FEDERAL UNIVERSITY OF MINAS GERAIS

School Of Engineering

Department Of Nuclear Engineering

Graduate Program In Nuclear Sciences And Technique

Raoni Adão Salviano Jonusan

ANALYSIS OF THE DISPOSAL OF SPENT NUCLEAR FUEL IN BRAZIL

Belo Horizonte

2021

Raoni Adão Salviano Jonusan

Analysis of the disposal of spent nuclear fuel in Brazil

Thesis presented to the Graduate Program in Nuclear Sciences and Techniques of the Federal University of Minas Gerais in partial fulfillment of the requirements for the degree of Doctor in Nuclear Sciences and Techniques

Concentration area: Nuclear and Energy Engineering

Advisor: Claubia Pereira Bezerra Lima

Co-advisor: Fernando Pereira de Faria

Belo Horizonte

2021

Jonusan, Raoni Adão Salviano.
J81a Analysis of the disposal of spent nuclear fuel in Brazil [recurso eletrônico] / Raoni Adão Salviano Jonusan. - 2021.
1 recurso online (177 f. : il., color.) : pdf.

Orientadora: Claubia Pereira Bezerra Lima.
Coorientador: Fernando Pereira de Faria.

Tese (doutorado) - Universidade Federal de Minas Gerais, Escola de Engenharia.

Anexos: f. 195-202.
Apêndices: f. 165-194.
Bibliografia: f. 150-164.
Exigências do sistema: Adobe Acrobat Reader.

1. Engenharia nuclear - Teses. 2. Análise térmica - Teses.
3. Combustíveis nucleares- Teses. 4. Resíduos radioativos – Teses.
I. Lima, Claubia Pereira Bezerra. II. Faria, Fernando Pereira de.
III. Universidade Federal de Minas Gerais. Escola de Engenharia.
IV. Título.

CDU: 621.039(043)

Ficha catalográfica elaborada pela Bibliotecária Letícia Alves Vieira - CRB-6/2337
Biblioteca Prof. Mário Werneck - Escola de Engenharia da UFMG

UNIVERSIDADE FEDERAL DE MINAS GERAIS

PROGRAMA DE PÓS-GRADUAÇÃO EM CIÊNCIAS E TÉCNICAS NUCLEARES

PCTN

FOLHA DE APROVAÇÃO

AN ANALYSIS OF THE DISPOSAL OF SPENT NUCLEAR FUEL IN BRAZIL

RAONI ADÃO SALVIANO JONUSAN

Tese submetida à Banca Examinadora designada pelo Colegiado do Programa de Pós-Graduação em CIÊNCIAS E TÉCNICAS NUCLEARES, como requisito parcial para obtenção do grau de Doutor em CIÊNCIAS E TÉCNICAS NUCLEARES, área de concentração ENGENHARIA NUCLEAR E DA ENERGIA.

Aprovada em 06 de outubro de 2021, pela banca constituída pelos membros:

Profa. Cláubia Pereira Bezerra Lima - Orientadora
Departamento de Engenharia Nuclear - UFMG

Dr. Fernando Pereira de Faria - Coorientador
Departamento de Engenharia Nuclear - UFMG

Profa. Antonella Lombardi Costa
Departamento de Engenharia Nuclear - UFMG

Dra. Patrícia Amélia de Lima Reis
Departamento de Engenharia Nuclear

Prof. Michel Melo Oliveira
Departamento de Engenharia de Minas - UFMG

Dra. Flávia Schenato
CNEN

Dr. Francisco Javier Rios
CDTN /CNEN

Belo Horizonte, 6 de outubro de 2021.

To my sunshine's: Juliana, Nanna, Sia, Nanninha, Silvia, Princen, and Odin.

Acknowledgments

First of all, I would like to thank my supervisor, Prof. Claubia Pereira, for the support and encouragement throughout these 4 years. I forgive you for the sad news on my dissertation defense day!!! Under your supervision, I could make my decisions and mistakes, learn my lessons, and achieve my goals.

My co-supervisors Fernando Pereira, I cannot thank you enough. This thesis would not exist without you. Your work was what motivated me to study nuclear waste disposal! Thanks for your guidance, encouragement, and friendship.

I would also like to express my deepest gratitude to my coauthors Raphael Henrique, Fidéllis Bitencourt e Dario Godino. This thesis would not have been possible without your contributions.

I thank all the PCTN teachers for creating an environment that felt like home. Thanks for the conversations and guidance. Special thanks to prof. Antonella Lombardi, who helped me and treated me as one of her mentees. Furthermore, I would like to thank Thales and Aline for their friendship and patience during my time as the student representative. My eternal teachers Prof. Angela and Prof. Ricardo, you got me ready to walk this Ph.D. path with your deeply educative supervision during my master thesis project.

I would like to thank the Coordination for the Improvement of Higher Education Personnel (CAPES), the National Council for Scientific and Technological Development (CNPq), and the Federal University of Minas Gerais (UFMG) for funding this research.

A big thank you to all my friends and colleagues! You guys encouraged and supported me during the student performance, I did my best for you! Once upon a time, there was this exceptional group of friends organized in a secret group: Angelina, Cláudio, Emílio, Esther, Fernanda Guerra, Fernanda Stephanie, Fidéllis, Igor, João, Raphael, Rodrigo, and Sarah. I could look at these guys as my siblings. Crazy Drop forever!!!

Thanks also to my extended family and my fantastic friends: You are simply the best! Words fail for Mom and Dad. Thank you for making all this possible in the first place. The fruit does not fall far from the tree!!! Thank you, João, Marina, and Ryana for their unconditional love and affection.

Last but most definitely not least, I want to thank my sunshine and soulmate, Juliana, for lighting up my life. Your support means so much. Thank you for your love and your bubbling and contagious joy and energy. Nothing is impossible with you by my side. Love you!!!

“Life,—does it disappoint thee?
Grieve not, nor be angry thou!
In days of sorrow gentle be:
Come shall, believe, the joyful day.

In the future lives the heart:
Is the present sad indeed?
'T is but a moment, all will pass;
Once in the past, it shall be dear”. (Alexander Pushkin, Poems, 1825)

ABSTRACT

The disposal of radioactive waste has been the subject of scientific research since the beginning of the nuclear industry. For high-level waste or spent fuel, the final disposal in deep geological repositories is the global scientific consensus. In this doctoral thesis, aspects related to the process of disposal of spent nuclear fuel (SNF) in Brazil were studied, from a purely academic point of view. The radioactive decay process releases thermal energy that is absorbed by the geological environment. However, some of the safety barrier components have a maximum operating temperature limit. Furthermore, the heat released can help the migration of fluids in the geosphere. As the heat transfer process is passive, the repository must be dimensioned so that the thermal limits are not exceeded during its operation. The simulation of heat transfer allows the determination of the smallest acceptable geometric dimensions of the repository for each type of SNF. Given the Brazilian Government's apparent interest in reprocessed nuclear fuels, the thermal behavior of two reprocessed fuels for the Angra 2 nuclear power plant, a Mixed Oxide (MOX) and a thorium-enriched reprocessed fuel was simulated. The MOX fuel can be disposed of in a repository after 50 years of its removal from the reactor. The spent fuel containing thorium, however, cannot be disposed of in a repository under the same conditions, since the maximum safe temperature would be exceeded. The dimensioning of the repository for the SNF is an important piece of information for the process of selecting areas with the potential to house a geological repository. With the application of a method based on geographic information systems and multi-criteria analysis for the selection of an area for the construction of a repository for the SNF, sites of interest were selected for further. Candidate sites have areas greater than the minimum areas estimated as necessary by the heat transfer simulation. As both the nuclear fuel cycle and the total number of nuclear power plants to be built in this century remain undefined, there is no estimate of back-end costs in Brazil. To estimate the costs associated with this phase of the nuclear fuel life cycle, strategic scenarios were created. These scenarios, together with the possible fuel cycles, were modeled in the energy planning tool MESSAGE to estimate the amount of SNF generated. Using stochastic methods, the most likely total cost was calculated. Values range from $12.84 billion to $83.71 billion depending on the scenario. With this

range, it was estimated that the energy sale value should be between 40% and 60% higher than the current value charged to finance the SNF disposal activities.

Keywords: Spent fuel. Deep geological repository. Cost estimation. Thermal analysis. Site selection.

RESUMO

O descarte de rejeitos radioativos tem sido objeto de pesquisas científicas desde o início da indústria nuclear. Para resíduos de alto nível ou combustível irradiado, a disposição final em depósitos geológicos profundos é o consenso científico global. Nesta tese de doutorado, foram estudados, de um ponto de vista puramente acadêmicos, aspectos relacionados ao processo de destinação do combustível nuclear usado (SNF) no Brasil. O processo de decaimento radioativo libera energia térmica que é absorvida pelo ambiente geológico. No entanto, alguns dos componentes da barreira de segurança têm um limite máximo de temperatura operacional. Além disso, o calor liberado pode facilitar a migração de fluidos na geosfera. Como o processo de transferência de calor é passivo, o repositório deve ser dimensionado de forma que os limites térmicos não sejam ultrapassados durante o seu funcionamento. A simulação da transferência de calor permite a determinação das dimensões geométricas mínimas aceitáveis para cada tipo de SNF. Dado o aparente interesse do governo brasileiro em combustíveis nucleares reprocessados, foi simulado o comportamento térmico de dois combustíveis reprocessados para a usina nuclear de Angra 2, um Óxido Misto (MOX) e um combustível reprocessado enriquecido com tório. O combustível MOX pode ser descartado em um repositório após 50 anos de sua remoção do reator. O combustível irradiado contendo tório, entretanto, não pode ser descartado em um repositório nas mesmas condições, uma vez que a temperatura máxima de segurança seria excedida. O dimensionamento do repositório para o SFN é uma informação importante para o processo de seleção de áreas com potencial para abrigar um repositório geológico. Com a aplicação de um método baseado em sistemas de informações geográficas e análise multicritério para seleção de área para construção de repositório do SNF, foram selecionados sítios de interesse para futuros estudos. Os locais candidatos têm áreas maiores do que as áreas mínimas estimadas como necessárias pela simulação de transferência de calor.

Como tanto o ciclo do combustível nuclear quanto o número total de usinas nucleares a serem construídas neste século permanecem indefinidos, não há estimativa de custos do *back-end* no Brasil. Para estimar os custos associados a esta fase do ciclo de vida do combustível nuclear, foram criados cenários estratégicos. Esses cenários, juntamente com os possíveis ciclos de combustível, foram modelados na ferramenta

de planejamento de energia MESSAGE para estimar a quantidade de SNF gerada. Usando métodos estocásticos, o custo total mais provável foi calculado. Os valores estão na faixa entre US $ 12,84 bilhões e US $ 83,71 bilhões dependendo do cenário. Com esses valores, estimou-se que o valor de venda de energia deveria ser entre 40% e 60% maior que o atual cobrado para financiar as atividades de descarte do SNF.

Palavras-Chave: Combustível irradiado. Repositório geológico profundo. Estimativa de custo. Análise térmica. Seleção de local.

LIST OF FIGURES

LIST OF TABLES

LIST OF ACRONYMS

Analytic Hierarchy Process	AHP
Areas Of Relevant Mineral Interest	ARIM
Autoridade Nacional De Segurança Nuclear	ANSN
Brazilian Geological Service	CPRM
Brazilian Institute of Geography and Statistics	IBGE
Central Nuclear Almirante Álvaro Alberto	CNAAA
Chicago Pile-1	CP-1
Chicago Pile-2	CP-2
Chicago Pile-3	CP-3
Closed Fuel Cycle	CFC
Comissão Nacional De Energia Nuclear	CNEN
Computer-Aided Design	CAD
Computer-Aided Engineering	CAE
Controladoria Geral Da União	CGU
Deep Geological Repository	DGR
Depósito Intermediário De Longa Duração De Combustível Usado	DICOMB
Dry Storage Unit	UAS
Energy Research Office	EPE
Ferriferous Quadrilateral	QF
Final Deposit of High Activity Radioactive Material	RAN
Finite Element Analysis Method	FEA
Geographic Information Systems	GIS
Graduate Program in Nuclear Sciences and Techniques	PCTN
Grid Convergence Index	GCI
High Level Long-Lived Waste	HL-LLW
High-Level Waste	HLW
Intermediate Geographic Regions	IGR
Intermediate Level Long-Lived Waste	IL-LLW

Intermediate Level Waste	ILW
International Atomic Energy Agency	IAEA
Korea Atomic Energy Research Institute	KAERI
Levelized Cost of Energy	LCOE
Long-Term Safety	LTS
Low Level Short-Lived Waste	LL-SL
Low Level Waste	LLW
Minas Gerais	MG
Mixed Oxide	MOX
Model For Energy Supply System Alternatives and Their General Environmental Impacts	MESSAGE
Multiple Criteria Decision Making	MCDM
National Academy of Sciences	NAS
National Department of Transport Infrastructure	DNIT
Nuclear Power Plant	NPP
Open Fuel Cycle	OFC
Operation And Maintenance	O&M
Organization For Economic and Co-Operation and Development/ Nuclear Energy Agency	OECD/NEA
Richardson Extrapolation	RE
Rio de Janeiro	RJ
Rough Order of Magnitude	ROM
São Francisco Craton	SFC
Socioeconomic And Environmental Viability	SEV
Spent Mixed Oxide	SMOX
Spent Nuclear Fuel	SNF
Spent Reprocessed Transuranic Fuel Spiked with Thorium	STRU
Spent Uranium Oxide	SUOX
Suitability Index	SI
Swedish Nuclear Fuel and Waste Management Company	SKB
Technical Feasibility	TF
Transuranic Fuel Spiked with Thorium	(TRU-Th)O_2

U.S Department of Energy	DOE
Underground Research Laboratories	URL
Unidade De Armazenamento A Seco	UAS
Unit Variable Cost	CVU
United States Atomic Energy Commission	AEC
Very Low-Level Waste	VLL
VTT Technical Research Centre of Finland	VTT

SUMMARY

1 – INTRODUCTION

1.1 – BRIEF HISTORY OF THE DISPOSAL OF HIGH-LEVEL WASTES

The generation of electricity using nuclear reactors creates radioactive wastes. As the radionuclides decay over time, they may provoke biological injuries to humans and animals. Despite the potential biological risks, its volume of waste per kWh is much smaller than that of other power plants that use fossil fuels (1). Radioactive waste is generated in every stage of the nuclear fuel cycle, as presented in Table 1.

Table 1 **–** Origin, nature, and management of nuclear waste. Adapted from (2).

Waste	Origin	Nature	Radioactive half-life	Activity	Management
Mine tailingns	Uranium mines	After chemical extraction of the uranium from crushed ore, the tailings still contain the daughter nuclides of uranium, and especially radium	A few thousand years	Very low (a few ten thousand Becquerel per kilogram)	In situ storage. Themine tailings are covered by a layer of sterile rock and soil to prevent their dispersion, to screen the gamma radiation and to limit radon exhalation
Very low level waste (VLL)	VLA waste comes mainly from dismantled nuclear facilities	Steels, and concrete rubble containing activation products	Variable	Very low (a few ten thousands Becquerel per kilogram)	Sort them, decontaminate whenever possible, then store in surface facilities (such a storage already exists in France in Morvilliers)
Low level short-lived waste (LL-SL)	Operation of nuclear plants	Gloves, boots, filters immobilized in concrete	Short (10-100 years) After 300 years, all the radioactivities will be disappeared	Low (smaller than 3.710^{8} Bq/kg)	Surface storage of the concrete blocks in dedicated surface installations. The waste is stored above the water table, covered with an impermeable clay layer and a few meters of soil. Two such storage facilities already exist in France in La Hague and Soulaines
Intermediate level long-lived waste (IL-LL)	Fuel reprocessing	Processing residues and fuel claddings immobilized in concrete	Long (up to million years)	Medium (smaller than3.710^{11} Bq/kg) This waste does not generate heat	Probably underground disposal (The WIPP facility is already in operation in USA; disposal is not yet decided in other countries)
High level long-lived waste (HL-LL)	This waste comes from spent fuel	Glass blocks (if the spent fuel is processed); spent fuel assemblies (if no processing)	Long (up to a million years)	High (of the order of 10^{13} Bq/kg)	No decision yet about what to do with this category of waste. Technical solutions already exist or are under study for the separation, transmutation conditioning of HLA waste, and for its storage or underground disposal In the mean time, these waste forms are stored in interim storage facilities (pools, or dry storage surface facilities)

The classification of wastes depends on each country. In Brazil, radioactive waste is classified into four classes: Class 0, Exempted Waste; Class 1, Very Short-Lived Wastes; Class 2, Low and Intermediate Level Wastes; Class 3, High-Level Wastes

(HLW) (3). The spent nuclear fuel (SNF) is not considered nuclear waste (4). The non-classification of the SNF as waste is due to the possibility of reprocessing (4, 5).

The accumulation of HLW initiated with the activities developed at the Manhattan Project during the Second World War. In December 1942, the first self-sustaining nuclear reaction was achieved on the world's first nuclear reactor, the Chicago Pile-1 (CP-1) (Figure 1), which was soon dismantled and reassembled in a new location, and the reactor was retitled as Chicago Pile-2 (CP-2). In 1943 the world's first heavy water moderated reactor, Chicago Pile-3 (CP-3), was assembled at the same site as CP-2. On May 15th, 1954, both reactors, CP-2, and CP-3, were decommissioned, dismantled, and buried in 1955 (6).

Figure 1 **–** An illustration depicting Chicago Pile-1.

(Image copyright Chicago Historical Society)

After the dismantling of CP-2 and CP-3, the extinct United States Atomic Energy Commission (AEC) contracted, in 1955, the National Academy of Sciences (NAS) to create a committee to evaluate possibilities for the disposal of HLW. The committee issued its first report in 1957, indicating the possibility of disposal in cavities mined in

salt beds and salt domes by the formation of a silicate brick or slag, which would be either stored in the surface or dry mines; or by injection of diluted liquid waste in profound rock strata (7).

At the end of the 1950s, as more countries began the development of their nuclear program, the disposal of radioactive wastes was recognized as an important field of knowledge. The first scientific conference on the disposal of radioactive wastes was sponsored by the International Atomic Energy Agency (IAEA) in 1959, with the attendance of scientists from 31 countries and 11 international organizations (8). Since then, many methods of disposal have been proposed. Kubo and Rose (9) proposed a taxonomy of nuclear waste disposal options for reprocessed SNF (Figure 2), but the options displayed may also be used for non-reprocessed SNF. There are three routes for disposal choice that depends on the disposal method. The first route (1 and 1A) is the disposal into geological formations with little to none, chemical or mechanical, work done to the waste. The second route (2 and 2A) is associated with the chemical separations of actinides and other heat-producing isotopes. The final route (3 and 3A) is the *in situ* melting of the waste. Other disposal options proposed were the disposition in Antarctic rocks; in permanent ice, i.e., long-lasting ice sheets; in engineered near-surface structures (mausolea) for future retrieval; on space; and oceans.

During the 1970s and 1980s, the effort was directed towards the disposal of a repository on land. The focus in a repository on land is supported by its effectiveness of sorption of radionuclides, confirmed by controlled experiments and at the Oklo formation, and the multi-barrier system which supplies more deterrents to the release of radionuclides to the biosphere (10, 11). In the next decades, the international community reached a consensus that the preferred method for the disposal of HLW should be in a deep geological disposal facility (12, 13). Nowadays, there are still no repositories in operation, although, in Finland, a construction license for one was granted in 2015, with the final disposal process being in the 2020s (14). The status of national waste disposal of HLW and SNF programs around the world is presented in Annex A (12).

Figure 2 – Taxonomy of nuclear waste disposal options (9).

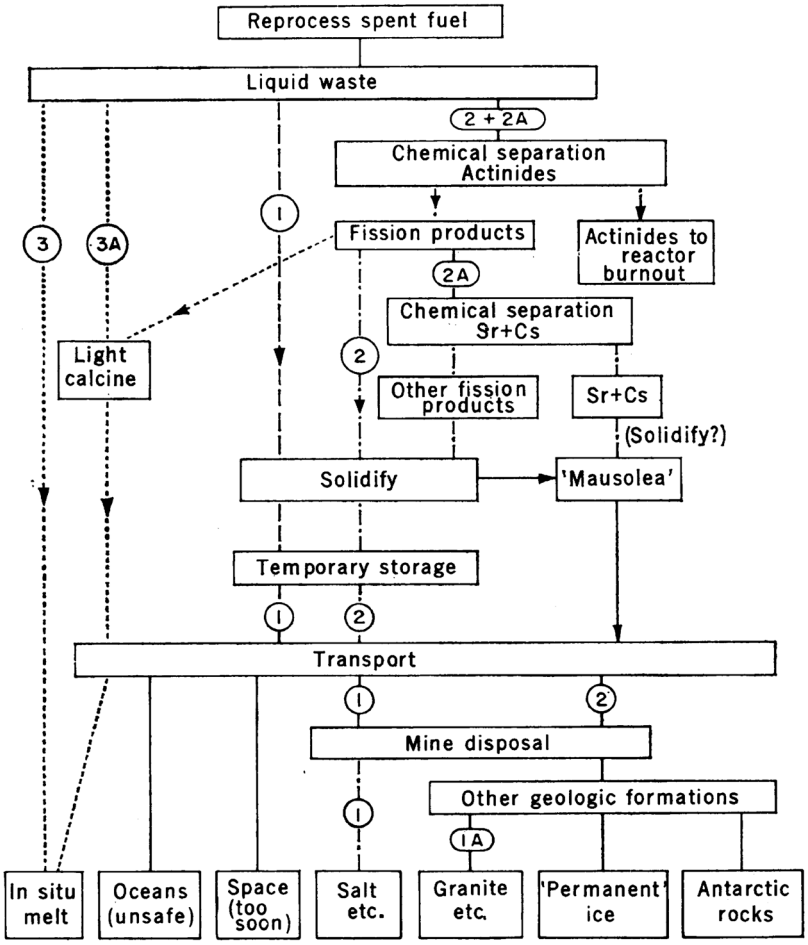

1.2 – DEEP GEOLOGICAL DISPOSAL

Most of the countries with either HLW or SNF stored in interim facilities have plans to construct a deep geological disposal facility (12). This type of repository was firstly proposed in the 1950s and, even though the advent of nuclear fuel reprocessing techniques, its importance stays unaltered. Since the 1980s, when the Beijer Institute undertook a review of the national waste disposal around the world, a deep geological repository has been the preferred method for disposal because (11):

1. The safety of the repository is not dependent upon human care: after its closure, the repository does not require human intervention.
2. Its depth, three hundred to 1000 m, provides a natural barrier between the waste and the biosphere hampering the release of the waste into the environment, by man nor natural process, if installed in a local without mineral resources.

3. The method of disposition is achievable with usual techniques: many mines are at the depth needed or deeper. In Brazil, according to data from 2015, 43 active mines were deeper than 300 m[1];
4. Multiple possibilities for finding such structures are available.
5. "...the wastes could either be retrieved or the effects mitigated if unprecedented events should occur to drastically alter the safety of the system" (11): The multiple-barrier system, similar to the defense-in-depth in nuclear reactors, is an approach to account for any uncertainties given the time scale involved.
6. It is possible to model the life cycle of the wastes at the repository under the influence of the various stresses[2] present in the host rock.

The deep geological repository may be constructed in different host rocks such as salt, granite, shale, and basalt. Each host rock has favorable and unfavorable characteristics. Table 2[3] shows a comparison between the host rocks. The associated disposal media were divided into 4 large groupings (15): 1) Sal: anhydrite, gypsum; Granite: general crystalline rock, granodiorite, periodontitis, gneiss, syenite; 3) shale: general argillaceous rock, carbonate; and 4) basalt: gabbro and some tuffs.

The most studied host rocks are granite (the preferred media in Finland (Figure 3) and Sweden), shale (the preferred media in France and Belgium), and salt formations (studied in Germany since it already operates two repositories for low-level waste (LLW) and intermediate-level waste (ILW) in former salt mines) (12). The physical properties are treated in a broad sense and do not reflect site-specific conditions such as deformation, metamorphism, or fracture of the rocks. These factors, although relevant, must be analyzed on a case-by-case, site-by-site basis.

[1] Among forty-three mines, twenty-five are in the State of Minas Gerais. Information was obtained by requesting to the National Mining Agency (Portuguese: Agência Nacional de Mineração – ANM) that is supported by the Information Access Law, law nº 12.527/11.
[2] Radiation and heat released from the waste; hydrogeological, lithostatic, chemical and biological conditions.
[3] The comparisons are based on the Final Environmental Impact Statement published by the U.S. Department of Energy (DOE) regarding the Management of Commercially Generated Radioactive Waste in 1980 (15).

Table 2 – Comparison between the rock types and their properties. Adapted from (11, 15).

Property	Host Rock			
	Salt	**Granite**	**Shale**	**Basalt**
Natural moisture content	3	3	2	3
Strength	1	3	2	3
Coefficient of linear thermal	2	3	3	3
Heat Capacity	3	2	2	2
Thermal conductivity	3	2	2	1
Permeability	3	3	3	3
Porosity	3	3	3	3
Solubility	1	3	3	3

1-Bad / 2-Medicore / 3-Good

Figure 3 – Layout of the Olkiluoto repository in Finland (16).

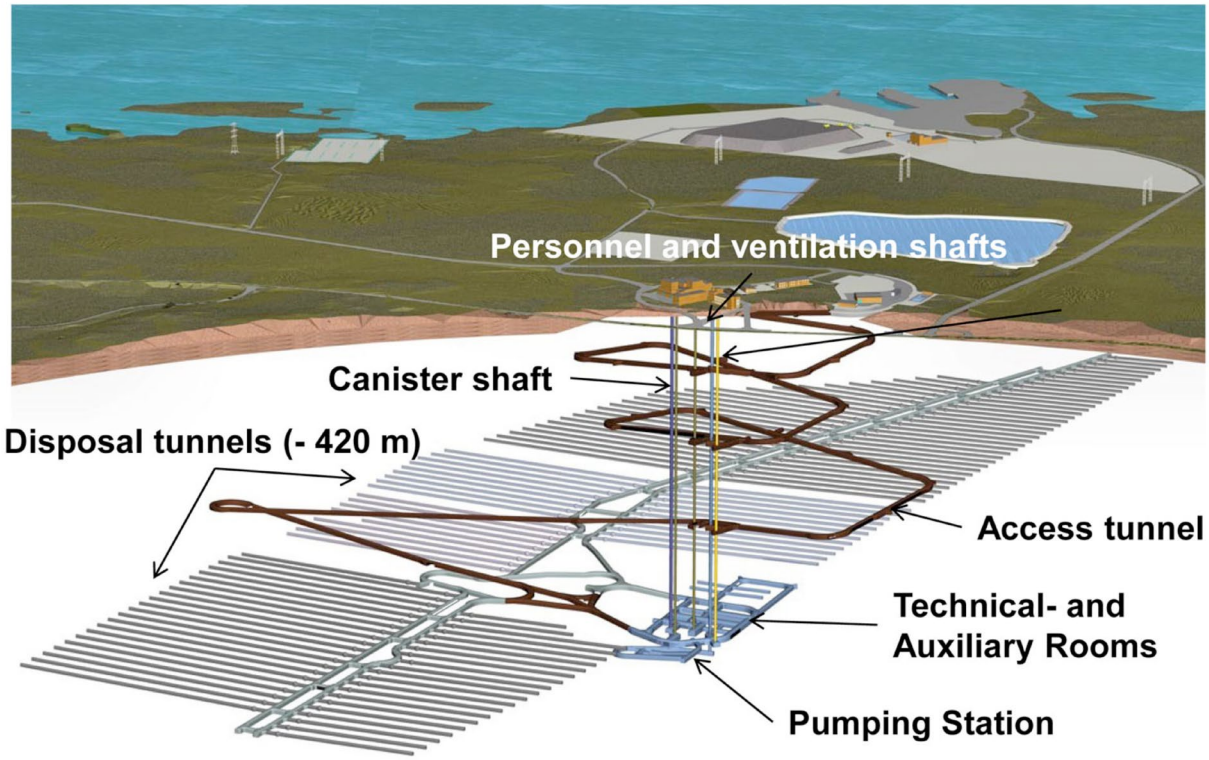

The multiple-barrier system has the host rock as the final barrier against the release of radionuclides to the biosphere. The barriers, as shown in Figure 4, are:

1. The HLW or SNF themselves: HLW is composed of wastes resulting from the reprocessing of SNF, which is solidified on an inert matrix, such as glass. SNF is composed of ceramic fuel pellets inserted into gas-tight metal rods.
2. The final disposal canister: both HLW and SNF are packed in a corrosion-resistant metal canister made of copper and cast iron. The canister provides mechanical, chemical, and biological protection for the HLW or SNF.
3. A bentonite barrier[4]: bentonite clay is used to enclose the final disposal canister. The bentonite provides mechanical stability since it slows down the water movement in the canister surroundings and adsorbs the radionuclides in case of leakage accidents.
4. The host rock: the bedrock provides an ambient with slow and predictable changes, chemical or physical.

Figure 4 – Engineered barriers.

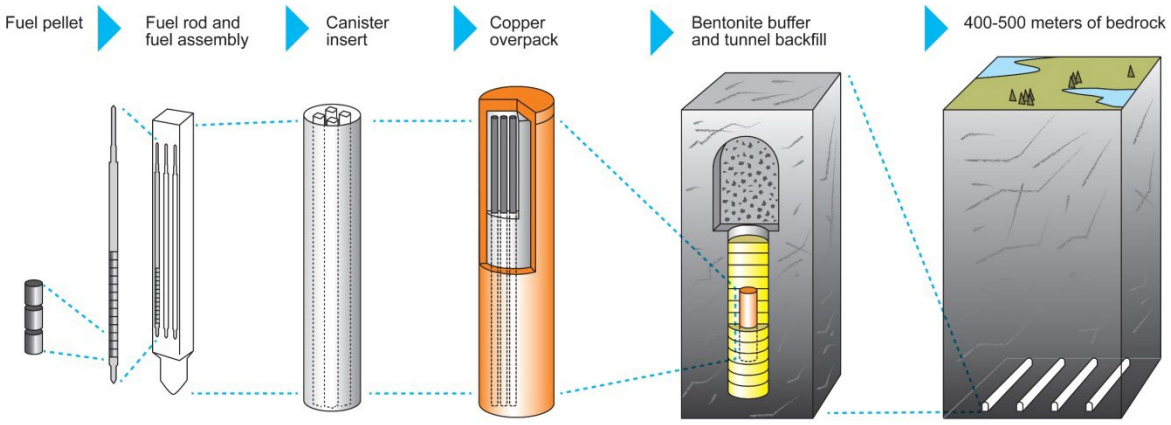

(Image copyright Posiva Oy)

To date, only three countries began or will begin to construct a repository in the following decade: Finland (2016), with the Olkiluoto[5]; France (2022, estimate)[6] with Cigéo; and Sweden (early 2020s) with Forsmark[7] (20).

[4] The bentonite buffer is one of the design constraints. Among the requirements, the buffer must transfer the heat emanating from the canister efficiently to keep its temperature below 100ºC, to maintain the mineralogical integrity of the buffer [15].
[5] The start of the geological final disposal of spent nuclear fuel is planned by the mid-2020s (17).
[6] The beginning of the operations of Cigéo is planned to 2030 (18).
[7] Forsmark should start its operations in the 2030s (19).

1.2.1 – Numerical analysis of the heat propagation

Idealized by Courant (21), the finite element analysis method (FEA)[8] helped the analysis of the physical phenomenon in a continuum of matter (solid, liquid, or gas) by the decomposition of the domain (continuum with a known boundary) into a finite number of subdomains (elements). By dividing the problem into smaller and manageable pieces FEA, alongside computer-aided design (CAD) and another computer-aided engineering (CAE) method, supplies the solution of many complex engineering and physical problems rapidly and effectively (22, 23).

Numerical modeling is a powerful tool used to simulate and optimize the repository and when associated with the field research in underground research laboratories (URLs)[9], it can be used not only for prediction of the performance of the repository along the time but also to design field experiments, to analyze the results, and to improve the understanding of the subsurface processes (25).

Earlier works also used numerical models to simulate the heat propagation of HLW and SNF disposed on a geological repository with hard rock as a host rock. The works published by Choi and Choi (26), Lee *et al.* (27), and Acar and Zabunoğlu (28, 29), alongside the technical reports from the Swedish Nuclear Fuel and Waste Management Company (SKB) (30), VTT Technical Research Centre of Finland (VTT) (16) and Korea Atomic Energy Research Institute (KAERI) (31), also used numerical modeling codes applied to the study of deep geological repositories. The simulation can be done by numerical models such as ANSYS, Code_Bright, COMPASS, FEFLOW, NISA, OpenFOAM©, PORFLOW, and TOUGH2.

[8] A brief account of the development of FEA was given by O.C. Zienkiewicz on his paper “The birth of the finite element method and of computational mechanics” (DOI: 10.1002/nme.951)

[9] According to the Nuclear Energy Agency (NEA) of the Organization for Economic Co-operation and Development (OECD) (24): “A URL is an underground facility in which site characterization and testing activities are carried out along with technology development and demonstration activities in support of the development of deep geological repositories for radioactive waste. URLs are in geological environments that are suitable for repository implementation such as granite, salt, clay/shale or volcanic tuff.”

1.2.2 – The Sitting Process

The sitting process is a major step during the construction of the repository as the site selected must have the right characteristics for the containment of the radioactive waste. Given the complexity of this process, a multi-stage approach is employed with four broad stages, as defined by the IAEA (32)[10]: conceptualization, area survey, site investigation, and detailed site characterization (Figure 5).

Figure 5 – Stages of the sitting process. Adapted from (31).

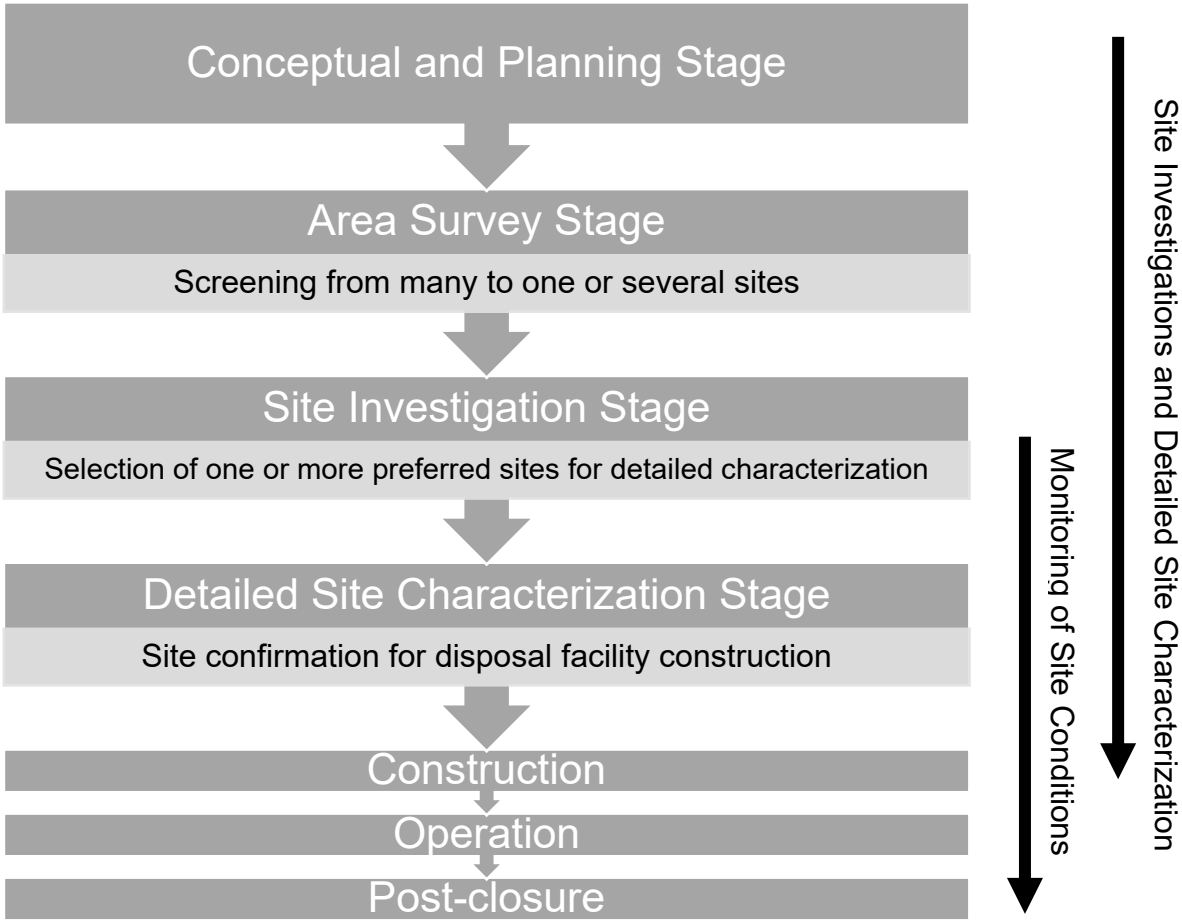

[10] The Appendix I of the IAEA Specific Safety Guide nº SSG-14 supplies detailed information about the stages and the data necessary during the sitting process.

1.2.3 – Cost estimation

The construction of a geological project is a long-term enterprise. The fastest that any country took since the beginning of the feasibility and site investigations studies to the submission of the application for construction was 24 years (20). In addition, the operation of the repository is a long-term activity, therefore it is necessary to set up the provision and/or financial reserve for the construction, operation, and decommissioning of the project. Cost estimation is an essential element of the studies of feasibility since it helps to address three fundamental questions: is it affordable? What is the budget necessary? What choice would yield the best results?

1.3 – SPENT FUEL MANAGEMENT IN BRAZIL

The Brazilian government has not yet decided about the nuclear fuel cycle to be followed in the country. The current policy for managing the SNF is to keep it in temporary storage, in the nuclear plants' cooling pools, and dry storage units in the next years, while the technical, economic, and political decision about the fuel cycle remains undefined (33). Therefore, spent fuel is not considered nuclear waste according to Brazilian law.

Currently, the SNF is initially stored into cooling pools installed in nuclear power plants (NPP) of Angra. In the short term, part of the SNF will be transferred to a dry storage unit (Portugues: Unidade de Armazenamento a Seco - UAS). Until April 2020, it was considered that the UAS would start receiving the first SFs in June 2021 (34)[11]. The UAS will have the capacity to store the SNF of the two NPPs currently in operation, ANGRA 1 and ANGRA 2, until 2045, at least, when it was considered the start of the Long-Term Intermediate Deposit for Fuel Elements (Portuguese: Depósito Intermediário de Longa Duração de Combustível Usado – DICOMB) (35). However, with the implementation of the UAS, the National Nuclear Energy Commission

[11] Obtained by requesting access to information, through the Integrated Ombudsman and Access to Information Platform (Fala.Br) of the Comptroller General of the Union (CGU), to Eletronuclear, number 99908.000235 / 2020-05, held on 04/16/2020 and answered on 04/29/2020.

(Portuguese: Comissão Nacional De Energia Nuclear – CNEN) abandoned the development of DICOMB[12].

1.3.1 – Related national legislation

The Brazilian national laws related to the management of spent fuel and radioactive waste in Brazil are, from the newest to the oldest:

- Provisional Measure Nº. 1,049 of May 14, 2021 (36, our translation): creates the National Authority for Nuclear Safety (Portuguese: Autoridade Nacional de Segurança Nuclear – ANSN). ANSN assumes, among others, the responsibilities of safety assessment, inspection, and licensing operations related to the management of radioactive waste.
- Decree Nº. 9,600 of December 5, 2018 (4, our translation): consolidates the guidelines on the Brazilian Nuclear Policy and establishes that spent fuel is not considered a radioactive waste and must be stored for future reuse.
- Norm CNEN NN 9.02 of 2012 (37, our translation): deals with the management of financial resources for technical and administrative activities for the removal of regulatory control of nuclear power plants
- Norm CNEN NN 9.01 of 2012 (38, our translation): deals with the decommissioning of nuclear power plants.
- CNEN Regulatory Position 1.26 / 001 2008 (39, our translation): deals with the management of radioactive waste in NPPs.
- Decree Nº. 5,935 of October 19, 2006 (40, our translation): promulgates the Joint Convention on the Safety of Spent Fuel Management and the Safety of Radioactive Waste Management.
- Norm CNEN NE 5.02 of 2003 (41, our translation): deals with the transport, receipt, storage, and handling of fuel elements of nucleoelectric plants.

[12] Obtained by requesting access to information, through the Integrated Ombudsman and Access to Information Platform (Fala.Br) of the Comptroller General of the Union (CGU), to Eletronuclear, number 01217.004257/2021-09, held on 06/22/2021 and answered on 07/12/2021.

- Law Nº. 10,308 of November 20, 2001 (42, our translation)[13][14]: establishes rules for the siting, licensing, operation, and regulation of radioactive waste storage facilities in Brazil. This law concerns all types of nuclear waste produced in Brazil.
- Law Nº. 9,765 of December 17, 1998 (43, our translation): establishes a license, control, and inspection fee for nuclear and radioactive materials and their installations.
- Norm CNEN NE 1.26 of 1997 (44, our translation): deals with safety in the operation of nucleoelectric plants.
- Articles 21, item XXIII, and 22, item XXVI, of the Brazilian Federal Constitution which establishes the competence of the Union through CNEN, attributed by Law Nº. 6,189 of December 16, 1974, modified by Law Nº. 7.781 of June 27 of 1989, as responsible for the final destination of the radioactive waste produced in the national territory (36, p. 1, 43, 45, our translation).
- and Law Nº. 6,453 of October 17, 1977 (46, our translation): establishes civil liability for nuclear damage and criminal liability for acts related to nuclear activities.

Additionally, during the environmental licensing process of Angra 3 NPP, two environmental conditions are related to the management of the Brazilian SNF:

- Condition 2.18 of Preliminary License 279/2008 (47, our translation), which determined "To present a proposal and start the execution of the project approved by the environmental agency for final disposal of high-activity radioactive waste before the start of operation of Unit 3.”.

- Condition 2.20 of the Installation License 591/2009 (48, our translation), which determined: "To present in 180 days a technical-financial and execution

[13] Technically, the SNF is not considered a nuclear waste given the possibility of reprocessing, according to Decree 9,600 of 2018. However, even with the reprocessing, high-level waste would be generated that would fall under the law.
[14]The Law 10,308 / 2001, in its article 18, also provides that the costs of the intermediate and final repositories will be paid to CNEN by the generator of the radioactive waste.

> schedule according to the analytical structure of the RAN Project - Long Term Waste Deposit for used fuels, approved by CNEN."

In the last available Analysis of Attendance Analysis Report of the Installation License n ° 591/2009 of Angra 3, issued by the Brazilian Institute of the Environment and Renewable Natural Resources (Ibama) in 2011 (49, our translation), it is said that

> "The Brazilian Political decision in postponing the recycling of Irradiated Fuel Elements - ECIs, CNEN decided that these fuels, originating from reactors at Brazilian nuclear plants, should be stored for long term in intermediate deposits, until it is considered convenient, politically and economically, to recycle such ECIs ",

This statement is confirmed by Decree No. 9,600 of December 5, 2018[15], and it is necessary then "[..] to reconsider the stipulation by condition 2.18 of the Previous License No. 279/2018 concerning the requirement for the Construction of a Final Deposit of High Activity Radioactive Material (RAN)." (49, our translation). In addition, the RAN Project was replaced by the DICOMB Project, under the responsibility of CNEN (49). According to this document, the environmental licensing process for this project was scheduled for 2017 (49). Electronuclear, started in 2021, the transfer of part of the irradiated fuel stored in the cooling pools of the Angra 1 and Angra 2 NPPs to the UAS, which is considered by the CNEN and by Eletronuclear as an initial storage unit[16]. The UAS consists of the storage of irradiated fuels in concrete and metal hulls of the HI-STORM type, by the company HOLTEC, in a location of the *Central Nuclear Almirante Álvaro Alberto* (CNAAA). With the adoption of the UAS, CNEN discontinued the development of DICOMB[17].

---

[15] “Art. 2 For the purposes of this Decree, it is considered: [...] II – spent nuclear fuel - nuclear fuel used in nuclear reactor and removed from its core, which will be stored in an appropriate place for future reuse [...] "

[16] Obtained by requesting access to information, through the Integrated Ombudsman and Access to Information Platform (Fala.Br) of the Comptroller General of the Union (CGU), to CNEN, number 01217.003113/2021-27, held on 05/13/2021 and answered on 06/14/2021.

[17] See footnote 12.

The lack of definition about the nuclear cycle model to be adopted and, consequently, the lack of a formal policy and strategy for the management of SNF in Brazil, resulting in several deficiencies. Among the deficiencies are the lack of criteria for the selection of the final disposal sites for SNF, and the lack of provision or financial reserve by the radioactive waste generator. As stated in Judgment 1,108 / 2014 of the Federal Court of Auditors (Portuguese: Controladoria Geral da União – CGU) (50, our translation):

> "the absence of a formalized policy and strategy on the management of nuclear fuel used in the national territory, with the absence of positioning on the solution to be adopted in the country (deposition, reprocessing or waiting for technological/economic maturation of the available options), can harm the fulfillment of the obligations assumed by Brazil through the caput and items of Article 4 of the Joint Convention on the Safety of Spent Fuel Management and on the Safety of Radioactive Waste Management, promulgated by Decree No. 5,935, of 2006, in addition to constituting an important risk to the fuel management process nuclear used in the country "[18]

1.4 – RESEARCH QUESTIONS AND OBJECTIVES

This thesis is based on the following research questions:

1. What is the minimum area necessary for the disposal of SNF, traditional or reprocessed, in the Brazilian territory depending on the rock temperature at a depth of 500m?
2. Where could a geological repository of spent Brazilian fuel be built, considering the thermal behavior of the SNF?
3. What is the cost of the spent fuel back-end in Brazil?
    - Would reprocessing be the best choice from a financial point of view?

[18] More specifically, art. 4, items VI ("Strive to avoid actions that impose reasonably predictable impacts on future generations greater than those permitted for the current generation") and VII ("Aim to avoid imposing undue burdens on future generations") and art. 22 (Human And Financial Resources) of the Joint Convention (40)and Article 18 ("The intermediary and final deposit service for radioactive waste will have its respective costs compensated to CNEN by the depositors, according to the table approved by the CNEN Deliberative Commission") of Law No. 10,308 of 2001 (42).

The main related goals are:

1. To study the heat propagation in the geological disposal environment with information from the Brazilian thermal gradient, and to find the smallest disposal area needed for disposal of the reprocessed Brazilian fuels.
2. To apply a method of site selection in one or more Brazilian states.
3. To conduct an economic analysis of the fuel back-end spent in Brazil for different nuclear power generation scenarios.

1.4.1 – Assumptions

To answer the research questions and to fulfill the research objectives, the following underlying assumptions were adopted:

- General assumptions
    - The DGR is considered to be constructed on granitic rocks. The choice for the SNF disposal in granitic rocks was made for two reasons: First, this thesis is part of a pre-existing line of research in the postgraduate program in nuclear sciences and techniques, which investigated the disposition in these rocks; Secondarily, the reference work for the selection of suitable sites for the construction of a DGR also considered the disposal in granitic rocks.
    - It was considered that the SNF remained 50 years in interim storage before final disposal.
    - This thesis is an academic analysis. The simplicity of the analysis methods was emphasized, given that the methods and assumptions considered here may be completely different from those used by the Brazilian government when deciding about the construction of a Brazilian DGR.
- Chapter 2 assumptions:
    - The simulations used a finite element code, ANSY, for the heat transfer of SNF in final disposal conditions.
    - The simulations only consider heat transfer by conduction and use constant thermophysical and isotropic properties.

  - Underground excavation stability, groundwater flow, or earthquake effects have not been considered in the simulations.
- Chapter 3 assumptions:
  - The methodology used for site selection is based on international standards and the CNEN 6.06 standard for Selection and Choice of Locations for Radioactive Waste Deposits, for low and medium-level wastes.
  - The selection process carried out corresponds to the area survey stage and was carried out on a regional scale, as shown in Figure 5.
  - Due to the lack of standardized data for all Brazilian states, only the states of Minas Gerais and Espírito Santo were studied.
- Chapter 4 assumptions:
  - The economic analysis used the analogy method and different generation scenarios.
  - The effects of reprocessing in the front-end of the fuel cycle, as well as multi-reprocessing and the use of depleted uranium, were not considered.

The remaining chapters are organized as follows:

- Chapter 2 deals with the analysis of heat transfer by conduction of several types of SNF, UO2, MOX, and TRU, in a DGR built-in granitic rocks. It was carried out a reproduction study to confirm the computational model, a mesh convergence study, and a simulation of the influence of rock temperature on repository dimensioning.
- Chapter 3 deals with the application of a proposed methodology for the area survey stage of a DGR in Brazilian granitic rocks, proposed by Martins (51). The methodology was applied to two Brazilian states.
- Chapter 4 presents an estimation study of the back-end costs of the Brazilian nuclear program. Six strategic scenarios and a Monte Carlo simulation were used.

2 – NUMERICAL ANALYSIS OF HEAT PROPAGATION

Numerical modeling has been used to investigate a large variety of research questions concerning the disposal of HLW (25). Earlier works have used FEA, or other similar numerical modeling approaches applied in the study of deep geological repositories (16, 26–31, 52). Since there is not a permanent disposal program proposed for Brazil, this work considered the geological disposal model developed by Sweden, KBS-3V, as the model for disposal of the Brazilian radioactive waste.

2.1 – KBS-3V DISPOSAL CONCEPT

The disposal of HLW or SNF on the KBS-3V concept is intended to be done into hard rock, such as granite. The waste is loaded into a canister composed of a cast iron insert, and a copper overpack, as represented in Figure 6. Each canister is then placed on individual boreholes, excavated along parallel tunnels at a depth of 500 m in the host rock, and it is surrounded by a bentonite buffer in the borehole, for mechanical protection, as well as to limit and retard the release of radionuclides on the canister failure (16, 53, 54). This concept was also adopted as a reference by the Finish Posiva and British Nirex companies during the development of their repository concept (55, 16).

Figure 6 – UK HLW/SNF repository concept (55).

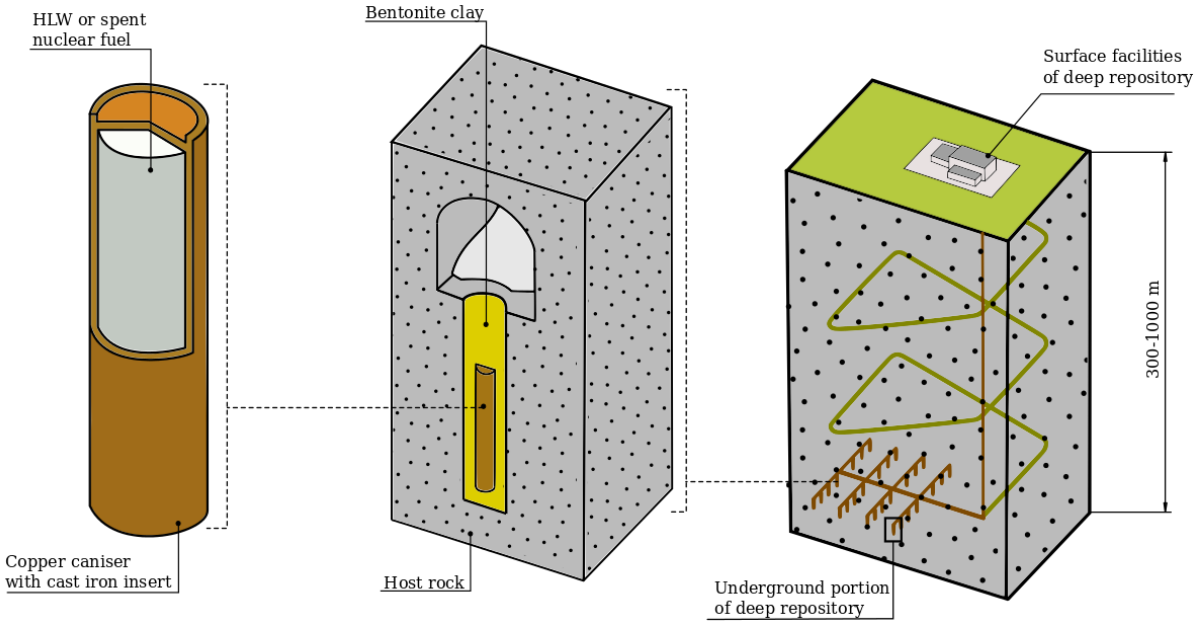

One of the key questions associated with the development of a deep geological repository (DGR) is how its containment barriers would behave in the presence of thermal loads emanating from nuclear waste. The heat transfer from the canister to the surrounding rock is determined by the heat output from the waste, thermal properties of the materials and the layout of the DGR, the canister spacing, and the distance between disposal tunnels. As the heat output and thermal properties are predetermined, the temperature profile of the surface of the canister is controlled by varying the distance between the tunnels and the spacing between the canisters.

The main purpose of this chapter is to investigate the thermal behavior of two types of SNF: the traditional Uranium Oxide, and reprocessed SFs that are composed of a MOX and a (TRU-Th)O_2. The latter was previously studied for the ANGRA 2 (56) NPP. The simulation considered a KBS-3V type and aims to determine the disposal area necessary for the disposal of each SNF type. To this end, a reproduction study of the work conducted by Acar and Zabunoğlu (28) was performed with the ANSYS® Academic Student 2019 R3 (57) and OpenFOAM© (OF) (58), to confirm the simulation. Afterward, a Grid Convergence Study as proposed by Roache (59, 60) was conducted using ANSYS to evaluate the influence of the mesh resolution and mesh type on the results. The canister spacing for MOX and (TRU-Th)O2 SFs were determined through simple thermal analysis with the ANSYS code. The disposal area was then compared against the original findings of Acar and Zabunoğlu (28). The analysis suggested the impossibility of the disposition of the (TRU-Th)O2 SNF in a DGR with the current buffer thermal restrictions (100ºC). Finally, with geothermal data from Brazil, the minimum separation between canisters holding MOX was estimated for different temperature conditions at the depth of the DGR (500m). The results show the necessity of increasing the minimum spacing as the temperature of the rock is raised.

2.2 – PROCEDURES AND COMPUTATIONAL TOOLS

Although the DGR model is the KBS-3, in this work the final geometry modeled followed an earlier study developed by Acar and Zabunoğlu, which was chosen as a benchmark (28), and used a variant of the KBS-3 design performed by Nirex (55).

2.2.1 – The geometry of canister near-field

Figure 7 shows the dimensions and layout of the disposal hole and tunnel for the SNF canisters. The dimensions of the tunnels and boreholes for this work are as follows: the tunnels have a diameter of 5.5 m and are 40 m distant from each other, and the boreholes have a diameter of 1.75 m and a depth of 7.55 m. (16, 28). The spacing between the canisters varies according to the type of SNF and its burnup, as listed in Table 3.

Table 3 – Canister spacing for the SUOX and SMOX considered (28).

SNF	Burnup (GWd/tHM)	Canister Spacing (m)
SUOX	33	3.90
	40	5.54
	50	10.00
SMOX	33	3.00
	40	4.80
	50	13.00

Figure 7 – Nominal dimensions of the disposal hole and tunnel, in millimeters.

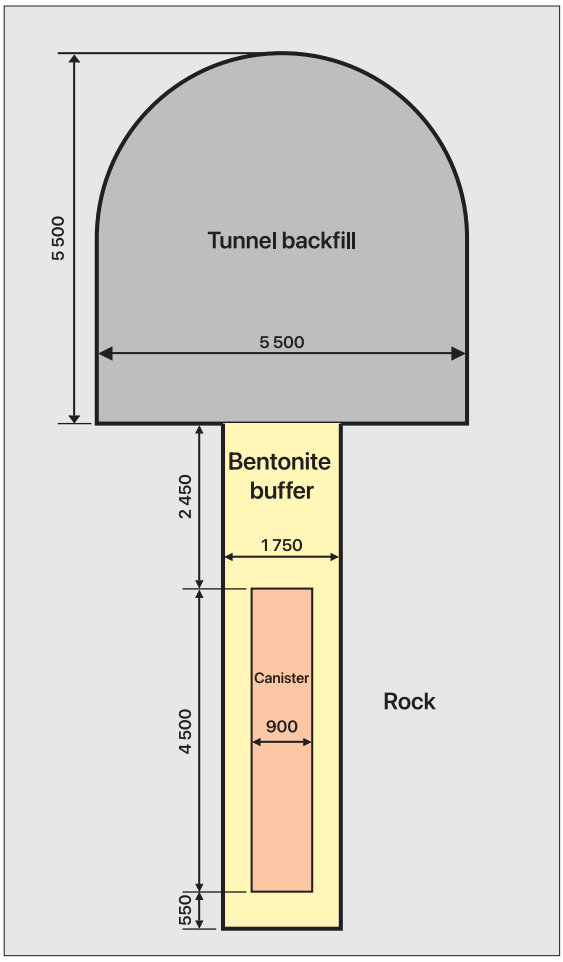

The canister design is the same for all SNF. However, the cast iron insert holds a different number of assemblies depending on the type of SNF, as shown in Figure 8. The canister is 4.5 m in height and has a diameter of 0.9 m. The canister designed for Spent Uranium Oxide Fuel (SUOX) accommodates a total of four assemblies. For Spent Mixed Oxide Fuel (SMOX) and Spent Reprocessed Transuranic Fuel spiked with Thorium Fuel (STRU), the canister accommodates only a single fuel assembly.

Figure 8 – SNF canister for UO_2 and reprocessed fuels.

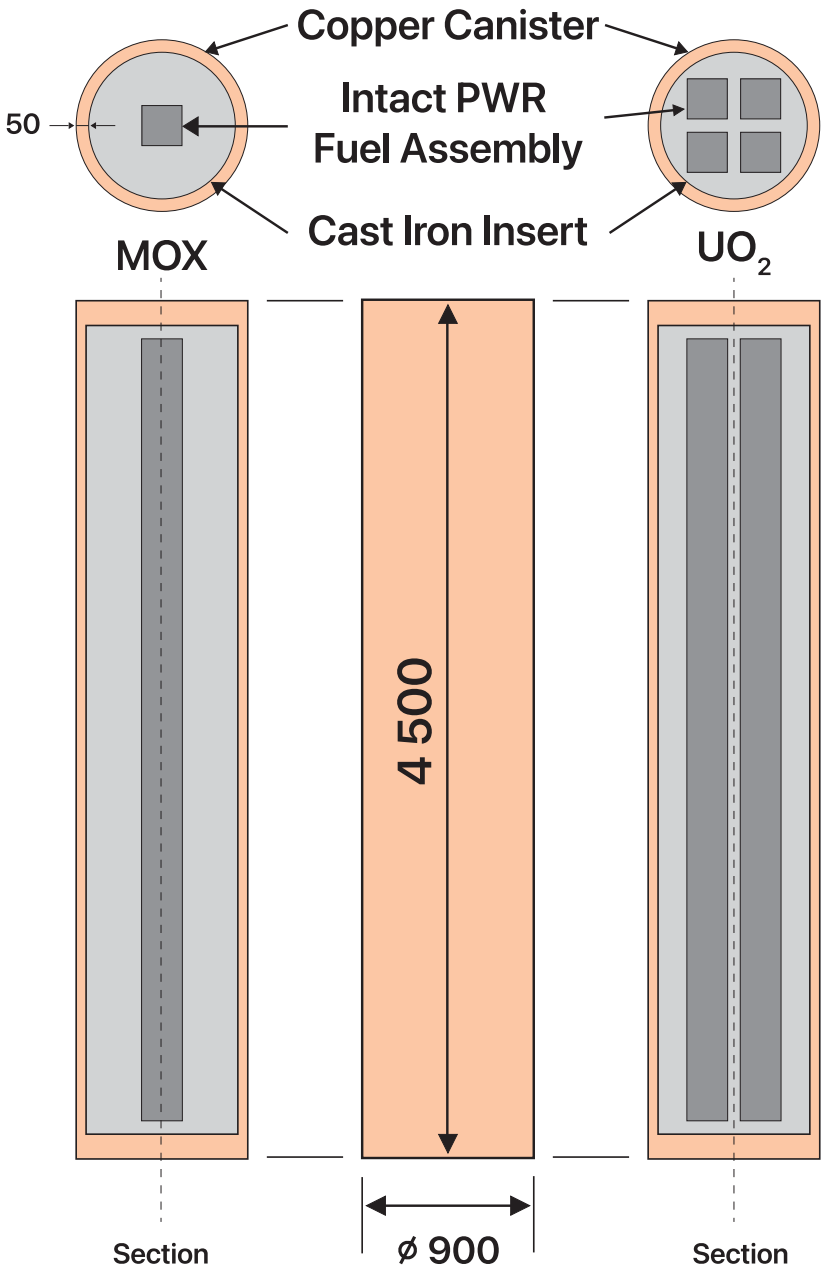

2.2.2 – Thermophysical properties

The thermophysical properties of the materials including thermal conductivity, the specific heat capacity, and the density are those used by Acar and Zabunoğlu and are presented in Table 4 (28, 29). As the initial temperature of the rock is an important parameter, a geothermal gradient of 30 °C/km and a ground surface temperature of the DGR of 15 °C (28) it was used to estimate this parameter at the depth of the DGR, 500m. These geothermal parameters are used for benchmark reproduction. The results of the reproduction study are then used as for later simulations using geothermal parameters estimated for Brazil.

Table 4 – Thermal properties of the materials (12,16).

Material	Density (kg/m^3)	Thermal Conductivity (W/m ºC)	Specific Heat (J/kg ºC)
SNF	2,000	0.135	2,640
Cast Iron Insert	7,200	52.0	504
Copper Canister	8,900	386.0	383
Bentonite	1,970	1.0	1,380
Backfill Material	2,270	2.0	1,190
Rock	2,650	3.2	815

Although the thermophysical properties used vary depending on the temperature of the material, constant values were used for the simulations. It was also considered that the thermal conductivity of the rock is isotropic, although it is orientation-dependent due to the foliation of the constituent minerals (53). The choice for constant values is justified by the fact that simulations are preliminary, that is, they are merely an academic analysis. The simplicity of the simulation was emphasized, given that the materials and methods considered here may be completely different from those used by the Brazilian government when deciding about the construction of a Brazilian DGR. It is noteworthy that the thermal analyzes were carried out with theoretically well-founded methods and codes.

2.2.3 – SPENT FUELS (SFs)

The final composition as well as the decay heat of the SNF are dependents on the fuel burnup, which is defined as the amount of energy generated by the nuclear fuel. The increase of the fuel burnup is desirable under the economic viewpoint since the higher

is the burnup, the higher is the core residence time and the smaller the power costs also will be. This work addresses three SNF types: SUOX, SMOX, and STRU.

Four types of SUOX are considered:

I. SOUX 33: 3.3% enrichment for a burnup of 33 GWd/tHM (28).

II. SOUX 40: 3.8% enrichment for a burnup of 40 GWd/tHM (28).

III. SOUX 50: 4.56% enrichment for a burnup of 50 GWd/tHM (28).

IV. SUOX 48: 4.3% enrichment for a burnup of 48 GWd/tHM (56).

Four types of SMOX are considered:

I. SMOX 33: 4.064% total fissile content for a burnup of 33 GWd/tHM (28).

II. SMOX 40: 4.852% total fissile content for a burnup of 40 GWd/tHM (28).

III. SMOX 50: 6.045% total fissile content for a burnup of 50 GWd/tHM (28).

IV. SMOX 48: 5.136% total fissile content for a burnup of 48 GWd/tHM (56).

The STRU has a 10% of fissile material for a burnup of 48 GWd/tHM (56). Both SMOX 48 and STRU result from earlier burnup studies performed to investigate the storage of these SNF into Angra 2 pool (56). The temporal decay heat data of the SUOX 30, SUOX 40, SUOX 50, SMOX 30, SMOX 40, and SMOX 50 SNFs were adjusted by the following function (61),

$$Q(t) = \sum_{i=1}^{4} A_i e^{-b_i t} \quad (1)$$

Where ***Q(t)*** is the heat released from the SNF in W/tHM at time ***t*** that is the time elapsed since the generation of the waste, in years, and $\boldsymbol{A_i}$ and $\boldsymbol{b_i}$ are fit coefficients of the decay heat curves. The coefficients values adopted in this study are listed in Table 5, being valid in the first 1,000 years (28). The decay power of the SUOX 48, SMOX 48, and STRU, SNFs, for the first 100 years, was calculated by Pereira *et al* (56) as part of the criticality studies with the KENO-V sequence of the SCALE6.0 computer

code making use of CSAS5 module and v7-238-energy-group library, including bias and uncertainty. Numerical values of the decay power are shown in Table 6.

Table 5 **–** Values of the ***Ai*** and ***Bi*** coefficients in Eq. 1 (28)

Waste type	**SUOX**			**SMOX**		
Burnup	**33**	**40**	**50**	**33**	**40**	**50**
A_1	990.18	1219.81	1535.27	1131.78	1495.38	2100.53
A_2	120.73	138.18	157.30	703.28	865.25	1058.92
A_3	14.27	15.76	48.54	390.09	552.25	660.44
A_4	11.60	13.02	27.20	116.68	138.58	177.22
b_1	11.60	13.02	27.20	116.68	138.58	177.22
b_2	0.00166	0.00167	0.00152	0.00152	0.00155	0.00159
b_3	0.00013	0.00014	0.00869	0.00692	0.00788	0.00765
b_4	$3.3175\ 10^{-5}$	$3.2642\ 10^{-5}$	$5.5445\ 10^{-5}$	$6.7581\ 10^{-5}$	$6.9608\ 10^{-5}$	$8.0955\ 10^{-5}$

Table 6 – Decay heat of SUOX 48, SMOX 48, and STRU SNFs (56)

Time (years)	**Decay heat (W/tHM)**		
	SUOX 48	**SMOX 48**	**STRU**
10	886	2,263	10,150
20	790	2,327	8,851
30	708	2,320	7,837
40	635	2,272	7,041
50	572	2,203	6,407
60	518	2,126	5,895
70	473	2,047	5,474
80	434	1,971	5,122
90	401	1,898	4,823
100	374	1,830	4,565

2.3 – SIMULATIONS

To ensure the safety and stability of the DGR is necessary to set up a thermal temperature constraint at the canister surface. This constraint guarantees the chemical stability of the bentonite buffer over the DGR life (16, 26, 28). The usual constraint is 100 ºC, however, deviations in the environmental parameters in the SNF data, as well as the occurrence of air gaps between the canister and the buffer, require a reduction

of the temperature constraint to 80 ºC (28, 52). To simplify the simulations, the air gap was suppressed, such that the only heat transfer mechanism is by conduction.

The DGR is geometrically symmetric, which simplifies the computational execution of the model. The symmetry planes are at the center of the deposition holes (28). Thus, only a quarter of one borehole was modeled. All symmetric boundaries are set as adiabatic.

All SNF types are assumed to be disposed of after 50 years under interim storage. The analysis was carried out over the critical period of 20 years after the deposition of the SNF (16, 28). The thermal analysis is used to calculate the temperature distribution in the critical points of the DGR that are: the canister-bentonite interface and the bentonite-rock interface. It is assumed that the vertical (Z-axis) boundaries are at 25 m above the top of the disposal tunnel and 25 m below the bottom of the disposition borehole (28). The temperature field deriving from the geothermal gradient is modeled by applying constant temperature boundary conditions at the top and the bottom of the model.

The temporal discretization of the analysis was done considering four end times for the time steps, as shown in Table 7. The smallest time steps are used during the first year of simulation, with the superior boundaries being either the first day or the first month, or the end of the first year. From the second year to the end of the simulation (20 years after the disposal), the time steps correspond to a period of three months.

Table 7 **–** Step end time and time steps used.

Step end Time	**Time Step**
86,400	180
2,592,000	10,800
28,927,800	259,200
631,152,000	7,889,400

On ANSYS, the Steady-State Thermal option was firstly conducted to set up the initial conditions, such as the geothermal gradient of the host rock, and the Transient Thermal analysis option was chosen to perform the time-dependent simulations. The meshes in the ANSYS were built using both unstructured and structured mesh tools. The solution method was the QUASI-solution method, which is associated with a Picard algorithm to solve the problem directly for the temperature (62). As the QUASI method was used, small-time steps (Table 7) were used to minimize inaccuracies (62). Simulations with ANSYS® were performed in a single machine using six cores (i7-8750H, 8GB-RAM DDR4,128GB SSD/ 1TB HD).

The computational domains used in OF were discretized using structured grids. The different domains were thermally coupled through the CHT solver, which is based on the combination of the solvers heatConductionFoam and buoyantFoam for conjugating the heat transfer between the solid and fluid regions. The solver employs an iterative method to find the temperatures shared by neighboring regions. The energy equation was resolved by the solver linear Preconditioned Conjugate Gradient (PCG). The preconditioner Diagonal Incomplete Cholesky (DIC) was used. Second-order convergence schemes were used for the temporal and gradient terms. For the linear solver, the convergence criteria for each time step were an absolute residual lower than 10^{-6}, or the reduction of the relative residual by three orders of magnitude. The OF version used was 4.1.a (58). Simulations in OF were performed in parallel distributed computing using eight cores (E5-1660-v3, 26GB-RAM DDR3, 160GBHD, Infiniband QDR4 Gbps).

2.3.1 – Reproduction study

To assure the correctness of the later simulations, since it is not possible to validate the simulations and that the simplified analytical solutions are corrected by numerical simulation results (16), it was decided to perform a reproduction study of Acar and Zabunoğlu (28) in ANSYS and OF codes. Acar and Zabunoğlu conducted their study by comparing the disposal area required by the SNF and HLW from the once-through and the standard closed nuclear fuel cycles. For the closed cycle, they simulated, among others, the disposal of a MOX SNF with a burnup of 50,000 MWd/tHM, similar

to the burnup of the reprocessed SFs studied for the Angra 2 NPP, 48,000 MWd/tHM (56).

However, the benchmark does not supply details of grid refinement adopted, nor the temporal discretization. Thus, for the reproduction study and later simulations, the temporal discretization shown in Table 7 was adopted. Numerous studies adopt different meshing strategies depending on the computational code and level of detail. However, it is known that some levels of grid refinement do not affect the results of the simulations significantly, depending on the type of simulation (16). Considering that the mesh adopted by the benchmark has not been informed, the meshing adopted for the reproduction study is significantly different. The meshes considered for each case are presented in Table 8. To quantify the effect of meshing resolution on the results, a grid convergence study was conducted following the recommendations of Roache's method (59, 60).

Table 8 **–** Number of elements in the reproduction study.

Case	ANSYS	OpenFOAM
SUOX 33	10,661	176,831
SUOX 40	12,848	180,037
SUOX 50	13,249	186,449
SMOX 33	11,250	146,293
SMOX 40	7,929	169,246
SMOX 50	7,725	172,685

2.3.1.1 – The Grid Convergence study

Roache proposed a method aiming to unify the reporting of grid refinement studies, named as Grid Convergence Index (GCI) (59, 60). The GCI is based on the generalized Richardson Extrapolation (RE) with the inclusion of a Factor of Safety, ***Fs***. The generalized RE for a ***p-th*** method with a grid ratio, ***r,*** is as follows:

$$f_{exact} \cong f_1 + \frac{f_1 - f_2}{r_{12}^p - 1} \tag{2a}$$

$$r = \frac{\text{number of elements of the coarse grid}}{\text{number of elements of the fine grid}} \tag{2b}$$

Where f_{exact} is a higher-order estimate of the quantity of interest at zero grid spacing limit; f_1 is the value of the quantity for the finest grid, f_2 is the coarser grid; r is the grid refinement ratio between two successive grids, and p is the theoretical order of convergence.

The estimated fractional error E_1 and the relative error ε for the finer grid solution is defined as follows:

$$E_1[fine\ grid] \cong \frac{\varepsilon}{r_{12}^p - 1} \tag{3}$$

$$\varepsilon = \frac{f_2 - f_1}{f_1} \tag{3a}$$

The estimated dimensional error can be expressed by the dimensional form, ε_d:

$$\varepsilon_d = f_2 - f_1 \tag{3b}$$

The actual fractional error, A_1, of the finer grid is given by:

$$A_1[fine\ grid] \cong \frac{f_1 - f_{exact}}{f_{exact}} \tag{4}$$

The observed order of convergence p_{obs} is obtained after the solution of the following equation for p:

$$\frac{\varepsilon_{23}}{r_{23}^p - 1} = r_{12}^p \left(\frac{\varepsilon_{12}}{r_{12}^p - 1} \right) \tag{5}$$

For a not constant r, Eq. 5 can be solved by usual solution techniques such as direct substitution refinement. The iteration equations are, with ρ being the earlier iteration for p, ω being the relaxation factor, and β being the function to be solved for p on a direct substitution refinement method,

$$p_{obs} = \omega\rho + (1 - \omega)\frac{\ln \beta}{\ln r_{12}} \tag{6a}$$

$$\beta = \frac{(r_{12}^{\rho} - 1)\varepsilon_{23}}{(r_{23}^{\rho} - 1)\varepsilon_{23}} \tag{6b}$$

The CGI for the finer grid is expressed as:

$$GCI\ [fine\ grid] = F_s\ \frac{|\varepsilon|}{r_{12}^{p} - 1} \tag{7}$$

The asymptotic range is achieved when,

$$GCI_{23} = r_{12}^{p}\ GCI_{12} \tag{8}$$

The apparent convergence condition is given by the convergence ratio[19], ***R*** (60)

$$R = \frac{f_1 - f_2}{f_2 - f_3} \tag{9}$$

(i) Monotone convergence for $0 < \mathrm{R} < 1$

(ii) Oscillatory convergence for $\mathrm{R} < 0$ and $|\mathrm{R}| < 1$

(iii) Monotone divergence for $\mathrm{R} > 1$

(iv) Oscillatory divergence for $\mathrm{R} < 0$ and $|\mathrm{R}| > 1$

For the grid convergence analysis were considered four structured and seven unstructured grids: The total number of elements is presented in Table 9 for each grid.

[19] As Coleman *et al* (63) remarks "If there is the possibility of oscillatory behavior of the value of a computed variable as grid size is refined in a simulation, then interpretation of the results of grid convergence studies seems impossible to achieve unambiguously". Since that for an oscillatory convergence, depending on the relationship between the chosen grid size and the (unknown) period(s) of oscillation(s), it is possible to observe a converging, oscillating or diverging behavior of the results (63).

Table 9 – Number of elements for the grid convergence study.

Case	Number of Elements
Structured 1	469,075
Structured 2	275,075
Structured 3	178,075
Structured 4	129,575
Unstructured 1	920,535
Unstructured 2	435,902
Unstructured 3	310,706
Unstructured 4	196,813
Unstructured 5	132,257
Unstructured 6	58,121
Unstructured 7	28,560

2.3.2 – Brazilian Disposal Parameters

Given the low thermal conductivity of granitic rocks, the temperature of the host rock in the depth of the DGR has a major influence on the density of disposal of the SNF. It is therefore necessary to simulate the disposal of the SNF using data from the Brazilian geothermal gradient.

The first step is to calculate, using geostatistical methods, the temperature of the rocks in the depth of the DGR, 500m. The details of these calculations can be found in Appendix A. Then, keeping all other input data constant, the minimum distance between each canister of SUOX 48 and SMOX was calculated for nineteen locations in Brazil. The temperature at a depth of 500m varies between 27.9ºC (Juiz de Fora, Minas Gerais) to 46.37ºC (Quixadá, Ceará). Table 10 shows the locations, the geothermal gradient and local surface temperature, and the temperature at a depth of 500m. Then, the spacing between canisters was adjusted such that the maximum temperature on the canister surface does not exceed 80ºC.

Table 10 – Temperature at 500m depth for selected locations in Brazil. Adapted from (64, 65).

Location	Geothermal Gradient (ºC/km)	Mean Surface Temperature - 2020 (ºC)	Temperature at 500m (ºC)
Ponta Grossa - PR	19.94	18.13	27.90
Juiz de Fora - MG	16.68	20.94	28.93
Passo Fundo - RS	23.48	18.27	30.03
Ijuí - RS	22.47	19.93	31.03
Irecê - BA	18.82	23.95	31.94
Passos - MG	23.06	21.73	33.02
Governador Valadares - MG	22.33	23.22	34.04
Florianópolis - SC	26.01	21.89	35.01
Maringá - PR	25.90	23.04	35.99
Sinop - MT	23.73	25.62	36.99
Redenção - PA	23.32	26.95	37.99
Bragança - PA	24.36	26.85	38.98
Aracaju - SE	26.92	26.63	40.04
Santa Inês - MA	27.50	27.24	40.79
Caicó - RN	28.15	27.78	42.04
Mossoró - RN	30.51	27.56	42.92
Pau dos Ferros - RN	31.96	27.52	44.03
Crateús - CE	35.25	26.98	45.36
Quixadá - CE	38.25	26.79	46.37

2.4 – RESULTS AND DISCUSSION

2.4.1 – Reproduction of the Benchmark

2.4.1.1 – SUOX

The comparison of the results obtained with ANSYS and OpenFOAM© for the SUOX cases shows good agreement between both codes and between the codes and the benchmark. Figure 9 shows the temperatures at the canister surface and the bentonite-rock interface, for the period analyzed (20 years after the disposal). The differences for the canister surface temperature are below 2°C in all cases, except for the SUOX 50 GWd / tHM case, for which the simulations predicted temperatures below 5°C. For the lowest burnup, 33 GWd/tHM, the maximum temperature occurred at the time of 12 years after the disposal in all simulations. For the intermediate burnup, 40 GWd/tHM, the maximum temperature in simulations occurred at the time of 11 years after the disposal, while in the benchmark it occurred at the time of 10 years. For the 50

GWd/tHM burnup, the canister surface temperature reached its maximum value after 9 years after the disposal, while in the benchmark the maximum occurred after 6 years.

Figure 9 – Maximum temperature at the canister surface and at bentonite- rock interface for the SUOX cases as a function of time.

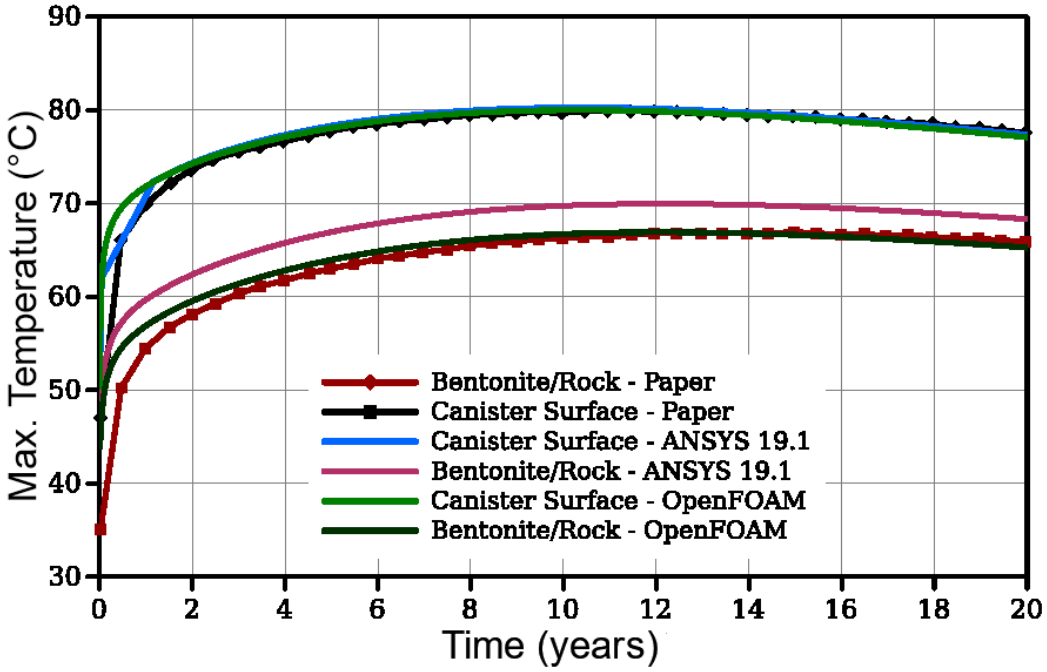

(a) SUOX 33 GWd/tHM.

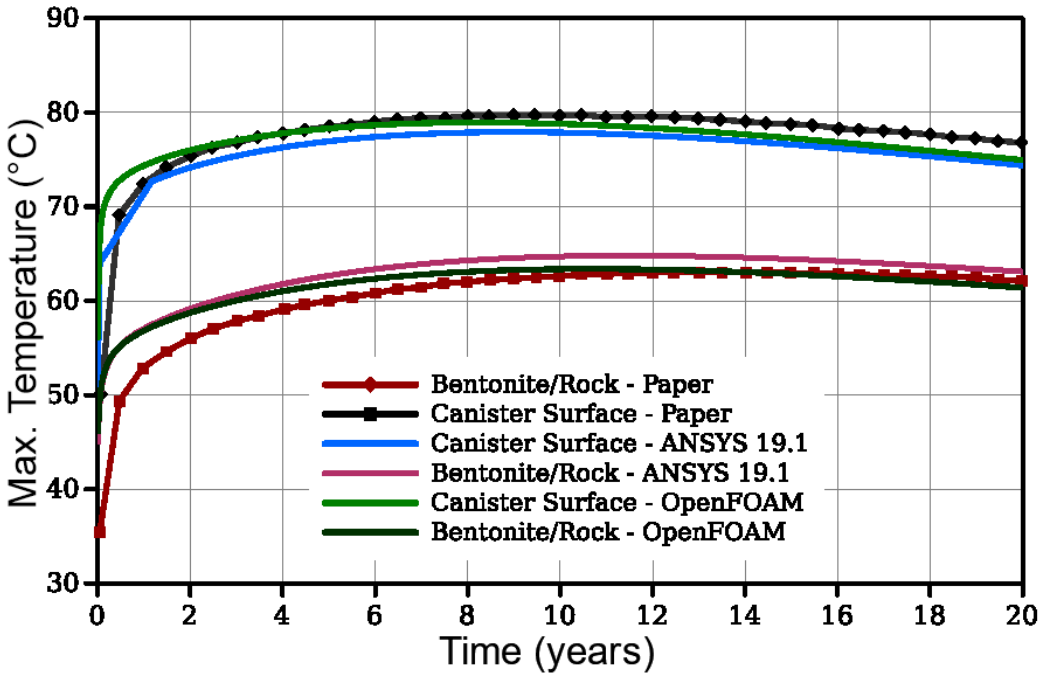

(b) SUOX 40 GWd/tHM.

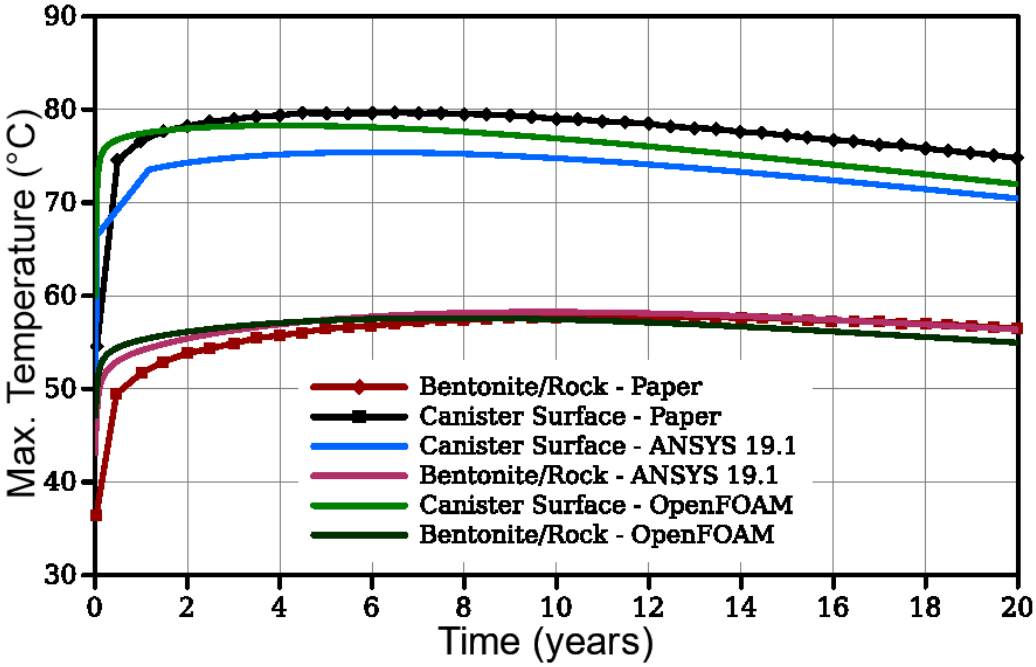

(c) SUOX 50 GWd/tHM.

2.4.1.2 – SMOX

The temperatures at the canister surface and the bentonite-rock interface during the period analyzed of 20 years after disposition, for the SMOX cases are presented in Figure 10. As expected, the canister temperature increased rapidly in the first days after the disposal, going towards the saturation regime slowly. The same temperature profile can be seen in (16). For the lowest burnup, 33 GWd/tHM, the maximum temperature occurred at the time of 16 years after the disposal in all simulations. For the intermediate burnup, 40 GWd/tHM, the temperature also reached its maximum value at the time of 15 years after the disposal in all studies. For the 50 GWd/tHM burnup, the maximum temperature occurred at the time of 11 years after the disposal, which is 3 years lower than the time documented in the work considered as a benchmark.

Figure 10 – Maximum temperature at the canister surface and at bentonite- rock interface for the SMOX cases as a function of time.

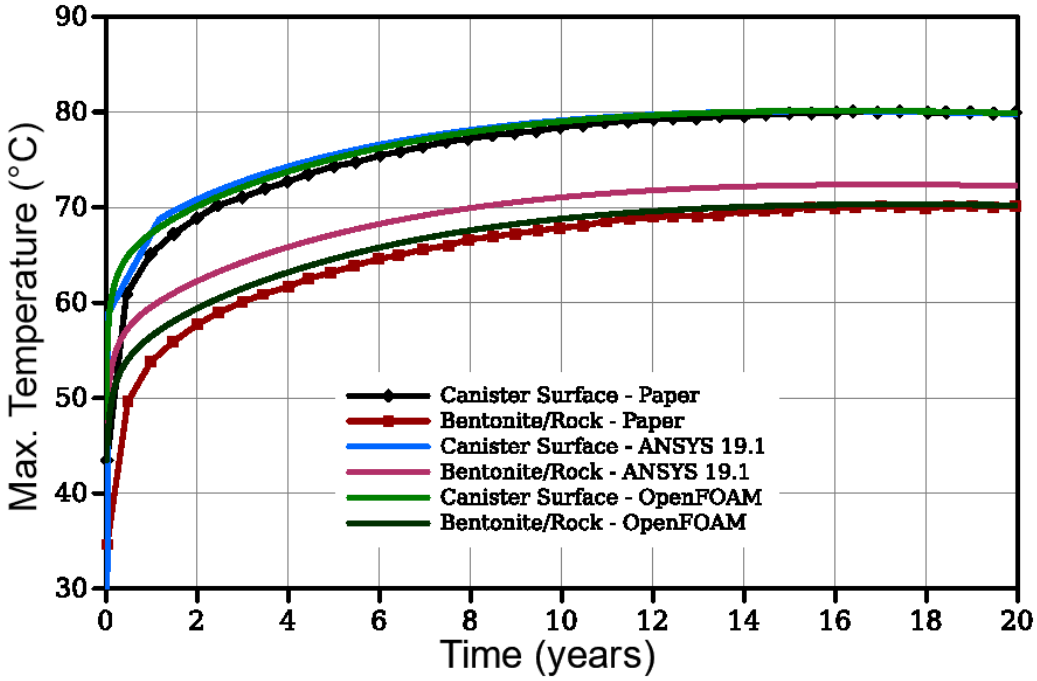

(a) SMOX 33 GWd/tHM.

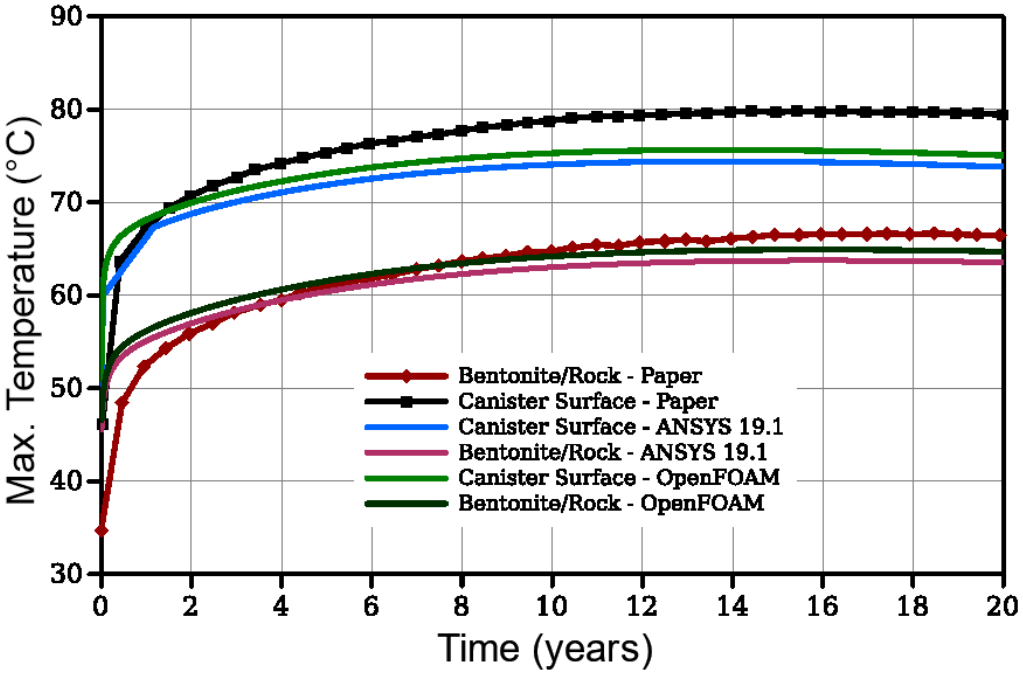

(b) SMOX 40 GWd/tHM.

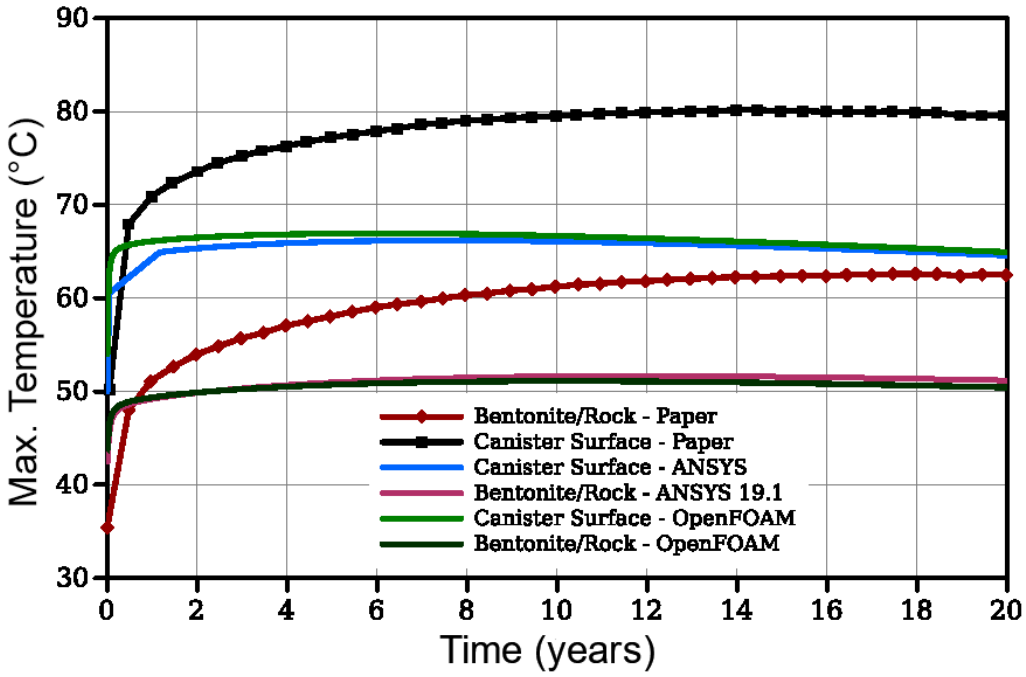

(c) SMOX 50 GWd/tHM.

Despite the behavior of the temperature curves being the same as the benchmark, the values of the maximum temperature at the canister surface differ by more than 5°C for the SMOX 40, and more than 15°C for the SMOX 50 cases. More simulations were carried out to see if reducing the spacing between the canisters would reduce the discrepancies, the results are presented in Figure 11. Since an explanation for the discrepancy would be a spacing greater than necessary between the SMOX 40 and SMOX 50 canisters. This hypothesis was raised considering that the mesh size and different time steps of the benchmark would not significantly influence the result of the simulations in two distinct codes. And the simulations of all the other cases demonstrate that this statement is true. Assuming, also, that the values of the indices for the calculation of the heat of decay are true since it would not be possible, for this work, to perform a simulation of the nuclear fuel life cycle, the only remaining variable that would explain the discrepancy is the distance between the canisters. As expected, after the reduction of the canister spacing from 4.8 m to 4.0 m for the SMOX 40 case, and from 13 m to 5.8 m for the SMOX 50 case, the discrepancies between the simulations and the benchmark were significantly reduced.

Figure 11 – SMOX canister temperature with adjusted spacing.

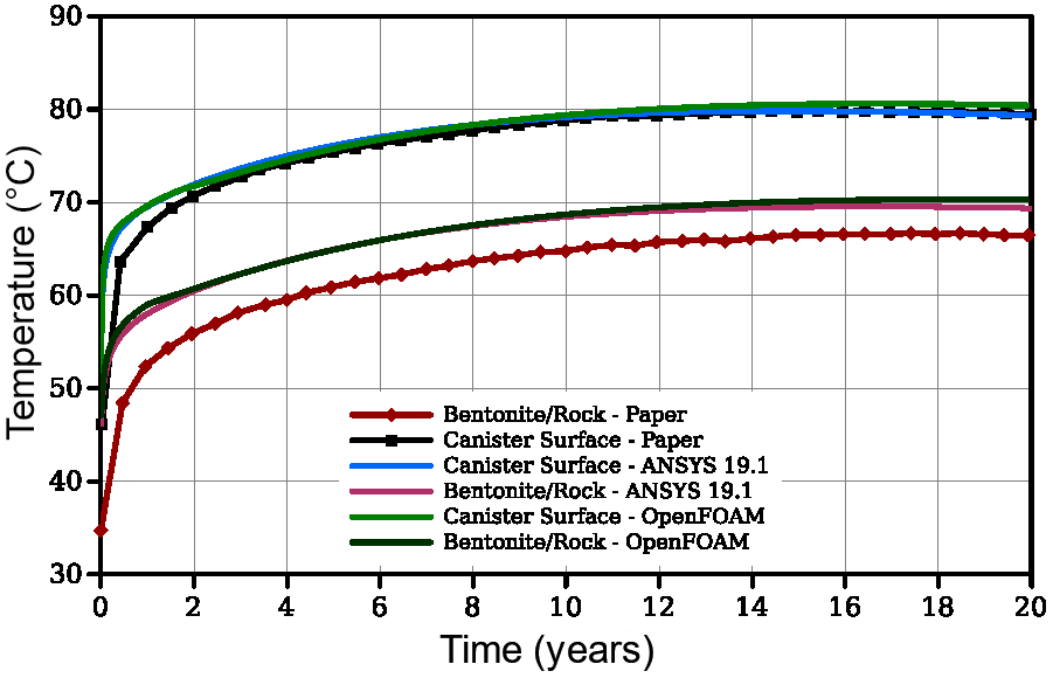

(a) SMOX 40 GWd/tHM – adjusted spacing.

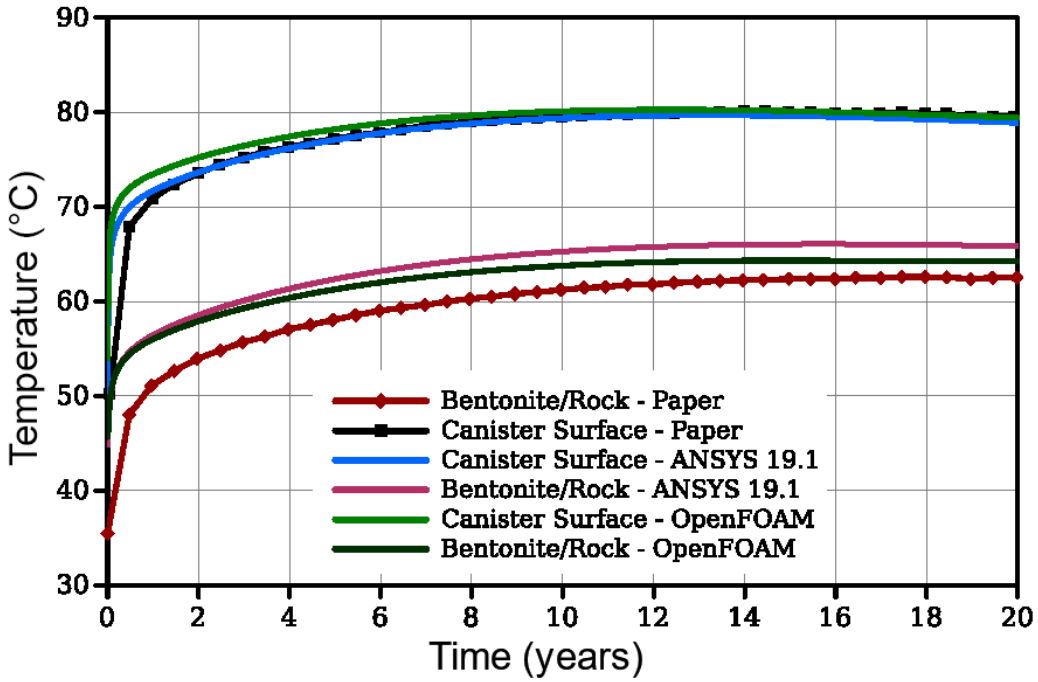

(c) SMOX 50 GWd/tHM – adjusted spacing.

2.4.1.3 – Temperature distribution around the canister

To compare the temperature distribution between ANSYS and OF at the specific time of 20 years after the disposition, it was plotted graphs along three axes by sectioning

the domain. In the X coordinate, all curves extend up to 10 m from the canister center. In the Y-axis, the domain extends from the canister center to a distance equal to half of the distance between two successive canisters. In the vertical axis Z, the temperature from the upper surface of the canister to the lower surface of the tunnel (backfill) was reported. Figure 12 shows the temperature distributions along each axis for SUOX and SMOX fuels. From the analysis of the graphs, a good agreement between ANSYS and OF can be seen for all the positions and burnups.

Figure 12 – Temperature distribution along the three axes for SUOX and SMOX cases.

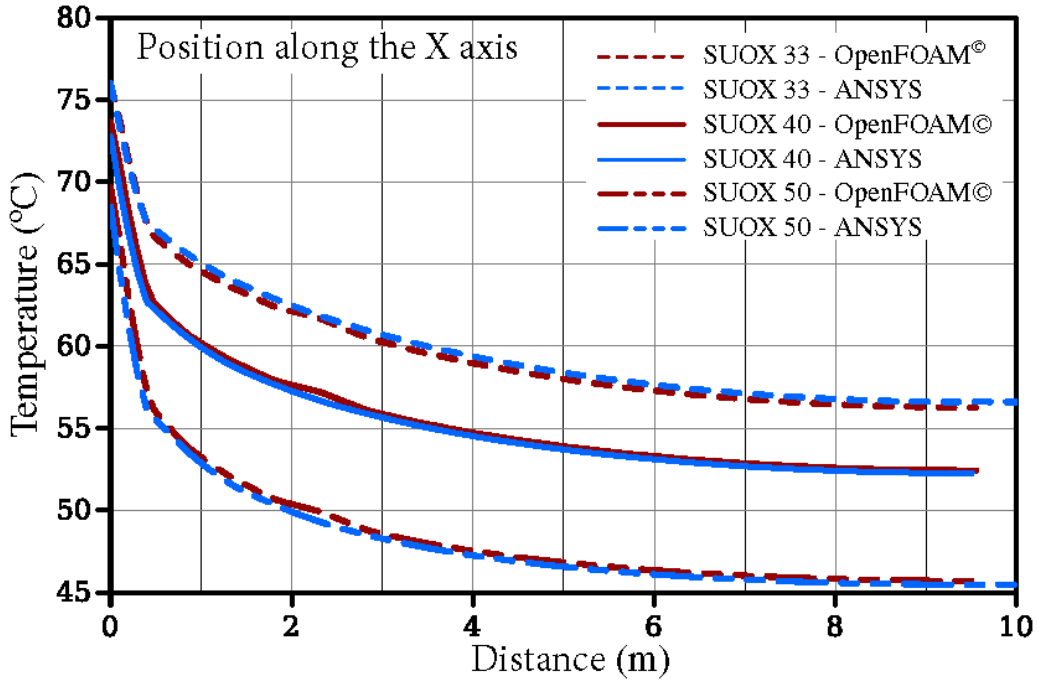

(a) SUOX – X Axis

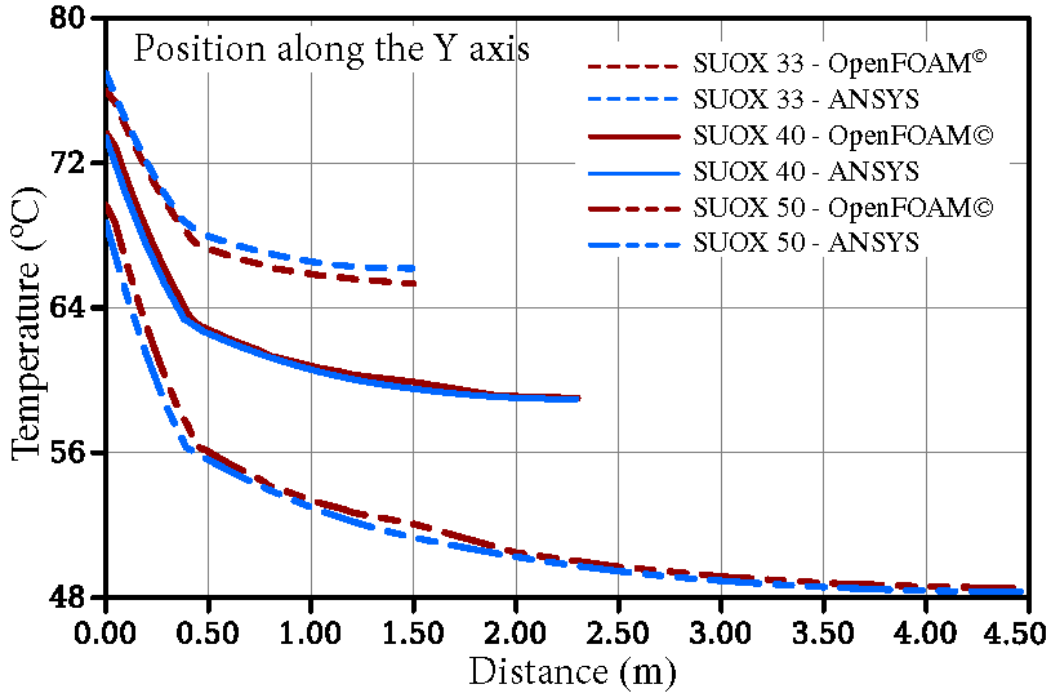

(b) SUOX – Y-Axis

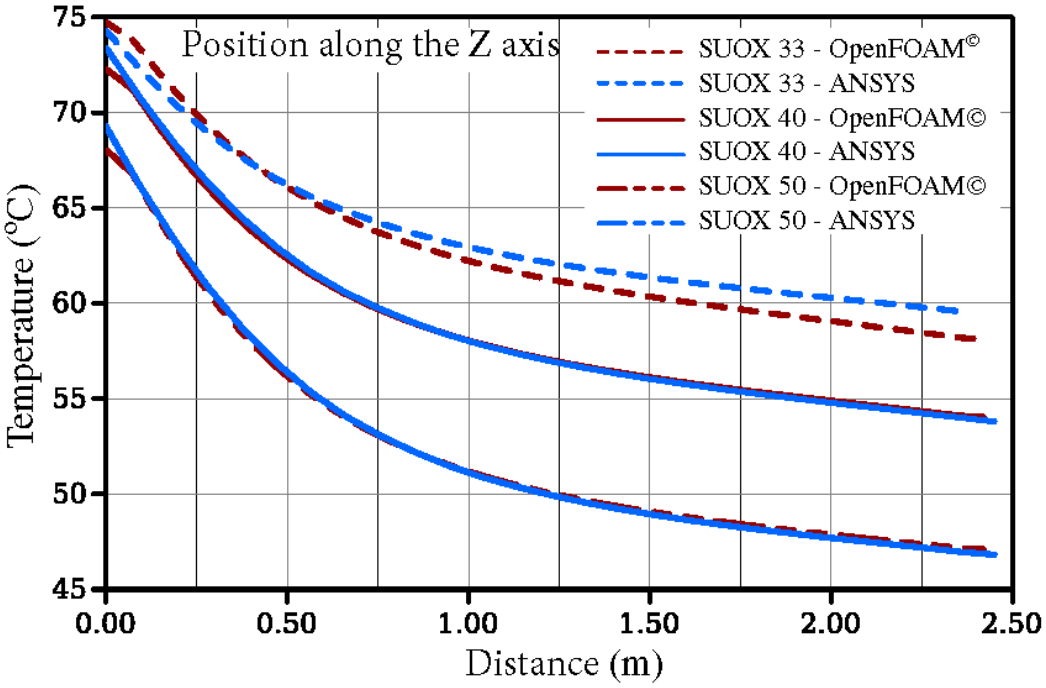

(c) SUOX – Z-Axis

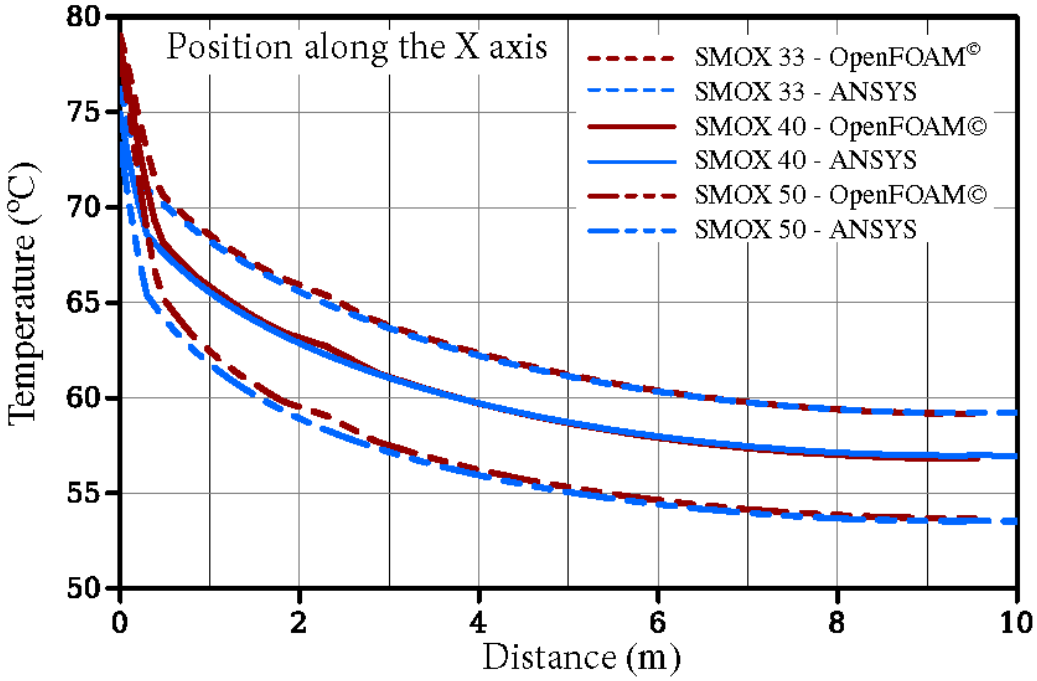

(d) SMOX – X Axis

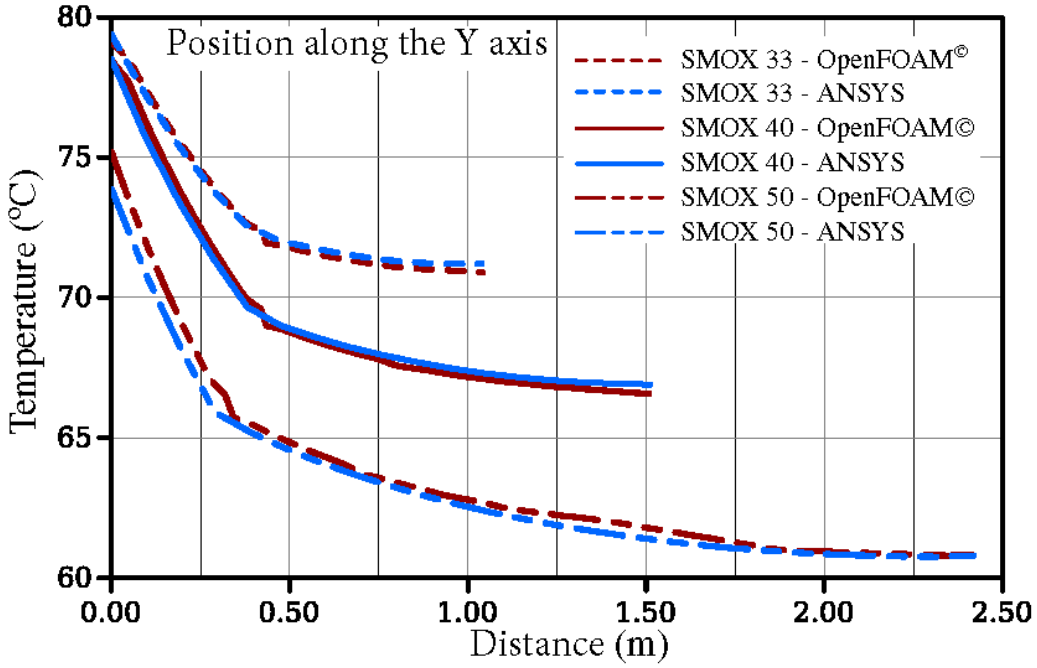

(e) SMOX – Y-Axis

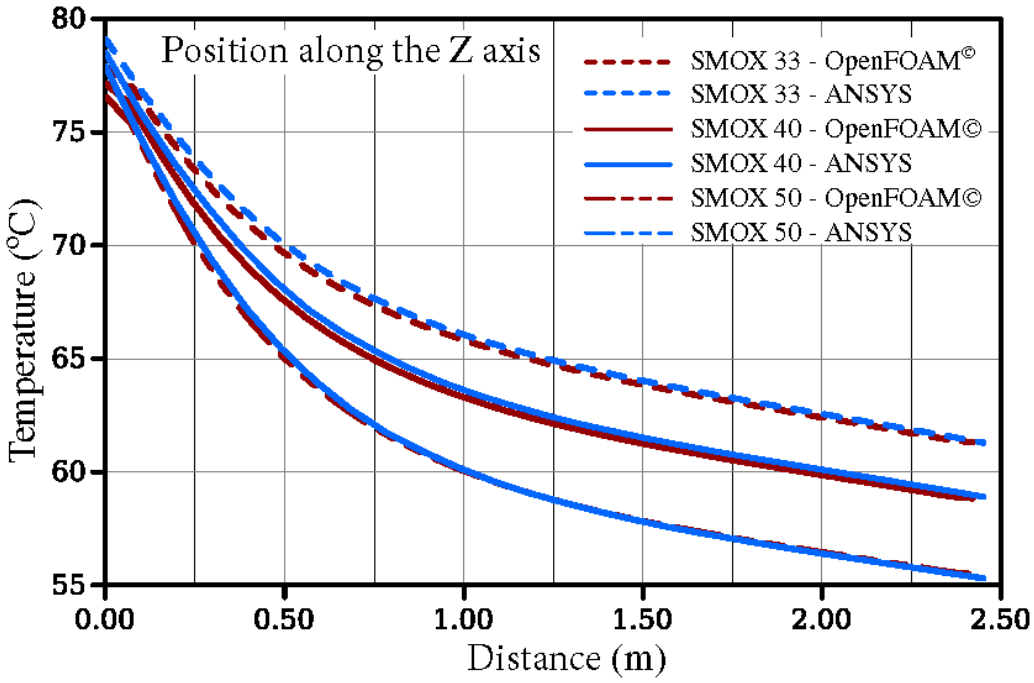

(f) SMOX – Z-Axis

Figure 13-a shows part of the geometry of the SOUX 33 case. In Figure 13-b and c, the temperature field is shown for the simulations of the same case performed with ANSYS 19.1 and OpenFOAM©, respectively. As observed, the field obtained with ANSYS is slightly more diffusive due to the refinement of the mesh that is lower than that in OpenFOAM©. This is clear for the bentonite region and for regions where temperature gradients are maximum. Figure 13-d shows the 3-D temperature field for the SUOX 33 case.

Figure 13 – Temperature distribution around the fuel (SUOX 33 GWd / tHM): a) Mesh regions, b) ANSYS 19.1 simulation, c) OpenFOAM© simulation, d) Reconstruction of the case.

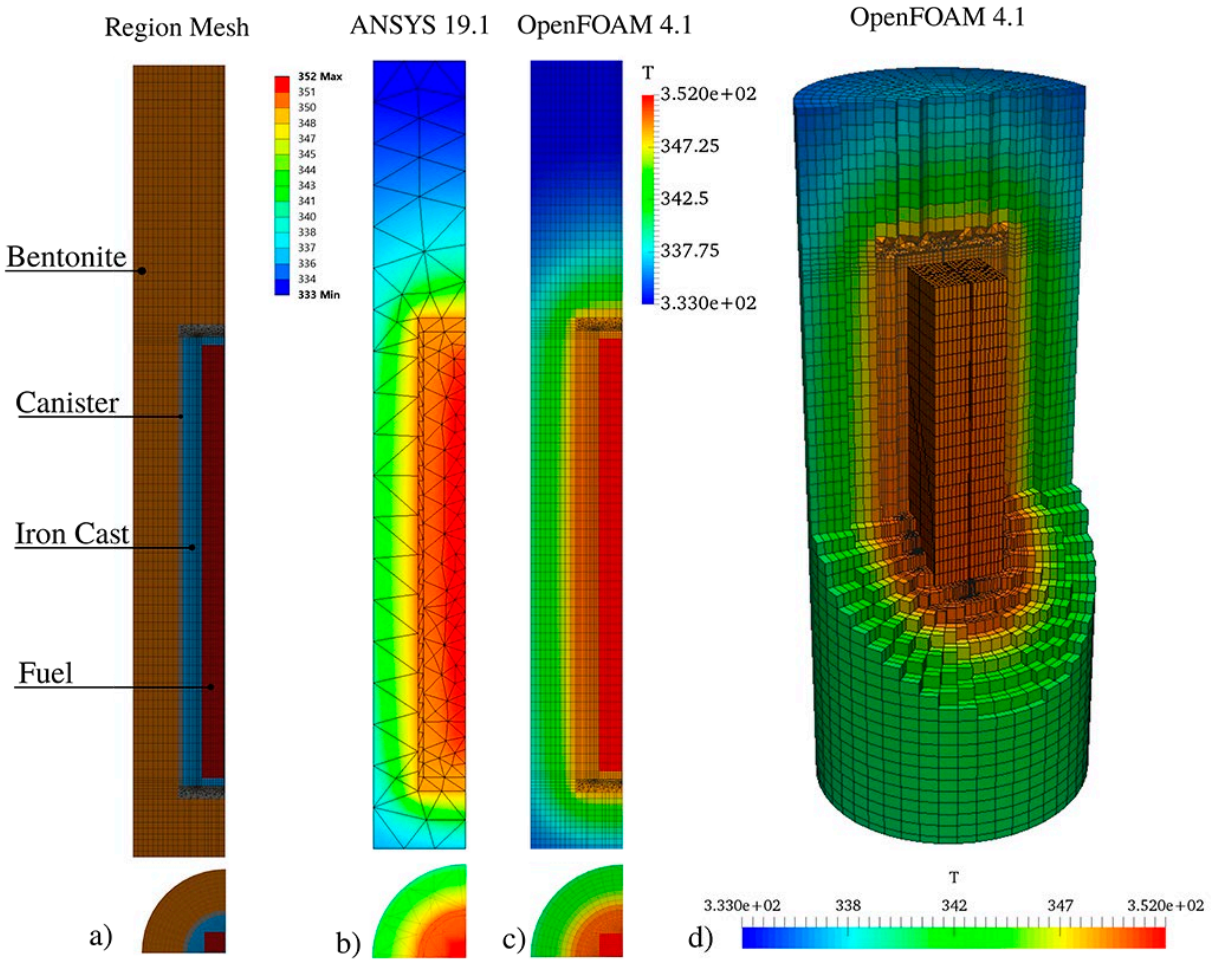

2.4.1.4 – Disposal area required

As seen in Table 11, the increase of fuel burnup enhances the disposal area required for the Spent Uranium Oxide (SUOX) and SMOX fuel. For the 50,000 MWd/tHM, the disposal area needed calculated in this work is significantly lower than those found by Acar and Zabunoğlu (28). The disposal area per canister or ton of waste is calculated by:

$$Disposal\ area\ per\ canister = Canister\ spacing\ \times\ tunnel\ spacing \tag{10a}$$

$$Disposal\ area\ per\ ton\ of\ waste = \frac{Disposal\ area\ per\ canister}{ton\ of\ waste\ /_{Canister}} \tag{10b}$$

Each SNF assembly holds, approximately, 0.48 t of heavy metal, regardless of whether it is SUOX, SMOX, or STRU (28). Thus, a SUOX canister holds approximately 1.92 t of waste, while SMOX or STRU canisters hold 0.48 t of waste.

Table 11 – Disposal area per canister and ton of waste for a generic DGR. Adapted from (28).

SNF	Burnup (GWd/tHM)	Canister spacing (m)	Disposal area per ton of waste (m^2/t)	Adjusted Canister Spacing (m)	
				Canister Spacing (m)	Disposal area per ton of waste (m^2/t)
SUOX	33.00	3.90	80.73	-	
	40.00	5.54	114.68		
	50.00	10.00	206.99		
SMOX	33.00	3.00	248.39		
	40.00	4.80	397.43	4.00	331.19
	50.00	13.00	1,076.36	5.80	480.22

2.4.1.5 – Grid Convergence analysis

The grid convergence test was based on the results from transient-thermal simulation for the SMOX 50 case (with the canister spacing adjusted to 5.8m) in ANSYS. Three consecutive grids were created to estimate the value of the maximum temperature at the canister surface, as well as to estimate the magnitude of the discretization error. Table 12 shows the grid details and the maximum temperature at the canister surface computed from the solutions.

Table 12 **–** Grid details and the maximum temperature at the canister surface.

Grid	Normalized refinement ratio (r)*	Maximum Temperature at the Canister Surface (°C)
1	1	79.788
2	1.374301	79.782
3	2.122902	79.767

*Grid refinement ratio normalized by the number of cells of the finest grid.

The theoretical order of convergence of p is 1.0 since thermal problems are treated as a first-order system by ANSYS (66). The p_{obs}, as calculated by Eq. 5, is 2.360241. For all later calculations, p_{obs} were considered instead of p. The estimate of the maximum temperature at the canister surface at zero grid spacing, given by Eq. 2, was f_{exact} = 79.79. Figure 14 shows the plot of the maximum temperature at the canister surface with three successive grid spacings and f_{exact}. As the grid spacing is reduced the temperature approaches towards an asymptotic zero-grid spacing value.

Figure 14 – The maximum temperature at the canister surface with different grid spacings.

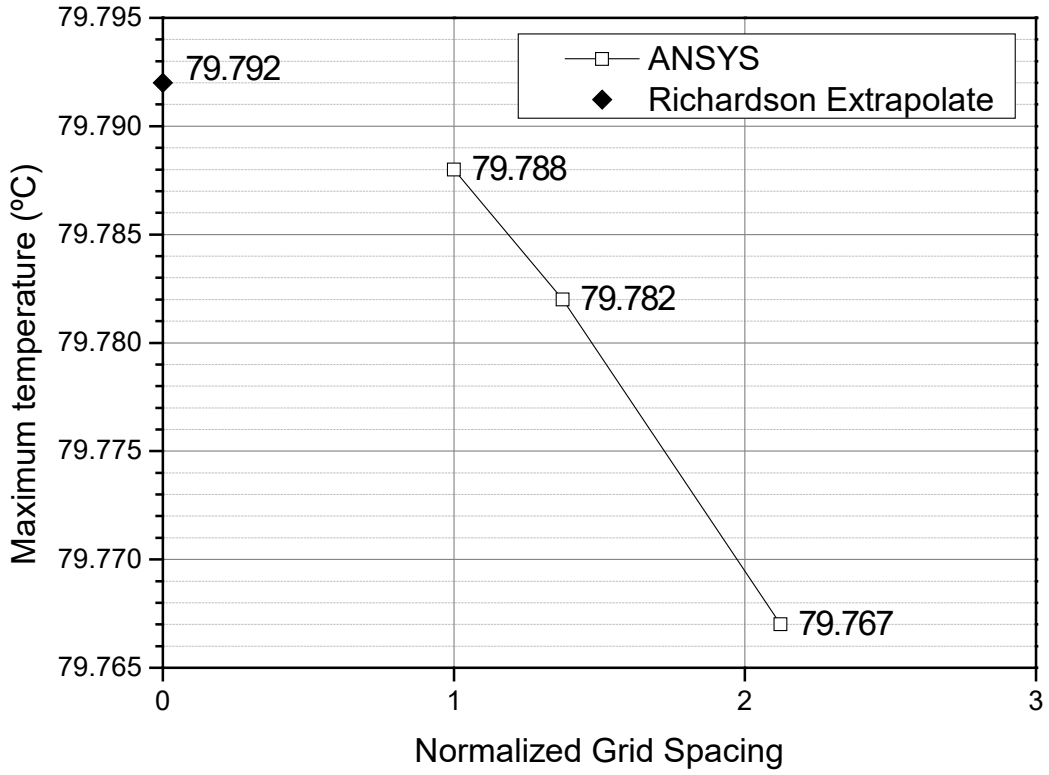

The computation of the GCI was very conservative because of the use of p_{obs}, instead of p. Since the value of p_{obs} >> p, an F_s of 3 was used. The GCI for the pairs of solutions is presented in Table 13 along with ε, ε_d, E, and the A for each solution. The first pair is composed of grids 1 and 2, while the second pair is composed of grids 2 and 3.

Table 13 – GCI and error estimates.

Solution Pairs	*GCI*	*ε*	ε_d	*E*
1,2	0.0346%	0.0075%	-0.01	0.0115%
2,3	0.0572%	0.0188%	-0.02	0.0191%
Solution		***A***		
1		-0.0115%		
2		-0.0191%		
3		-0.0379%		

From the values of the GCI_{12} and GCI_{23}, and Eq. 8 we can verify that the asymptotic range was achieved. Eq. 9 yields R = 0.4, hence the results of the grid refinement show monotone convergence. Further mesh studies were conducted to find if this problem was grid-independent. We simulated the problem with an added coarser structured grid and seven unstructured grids. The results of all simulations along with the actual fractional error, A, are presented in Figure 15. For all cases, the actual fractional error is lower than 0.1%, even when cases had less than thirty thousand elements.

Figure 15 **–** The maximum temperature at the canister surface and actual fractional errors.

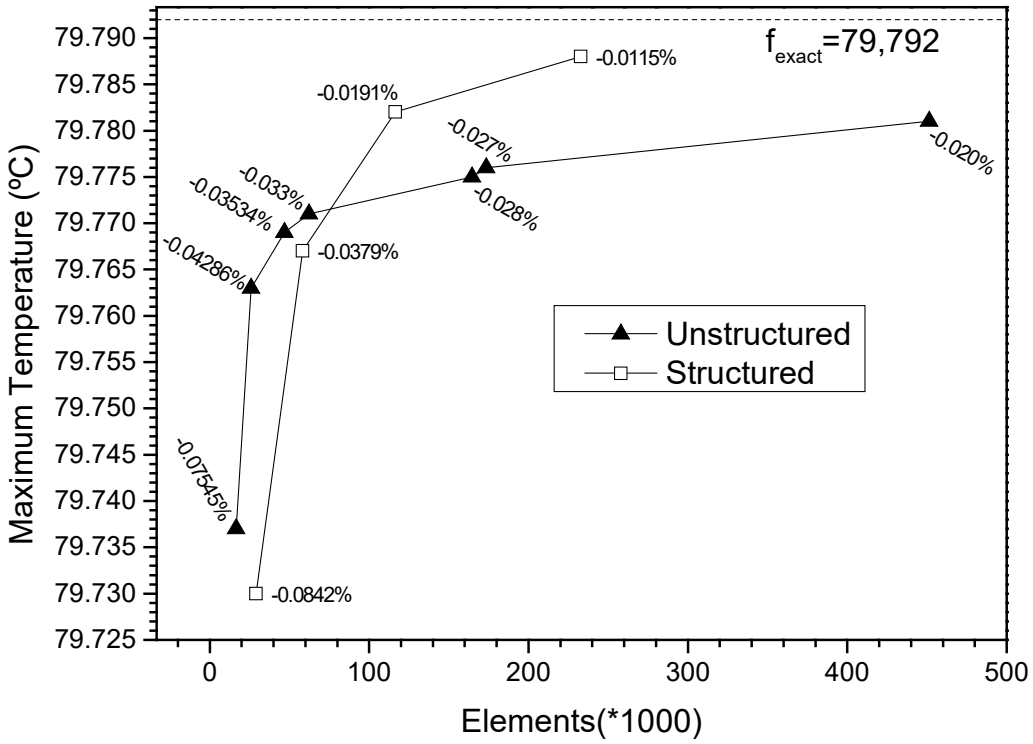

The structured grid, as expected, presents a faster rate of convergence when compared with the unstructured grid. An illustration of both grids is presented in Figure 16.

Figure 16 **–** The coarsest meshes: (a) structured and (b) unstructured.

(a)

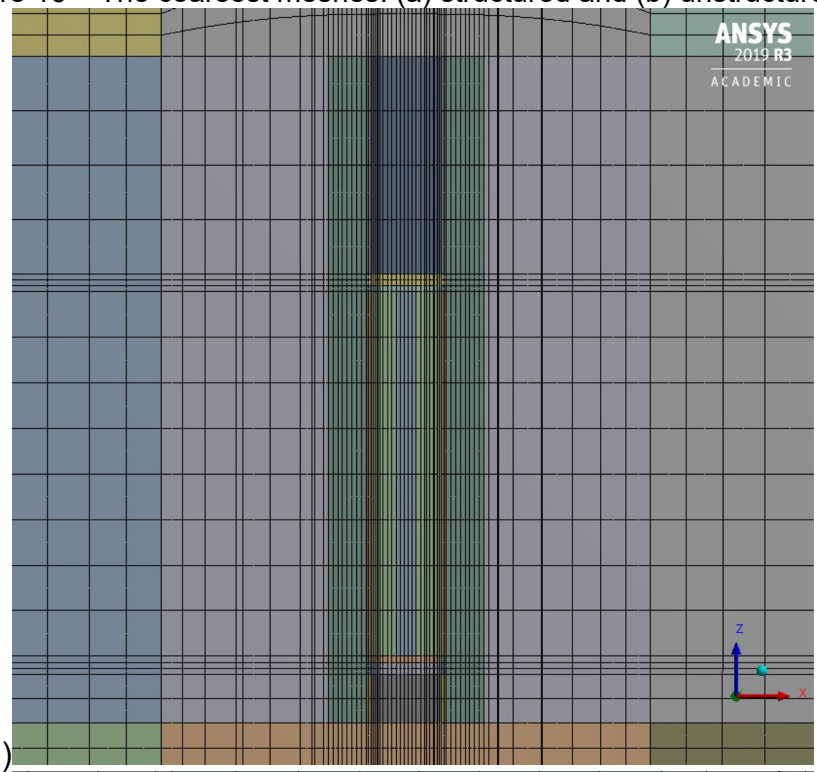

(b)

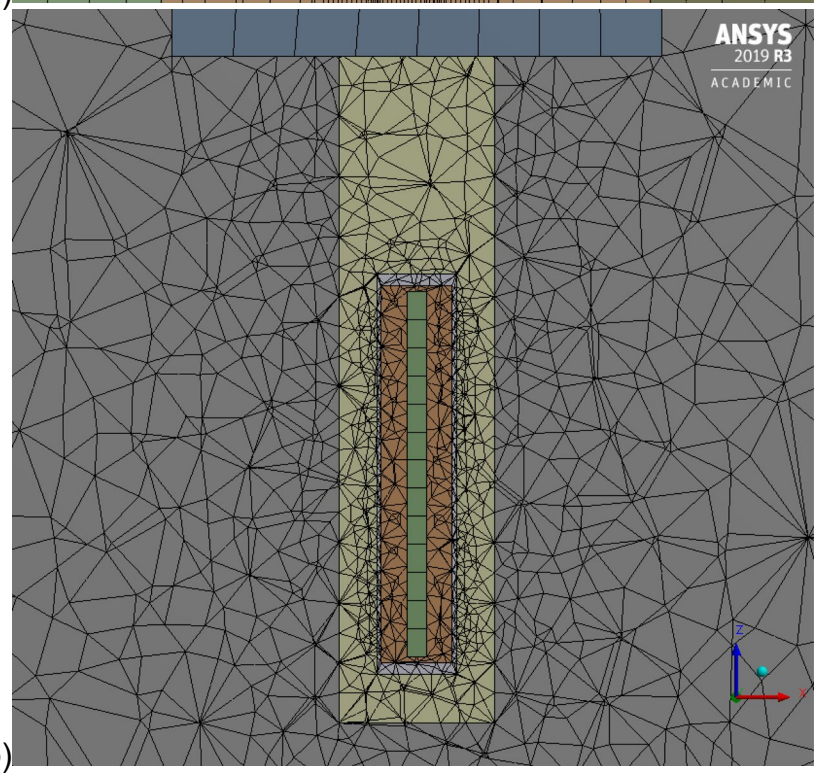

It was also investigated the temperature distribution along each axis for all cases, as presented in Figure 17. In all cases, except the Unstructured 1 grid, the temperature gradient along the axis was almost the same. In this case, the small number of elements in the SNF did not allow the correct simulation of the internal temperature distribution, although, at the interface SNF-cast iron, the temperature was correctly simulated, as shown in Figure 17(d). These results assure that the mesh type and its resolution do not affect the results significantly. Thus, the temperature at the canister surface can be considered grid-independent.

These results indicate that for simplified studies, related only to the heat propagation process by conduction, meshes with a small number of elements do not significantly affect the results. This is a key factor for further studies that require many simulations. The simulation of the coarsest unstructured mesh was completed in less than one hour, while the finer structured mesh required 3 days to complete. In these cases, where simulation speed is more important than simulation accuracy, it is advisable to use coarser meshes, as the geometry chosen at the end can be simulated later with a finer mesh if necessary.

Figure 17 – Temperature distribution on the three-axis SMOX 50 fuel: (a) along with the X-axis; (b) along the Y-axis; (c) Along the Z-axis; (d) temperature distribution between the cast iron insert and canister external surface.

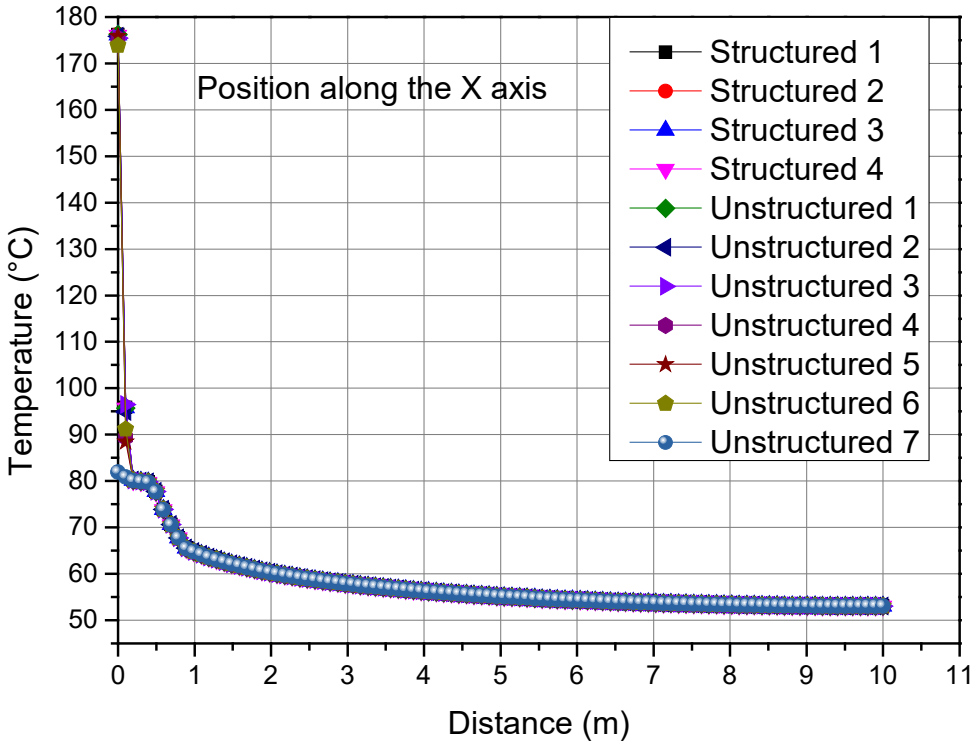

(a)

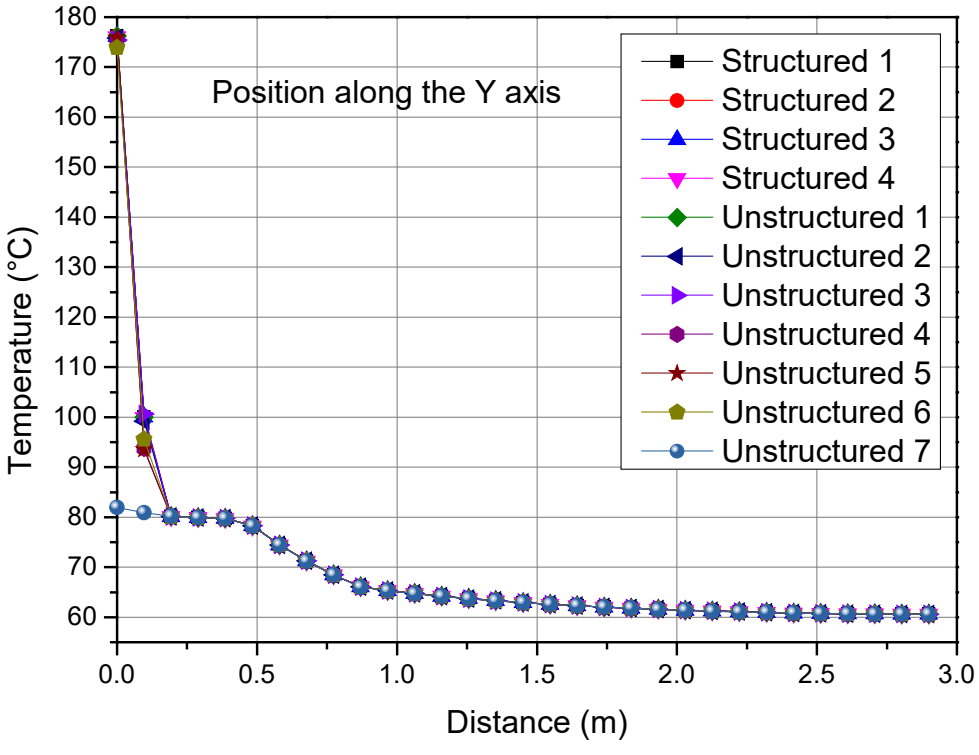

(b)

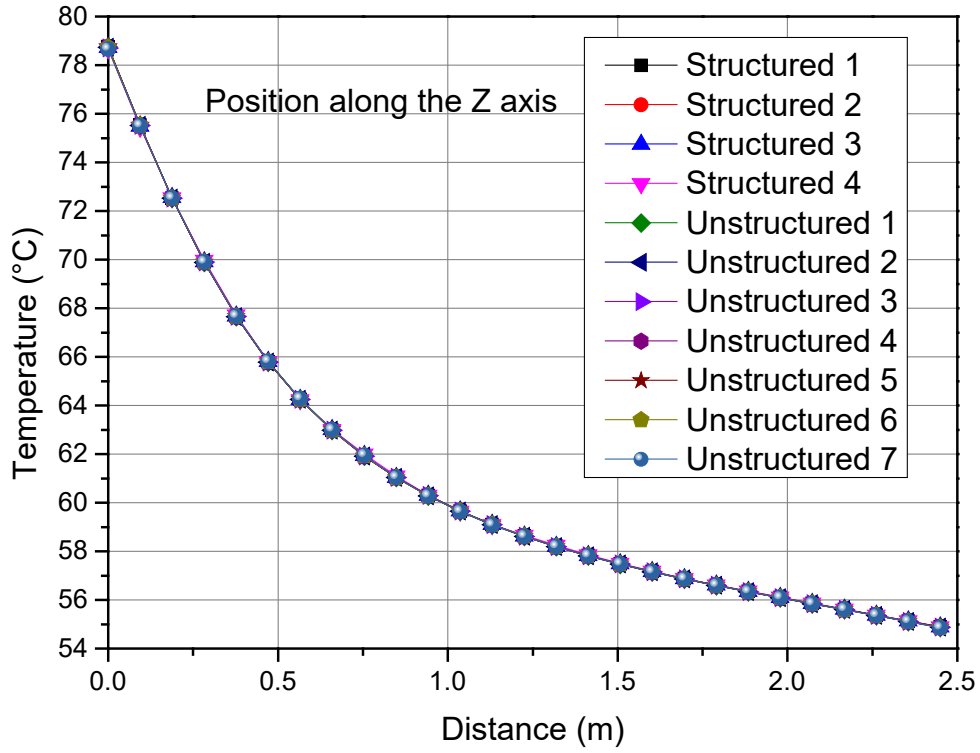

(c)

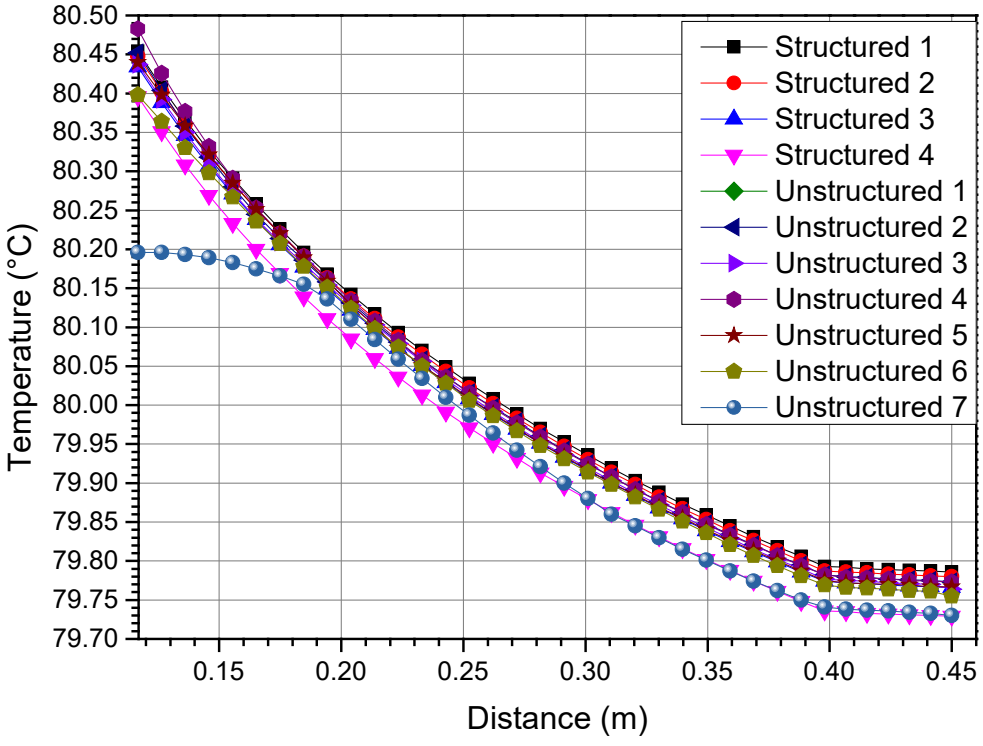

(d)

2.4.2 – Disposal of simulated ANGRA 2 SNF

Since the burnup values of the SNFs studied for ANGRA 2 are similar to those of the benchmark with a burnup of 50 GWd/tHM, the initial spacing between the canisters

was assumed to be the same: 5.0 m for the SUOX 48 case and 5.8 m for the SMOX 48 and STRU cases.

As shown in Figure 18, despite the SUOX 48 having gone through a burning cycle similar to SUOX 50, specifically the burnup value, the composition and, consequently, the decay heat is distinct. For this reason, the spacing required between the canisters of SUOX 48 is smaller. The spacing required for the SUOX 48 is 8.2 m versus 10 m for the SUOX 50. The maximum temperature in this spacing occurs approximately 12 years after disposal.

Figure 18 **–** The maximum temperature for the SUOX 48: (a) at the canister surface as a function of the spacing between canisters; (b) temperature distribution along the time at the canister surface.

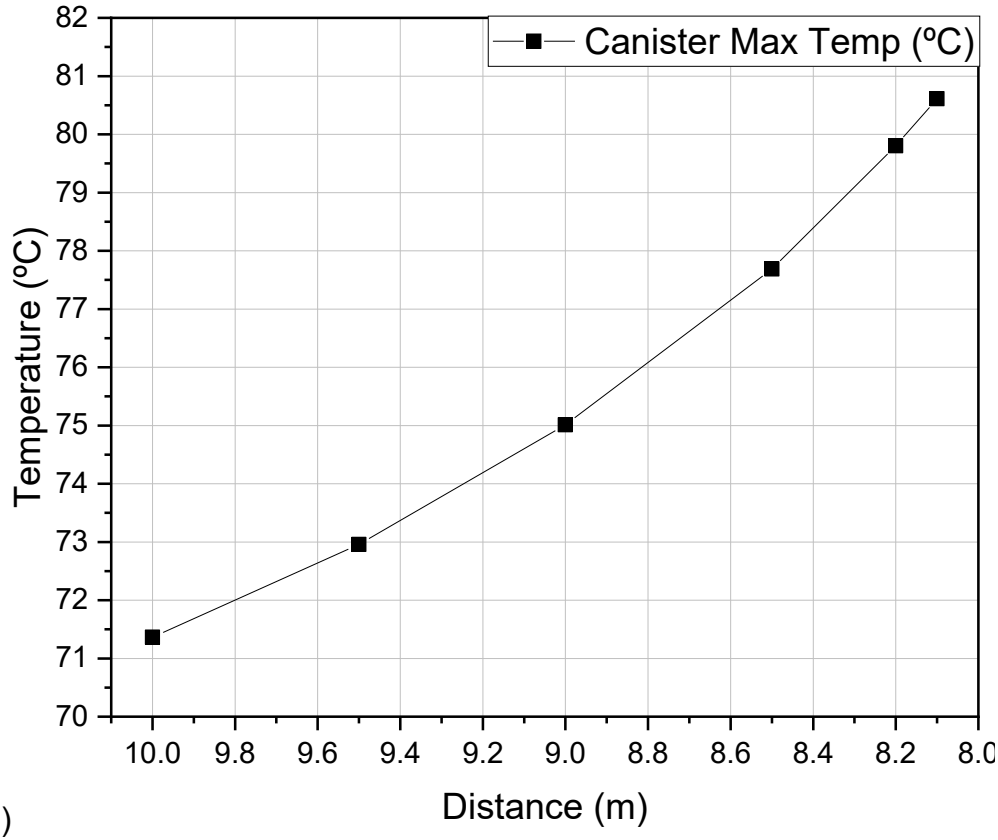

(a)

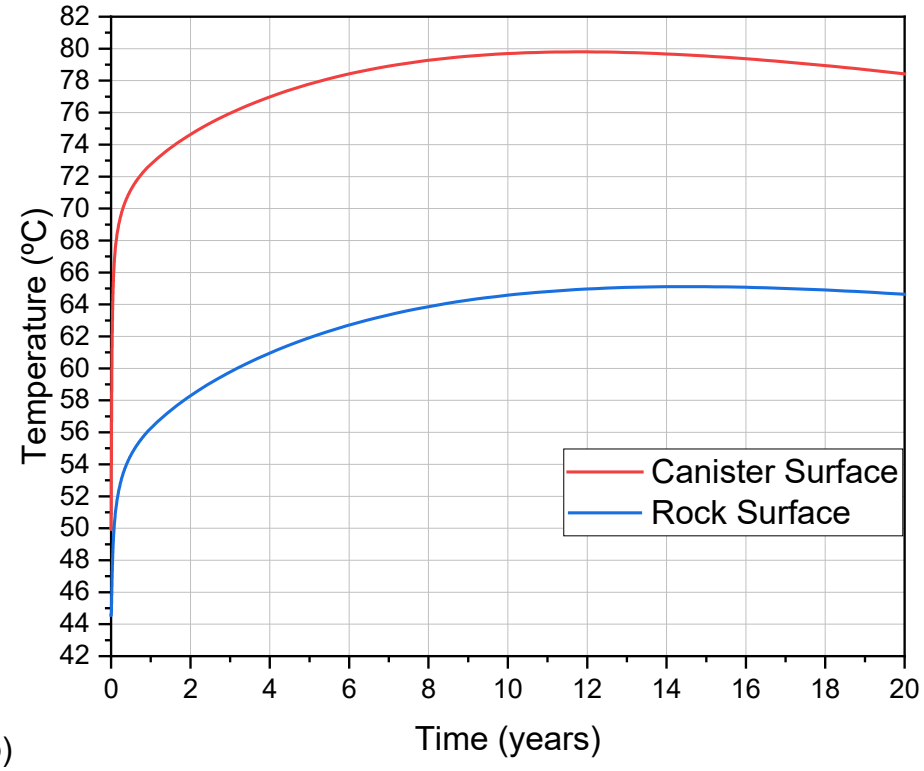

(b)

In the case of the SMOX 48, Figure 19, the decay heat released by the fuel element is greater than that of the SMOX 50. Therefore, it is necessary to increase the spacing between the canisters from 5.8 m to 6.8 m. The maximum temperature of 80°C is reached around 17 years after disposal.

Figure 19 – The maximum temperature for the SMOX 48: (a) at the canister surface as a function of the spacing between canisters; (b) temperature distribution along the time at the canister surface.

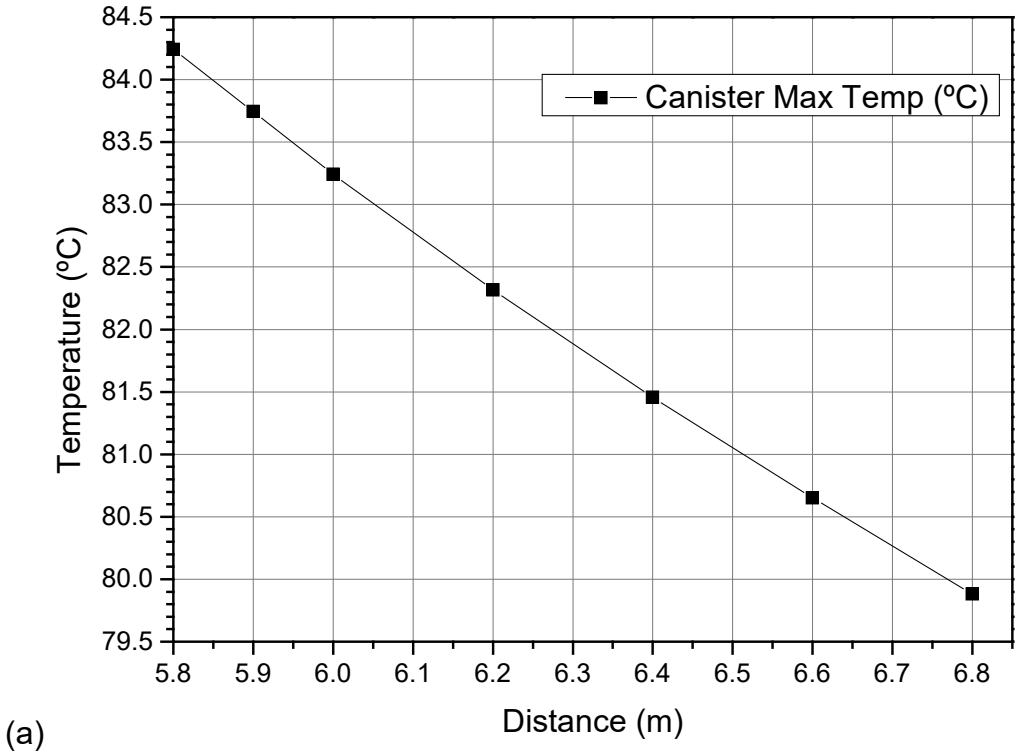

(a)

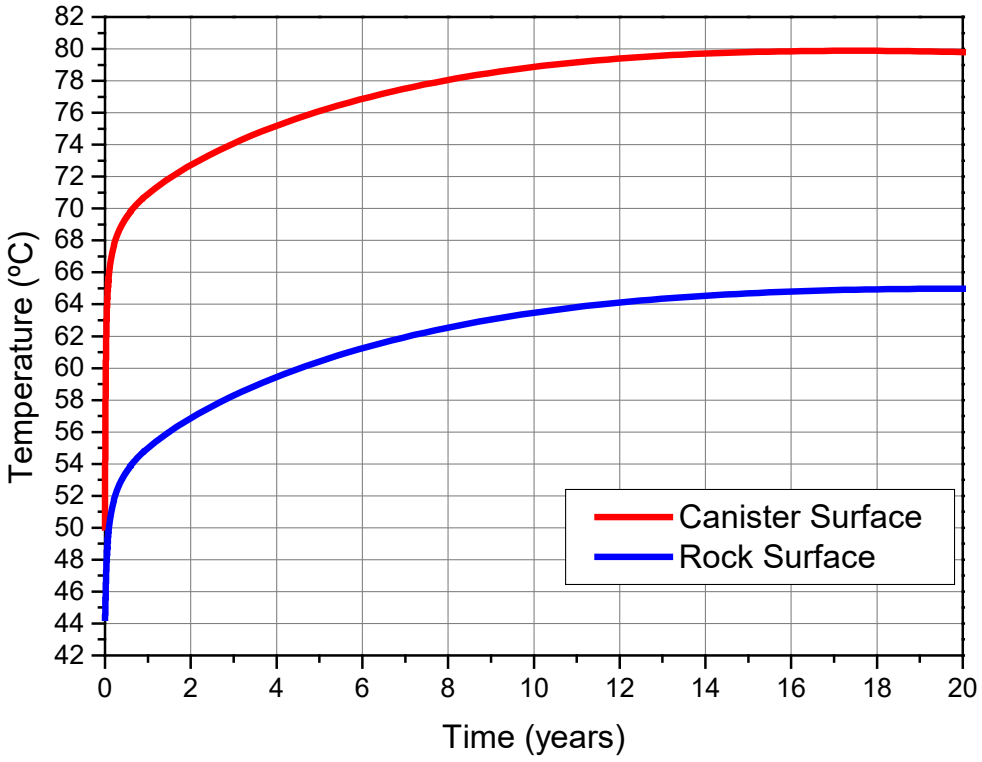

(b)

As shown in Figure 20, for the STRU case, the temperature does not drop below 80 °C, even for a spacing of 60 m. The STRU generates ten times more heat in comparison with SMOX 48. Since the thermal conductivity of the rock mass is small,

the thermal gradient in the proximity of the canister increases remarkably as the heat released spreads slowly. This result shows that the STRU must remain longer in the intermediary storage while it reaches an acceptable level of heat decay before the final disposal.

Figure 20 **–** Temperature profile for the STRU case: (a) at the canister surface as a function of canister spacing; (b) along with the X-axis; (c) along the Y-axis; (d) Along the Z-axis.

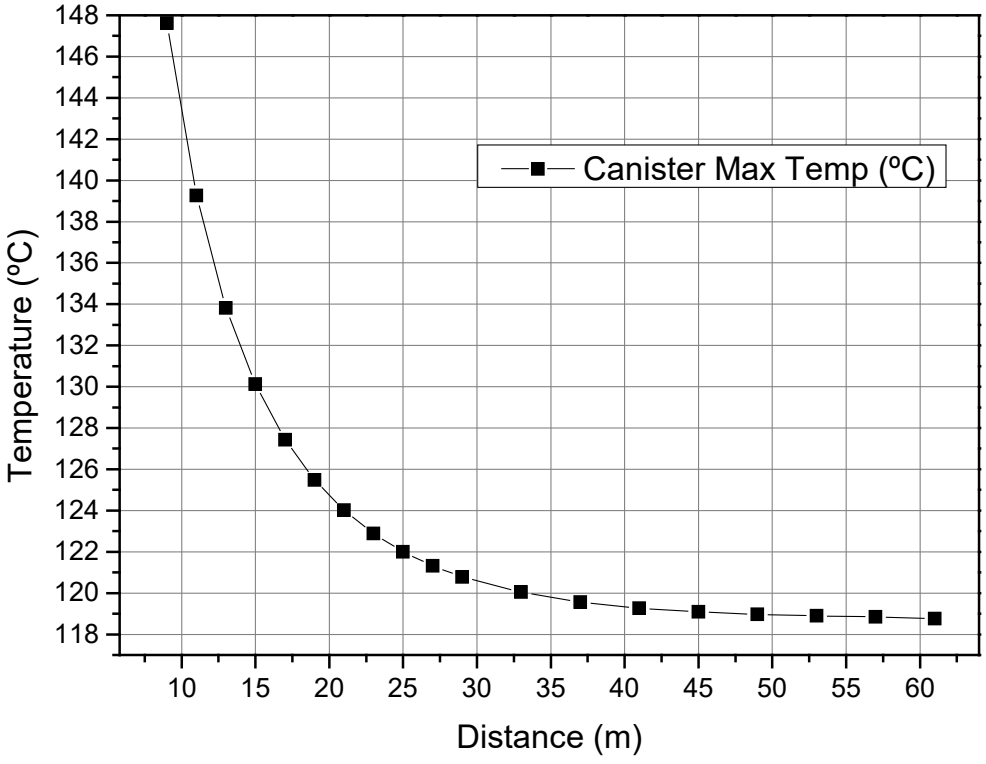

(a)

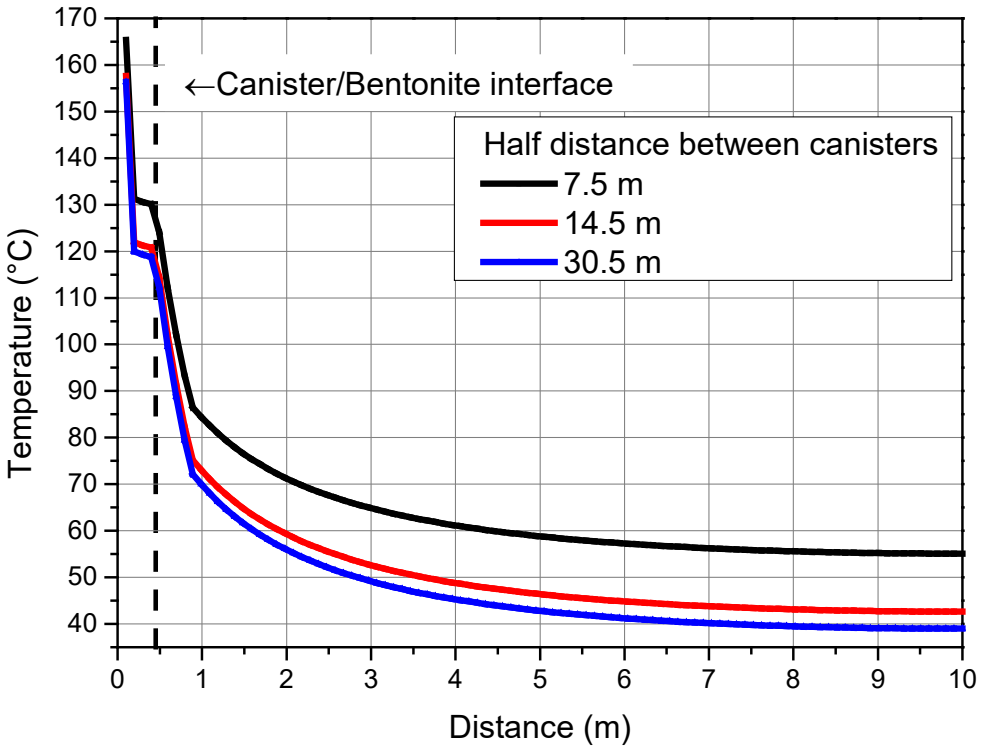
←Canister/Bentonite interface
Half distance between canisters
7.5 m
14.5 m
30.5 m
Temperature (°C)
Distance (m)

(b)

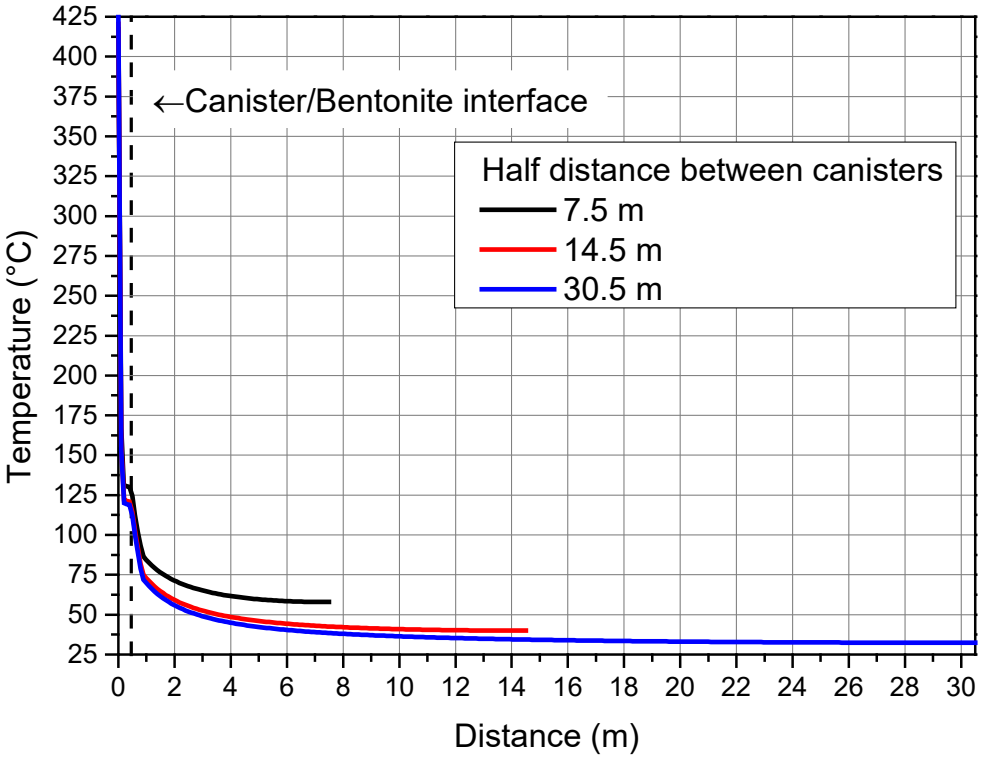
←Canister/Bentonite interface
Half distance between canisters
7.5 m
14.5 m
30.5 m
Temperature (°C)
Distance (m)

(c)

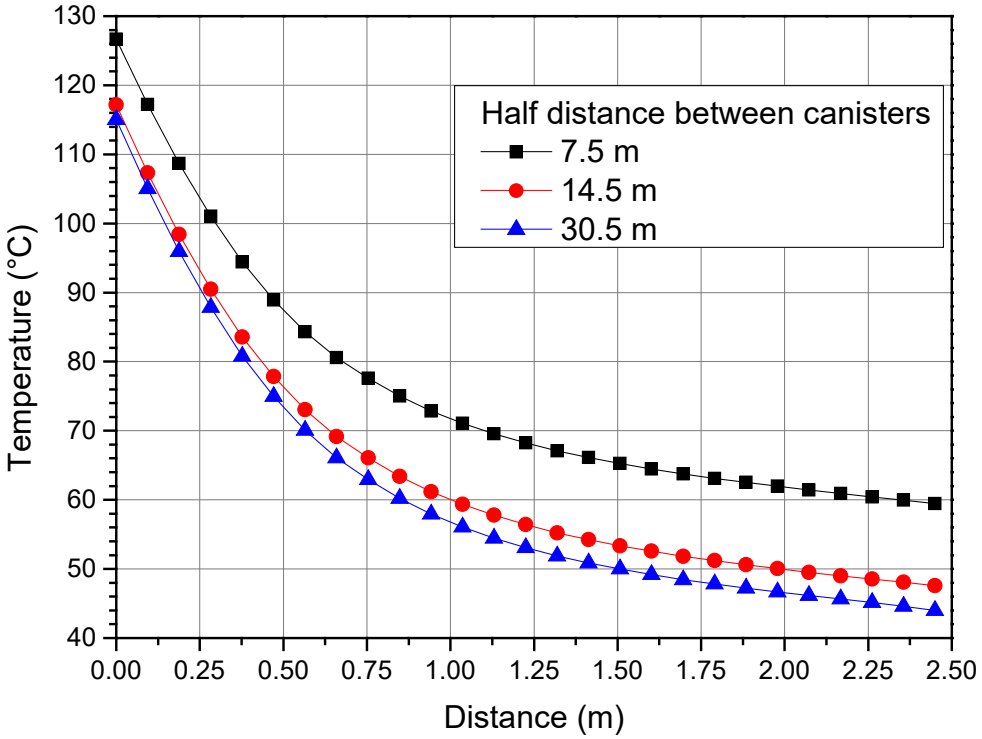

(d)

2.4.2.1 – Disposal area required

As shown in Table 14, each SUOX 48 canister requires a placement area of 328 m² vs 272 m² of a SMOX 48 canister as per equation 10a. However, as each SUOX canister holds 4 fuel assemblies, the disposition density (m²/t) is greater than that of SMOX, even requiring a greater spacing between the canisters. The STRU cannot be disposed of on DGR with the restrictions considered, as shown in Table 14. This suggests that STRU should stay longer on an interim storage facility. Another possibility is the adoption of a new thermal criterion for the buffer, as suggested by Cho and Kim (68), from 100 °C to 125°C. With this new limit, the disposal of STRU should be possible with canister spacings of 20 m.

Table 14 – Disposal area per canister and ton of waste for the SUOX 48, SMOX 48, and STRU SNF.

SNF	Burnup (GWd/tHM)	Canister spacing (m)	Disposal area per canister (m²/canister)	Disposal area per ton of waste (m²/t)
SUOX	48.00	8.20	328.00	169.73
SMOX	48.00	6.80	272.00	563.02
STRU	48.00	-	-	-

2.4.3 – DISPOSAL OF SUOX 48 AND SMOX 48 USING BRAZILIAN GEOTHERMAL DATA

The disposal of the SMOX 48 was simulated for selected locations in Brazil, as shown in Table 10. The geothermal gradients range from 16.68 ºC/km on Juiz de Fora, Minas Gerais to 38.25 ºC/km on Quixadá, Ceará. Regardless of the type of SNF to be disposed of, an increase of 1ºC in the initial temperature of the rock at a depth of 500 m corresponds to an increase of approximately 1ºC in the maximum surface temperature of the canister, as shown in Figure 21. The rock temperature at Ijuí, Rio Grande do Sul, corresponds to the rock temperature conditions previously assumed for the generic DGR (31ºC at 500 m depth). It was then analyzed what would be the necessary spacing between the canisters at selected rock temperatures: 31ºC, 35ºC, 40ºC, and 45ºC.

As shown in Figure 22, Starting from an initial spacing between the canisters of 10m, for the SUOX 4.8, two different situations occur: For rock temperatures below 40ºC it is necessary to reduce the spacing; above 40°C it is necessary to increase the spacing. Thus, for a rock temperature of 31ºC the spacing required is 6.4 m, while for a temperature of 45ºC the spacing required is 15.8 m.

Figure 21 – Relationship between maximum canister temperature and rock temperature at 500 m for SUOX 48 and SMOX 48 SNFs for a fixed canister spacing.

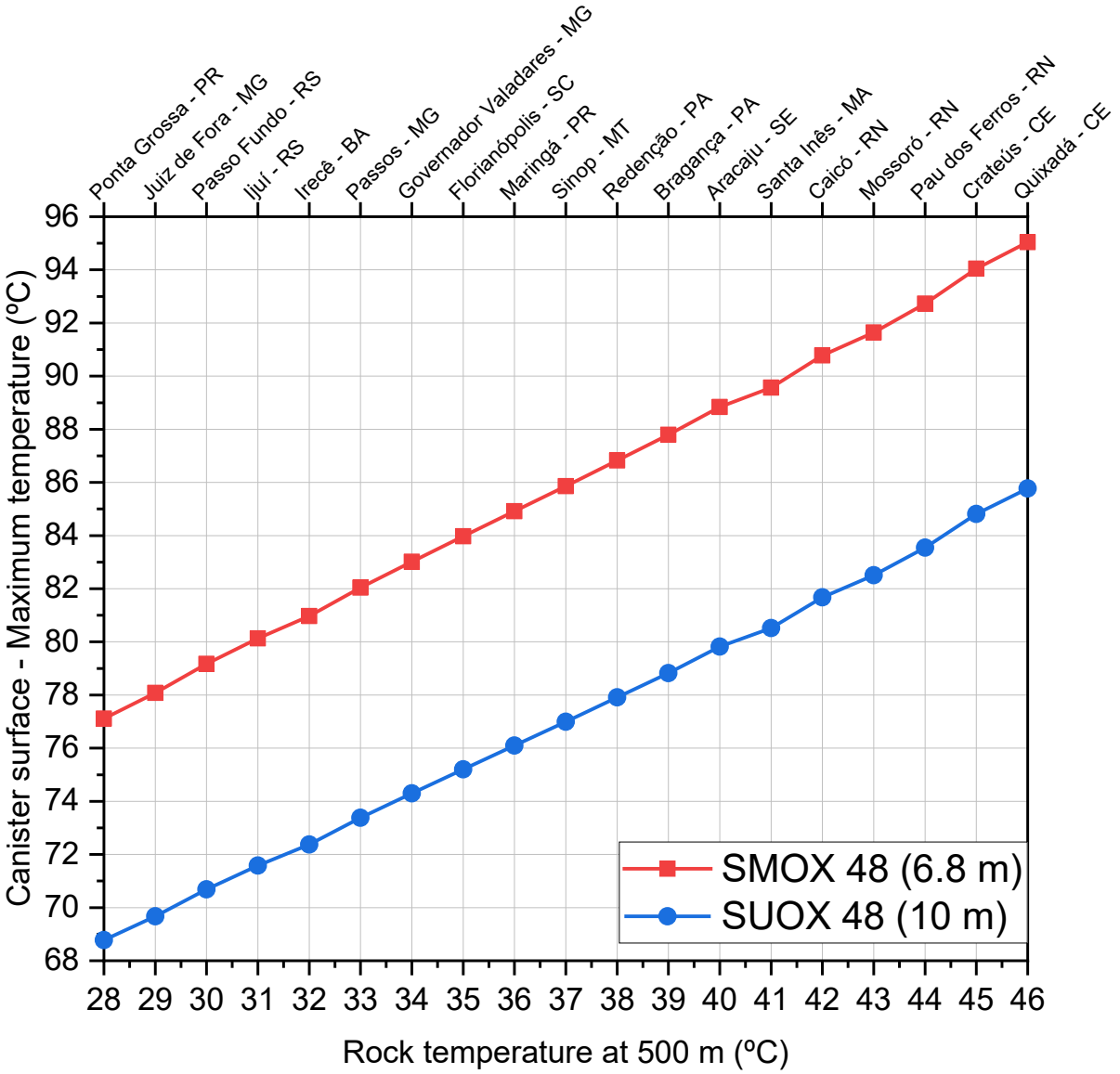

The required canister spacing was adjusted according to locations with higher temperatures at 500m depth than the generic case, with 5ºC increments, as shown in Figure 23. With the rock temperature set at 35ºC, the minimum spacing between canisters must increase by 1.4 m, from 6.8 m to 8.2 m. For a rock temperature set at 40ºC, the new canister spacing is 10.8 m, and that temperature is set at 45 ºC, the canister spacing must be 17.8m.

Figure 22 – The maximum temperature for the SUOX 48 at the canister surface as a function of the spacing between canisters for selected rock temperatures.

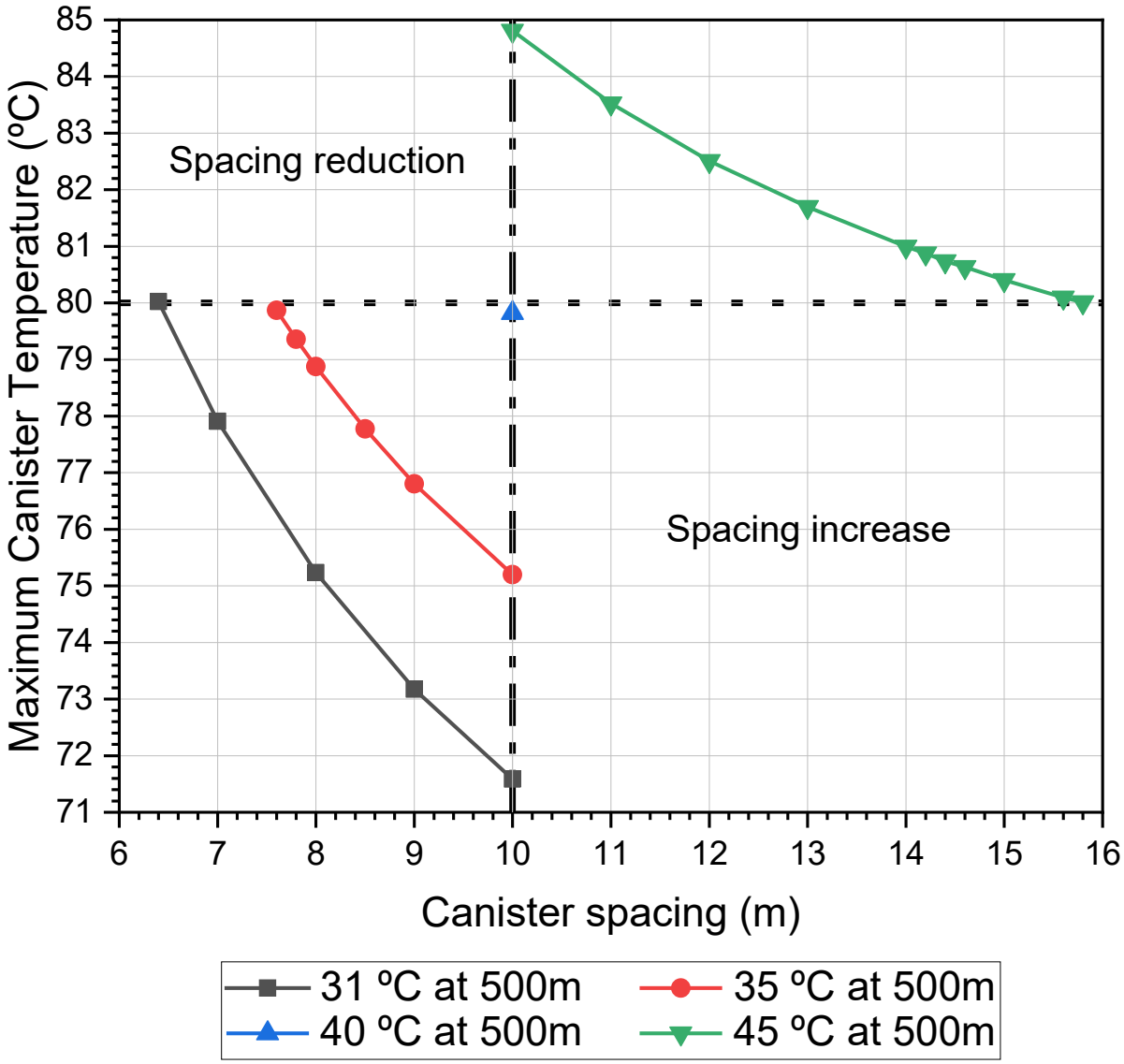

The SMOX 48 situation is different, as shown in Figure 23. Starting with a spacing of 6.8 m between the canisters, it is necessary to increase the spacing for all cases. With the rock temperature at 31ºC, the spacing required is 8.2 m, while for 45ºC 17.8 m are needed between each canister.

Figure 23 – The maximum temperature for the SMOX 48 at the canister surface as a function of the spacing between canisters for selected rock temperatures.

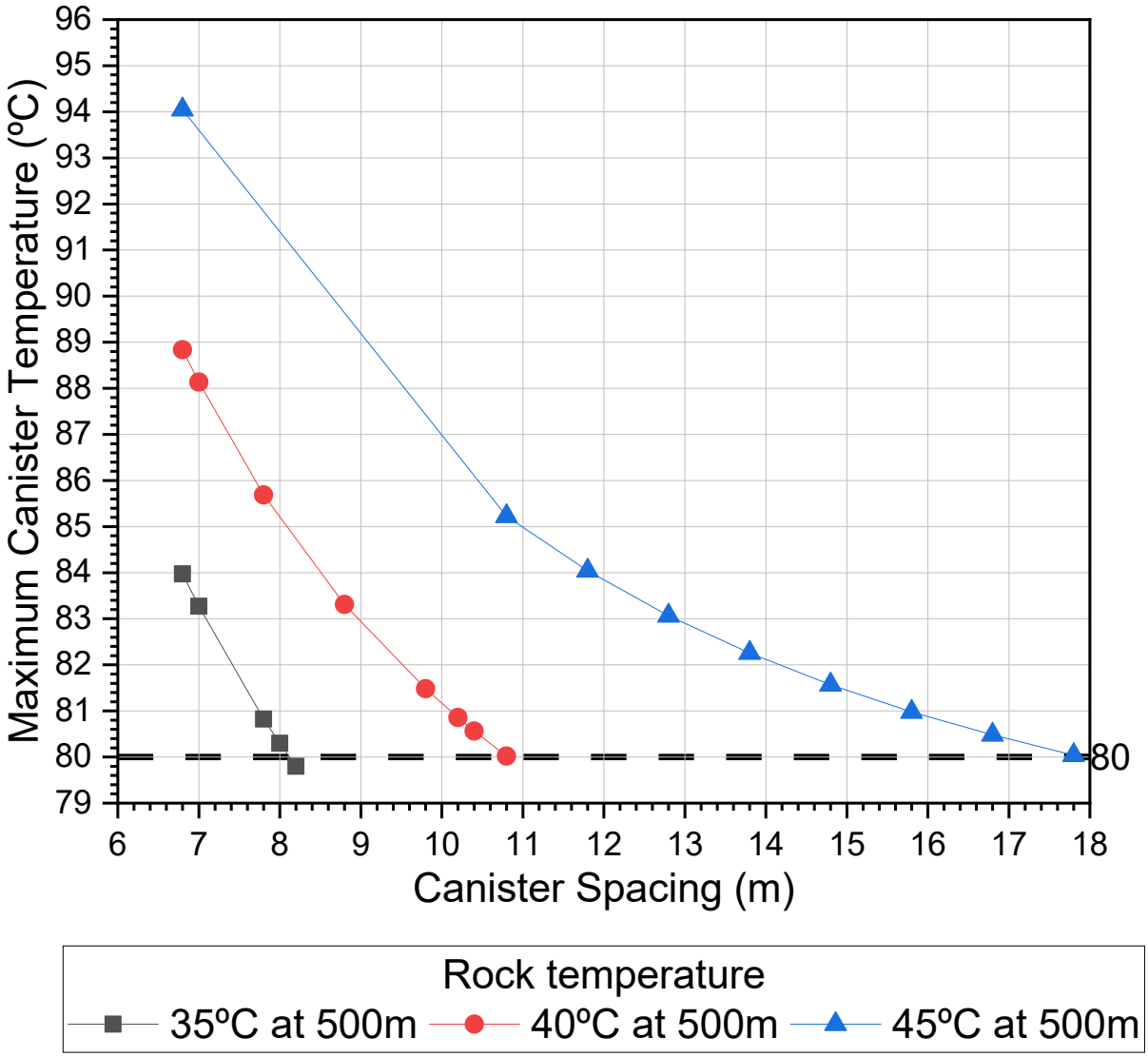

2.4.3.1 – Disposal area required

With the estimated spacings for the different temperatures of rocks existing in Brazil, it is possible to estimate the total disposal area needed for the Brazilian SNF. For this purpose, nuclear power generation scenarios, detailed in Chapter 4, were used to estimate the total amount of SNF to be disposed of. Table 15 shows the minimum area needed for each canister, per ton of waste, and the total area needed for the Brazilian nuclear program according to different nuclear generation scenarios.

Table 15 – Disposal area per canister and per ton of waste, and total area needed for different rock temperatures and amounts of SNF to be disposed of.

Rock Temperature at 500m (ºC)	**Disposal area per canister (m²/canister)**	**Disposal area per ton of waste (m²/t)**	**Total area needed for the following amount, in tHM, of SNF (km²)**		
			1,469*	**2,461****	**14,347*****
Open Fuel Cycle (SUOX 48)					
31.00	256.00	132.47	0.19	0.33	1.90
35.00	304.00	157.31	0.23	0.39	2.26
40.00	400.00	206.99	0.30	0.51	2.97
45.00	632.00	327.05	0.48	0.80	4.69
Closed Fuel Cycle (SMOX 48)					
31.00	272.00	563.02	0.83	1.39	8.08
35.00	328.00	678.93	1.00	1.67	9.74
40.00	432.00	894.20	1.31	2.20	12.83
45.00	712.00	1,473.78	2.17	3.63	21.14

* **ANGRA1&2** scenario.
** **ANGRA3** scenario.
*** **ANGRA+8** scenario.

The total required disposal area increases with increasing temperature. When compared to a rock temperature of 31°C the total disposal area increases by 1.2, 1.6 and 2.5 times larger for rock temperatures of 35°C, 40°C, and 45°C, respectively. Furthermore, the total disposal area increases with the use of reprocessed fuel, compared to direct disposal. For rock temperatures of 31ºC, 35ºC, 40ºC, and 45ºC, SMOX 48 needs, respectively, disposal areas 4.3, 5.1, 6.8, and 11.1 times larger than SUOX 48.

2.5 – CONCLUSION

This part of the work reproduced an earlier study of Acar and Zabunoğlu (28). The initial simulations performed with ANSYS and OF did not obtain results concordant with the benchmark paper for the SMOX 40 and SMOX 50 cases. The reduction of the canister spacing was sufficient to minimize the differences. Neither the type of mesh nor the number of elements significantly affected the results of the maximum temperature at the canister/bentonite interface.

A mesh convergence study was conducted to further investigate the effects of the mesh on the simulations. Using the SMOX 50 as the base case, the estimated maximum temperature of the canister surface, for a zero-grid spacing (Richard extrapolation), was 79.79 ºC. The actual fractional error between the meshes and the calculation of the Richardson extrapolation was lower than 0.1%. Thus, the mesh refinement has no significant effect on the evaluation of the maximum canister surface temperature.

New reprocessed SF types proposed and modeled for Angra 2 in earlier published works by Pereira *et al* (56), MOX and TRU, were also analyzed. According to the results, SMOX 48 would require canisters spacing of 6.8 m or a disposal area of 272 m². Due to the high decay heat generation of the STRU, it cannot be disposed of on a DGR with the thermal restrictions (80 °C), so that and residence time in interim storage (50 years) should be considered.

Using data from the Brazilian geothermal gradient and some projections of the total SNF to be produced in Brazil, the total required waste disposal area was calculated considering that the reprocessing of fuels is adopted. The results show that the minimum area, depending on the rock temperature at the chosen location, in a scenario with only two NPPS in operation ranges from 0.83 km² to 2.17 km². For a scenario with three NPPs in operation, the minimum area varies between 1.39 km² and 3.63 km². For a scenario with eleven NPPs in operation, the minimum area varies between 8.08 km² and 21.14 km². These results show the need to prioritize places that, in addition to having the required characteristics for disposal, have rocks with lower temperatures, to increase the density of disposal.

3 – SITE SELECTION

The planning and site selection stages for implementing a DGR consist of several steps (69). Despite being commonly grouped into five distinct phases, the final number of steps depend on each country's regulation. The phases are:

- Phase 1: Evaluation and selection of areas.
- Phase 2: Characterization of the areas.
- Phase 3: Construction of the facility.
- Phase 4: Operation and closing of the installation.
- Phase 5: Post-closing of the DGR.

The site selection for a future DGR must consider the following factors: long-term safety; technical feasibility; and socioeconomic, political, and environmental aspects (32). These factors are somehow self-conflicting, such that, to ensure the safety of the enterprise, they demand numerical and judgment analyses in a variety of areas, such as geology, engineering, and environmental protection (32, 51).

The current Brazilian thermonuclear plants are in the State of Rio de Janeiro (RJ). The National Energy Research Office (Portuguese: Empresa de Planejamento Energético – EPE), through the National Energy Plan 2030 (PNE 2030) confirmed the need for an expansion of the thermonuclear generation by more than 4,000 MW in addition to Angra III. From this value, 2,000 MW would be allocated in the Southeast (possibly on Minas Gerais), and 2,000 MW in the Brazil Northeast (70, 71). In 2011, the Eletronuclear agency, together with EPE, prepared an Atlas of the Brazilian Nuclear potential, identifying suitable areas for the installation of future NPPs throughout the country (72). Therefore, the evaluation of areas for implementing a DGR should be done from a national perspective, owing to the possibility of new NPPs to be constructed in different states in the future (69).

The difficulty to find out a suitable region for the DGR is amplified by the Brazilian territorial extension, besides the expectation of rational use of human and financial resources available. To attend to these requirements, the method developed by Martins was employed in this work (51). It combines the multicriteria analysis based on expert judgment and Geographic Information System (GIS) to identify preliminary areas in a given region of interest for further studies, becoming the searching process quicker and cheaper (51).

However, Brazil still lacks a specific rule available to the SNF by the responsible government agency, as discussed in Chapter 1, which means that there are no national criteria for choosing the type of host rock or even criteria for the process of choosing the DGR site. Thus, research related to this topic remains incipient in the country, given the impossibility of in-depth studies in the absence of clear criteria. To date, there are only five works, as far as it is known, aimed at selecting sites for the construction of a national SNF DGR:

1. Mattos (73) in 1981, conducted a preliminary analysis of the deposition of HLW, including SNF, in existing geological formations in the state of São Paulo.
2. Enokihara (74) in 1983, carried out an analysis, also preliminary, on the disposal of radioactive waste in rock salt, granite, and basalt from various locations in Brazil.
3. In 2009, Martins (51), proposed an area selection method based on a DGR model that uses hard rocks as hosts and applied the method to the state of Rio de Janeiro.
4. In 2015, Silva *et al* (75), was building a geospatial database to be used for a site selection in the state of Rio de Janeiro; and
5. In 2019, Jonusan *et al* (76), applied the method proposed by Martins for the state of Minas Gerais and found areas of interest.

This chapter aims to apply the methodology proposed by Martins (51) to the states of Espírito Santo and Minas Gerais and to, systematically, expand the number of sites studied for a future Brazilian SNF DGR. Geospatial data available from Brazilian government agencies – Brazilian Geological Service (Portuguese: Serviço Geológico

Brasileiro - CPRM) (77, 78), Brazilian Agricultural Research Corporation (Portuguese: Empresa Brasileira de Pesquisa Agropecuária – Embrapa) (79), National Department of Transport Infrastructure (Portuguese: Departamento Nacional de Infraestrutura de Transportes – DNIT) (80), and Brazilian Institute of Geography and Statistics (Portuguese: Instituto Brasileiro de Geografia e Estatística - IBGE) (81) – were used for creation of a map of the Suitability Index (SI) for the construction of a geological DGR. The results show that both Minas Gerais and Espírito Santo have areas considered as good and meritorious for further investigation.

3.1 – GEOLOGICAL DESCRIPTION

Minas Gerais is a state in southeastern Brazil and borders São Paulo (south), Bahia (north), Rio de Janeiro and Espirito Santo (east), Goiás (west) and Mato Grosso do Sul (extreme west). Espírito Santo is also located in southeastern Brazil, having as limits the states of Minas Gerais (west), Bahia (north), Rio de Janeiro (south), and the Atlantic Ocean (east). Five main outcropping geological units stand out (77):

- São Francisco Craton (SFC).
- Brasília Belt.
- Colluvium-Alluvial and Eluvial Coverages.
- Paraná Basin.
- Araçuaí/Ribeira Orogen.

Minas Gerais is composed, roughly, of two types of land: the ancient, of pre-Cambrian age (> 541 million years); and young, of Phanerozoic ages (<541 million years) (82). Espirito Santo, meanwhile, is completely inserted in the evolutionary geotectonic context of the Mantiqueira province (Araçuaí Mobile Belt), in which it is dated to the Neoproterozoic - Cambrian age, having as its base Archean blocks agglutinated between 2.2 to 2.0 billion years. Neoproterozoic to Cambrian igneous and metamorphic rocks represents about two-thirds of the territory. The rest is composed of phanerozoic covers (78).

The São Francisco Craton (SFC), present in Minas Gerais, is a geologically stable continental block, occupying a large part of the state territory (in the center) and limited by the Brazilian orogenic systems Araçuaí / Ribeira (south and east) and the Brasília strip (west) (77). Much of the SFC is formed of Precambrian and Phanerozoic sedimentary rocks, in the so-called São Francisco Sedimentary Basin. To the south are found rocks of its foundation, with ages of up to 3.2 billion years (82).

The Brasilia Belt is part of the Tocantins Orogenic system. This unit is the result of the addition of metasediments of marine origin (82). The Belt is still composed of granite rocks formed before the event of collision and uplift of the Tocantins System (77). The Brasília Belt is present on the southeastern portion of Minas Gerais.

The Paraná Basin is in the Triângulo Mineiro region. The Basin is composed of a sedimentary-magmatic succession (77). In Minas Gerais there are two main groups, São Bento and Bauru. The São Bento Group is made up of sandstones, fluvial conglomerates, and fine-grained basalt (82). The Bauru Group is composed of sandstones of alluvial origin containing fragments of volcanic rocks and conglomerates, calcareous sandstones, and claystone (82).

The Colluvium-Alluvial and Eluvial Coverings covers extensive areas of Minas Gerais. These soil coverings are the result of intense inter-activity over millions of years in regions with elevated levels of humidity and rainfall (77).

The Araçuaí / Ribeira orogens constitute the eastern and southern limit of the SFC. The Araçuaí Orogen can be subdivided into two parts. The outer part is composed of low to medium metamorphic metasedimentary rocks. The internal part is composed of high-grade metamorphic rocks and granites (82). The Ribeira strip is the result of a change in the direction of Brazilian structuring - from north-northeast to north, to the northeast to the south - without the occurrence of a stratigraphic or metamorphic discontinuity (77). The Ribeira Belt overlaps with the southern terminal of the Brasilia

Belt. The base of the Ribeira Belt is composed of gneisses and granites of the Archaean and Paleoproterozoic ages (82).

The Araçuai Orogen constitutes the eastern boundary of the SFC in Minas Gerais, while Espirito Santo is located entirely within the domain of the orogen. In Minas Gerais, the orogen basement is formed by gneiss, TTG migmatites (tonalite-trondhjemite-granodiorite), granitic plutons and greenstone belt sequences (Guanhães, Gouveia and Porteirinha Complexes); banded orthogneisses (Mantiqueira Complex) and granulitic orthogneisses (Juiz de Fora Complex) (77). In Espirito Santo, the orogen basement comprises two units: the Caparaó Suite and the Pocrane Complex. The Caparaó Suite is formed by granulites of different compositions. The Pocrane Complex is formed by biotite hornblende gneisses, metasedimentary and metaultramafic rocks (78).

3.2 – MULTICRITERIA ANALYSIS

Multiple Criteria Decision Making (MCDM) is a framework developed to support the decision-making process of different sets of alternatives. The site selection for the accommodation of a geological DGR is a prime example of an application of the MCDM framework, more specifically, a multiple criteria discrete alternative problem (83). To deal with the complex relationship between each criterion[20] and attribute[21], the Analytic Hierarchy Process (AHP) is used to “derive priorities for criteria concerning the goal” (85).

Martins has developed a method to apply the MCDM and AHP in conjunction with expert judgment and GIS systems to ease the initial selection of suitable areas for the implementation of an SNF DGR in Brazil (51). In the absence of specific guidelines for HLW repositories, including SNF, Martins has used international standards, such as those published by the IAEA, and the NE 6.06 standard from CNEN that is applied to

[20] Criteria can be defined as: alternatives, usually being assumed to be finite, that represent different choices of action available to the decision-maker (84)
[21] Attributes can be defined as: goals or decision criteria. According to Navneet and Kanwal (84), “Different attributes represent different dimensions of looking at the alternatives […]”.

"[...] the location of final or intermediate or provisional deposits for low and medium radiation wastes [...]" for creating the criteria and attributes necessary for multicriteria analysis (3, 32, 51).

The method[22] consists of sending a questionnaire to experts in fields related to the construction and operation of a DGR to generate a comparison matrix of the different criteria and attributes. The results obtained from the matrixes are the weights of each attribute that compose a criterion, which will compose the goal afterward. The weights are used in conjunction with spatial data to generate a Suitability Index (SI). The index is the result of the classification and combination of spatial data, and it shows, numerically, the most suitable areas for building the geological DGR.

3.2.1 – Criteria

Martins has developed a set of criteria for the initial step of the area survey stage (51). Each criterion is composed of a set of attributes that are judged by specialists. The criteria follow national and international legal requirements (3, 32, 51). The criteria and their hierarchical relationship are presented in Figure 24.

[22] The original comparison matrices, as well as the consulted specialists, are available in Martins' Thesis (51). Martins consulted experts in the areas of transport, environment, mineral resources, land use, hydrogeology, structures, among others to define the criteria and the exclusion criteria. Latter these specialists filled out the decision matrix. This matrix was used to calculate the weights of each criterion and attribute.

Figure 24 – Hierarchical relationship between criterion and attributes. Adapted from (51).

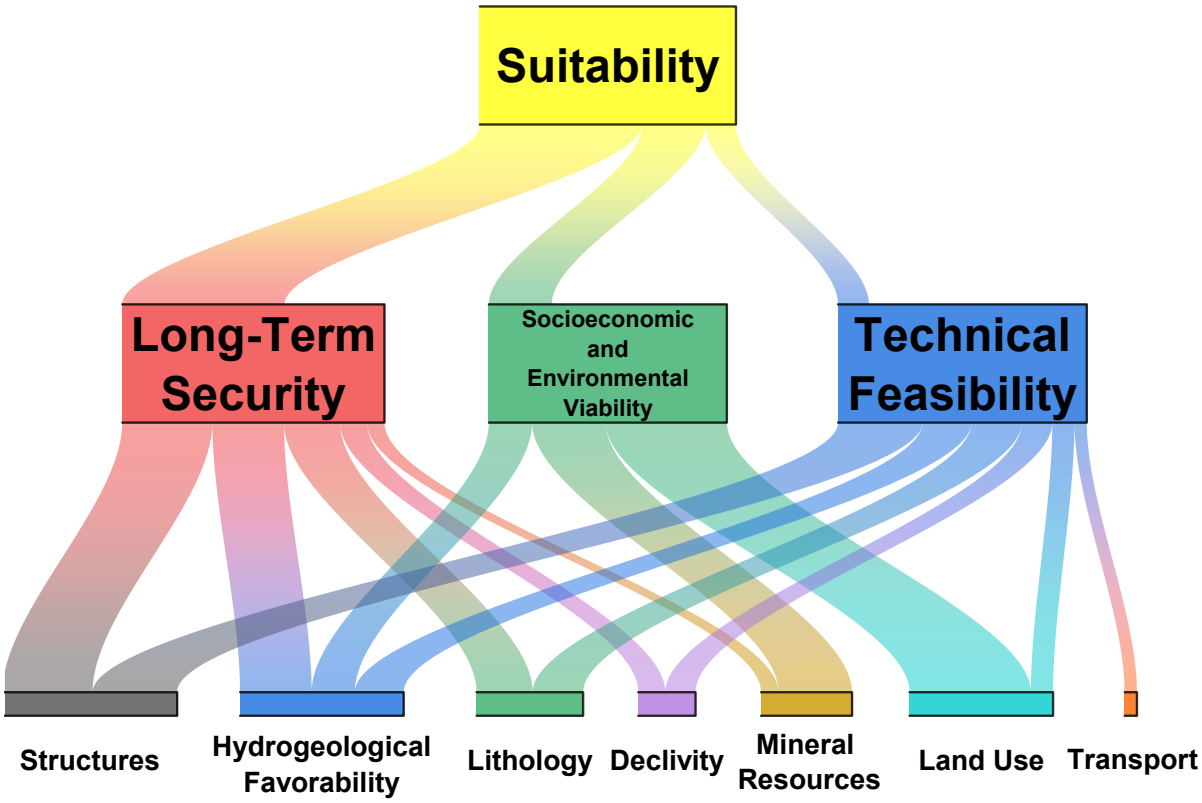

The Long-Term Safety (LTS) criterion refers to the geotechnical safety of the DGR from its construction to its post-closure insulation. The Socioeconomic and Environmental Viability (SEV) refers to the relationship between the construction and operation of the DGR, as well as to the social and natural environment domains related to the area of implementation. Technical Viability (TV) refers to the most important technical criteria[23] in the construction and operation of the DGR (51).

3.2.2 – Attributes

The attributes considered by Martins and used in this work were: Structures, Lithology, Mineral Resources, Hydrogeological Favorability, Declivity, Land Use, and Coverage, Demography, Conservation Units, and Transportation (51). This work, as well as Martins one, was based on a geological DGR built on hard rocks, such as granites. Such choice comes from the integration between the analysis of this chapter and those

[23] Structures (fractures and faults), lithology, hydrogeology, declivity, land use, coverage, and transportation.

of the next chapter, the evaluation of the thermal performance of the SNF in a DGR built-in hard rock. However, it is not possible to exclude other types of rocks in the choice of areas a priori, given that several countries consider other types of rocks for constructing a geological DGR, and considering the Brazilian geological diversity and its immense territorial extension. To analyze the criteria, attributes, and restrictions involved, a geospatial database holding the information specified in Table 16 was organized:

Table 16 – Spatial data sources.

Data	Scale / Spatial Resolution		Source	
	ES	**MG**	**ES**	**MG**
Declivity	90 m		EMBRAPA (79)	
Hydrogeological Favorability	1:2,500,000	1:2,500,000	CPRM (78)	CPRM (77)
Land Use	~30 m		IBGE (86)	
Lithology	1:1,000,000	1:1,000,000	CPRM (78)	CPRM (87)
Minera Resources	1:100,000	1:100,000	CPRM (78)	CPRM (77)
Structures	1:1,000,000	1:1,000,000	CPRM (78)	CPRM (77)
Transportation	Unavailable		*Ministério dos Transportes* (88) and DNIT (80)	
Demography	1:50,000		EMBRAPA (89)	
Conservation Units				
Water Mass	1:250,000		IBGE (81)	
Indigenous Land				

Both criteria and attributes are classified according to a standardized score ranging from 1 to 5, following qualitative parameters, which are: *1 - very bad*, *2 - bad*, *3 - regular*, *4 - good*, *5 - very good*. The scores of each attribute were obtained and adapted from Martins (51). Table 17 shows the classification of each attribute.

The effects of earthquakes or micro-earthquakes were not considered. Despite their importance, especially for the safety of surface installations, it is expected that the underground movement of the rock mass caused by an earthquake would be lower than that of the surface (90, 91). Specifically for tunnels in crystalline rocks, the effects of an earthquake are expected to be insignificant (91). However, movements caused by earthquakes must be considered, as they can result in changes in the flow, level,

pressure, and chemical properties of groundwater, and may result in failures of the SNF safety mechanisms (91).

Table 17 – Attribute classification. Adapted from (51).

Attribute	**Classification**				
	1- Very Bad	**2- Bad**	**3 - Regular**	**4 - Good**	**5 - Very Good**
Lithology	Unconsolidated sediments (clastic and lateritic sediments)	Sedimentary (sandstone, claystone)	Metamorphic (quartzite and shale)	High Metamorphic (paragneiss)	Igneous (basalt, granite)
Land Use	Wet area	Forest vegetation, natural grassland	Mosaic of vegetation	Agricultural area, pasture, forestry, agricultural mosaic	Uncovered area
Hydrogeological Favorability	High	Variable	Low	Very Low	No favorability
Mineral Resources	Indicative areas for mineral exploitation	-	Areas with potential for mineral exploitation	-	Areas without the potential for mineral exploitation
Transportation	18-30 km	12 - 18 km	7 - 12 km	3 - 7 km	0 - 3 km
Declivity	Mountainous	Strongly rugged	Rugged	Gently rugged	Plain

3.2.2.1 – Structures

Structures are faults (shear zones) and fractures existing on rocky masses and may be areas of instability and weakness in the host rock. Structures can also help the transport of groundwater in the DGR region (51, 92). In addition, seismic events can reactivate geological failures, putting at risk the safety of surface facilities and SNF (91). All structures classified as faults, fractures, or shear zones were considered in this work. A buffer region of 200 m around the structures was created and classified as an inappropriate area. All remaining areas were rated *5 - very good*. The classification of the structural areas is shown in Figure 25[24].

[24] Due to the resolution, size and scale of the image, the 200 m buffer around the structures is difficult to see.

Figure 25 –Structures classification.

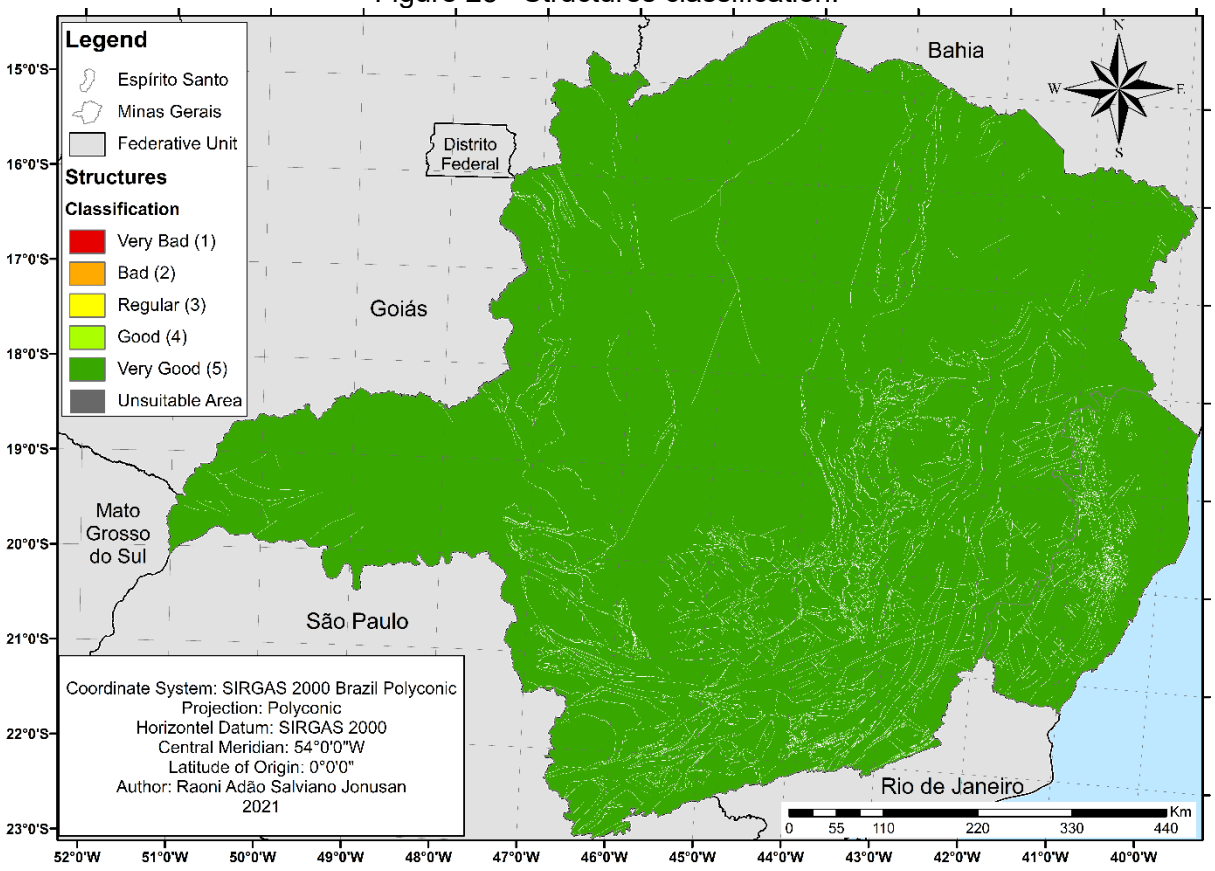

3.2.2.2 – Lithology

Lithology was also considered and analyzed since the DGR is a permanent underground installation having the host rock as its last containment barrier. In this work, the granite was the host rock considered. Therefore, sedimentary rocks and low and medium-grade metamorphic rocks received lower ratings. High-grade metamorphic rocks and igneous rocks received the highest ratings. Table 17 holds the classification for each type of rock as well as the examples and the classification of lithologies are shown in Figure 26.

Figure 26 – Lithology classification.

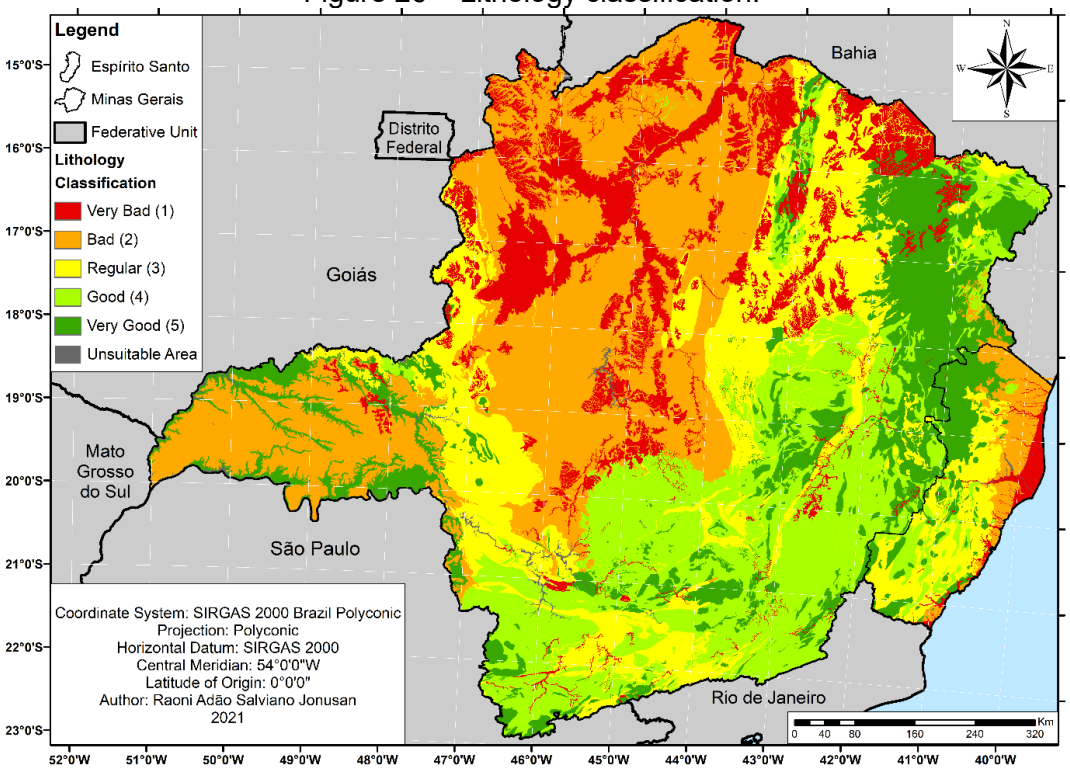

3.2.2.3 – Mineral resources

Future human actions e.g., the search for mineral resources may result in unintentional leakage of radionuclides from the DGR. Therefore, the DGR must be in regions without the recognized potential for mineral exploration (93–95). The Brazilian geological service (CPRM) produced a map of areas of relevant mineral interest in Brazil. The classification of this attribute, as shown in Table 17, follows the CPRM classification. Areas with proven mineral exploitation were classified as unsuitable areas. The classification of areas by this attribute is shown in Figure 27.

Figure 27 – Mineral resources classification.

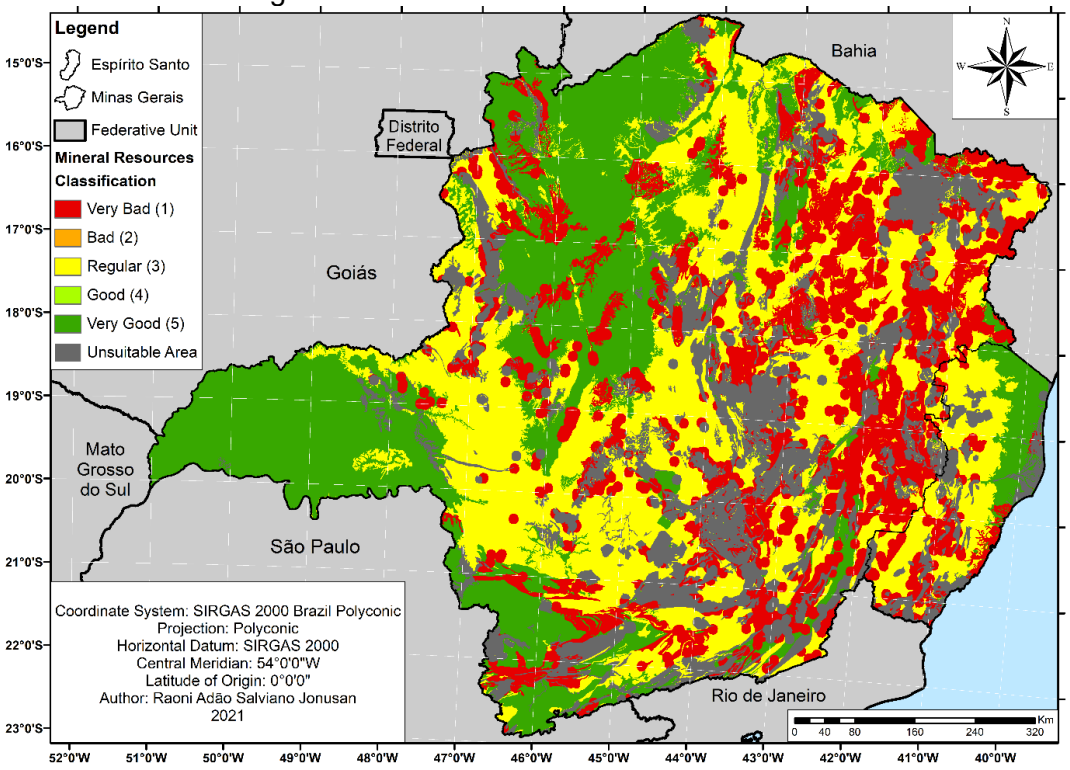

3.2.2.4 – Hydrogeology

Hydrogeological favorability may affect the long-term construction, operation, and safety of the DGR. Groundwater can affect the dynamics of heat transmission and corrosive processes within the DGR. The presence of groundwater does not prevent the construction of the DGR, although it can interact with the DGR containment barriers, easing the release of radionuclides to the biosphere in case of accidents (92–94). It is important to emphasize that an environment with low hydraulic conductivity and hydraulic gradients does not imply that the DGR would remain “dry” for hundreds or thousands of years (16). Areas with low favorability for the occurrence of groundwater are considered more suitable (see Table 17). The classification of hydrogeological favorability is shown in Figure 28.

Figure 28 – Hydrogeological favorability classification.

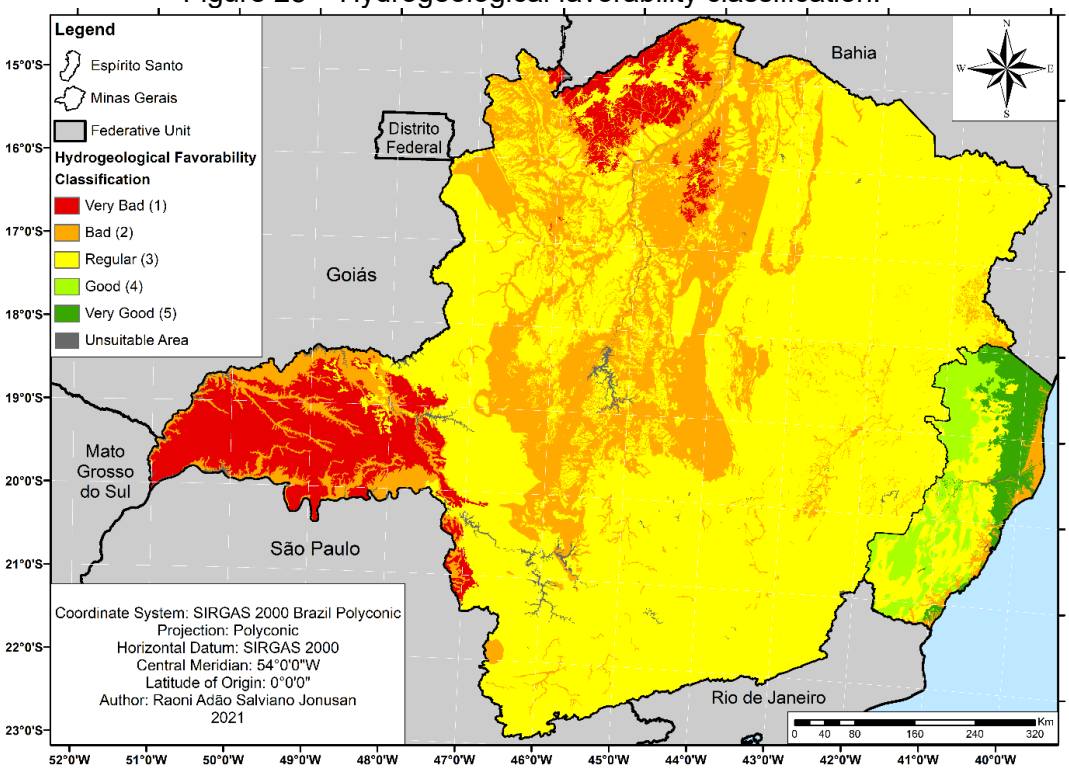

3.2.2.5 – Declivity

Rough terrain can hinder both the construction and operation of the DGR due to the unfavorable topography and natural phenomena, such as landslides (51, 94). The classification of this attribute, as shown in Table 17, follows the slope classification classes of Embrapa (79). The slope classification map is shown in Figure 29.

Figure 29 – Declivity classification.

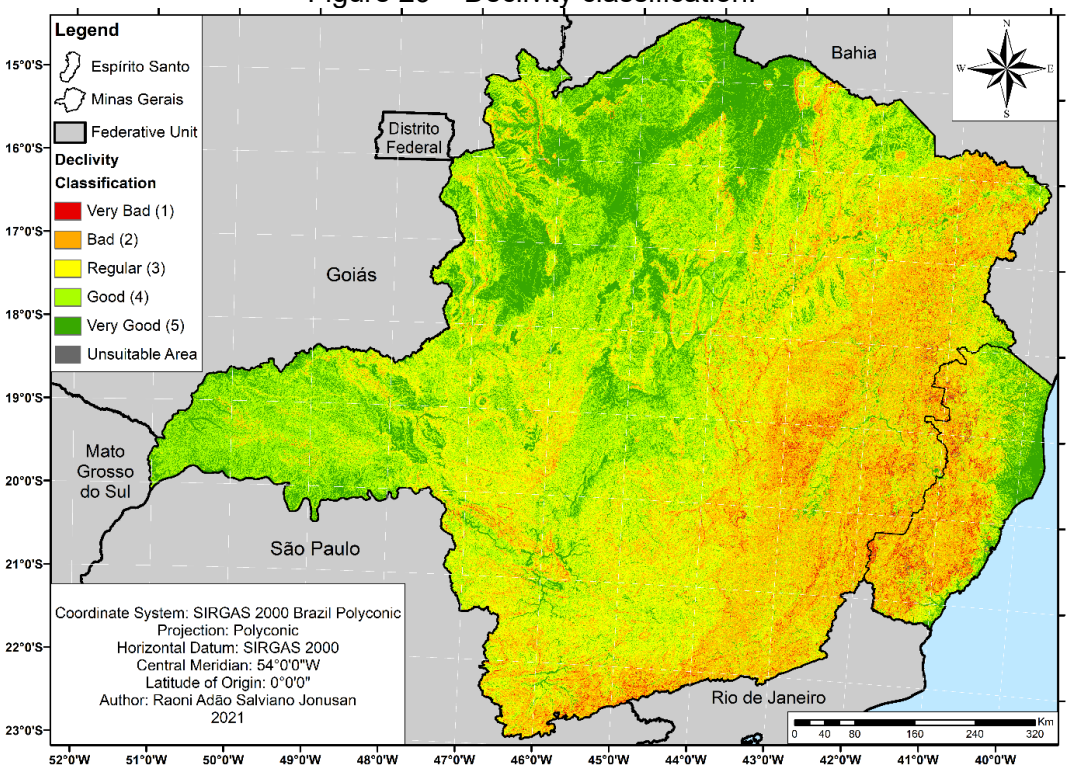

3.2.2.6 – Land use and Coverage attribute

This attribute is important in the construction and operation stages of the DGR, which, despite being an underground structure, the land use may hinder its construction and operation as occurs in protected areas. This is the reason wetlands (rivers, lakes, and marshes), urban areas (demography), and areas of environmental protection are classified as unsuitable for construction (92–94). The land use classification map is shown in Figure 30 (Appendix B). An attempt was made to carry out the selection of areas on public land of the Union, as recommended by the CNEN NE 6.06 standard (3, p. 06). However, no database was found with the data[25].

[25] A request, via the Access to Information Law, was made to the Secretariat for Coordination and Governance of the Patrimony of the Union (SPU), of the Ministry of Economy, to obtain data on georeferenced Brazilian public lands. The request, made under number 03950.000337 / 2019-94 on 01/31/2019, was denied on the grounds that there was no database with the data, at that time. In December 2020, the SPU + Geo program was launched, holding the georeferenced location of the Union's properties, however without having the polygons that define the area of the properties.

Figure 30 –Land use classification.

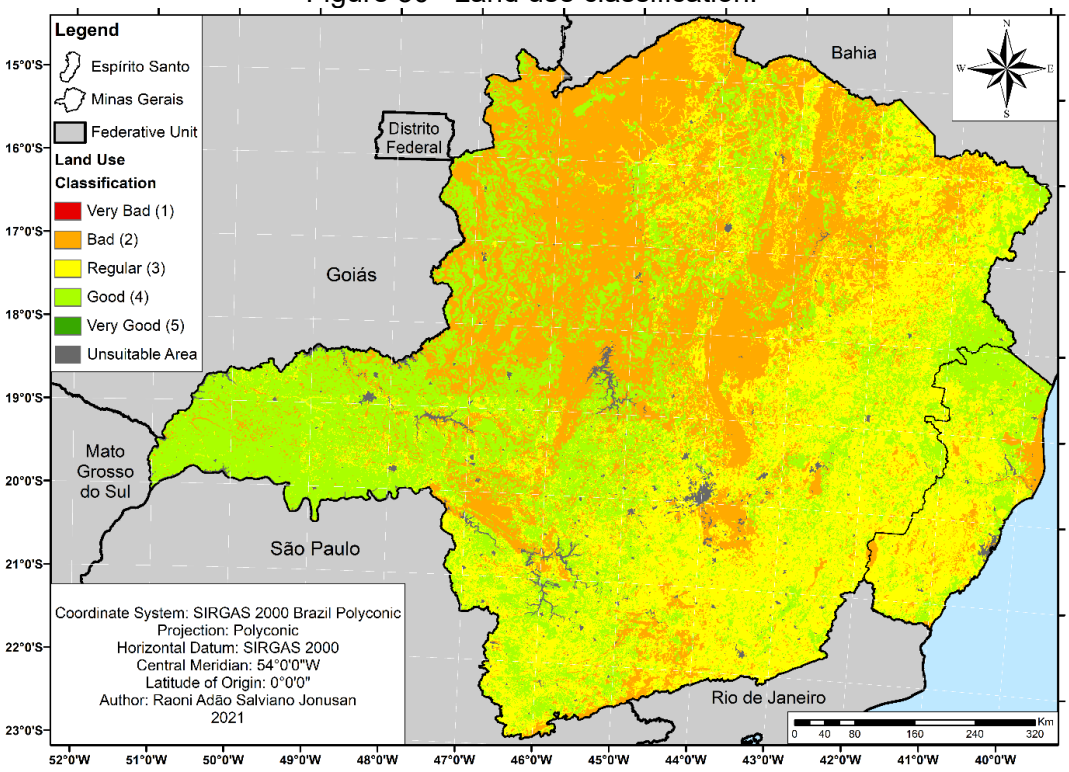

3.2.2.7 – Transportation of SNF/HLW

The transport of SNF/HLW from the intermediate storage site to the DGR requires that the latter should be built nearby to the transport system already established to reduce construction costs (92–94). Road, rail, and waterways can be used to transport spent fuel. Only rail transport was considered, as well as railroads classified as active, and road transport, those roads that meet the road rules of geometric design. The classification criterion was the Euclidean distance between the axis of the road and railway network (state and federal) and a predetermined maximum distance, as shown in Figure 31.

Figure 31 – Transport classification.

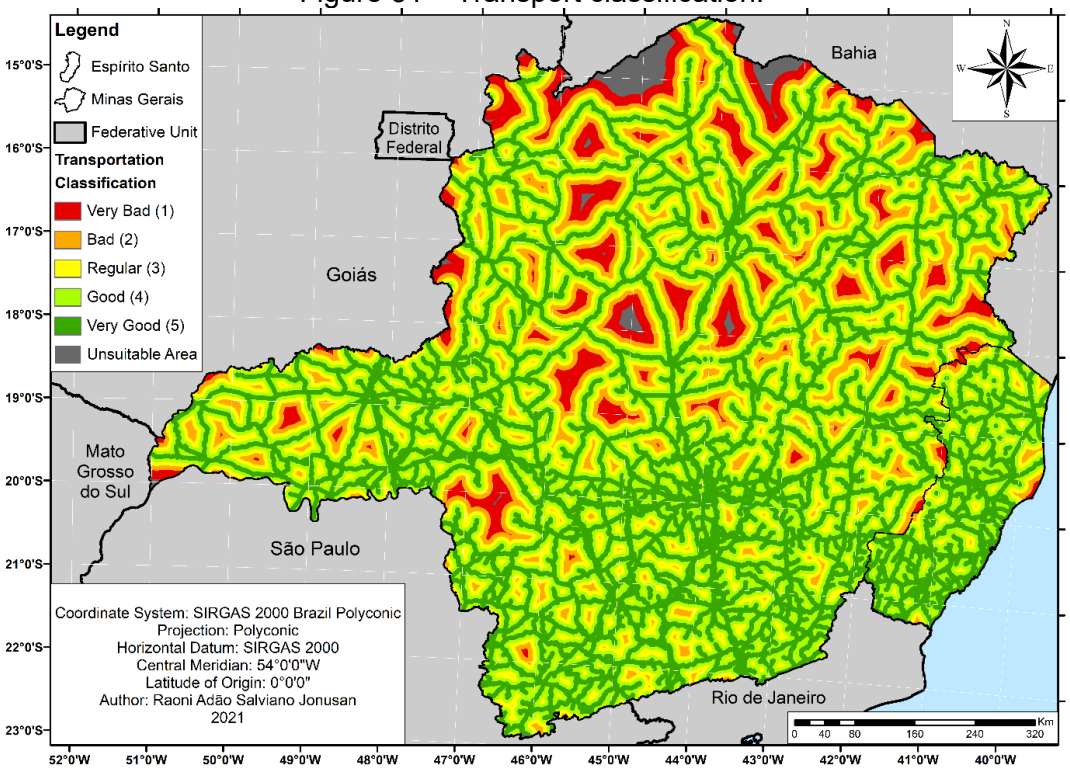

3.2.2.8 – Excluded areas

Integral protection units, indigenous lands, water bodies, flooded areas, urban areas, buffer regions around faults and fractures, and areas of proven mineral exploration were disregarded. The excluded areas are shown in Figure 32. In this criterion, modifications were made according to the criteria proposed by Martins:

- Units of sustainable use: It was considered that these areas are not prohibitive to host a geological DGR.
- 1 km buffer around mineral water occurrence sites: This buffer was not considered. The geospatial data used include mineral waters. Furthermore, as explained in more detail below, the types of spatial data used are different.
- Fracture density: Fracture density was not considered. Fractures received the same buffer as fault zones.
- Slope: In this work, steep terrains with a declivity higher than 75% were excluded. Mountainous areas, with slopes between 45 and 75%, were classified as Very Bad.

Figure 32 – Exclusion attributes.

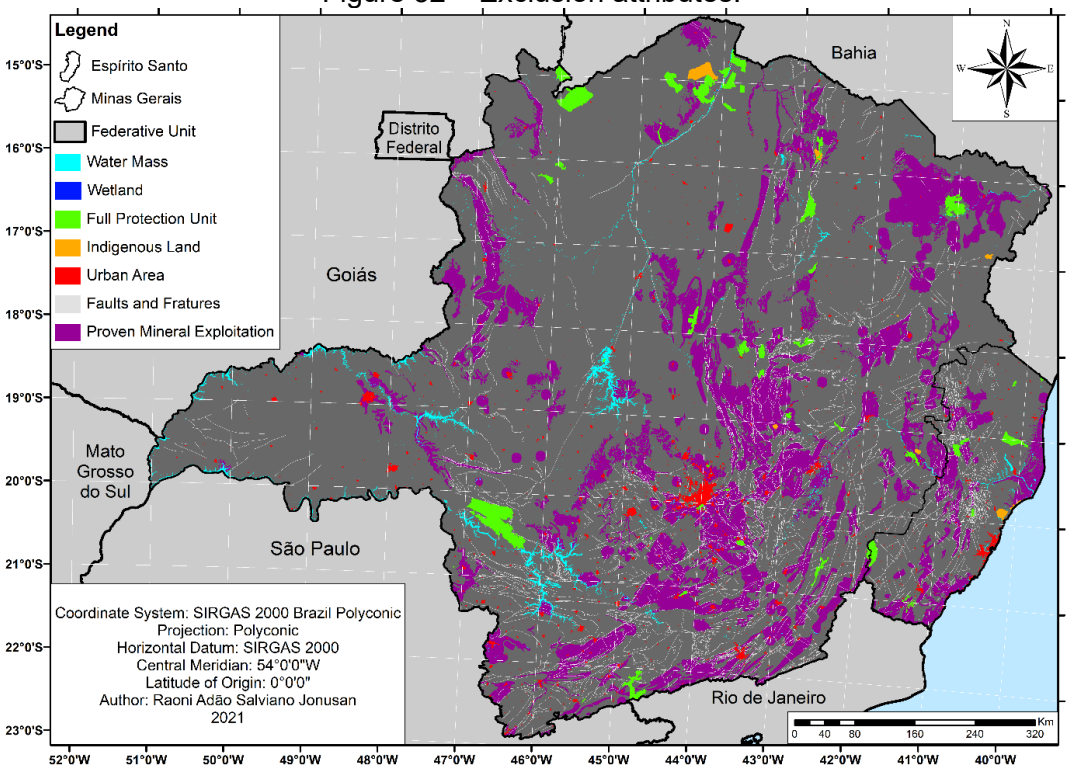

3.3 – DATA MANAGEMENT

The spatial data used in this work were obtained from several official sources, such as the CPRM, DNIT, and IBGE (77, 86, 96–99). Although all of them adopt the Brazilian geodesic reference system, SIRGAS 2000, some of them adopt the geographic coordinate system, and a projected coordinate system, which requires a standardization before the analysis. All data were projected to the UTM SIRGAS 2000 Brasil Polyconic Coordinate System[26]. In addition, all vector data were converted to raster data[27] with a spatial resolution of nine meters. The Esri® ArcMap software™ 10.6.1 was used for processing the data and generating the SI map.

[26] This projection was used because it has as the unit of measurement the meter, as well as being a projection applied to small scale mappings. This projection deals with interference caused in the boundary zones of each UTM Zone, which is fundamental, considering that Minas Gerais is crossed by 3 UTM Zones (22S, 23S and 24S). The SIRGAS 2000 Brazil Polyconic Projection holds the code EPSG:5880.

[27] Vector data, such as shapefiles, store data as geometric shapes. To represent geographic data, the shapes are linked to data attributes. Raster data, such as digital aerial photographs, store data in a matrix of cells. A more in-depth discussion about vector and data types can be found at the Encyclopedia of GIS (100).

Some geospatial data were used differently from the method proposed by Martins, such as those for mineral resources and transport. The classification of the mineral resources attribute by Martins [21] was performed considering the degree of exploitation of mineral resources, and the spatial data of the point type[28] were used. The use of points for this attribute disregards not only the spatial dimensions of mineral deposits or deposits but also the geological potential of an area. It is noteworthy that ARIM, a source of data for this attribute, in this study, was published in the same year as Martins ' work, so they were not available at the time of the study. For the transport attribute, Martins considered only the classes of highways (municipal, state, or federal), using spatial data of the line type[29]. The classification of this attribute considers only the type of highway, which is irrelevant, and analyzed only the axis of the highways, excluding all other areas. These changes are important because the method aims to classify areas. Thus, the use of point or line type geospatial data influences the final quality of the classification.

3.3.1 – Suitability Maps

The preparation of suitability maps demands the association of the classifications of attributes and weights with the corresponding spatial data. Following the input data preparation, the *reclassify tool*[30]*,* part of Esri® ArcMap spatial analyst extension tools, was used to assign the values described in Table 18 to the raster data. In the specific case of the transport attribute, the Euclidean distance tool was first used to calculate the Euclidean distance to the point nearest to the highway axis for each cell, allowing the later use of the *reclassify tool*.

The scores of the attributes represented in the layers[31] are represented by a square matrix, $\boldsymbol{M_{ij}}$, of order $\boldsymbol{m}$. The aggregated layer, represented by the criteria, is a square

[28] A spatial data of point type stands for an object with a single X, Y co-ordinate. A point normally is a geographic feature too small to be displayed as a line or area.
[29] Lines are used to represent the shape and location of geographic objects too narrow to depict as areas.
[30] The *reclassify tool* reclassifies or change cell values of raster data to alternative values using a variety of methods.
[31] A layer is a geographic dataset in ArcMap.

matrix, $R_{ij,}$ of order ***m*** that can be calculated by a linear combination between the matrices M_{ij} and the weights of each attribute, w_k,

$$R_{ij} = \sum_{l=1}^{l} M_{ij}^{l} * w_k^l \quad (11)$$

where ***l*** is the number of information layers (attributes) used in the analysis of each criterion. Similarly, the final SI of the studied region, A_{ij}, is obtained by the linear combination of the R_{ij} matrices and the weights of each criterion. Its expression is given by:

$$A_{ij} = \sum_{l=1}^{l} R_{ij}^{l} * w_k^l \quad (12)$$

Where ***l*** is the matrices of criteria obtained by equation 12. The matrix operation in equations 11 and 12 is performed with the aid of the Raster Calculator tool, which yields the Suitability Index (SI) map of the state for the construction of a DGR.

3.3.2 – Weights

The weights of each attribute result from the evaluation by experts in areas of knowledge relevant to the theme using the AHP method, while the weight of each criterion corresponds to the geometric mean of the attributes associated with it. To guarantee the feasibility of comparisons between works of different authors, the weight values defined by Martins were adopted (51). Table 18 shows the criteria and attribute weights.

Table 18 – Criteria and attribute weights.

Attribute	Criterion		
	Long-Term Security	**Socioeconomic and Environmental Viability**	**Technical Feasibility**
Declivity	0.096	-	0.108
Hydrogeological Favorability	0.255	0.154	0.174
Land Use	-	0.432	0.079
Lithology	0.200	-	0.180
Mineral Resources	0.062	0.262	-
Structures	0.321	-	0.301
Transportation	-	-	0.044
Final Weight	**0.578**	**0.224**	**0.110**

3.4 – RESULTS

To simplify the analysis given the large territorial extension of MG, it was adopted the regional territorial divisions, the so-called Intermediate Geographic Regions (IGR), former Mesoregions, as presented in Figure 33. The IGR is structured around metropolises, regional capitals, or representative urban centers of each state (101). Minas Gerais was divided into 13 IGRs and Espirito Santo into 4 IGRs.

Figure 33 – Map of the Intermediate Regions.

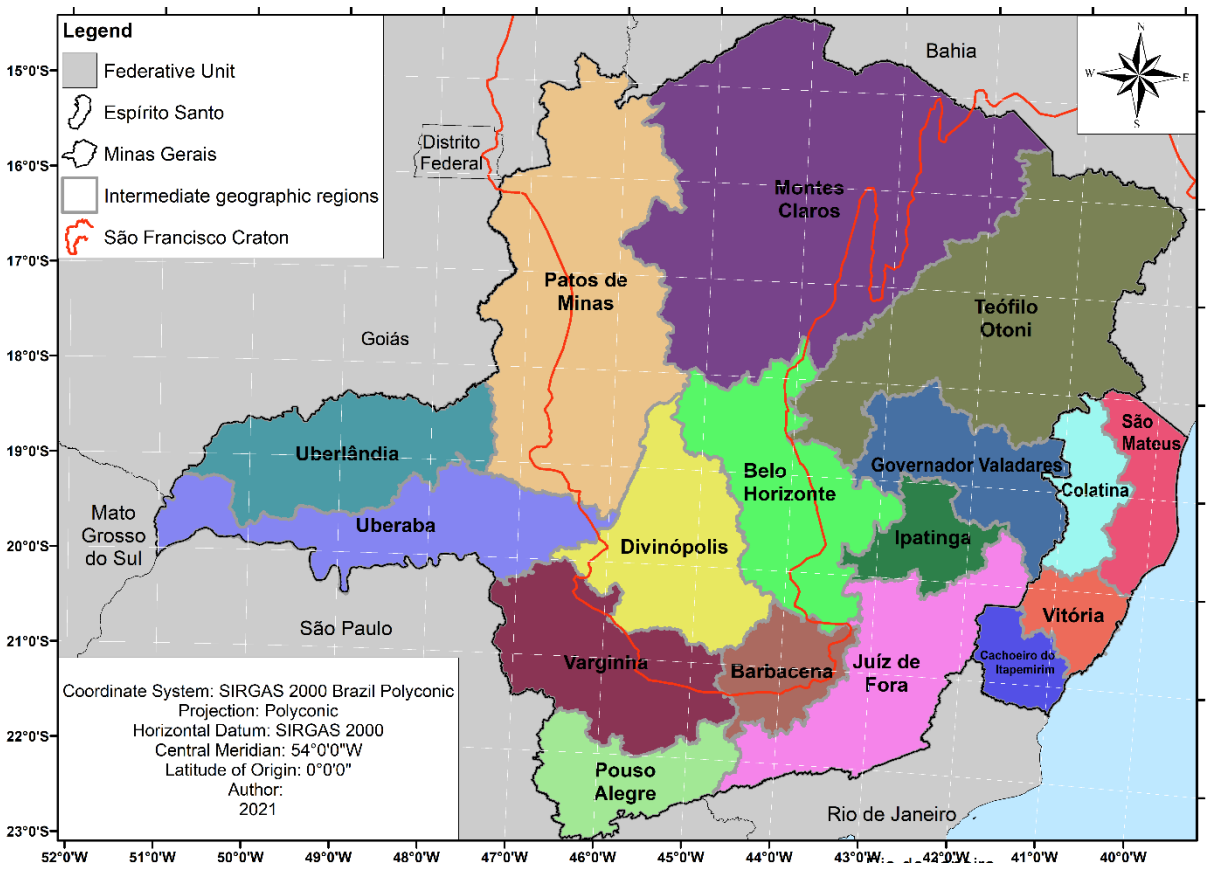

3.4.1 – Long-term Security

As shown in Figure 34, the areas classified as regular are concentrated in the eastern region of the state, while the western and northwestern parts concentrate areas classified as *2 - bad*. The eastern part, despite the classifications *4 – good* and *5 – very good* in the lithology attribute, is composed of regions of uneven terrain, with variable hydrogeological favorability and with good potential for mineral exploration, which reduces the classification of these areas.

The state of Espirito Santo has areas classified as *4 - good* in all IGRs, whereas Colatina and São Mateus have the largest areas with the classification of *4 - good*. These two IGRs have classification areas *4 - good* and *5 - very good* in hydrogeological favorability, lithology, mineral resources, and declivity attributes.

Figure 34 – Long-term safety map.

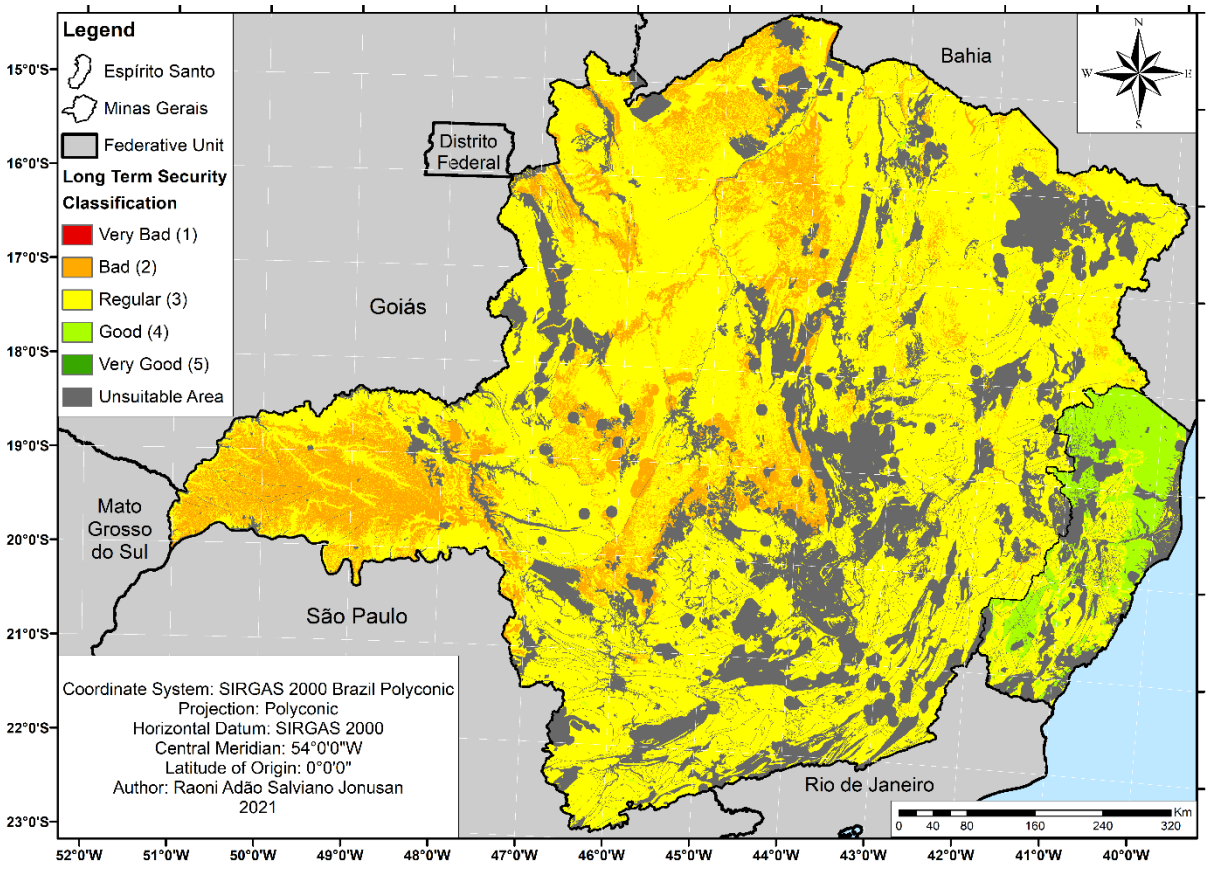

3.4.2 – Socioeconomic and Environmental Viability

As for the SEV (see Figure 35) Minas Gerais has regions classified as *2 - bad* and *3 - regular*. The areas classified as *3 - regular* are concentrated in the IGRs Uberlândia, Uberaba, Varginha, Divinópolis and Barbacena. The combination of areas rated as *5 - very good* in the lithology and land use attributes with low rated areas in hydrogeological favorability ensures the rating *3 - regular* in these IGRs.

Espirito Santo, in turn, has areas classified as *4 - good* in the São Mateus IGR due to the classification *5 - very good* in the Mineral Resources and Hydrogeological Favorability attributes and the classification *4 - good* in the land use attribute. The latter is the most important attribute for this criterion.

Figure 35 – Socioeconomic and environmental viability map.

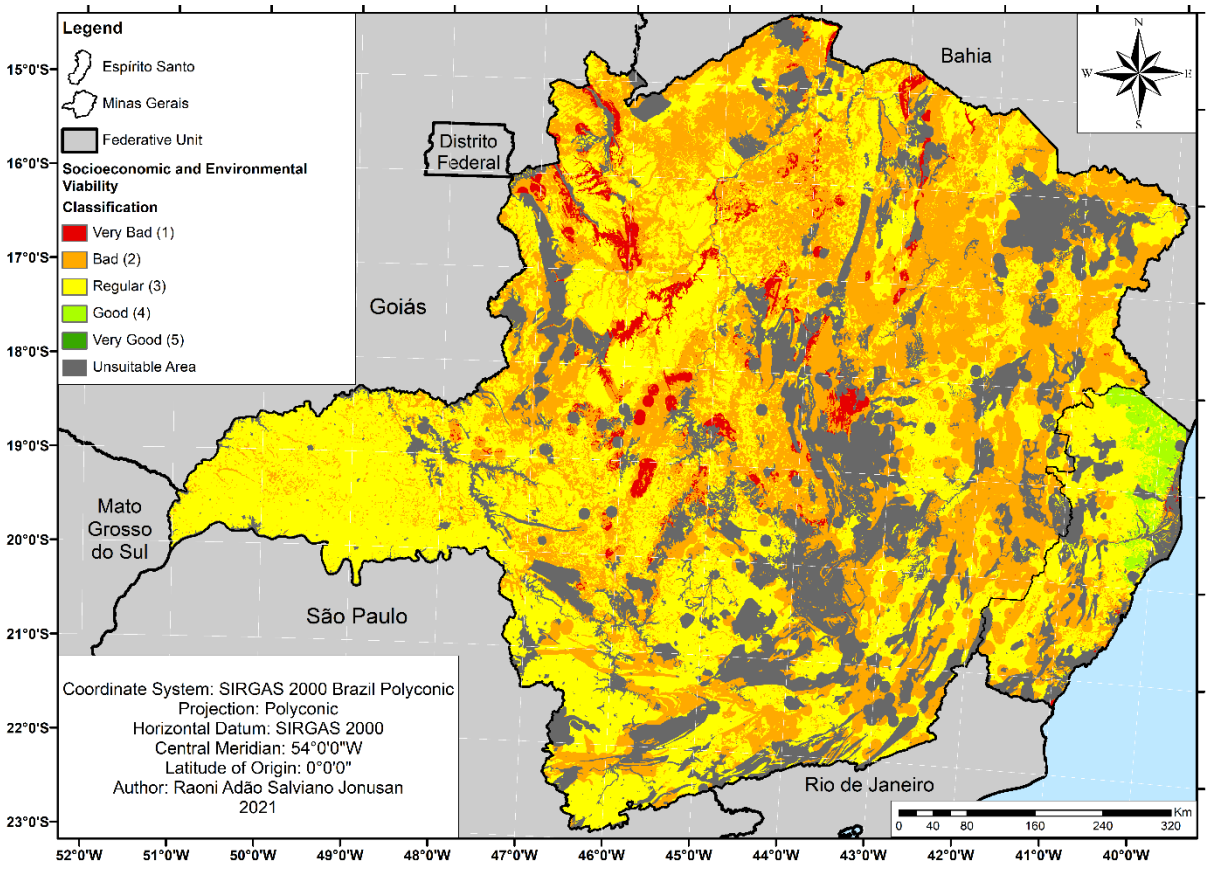

3.4.3 – Technical Feasibility

This is the only criterion in which Minas Gerais presents areas classified as *4 – good* (see Figure 36). These areas are concentrated in the regions outside the SFC. The regions internal to the craton have ratings *1 - very bad* and *2 - bad* in the main attributes of this criterion, including Hydrogeological Favorability, and lithology. The regions with classification *4 - good*, in turn, present good classifications in the lithology attribute and classification *3 - regular* in hydrogeological favorability.

Espirito Santo has areas classified as *4 - good* in all IGRs. As in the LTS criterion, the IGRs with the largest areas with this classification are found at Colatina and São Mateus IGRs.

Figure 36 – Technical feasibility map.

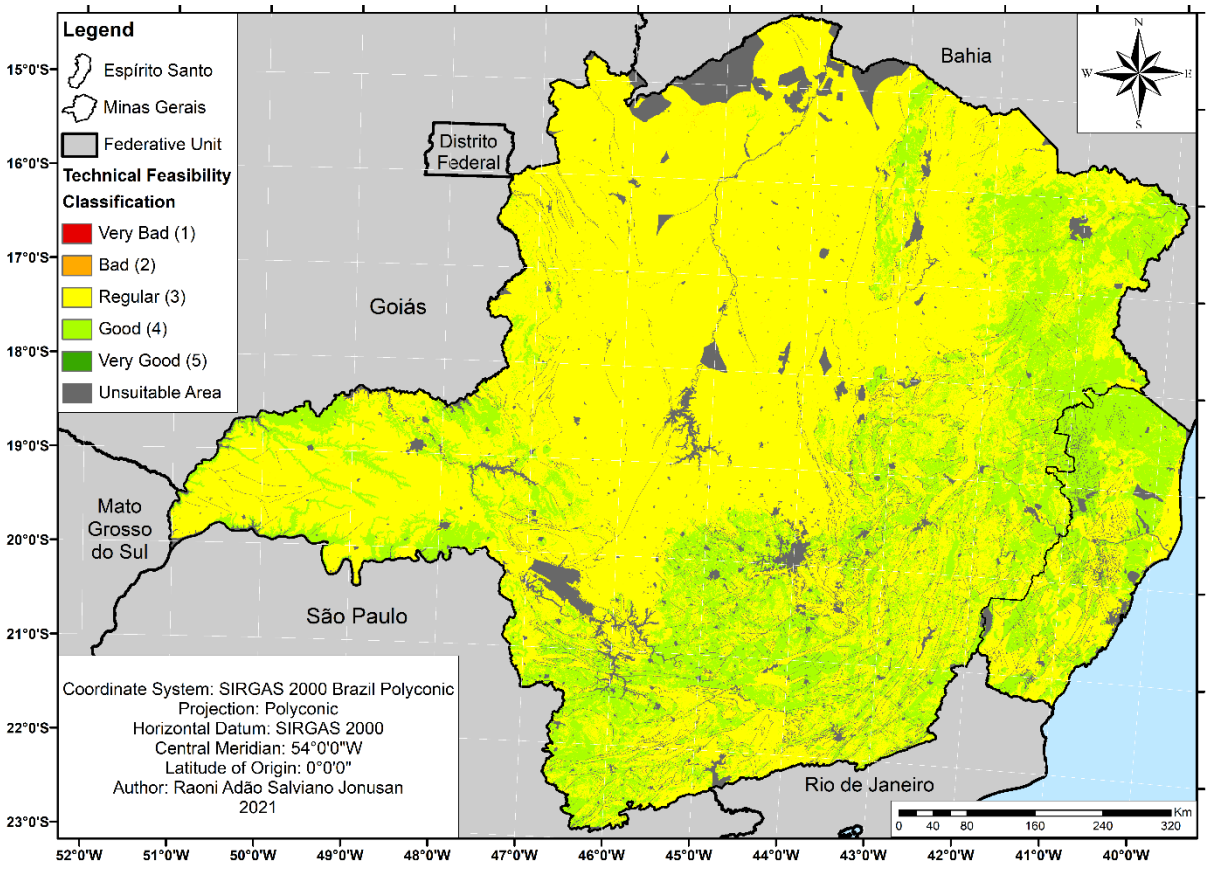

3.4.4 – Suitability Index

Espirito Santo is the single state with areas classified as *4 - good*, see Figure 37. Therefore, the analyzes presented below focused on the better classified regions.

Figure 37 – Suitability index map.

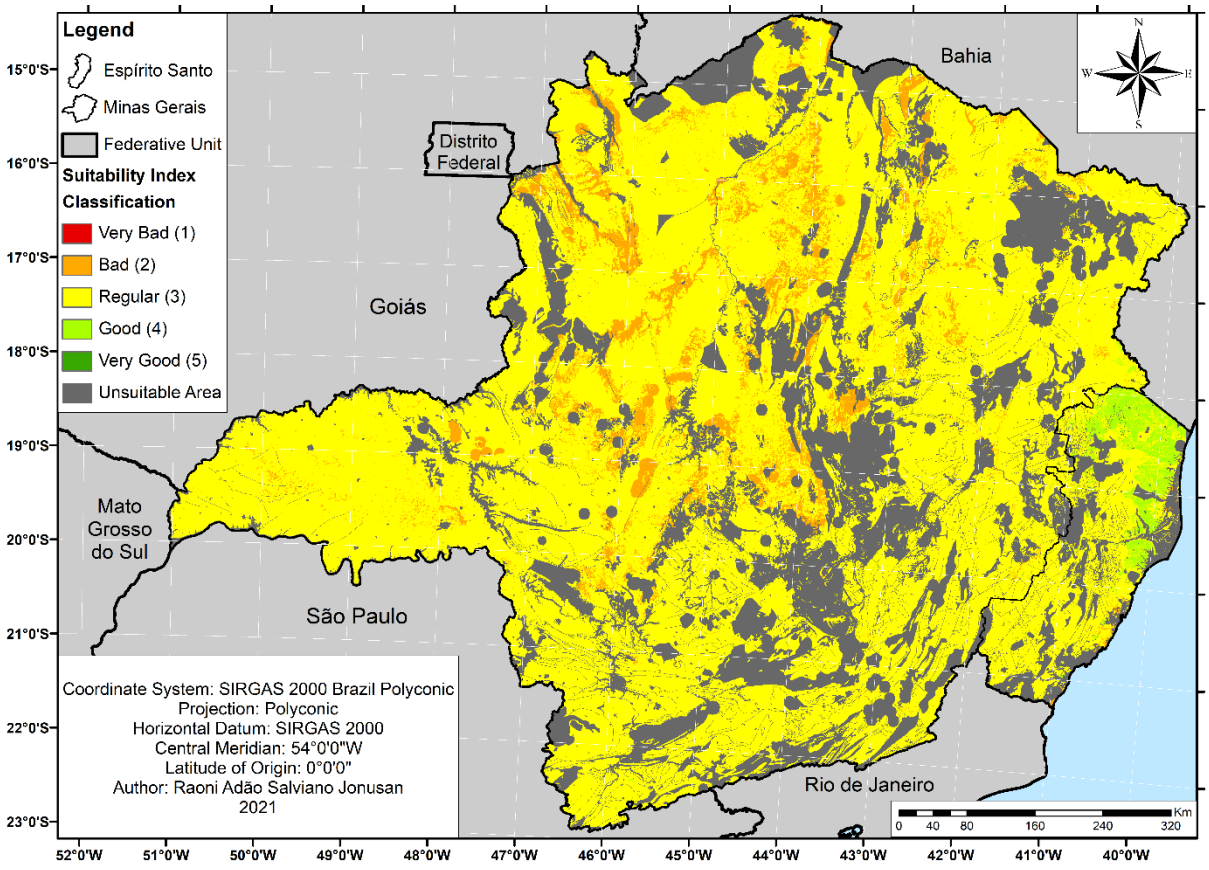

3.4.4.1 – Areas of interest

As shown in Figure 37, the regions classified as *4 - good* are concentrated in two IGRs: Colatina and São Mateus. However, not all areas are of interest since the weight of each attribute can mask unfavorable locations. It is noteworthy that the unfavorable term is applied only to the weights and criteria considered in this study. São Mateus IGR has areas with low classifications in the lithology attribute, nevertheless, they are still classified as *4 - good*.

To select the areas of interest for future studies, the following procedure was performed: All areas classified as *5 - very good* in the lithology attribute were selected in areas with SI classified as *4 - good*. This procedure was adopted to find the areas of granitoid rocks. As shown in Figure 38, these sites are concentrated in the northern region of the state, more specifically on the border of the IGRs Colatina and São Mateus.

Figure 38 – Detail of the lithology of the areas of interest.

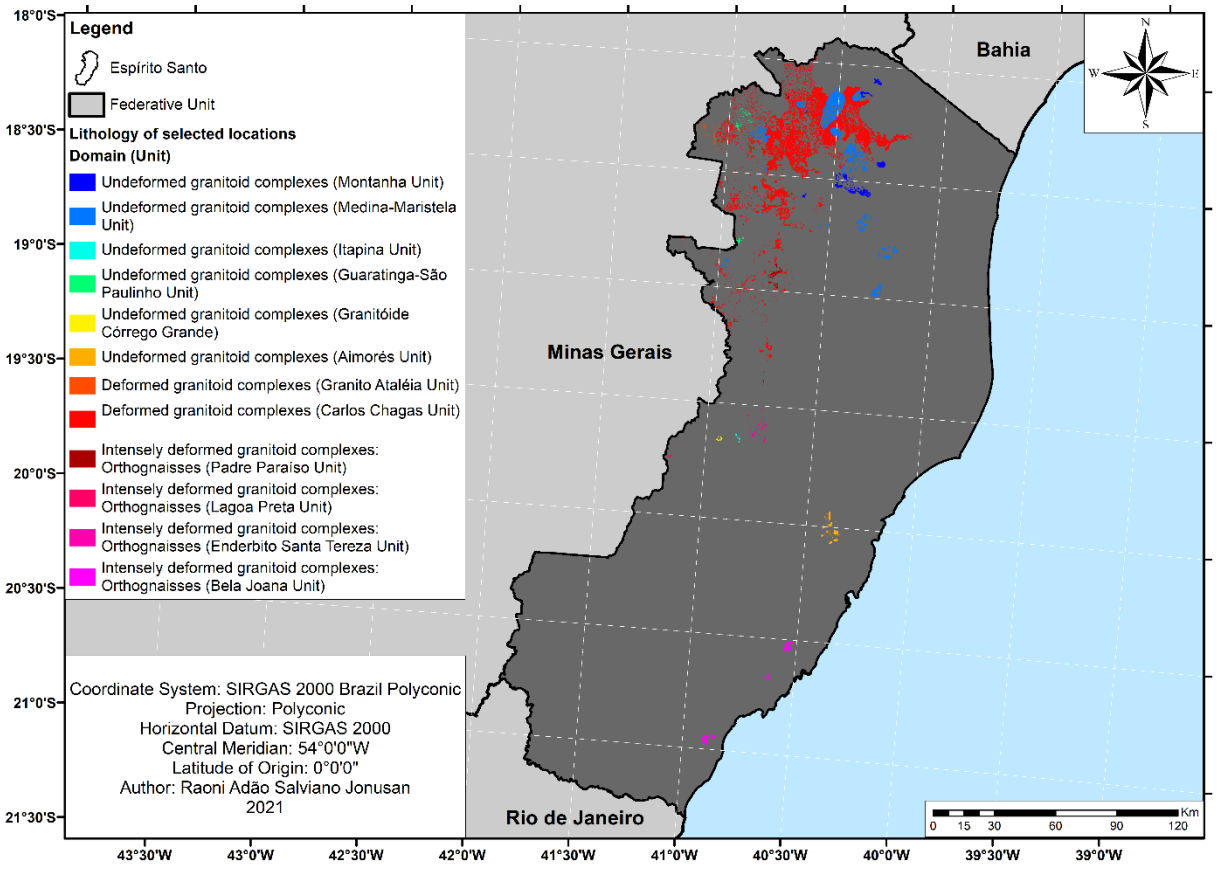

These areas can be subdivided into three according to the geological domain of the granitoid complexes: undeformed, deformed, and intensely deformed. This grouping refers to deformational events that occurred after its crystallization. According to Lopes *et al* (102), deformed granitic rocks show fluid migration when heated, while undeformed rocks do not show signs of fluid migration. Since one of the aims of a DGR is the containment or to delay the release of radionuclides in nature, this factor needs to be considered. Therefore, the selection work focused on the undeformed granitoid complexes.

The previously selected lithologies were then submitted to a new selection criterion. This criterion is the temperature of the rock at the depth of the DGR, 500 m, in this work. This selection associated with the amount of SNFN to be deposited allows the estimation of the minimum area needed for the DGR. As the amount and type of SNF are still uncertain, it was considered that SNF would be the studied MOX for Angra 2

plant. Figure 39 shows the estimated temperature of the rock at the previously selected sites. The minimum temperature found is 33.15ºC and the highest is 36.94ºC.

Figure 39 – Rock temperature at 500m map for selected locations.

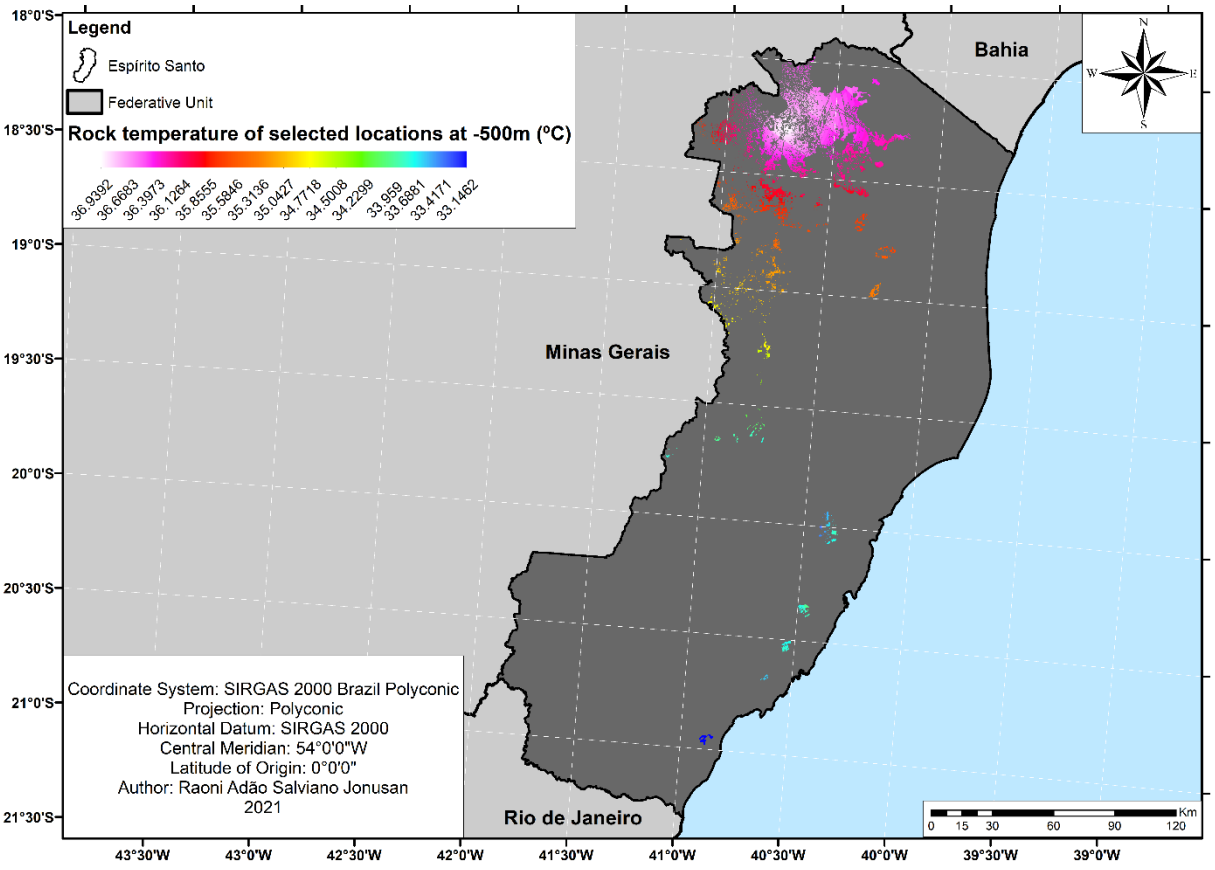

According to the proposed generation scenarios presented in detail in chapter four, and with the minimum areas for different rock temperatures presented in detail in the previous chapter, the estimated minimum area varies from 1 km² to 12.83 km², assuming minimum rock temperatures of 35 ºC and a maximum of 40 ºC.

Around the municipality of Ponto Belo, there is an area of 99.52 km² comprising the Medina-Maristela Unit of undeformed granite complexes, as shown in Figure 40. In addition to being an area composed of undeformed granitoids, this area features:

- A low hydrogeological favorability,
- Smooth to undulating terrains,

- Areas with low agricultural potential (78).
- Areas already impacted, composed of pastures.
- Paved highways nearby.
- Although the area has potential for the exploration of granite, it is considered that this potential is low, given that these granites are of low commercial interest (103).

Figure 40 – Detail map of candidate areas.

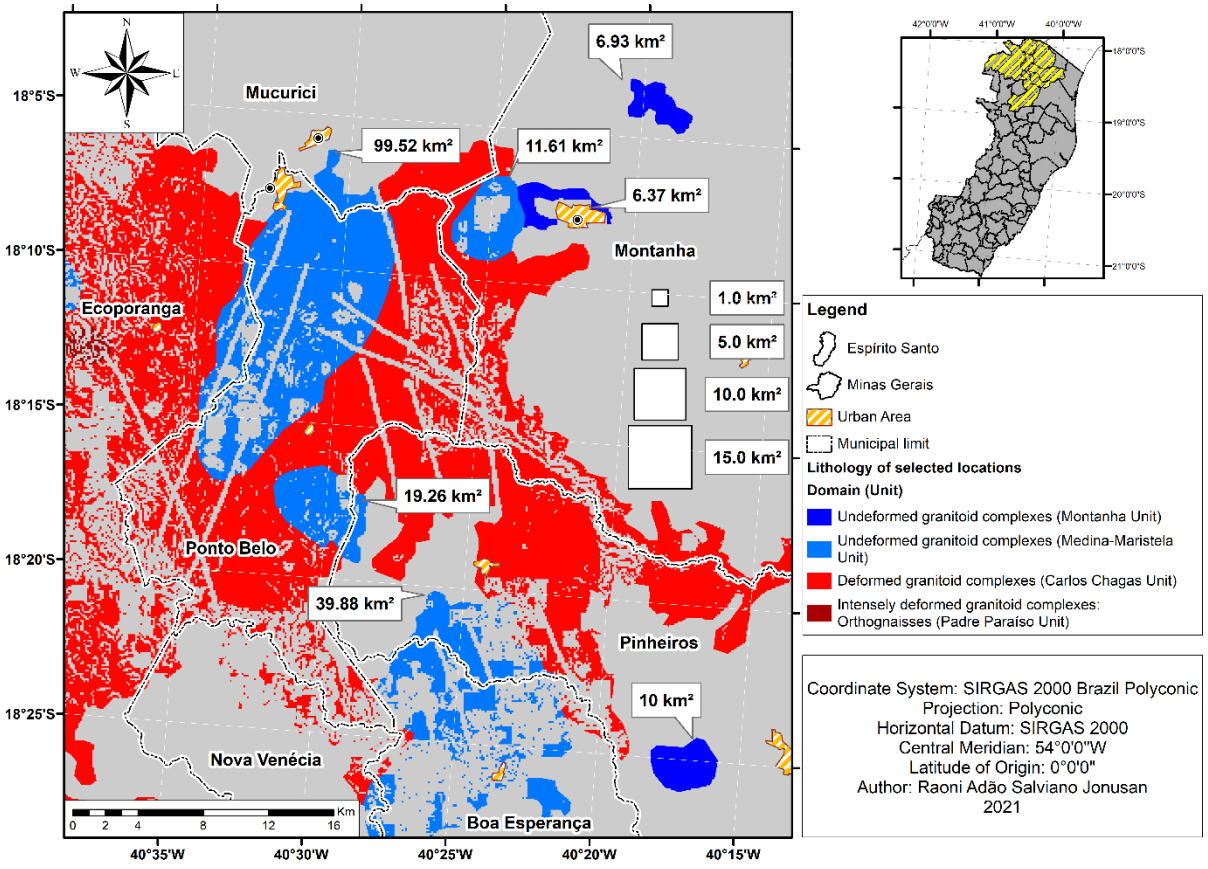

This area, together with smaller areas with similar characteristics in the vicinity, is considered promising for more detailed studies. Among future studies, those related to earthquakes, local rainfall, detailed hydrogeological analyzes, and social acceptance are suggested. These areas could be used for the installation of an analogous underground laboratory or the installation of a DGR if the Brazilian government chooses to use granitic rocks as the host rock. However, further studies would be needed to characterize the area and ensure the security of the repository. It is noteworthy that these results do not mean that this location should be chosen for the

construction of a Brazilian DGR, being only the result of an academic exercise of application of a method of selection of areas suggested for Brazil. For example, other rock types that are also considered internationally to host a DGR, such as clay rocks, were not considered. New studies must be carried out to improve and adjust the methodology.

3.4.4.1.1 – State laws about the disposal of SNF

Minas Gerais has prohibitive legislation about the disposal of nuclear waste. Law No. 9,547 of 12/30/1987 "Prohibits the installation of atomic waste or radioactive waste deposits in the state of Minas Gerais" (104). An exception is granted to low activity waste: "The provisions of the article do not apply to low activity waste, originating from equipment used in the state or from mining and processing of ores, which occur in the subsoil of the state of Minas Gerais.". In addition to this law, Decree 40.969 of 03/23/2000 prohibits the entry of radioactive waste into the state of Minas Gerais if it is outside the exemption limits established by CNEN and whose reuse is inappropriate or not foreseen (105).

The state legislation of Espiríto Santo, approved in the same period as that of Minas Gerais, in turn, is less restrictive. Law No. 4,033 of December 23, 1987 (106) establishes that:

> "The implementation in the State of Espírito Santo and the oceanic islands under its jurisdiction, of atomic plants for the production of nuclear energy, of plants for the enrichment of uranium, of plants for the reprocessing of nuclear fuels and deposits for atomic waste will depend on authorization from the Legislative Assembly and, also, on a popular referendum through the holding of a plebiscite, listening to the group of state voters."

State legislation must be analyzed in conjunction with relevant federal legislation during the selection process either to mobilize political resources for a change in local legislation or to mobilize political and popular resources for the approval and acceptance of the project by the population involved.

Recently, the current Attorney General of the Republic filed Direct Actions of Unconstitutionality requesting the annulment of the state and Federal District legislation that, as well as the legislation of Minas Gerais, restrict or prevent the implantation of NPPs, the reprocessing, or the construction of radioactive waste repositories. In total, nineteen lawsuits were filed referring to the states of Acre, Alagoas, Amapá, Amazonas, Bahia, Ceará, Distrito Federal, Goiás, Maranhão, Mato Grosso, Pará, Paraíba, Paraná, Pernambuco, Piauí, Rio de Janeiro, Rio Grande do Norte, Rondônia and Roraima (107).

3.5 – CONCLUSION

This part of the work focused on the selection of sites for the installation of a DGR in crystalline rocks. Other types of rocks were not considered since the method was developed for hard rocks. However, given the Brazilian territorial extent and its diversity of geological environments, the selection of sites for repositories based on other types of rocks should not be ruled out. This work modified the method proposed by Martins to avoid the use of point and line data types. Two modifications were made. The first consisted of the use of the Euclidian distance from the axis of the transportation network, including the railway network, instead of classifying the transportation network by the administrative responsible body. Secondly, instead of using point data for mineral resources, it was used the ARIM dataset.

Minas Gerais does not have areas considered as candidates for additional studies. Espírito Santo, however, has large areas considered as good candidates for future studies around the municipality of Ponto Belo. The candidate areas are composed of undeformed granites.

For future works, some other criteria could be added to the analysis process, such as the acceptance of the local population, the focus on the selection for lands of the Brazilian State, and the consideration of occurrence of natural disasters, including earthquakes.

4 – COST ESTIMATION OF THE BRAZILIAN NUCLEAR FUEL CYCLE BACK-END

4.1 – INTRODUCTION

How much it will cost? This question acquires another significance when projects without direct revenues are considered, such as the disposal of HLW and SNF. The disposal of these wastes is a cost resulting from the nuclear power generation process. There is a considerable time gap between the generation of waste and its disposal since the disposal activities can continue for a long time after the end of the generation of energy (108).

Over the last decade, different organizations have performed cost estimates for the back-end of the nuclear fuel cycle. When reviewing the specific literature (109–123), however, it is clear that different assumptions used - discount rate, types of waste, choice of the fuel cycle, etc. - create difficulty for comparison of estimated costs in each study (108, 124, 125). In addition to different assumptions, the lack of data for costs of deposition in a geological repository is evident, and when considered together with country-specific policies, practices, regulations, and the disposal timeframe involved, it is clear that cost estimates have many uncertainties (124). Although disposal of nuclear waste has been researched worldwide since 1957 (7), the first operational repository will, probably, be the ONKALO facility in Finland around 2025 (17), followed by Forsmark in Sweden, and CIGEO in France, both planned for the 2030s (12, 18, 19, 126).

4.1.1 – The Brazilian nuclear program

The Brazilian nuclear program for power generation consists of two NPPs in operation, Angra 1 and Angra 2, and a third under construction, Angra 3, at the Almirante CNAA, found in the city of Angra dos Reis, Rio de Janeiro state. The Angra complex is marked by delays and funding problems. As Spektor points out, the Brazilian “nuclear policy evolved from a low base and in a stop-and-go fashion in the face of political, managerial, and financial hurdles” (127). Angra 1, whose construction started in 1971 and the commercial operation started in 1985 (128), is at the end of its useful life and

is going through the procedures for the extension of its operating license for another twenty years. Angra 2, whose construction started in 1976 and the commercial operation started in 2001 (128), has the decommissioning projected for 2044. Angra 3 had its construction start in 1984, with commercial operation planned for 2026 (129). Besides Angra 3, the Brazilian government is planning the construction of six to eight new NPPs until 2050 (130).

The national nuclear policy considers that the SNF is not a waste and must be stored safely for future reuse (4). However, there are no official projects for the implementation of a national reprocessing center (131) or international partnerships for the SNF to be reprocessed abroad. Currently, the SNF already produced is stored, safely, in cooling pools inside Angra 1 and Angra 2 plants, with part of the spent fuel being transferred to another initial storage unit, the UAS, where it will remain for at least 40 years.

The vagueness associated with the fuel cycle to be effectively adopted also results in a lack of definition around the financing of the final disposal of the SNF. In Brazil, contrary to other countries, there is no obligation to create a specific fund to cover the costs of disposal of radioactive waste. Currently, Eletronuclear has a specific fund to cover the expenses of decommissioning Brazilian NPPs and temporary management of the SNF, after decommissioning, while the decision about the final repository is not taken by CNEN, following the relevant legislation. (37, 38).

Currently, Eletronuclear maintains a specific fund to cover the expenses of decommissioning Brazilian NPPs and temporary management of the SNF while the decision about the final repository is not taken by CNEN, following the relevant legislation. In addition, Law 10,308 of 2001 establishes that "the intermediary and final deposit service of radioactive waste will have their respective costs indemnified to CNEN by the depositors, according to the table approved by the CNEN Deliberative Committee" and that the costs of the said table will take into account " the cost of licensing, construction, operation, maintenance and physical security of the warehouse." (42). However, as the SNF is not considered waste, there are no reference values for the reimbursement to be carried out by Eletronuclear to CNEN.

Cost estimation is a crucial step of any project, being essential in the planning of expense and analysis of alternative options. To guide the cost estimation task, the Organization for Economic and Co-operation and Development/ Nuclear Energy Agency (OECD/NEA) published, in 2013, a study related to the economic aspects of the back-end of the nuclear fuel cycle to “develop a more in-depth understanding of economic issues and methodologies for the management of spent nuclear fuel and high-level waste from commercial power reactors”(124).

The purpose of this chapter is to estimate the back-end cost of the Brazilian nuclear fuel cycle employing the Levelized Cost of Energy (LCOE). The nuclear fuel cycle was modeled with the use of Model for Energy Supply System Alternatives and their General Environmental Impacts (MESSAGE) tool. The uncertainties about the nuclear policy were coped with the use of scenarios and Monte Carlo simulations. The scenarios proposed to encompass two nuclear fuel cycles (open and partially closed) and three possibilities about the number of NPPs.

4.2 – METHOD

The choice of cost estimation method depends on the maturity of the waste disposal program, as well as on factors such as the purpose of the estimate, program stage, availability, and reliability of data, assumptions adopted, staff, and time available to prepare the cost estimate (108, 115, 132–134). In general, there are 3 methods for estimating costs, shown in Figure 41 from the least detailed to the most detailed (108, 115, 134):

- analogy: this method uses the costs of similar programs for the estimate. Colloquially "It's like one of those".
- parametric: also known as statistical method, which uses a database of several similar programs to statistically estimate costs. Nicknamed "This pattern is kept".
- engineering: It is the technique with the most detailed estimates, it uses cost data from each part of the program for the estimate. Colloquially called "is made of these".

Figure 41 – Cost estimating methods as a function of program maturity. Adapted from(133).

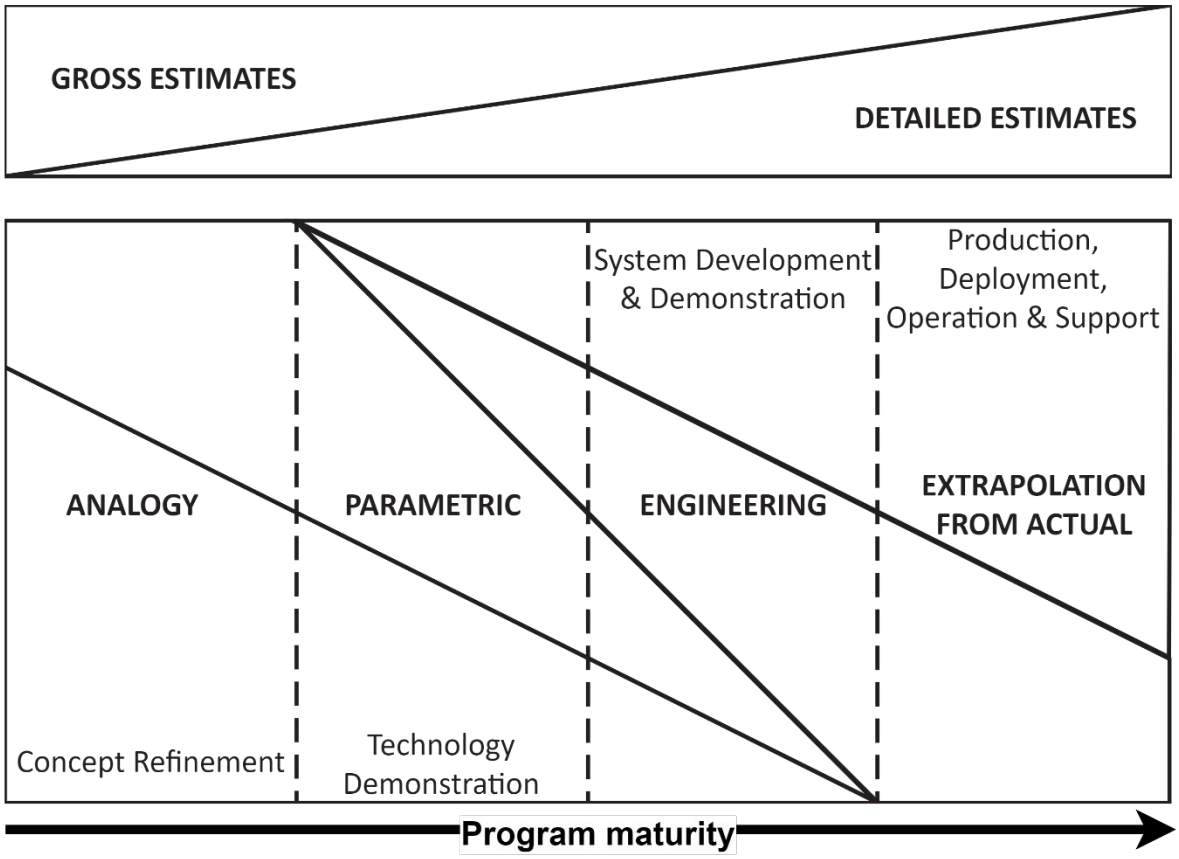

As there are no details on the Brazilian waste disposal program, the analogy method will be used. The advantage of this method is that it is based on data and experience of existing programs, which makes the estimation process fast and possible with little data and staff. However, as the data used are not specific to the proposed program, it is necessary to find program data as similar as possible. Furthermore, the resulting estimate is insensitive to the real drivers of cost and design changes (108, 115, 132, 134).

Due to the lack of definition of the Brazilian nuclear program on the choice of the nuclear fuel cycle and the final number of NPPs, it was decided to create three strategic scenarios with two variations of each scenario. The scenarios are structured around the final number of NPPs to be built in Brazil. The variations of the scenarios are the possible fuel cycles to be adopted.

Each material balance of each scenario/variation is then modeled by aiding the energy planning tool MESSAGE, having as output the amount of electrical energy produced

and the amount of spent fuel generated. The amount of SF generated is used for three deterministic cycle cost estimates, carried out with the aid of the parameterizations of an OECD/NEA study (124): a reference estimate, a low cost, and a high cost one. Each estimate then serves as inputs to a stochastic cost estimate, performed with the aid of a Monte Carlo simulation. Figure 42 shows the cost estimate flowchart.

The choice for the OECD/NEA study was based on the following reasons:

- There is little data about the waste disposal costs since only three projects have the beginning of the planned operation for the next 15 years: Olkiluoto (Finland) (17), Cigéo (France) (18), and Forsmark (Sweden) (19).
- Questionnaires were answered by the national authorities of the NEA member countries about the waste disposal costs, including the most advanced countries in the construction/operation of a geological repository.
- Parameterization of costs on a common basis. Capital and operation and maintenance cost curves were created for the main facilities in the fuel cycle. The curves for each facility are presented in Annex B.
- The parameterization was conducted in three cost modalities: reference, high and low. This makes it possible to use stochastic techniques to estimate the value of the cost and to decide about contingency funds.

Figure 42 – Cost estimation flowchart.

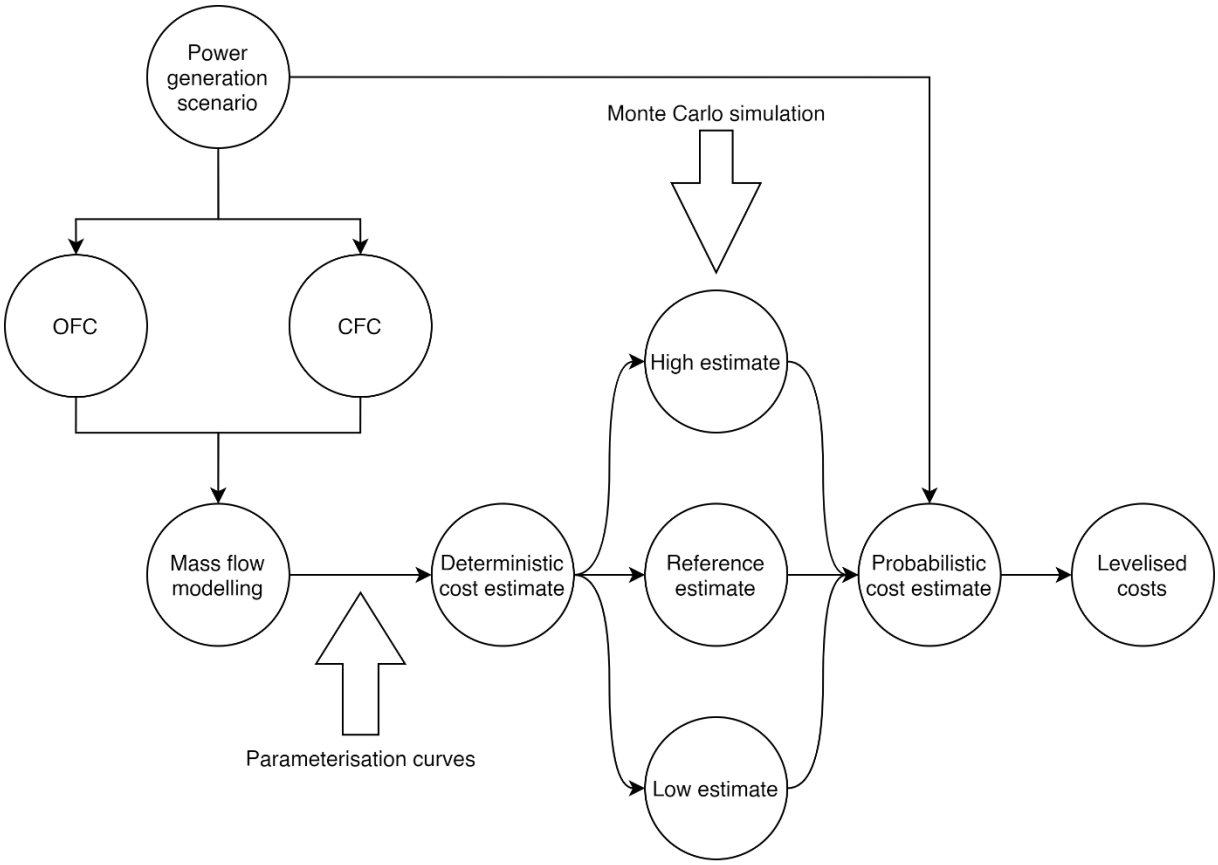

4.2.1 – Scenarios

To deal with the uncertainties related to the final number of NPPs and the nuclear fuel cycle, three nuclear generation scenarios were created and each of them was associated with a fuel cycle option. These strategic scenarios aim to answer the question: What will the cost of the following choices be? The scenarios are general and aim to point out the possible economic consequences of future political decisions on the choices that Brazil faces concerning the continued use of nuclear energy. Given their general character, the scenarios are not optimized and consider that both commissioning and decommissioning occur overnight. Figure 43 and Figure 44 show, respectively, the implementation and decommissioning calendar of each installation considered, and the general operating calendar of all NPPs considered.

Figure 43 – General timetable for each scenario.

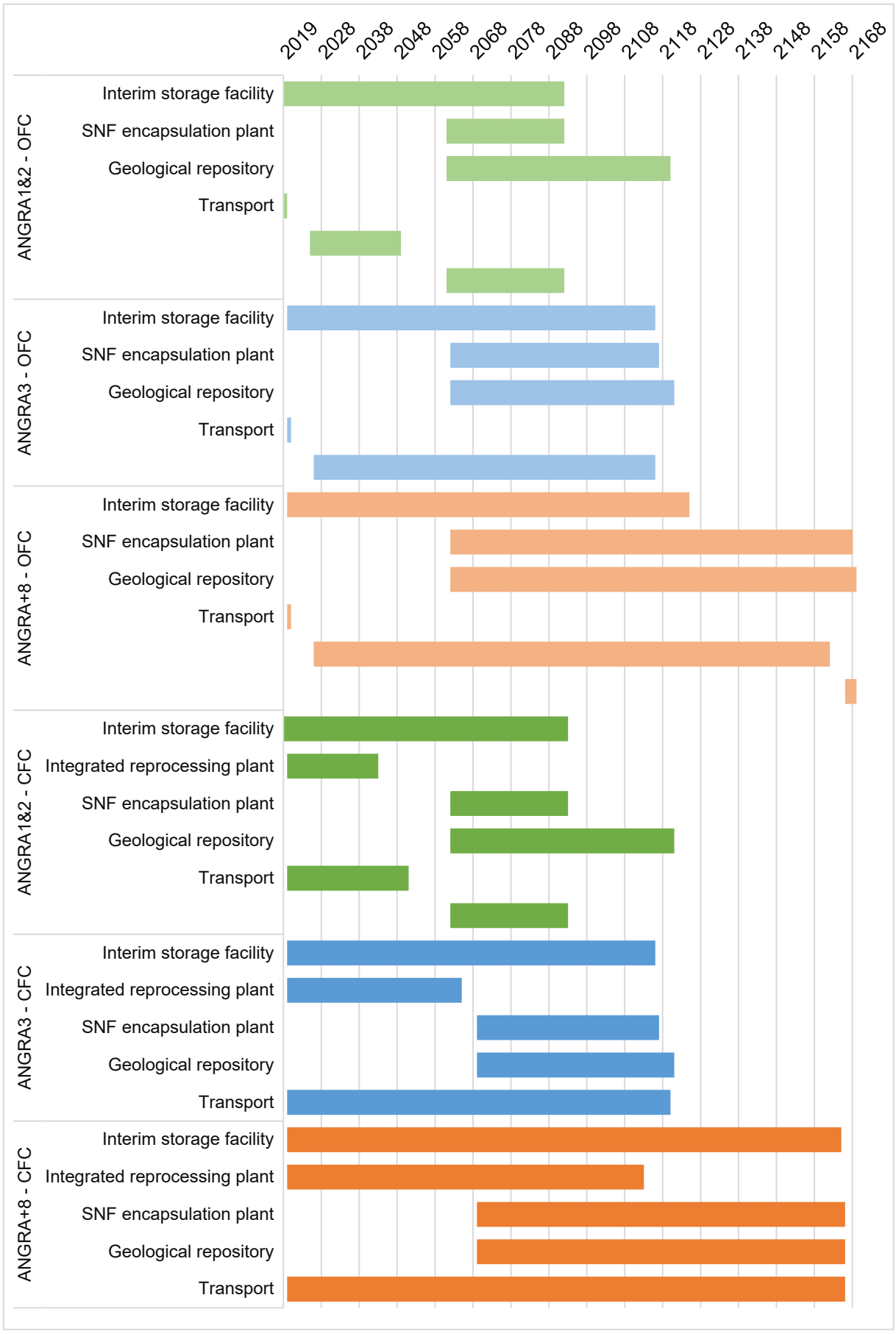

Figure 44 – Timetable of operation of nuclear reactors.

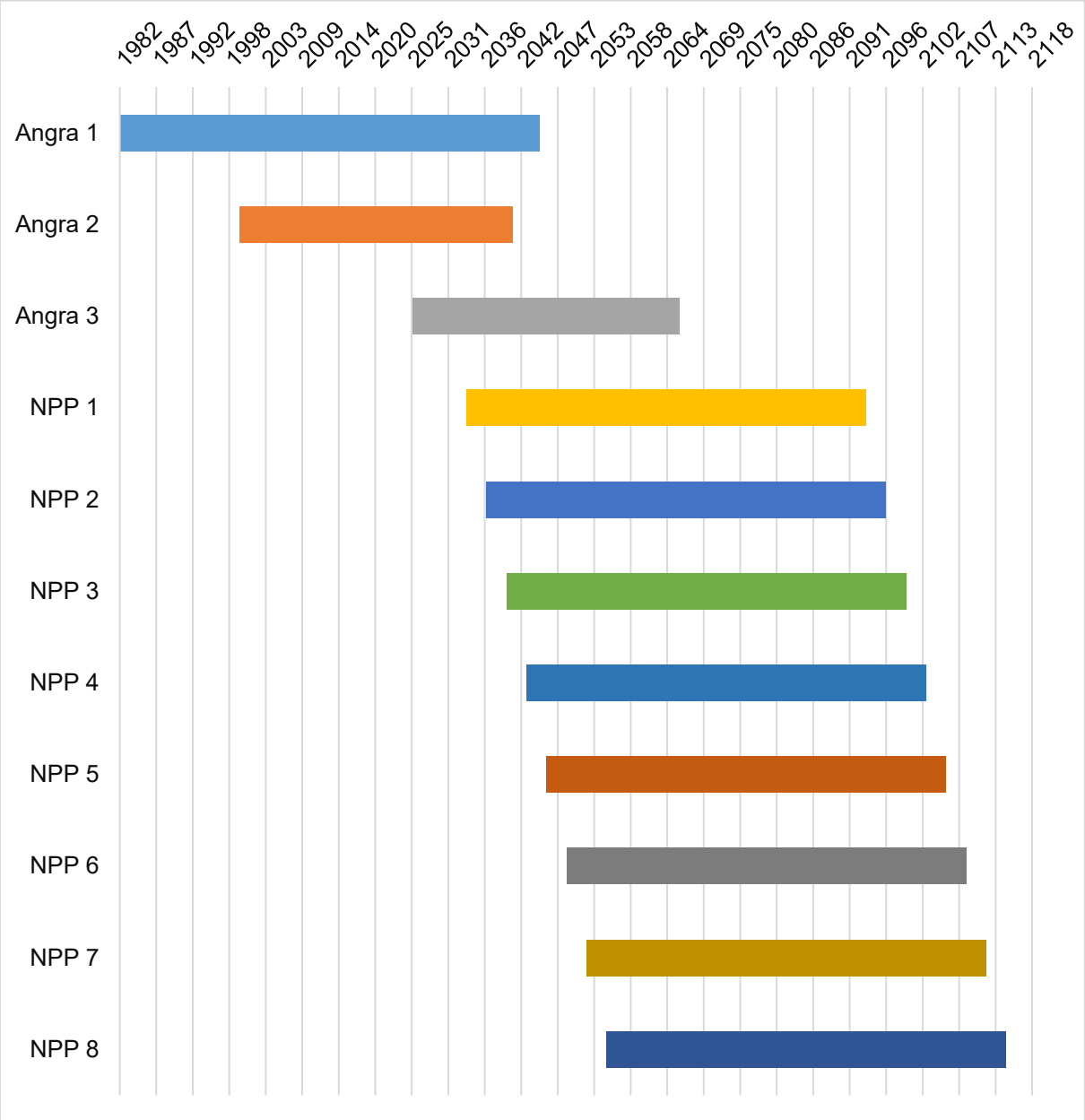

4.2.1.1 – ANGRA1&2 scenario

The first scenario, called ***ANGRA1&2***, can be considered a pessimistic scenario. This scenario considers that no other NPP, in addition to those in operation - Angra 1 and Angra 2, will be built in Brazil. This scenario was built considering the historical financing difficulties faced by the nuclear sector in Brazil. The amount of energy generated by the NPPs considered in this scenario is shown in Figure 45. Angra 1

would have its useful life extended by 20 years, being decommissioned in 2045, while Angra 2 would remain in operation until 2042.

Figure 45 – Electricity supplied, ***ANGRA1&2.***

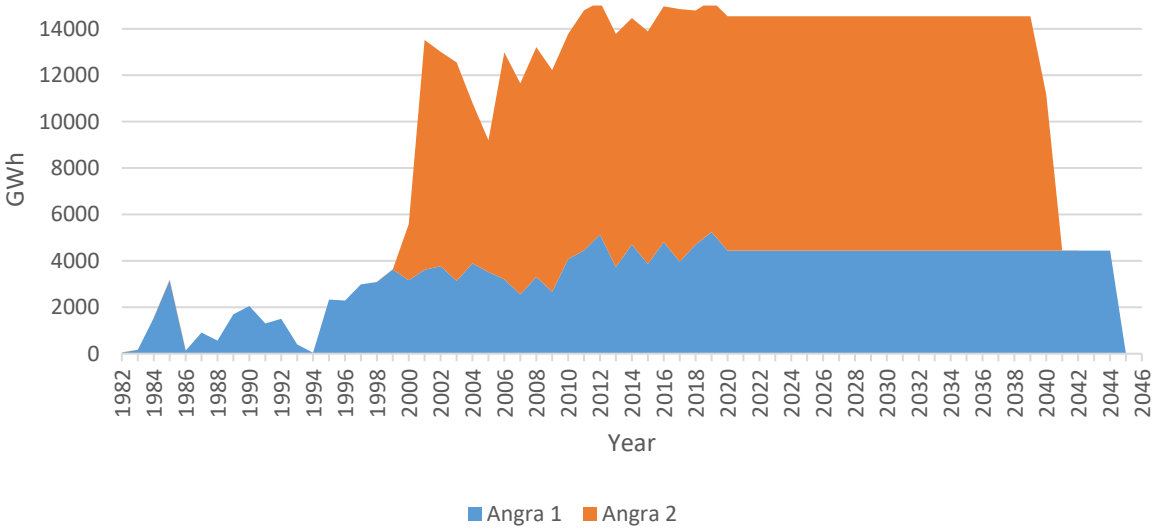

As a guide for the construction of this scenario, the "Audit in ongoing actions, promoted by CNPE, MME, Aneel, Eletronuclear and Eletrobras for the resumption or discontinuity of UTN Angra 3", process 036.751/2018-9, promoted by TCU, in which the following judgments were issued (135):

- It was decided that detailed documents should be presented to the Court to ensure the feasibility of the project.
- That the costs of continuing the construction of Angra 3 NPP should be compared with the costs of its cancellation.
- Recommended, of a non-mandatory nature, the holding of public consultation with agents in the electricity sector about the resuming or cancellation of Angra 3 NPP, both with specific studies to support the consultation process.

These judgments are based on the following arguments:

- Angra 3's cost escalation in relation to its twin sister, Angra 2. Angra 3 is projected to cost 40% more than Angra 2.
- The huge delay in the implantation of Angra 3. In 2021 the project completed 37 years and, given the start of works until the new date scheduled for entry into operation in 2026.
- The financial difficulties faced by Eletronuclear.
- Studies by the consulting firm PSR that show savings of $3.1 billion over 35 years with the cancellation of the project in relation to the continuity of its construction.

Allied to these factors, it was considered the resistance, not measured by opinion polls, of part of the population to the construction of new NPPs and legal problems for locations selected for new plants, as is the case in the state of Pernambuco. This state, indicated as the location for the installation of the next NPPs in Brazil (136, 137), prohibits the construction of NPPs in its territory (138). In addition, there are articulations of social movements to prevent the state legislation of Pernambuco from being changed (139, 140).

4.2.1.2 – *ANGRA3* scenario

The intermediate scenario, called ***ANGRA3***, considers that the challenges for completion of NPP Angra 3 will be overcome. It was considered that the status of 60% of the construction works is a crucial factor for the completion of the works, in addition to the need for the national electric system for dispatchable and highly available energy sources (135, 141). However, it was considered that no new NPP would be built after Angra 3. In this scenario, Angra 3 would start to operate in 2026 and would be decommissioned in 2063 (129). Angra 1 and Angra 2 would continue with the same operation dates considered in the previous scenario. Figure 46 shows the foreseen amount of energy supplied annually by the ***ANGRA3*** scenario.

Figure 46 – Electricity supplied, ***ANGRA3.***

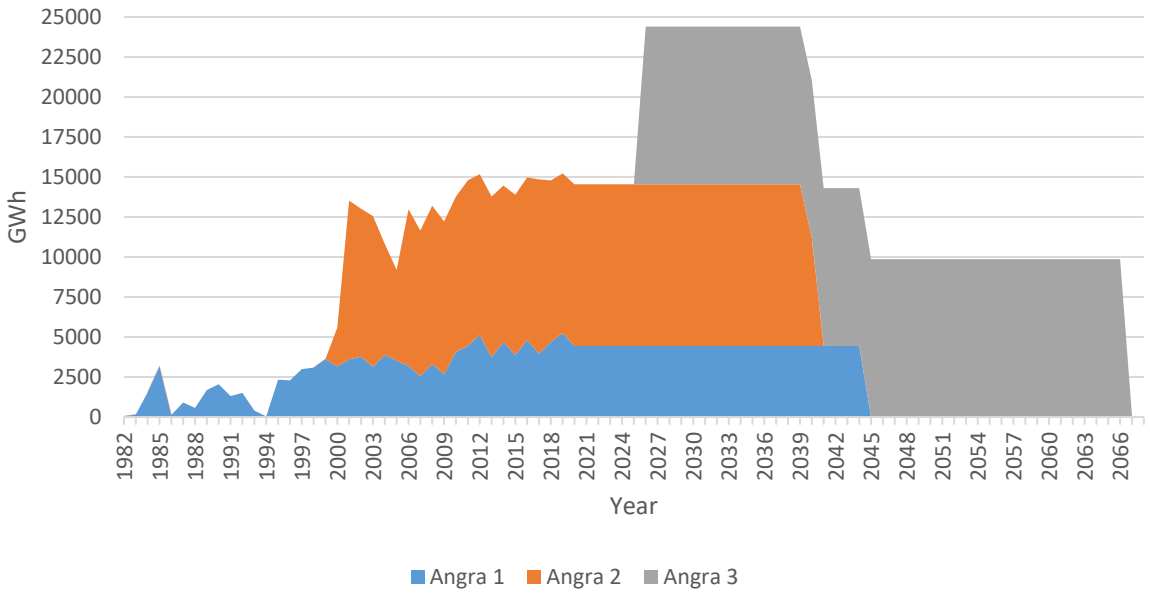

4.2.1.3 – *ANGRA+8* scenario

The optimistic scenario, called ***ANGRA+8***, was built based in part on the premises of the ANGRA3 scenario. In this scenario, eight new NPPs would be built in addition to Angra3, adding a total of 10 GW of installed capacity to the Brazilian electricity sector. This scenario is based on studies by the EPE, which, at various times, considered the construction of 6 (70) to 14 (142) new NPPs in Brazil. The first of the eight plants would come into operation in 2034, eight years after Angra 3, with the next seven NPPs being inaugurated at a three-year interval. In this way, the last NPP would come into operation in 2055 and would be decommissioned in 2114. Figure 47 shows the foreseen amount of energy supplied annually by the ***ANGRA+8*** scenario.

Figure 47 – Electricity supplied, ***ANGRA+8.***

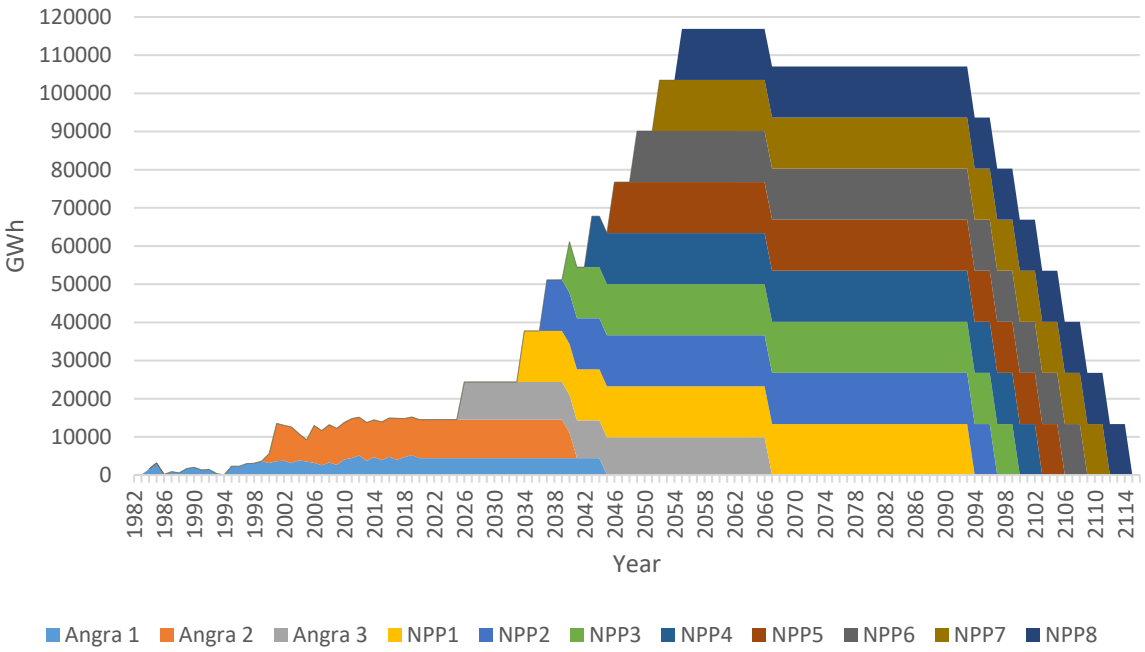

4.2.2 – Nuclear Fuel Cycles

Two nuclear fuel cycles were considered for each scenario. The first denoted Open Fuel Cycle (***OFC***) (Figure 48) consists of a once-through fuel cycle with a direct disposal route. After burnup, the SNF is transferred to initial storage, i.e., the cooling pools for seven years. After that, it is transferred to interim storage staying there for forty-three years before its encapsulation for final disposal.

Figure 48 – OFC route. Adapted from (124).

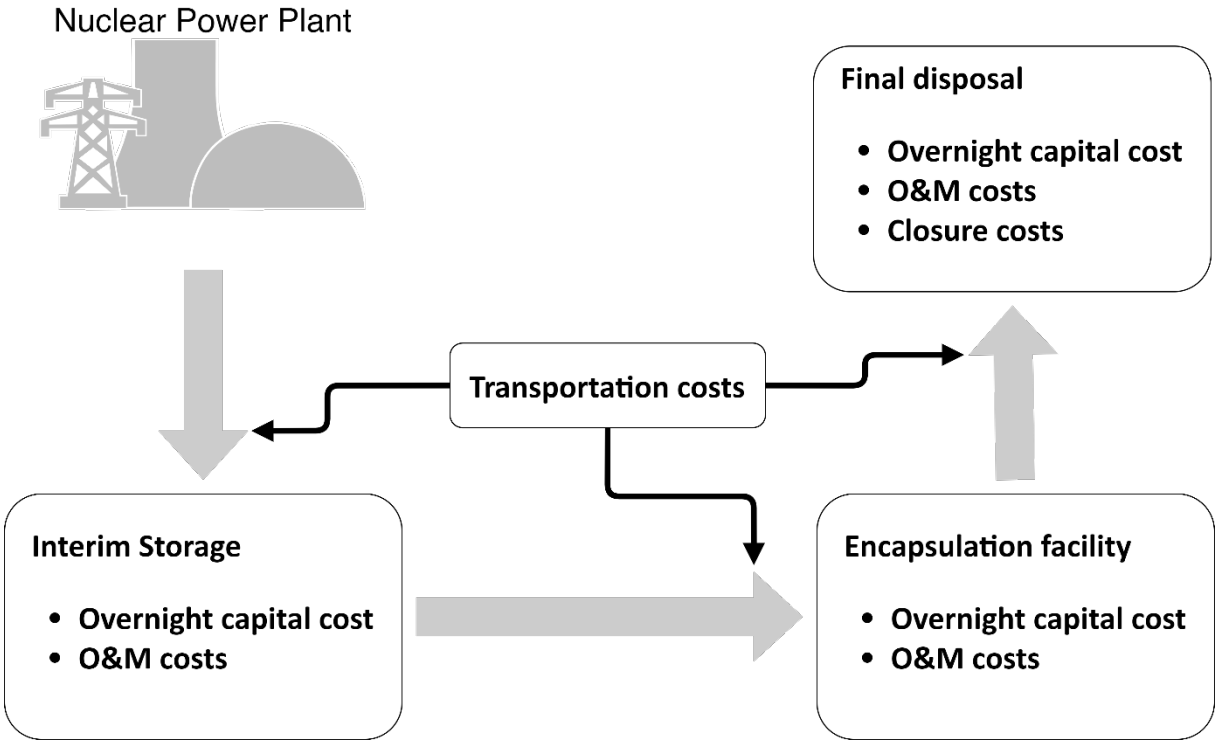

The second route denoted Closed Fuel Cycle (***CFC***), (Figure 49) includes a partially closed fuel cycle, in which SNF is carried to reprocessing plant after seven years under initial storage where Plutonium may be recycled for fabricating of Mixed Oxide Fuel (MOX). Other products generated at reprocessing plants are considered waste, such as reprocessed uranium, fission products, and minor actinides. Nuclear waste from reprocessing must be stored for fifty years, encapsulated, and sent to the final disposal. After burnup, MOX fuel must be sent to the cooling pool, remaining there for seven years. After that, it is transported to interim storage staying there for a total of fifty years. Finally, MOX SNF must be encapsulated and transported to the final disposal.

Figure 49 – CFC route for LWRs with MOX recycling in LWRs. Adapted from (124).

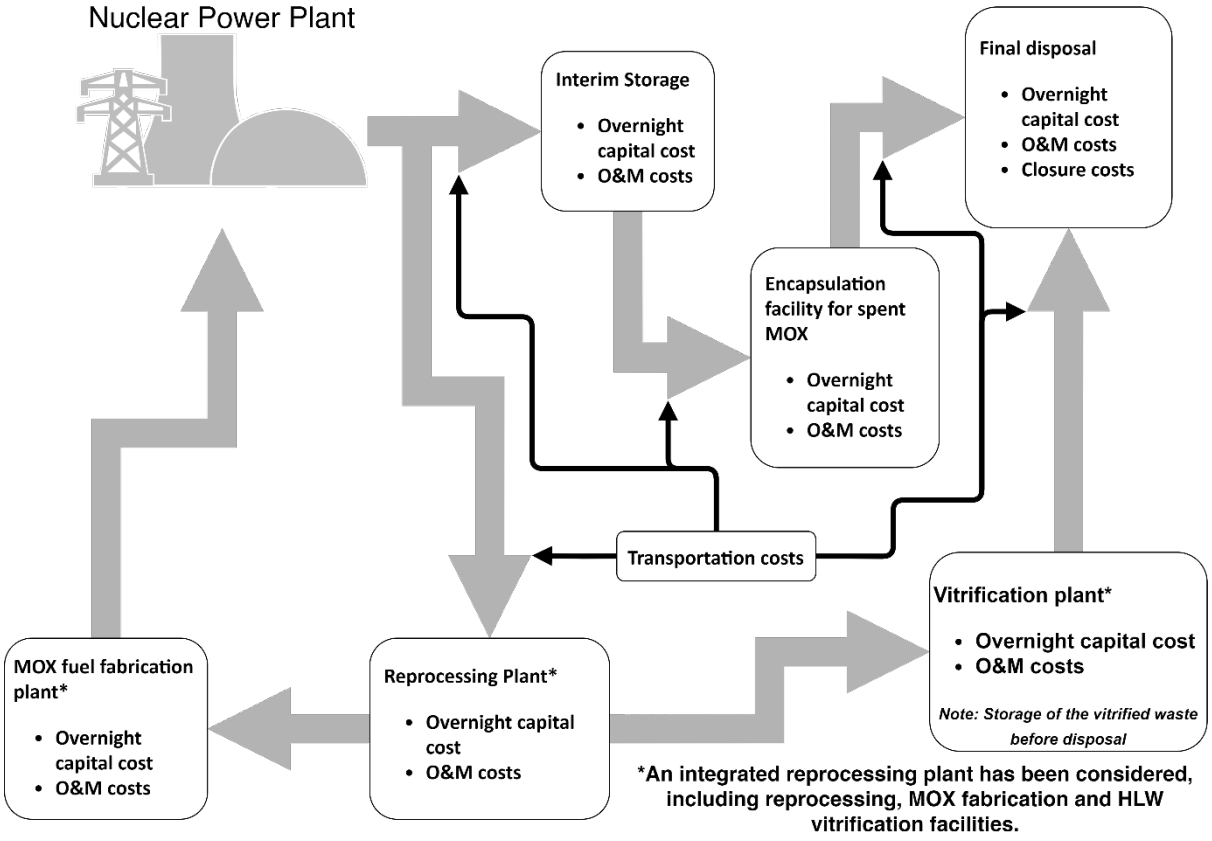

4.2.3 – Material Flows - MESSAGE

To estimate the back-end LCOE, the capacities of the facilities of storage, reprocessing, and the electricity supply data are needed. Therefore, the MESSAGE code was used to model the scenarios. MESSAGE is a tool for modeling and analyzing nuclear energy systems, capable to model nuclear technologies with their specific features (143). Outputs associated with the mass flow waste between processes and storages, annual use of the total capacities, and the total electricity supplied were used to calculate the back-end LCOE.

Features of each NPP and mass flows of the fuel cycle are used as inputs in MESSAGE. The average mass flows of nuclear materials are estimated using some well-known equations (143) and assuming that there are no losses at any stage of the fuel cycle.

The annual fresh fuel loading, G_x in tHM, fuel consumption, is calculated as follows:

$$G_x = \frac{365 \times W \times \varphi}{\eta \times B} \tag{13}$$

Where φ is the capacity factor, W is the reactor installed capacity in MW, B is the fuel burnup in MWd/tHM, and η is the thermal efficiency.

The first loading, G_f in tHM, is defined by.

$$G_f = \frac{W \times T_{eff}}{\eta \times B} \tag{14}$$

Where T_{eff} is the mean nuclear fuel residence time in days.

To generate the fuel for the fresh fuel loading, G in tHM, with x enrichment compared to natural uranium, with an amount of depleted uranium, the tail assay, with x_{dep} enrichment is calculated by:

$$G = G_x \times \left(\frac{x - x_{dep}}{0.007114 - x_{dep}}\right) \tag{15}$$

The natural enrichment of natural uranium is defined as 0.00714.

To produce a certain amount of fuel, with enrichment x in relation to natural uranium, some separative work units (SWU) are necessary, where V is the separation potential:

$$SWU = G_x \times \left[V(x) + V(x_{dep})\left(\frac{x - 0.00714}{0.00714 - x_{dep}}\right) - V(0.00714)\left(\frac{x - x_{dep}}{0.00714 - x_{dep}}\right)\right] \tag{16a}$$

$$V(x) = (1 - 2x)\ln\left(\frac{1 - x}{x}\right) \tag{16b}$$

The amount of depleted uranium, G_{dep}, generated per unit of fresh fuel is:

$$G_{dep} = G_x \times \left(\frac{x - 0.00714}{0.007114 - x_{dep}}\right) \tag{17}$$

Finally, the amount of ***SNF*** discharged at each loading is defined by:

$$SF = G_x \tag{18}$$

To calculate the mass flows for each reactor in each scenario, the data listed in Table 19, Figure 43, Figure 44, and the following assumptions were used.

- The NPP Angra 1 will have its useful life extended from 40 to 60 years. The analysis process for the extension has already started (144).
- NPP Angra 3 will start operating in 2026, in ***ANGRA3*** and ***ANGRA+8*** scenarios, according to the most recent forecasts (129, 144).
- For the ***ANGRA+8*** scenario, a new PWR will be included every three years, starting in 2034.
- An average of the last 10 years of the capacity factor was used for the NPPs Angra 1 and Angra 2 (128),
- The simulations started in 2019 and would finish with the closure of the repository. The timetable with the operating dates of each facility in each scenario is shown in Figure 43.
- SNF stored before 2019 is estimated to account for 659.86 t, according to a background historical simulation[32].
- For the closed fuel cycle, the assumptions are:
    - The MOX fuel composition is 7.23% of plutonium and 92.77% of depleted uranium, with an energy efficiency equivalent to a conventional fuel (UOX) (143).
    - NPPs in the partially closed fuel cycle use one-third of MOX and two-thirds of UOX in their core.

[32] Researcher Fidéllis Bitencourt, co-author of the studies in this chapter, requested, via the access to information law, the most current data about the amount of SNF stored in Brazilian nuclear plants and the request was denied. An outdated version of the Eletronuclear website held the data for an older date, 2017. A simulation with MESSAGE was then performed to estimate the amount of SNF until 2019.

- In the partially closed fuel cycle, whether UOX spent fuel reprocessed is not sufficient to supply the reactors, an extra content of fissile material (Pu) is acquired from an external source (External Pu).
- The savings generated by the reduction in fresh fuel requirements (fresh UO2) at the front end of the fuel cycle resulting from reprocessing were not considered in the cost estimates.
- The use of depleted uranium or multi-reprocessing was also not considered.

Table 19 – Technical features (128, 145–147).

Parameters	**Angra 1**	**Angra 2**	**Angra 3**	**PWR**
Nuclear Capacity (MWe)	626	1,275	1,245	1,660
Capacity Factor[33]	0.837	0.904	0.904	0.920
Thermal Efficiency	0.342	0.358	0.358	0.360
Discharged Burnup (GWd/tHM)	55	50	50	65
Residence time (days)	1,168	1,168	1,168	1,168
Enrichment of Fresh fuel	0.04	0.04	0.04	0.05
Tail assay	0.003	0.003	0.003	0.003

The mass flows used in the MESSAGE simulation for the two fuel cycles analyzed are shown in Table 20.

[33] In PRIS a term Load Factor (LF) is used for CF.

Table 20 – Mass flows.

Mass flow (kg/TWh)	**Angra 1**	**Angra 2**	**Angra 3**	**PWR**
Once-through fuel cycle				
Natural uranium	1,6674.9	18,925.25	18,925.25	18,715.19
Fuel fabrication (UOX)	1,854.1	2,104.283	2,104.283	1,638.177
Partially closed fuel cycle				
Natural uranium	11,116.6	12,616.8	12,616.8	12,476.8
Fuel fabrication (UOX)	1,236.0	1,402.9	1,402.9	1,092.1
Fuel fabrication (MOX)	618.0	701.4	701.4	546.1
Pu	12.3	14.0	14.0	10.9
External Pu	32.4	36.8	36.8	28.6
Spent fuel (MOX)	618.0	701.4	701.4	546.1
FProd+Mac+RepU	1,223.8	1,388.9	1,388.9	1,081.3

4.2.4 – Cost estimation

The cost estimation process is composed of two stages. The first considers the amount of waste produced by each scenario and cycle described above and uses the cost curves as a function of the amount of waste for each installation.

Data on overnight investment cost, operation, and maintenance (O&M) were acquired from “The Economics of the Back-End of the Nuclear Fuel Cycle” (124). These costs change according to the capacities of the storage (interim and final) activities, encapsulation, and reprocessing processes. However, for this study, it was necessary to extrapolate the costs from the cost curves, given the small size of the fleets considered. Therefore, the results of the MESSAGE simulation obtained for each scenario, related to mass flows, were used to find the maximum capacities for the reprocessing and encapsulation facilities. The maximum capacities needed for interim

and final storage under geological conditions were also estimated for all cases with MESSAGE. The original cost curves were at a constant 2010 dollar, so the values were updated for the start year of the scenarios, 2019, using the inflation observed in the United States in the period 2010/2019. The amount of electricity generated, considering the operating time of the plants shown in Figure 44, and the capacities of each facility for each scenario are shown in Table 21.

Table 21 – Cost estimation parameters.

Facility	***ANGRA1&2***		***ANGRA3***		***ANGRA+8***	
	OFC	**CFC**	**OFC**	**CFC**	**OFC**	**CFC**
	Electricity generated (TWh)					
	608		1,012		7,434	
	Facility capacity (tHM)					
Integrated reprocessing plant	**-**	81	**-**	109	**-**	145
Interim Storage	1,481	1,469	2,160	2,461	8,603	9,642
Encapsulation Plant	94	91	94	126	273	234
Geological Repository	1,481	1,469	2,479	2,461	14,445	14,347

For each scenario, three cost estimations were made: i) a low-cost case; ii) a reference cost case; iii) a high-cost case. The low-cost case corresponds to the lower bound of the estimated cost for a given facility. The reference cost case corresponds to the most probable value of cost, according to the data available to date. The high-cost case corresponds to the upper bound of the costs for a given type of facility or service. From this step, three fixed values of construction and O&M costs are obtained for each installation, denoted: Low, reference, and High. Table 22 presents the cost estimate as a function of the installation and cost case.

Table 22 – Cost estimate as a function of the installation and cost case in $\$_{2019}$ Million.

Facility	Cost Case	*ANGRA1&2*		*ANGRA3*		*ANGRA+8*	
		OFC	**CFC**	**OFC**	**CFC**	**OFC**	**CFC**
Interim storage facility: Overnight investment	Low	$456.62	$455.85	$504.68	$525.95	$960.24	$1,033.71
	Reference	$624.75	$623.06	$728.77	$774.80	$1,714.74	$1,873.74
	High	$818.62	$816.03	$978.61	$1,049.42	$2,495.15	$2,739.71
Interim storage facility: O&M	Low	$12.13	$12.13	$11.78	$12.36	$13.81	$14.05
	Reference	$15.08	$15.07	$15.56	$15.77	$20.11	$20.84
	High	$19.40	$19.38	$20.20	$20.55	$27.78	$29.00
Integrated reprocessing plant: Overnight investment	Low	-	$5,091.16	-	$5,337.55	-	$5,660.04
	Reference	-	$6,881.17	-	$7,207.08	-	$7,633.68
	High	-	$8,499.82	-	$8,911.19	-	$9,449.57
Integrated reprocessing plant: O&M	Low	-	$411.82	-	$421.23	-	$433.51
	Reference	-	$495.27	-	$506.72	-	$521.67
	High	-	$577.71	-	$591.15	-	$608.70
SNF encapsulation plant: Overnight investment	Low	$187.45	$184.05	$187.45	$221.53	$378.29	$336.73
	Reference	$249.93	$245.39	$249.93	$295.37	$504.38	$448.98
	High	$312.41	$306.74	$312.41	$369.21	$630.48	$561.22
SNF encapsulation plant: O&M	Low	$18.57	$18.35	$18.57	$20.72	$30.65	$28.02
	Reference	$24.75	$24.47	$24.75	$27.63	$40.87	$37.36
	High	$30.94	$30.58	$30.94	$34.54	$51.09	$46.70
Geological repository: Overnight investment	Low	$909.78	$909.32	$952.20	$951.43	$1,460.41	$1,456.26
	Reference	$2,269.20	$2,268.02	$2,375.60	$2,373.65	$3,650.28	$3,639.86
	High	$6,265.99	$6,262.78	$6,557.79	$6,552.47	$10,053.57	$10,025.00
Geological repository: O&M	Low	$22.71	$22.69	$24.01	$23.99	$39.63	$39.51
	Reference	$76.67	$76.66	$78.09	$78.06	$95.06	$94.92
	High	$202.54	$202.52	$204.22	$204.19	$224.36	$224.20
Geological repository: Closure	Low	$235.40	$235.40	$235.40	$235.40	$235.40	$235.40
	Reference	$470.80	$470.80	$470.80	$470.80	$470.80	$470.80
	High	$1,412.40	$1,412.40	$1,412.40	$1,412.40	$1,412.40	$1,412.40
Specific Transport	Low	$0.02	$0.02	$0.02	$0.02	$0.02	$0.02
	Reference	$0.06	$0.06	$0.06	$0.06	$0.06	$0.06
	High	$0.16	$0.16	$0.16	$0.16	$0.16	$0.16

To deal with variations and uncertainties that may occur in the cost estimate, Monte Carlo simulations were used, using the @Risk software by the Palisade Corporation. For each cost item shown in Table 22, associated probability functions were created. We opted for using triangular distribution functions, shown in Appendix D. Triangular functions were chosen given the values calculated for each facility, enough for a three-point estimate, and because they work for any type of system (132, 148). Furthermore, the calculated estimates are off, at best, rough order of magnitude (ROM) fidelity (132). For each installation and the total cost, 5,000 interactions were performed and the confidence interval, mean values, and standard deviation were calculated. In addition, the procedure conducted by SKB was adopted to estimate a supplementary amount for costs arising from unforeseen events. This value is determined to be the value of P90 minus the average value of the Monte Carlo simulations (108). Additionally, sensitivity analyzes were conducted to verify the impact of each installation on the total cost of the repository.

4.2.5 – Levelized Cost of Energy, LCOE

The last step is to calculate the cost on a level basis for different fuel cycles. A usual method of comparison is the LCOE, which is a ratio between the sum of all discounted costs of the energy generation stages and the discounted cash flow from energy sales at a constant price. In this work, we chose to use the LCOE of the fuel cycle back-end, as defined by the OECD/NEA: (124)

$$LCOE_{Back-end} = \sum_{Back-end\ facilities,i} \left[\frac{\sum_{t=T_{i,start}-T_{ref}}^{T_{i,end}-T_{ref}} \left(\frac{Investment_{i,t}+O\&M_{i,t}+Transport_{i,t}+Decommissioning_{i,t}}{(1+r_i)^t} \right)}{\sum_{t=T_{NPP,start}-T_{ref}}^{T_{NPP,end}-T_{ref}} \left(\frac{Electricity_t}{(1+r_E)^t} \right)} \right] \quad (19)$$

Where:

- T_{ref}: The reference year (all cash-flows are discounted from the reference year). In this work, T_{ref} is 2019.
- $T_{i,start}$: first year of the lifecycle of a facility "***i***."
- $T_{i,end}$: Final year of the lifecycle of a facility "***i***."
- $T_{NPP,start}$: Starting-operation year of NPPs.
- $T_{NPP,end}$: Shutdown year of NPPs.
- r_E: Annual discount rate for electricity cash flow.
- r_i: Annual discount rate for the cash-flows associated with construction and operation of the facility "***i***."
- $Electricity_t$: The amount of electricity produced at NPPs in year "***t***."
- $Investment_t$: Investments associated with the fuel cycle back-end, in year "***t***."
- $O\&M_t$: Operations and maintenance costs at various steps of the fuel cycle, in year "***t***."
- $Transport_t$: Transportation costs associated with the fuel cycle in year "***t***."
- $Decommissioning_t$: Decommissioning of the back-end facilities, with costs in year "***t***."

Equation 19 allows the comparison among different generation scenarios and fuel cycles on a common basis, resulting in the cost of this part of the cycle expressed in terms of the unit of currency per unit of energy produced. This output is useful for estimating disposal costs compared to the generation cost of current Brazilian NPPs. Regulatory authorities can use these values to calculate the minimum sale value of energy that supports the payment of waste disposal activities.

The use of LCOE as a critical element. As it is a present value analysis, the relative contribution of installations close to the start date of the analysis is greater than that of installations that are implemented late, for any non-zero discount rate. The greater the discount rate and the more distant from the present, the greater the effect.

The discount rate to be used varies with the country and industry and with the period considered. For long-term projects in the nuclear area, OECD/NEA recommends the use of low discount rates, so as not to mask the costs to be paid in the distant future (124). In Brazil, the EPE established the discount rate at 8 % to be adopted in energy projects (149, 150). An alternative, for intergenerational projects, such as those considered here, some analysts, as the French economist Christian Gollier (151), Oxera Consulting Ltd. (152), and the Lebègue report (153), argue in favor of the utilization of a varying discount rate that decreases over time for long-term projects (over 30 years), as shown in Table 23 and Figure 50, which illustrates the variation of discount rates over time for a period of two hundred years. To deal with the uncertainties about the discount rate, a sensitivity analysis was performed using fixed discount rates, ranging from 0-10%, and by decreasing discount rates, associated with Monte Carlo simulations. In simulations, each discount rate was considered independently and, as in the earlier step, with 5,000 interactions. For simplicity, this work assumed that the discount rates r_i and r_E are the same (124).

Table 23 – Varying discount rates (151–153).

Christian Gollier	$t \leq 30$ years, r_i=5% and $t \geq 31$years, r_i = 2%
Oxera Consulting	$t \leq 30$years, r_i=3.5% 31 years ≤ $t \leq 75$ years, r_i = 3% 76 years ≤ $t \leq 125$ years, r_i = 2.5% 126 years ≤ $t \leq 200$ years, r_i = 2% 201 years ≤ $t \leq 300$ years, r_i = 1.5% $t \geq 301$ years, r_i=1%
Lebégue Report	$t \leq 30$years, r_i=4% $t > 30$ years, $r_i = \sqrt[t]{(1.04^{30}\ 1.02^{(t-30)})} - 1$

Figure 50 – Varying discount rates over two hundred years.

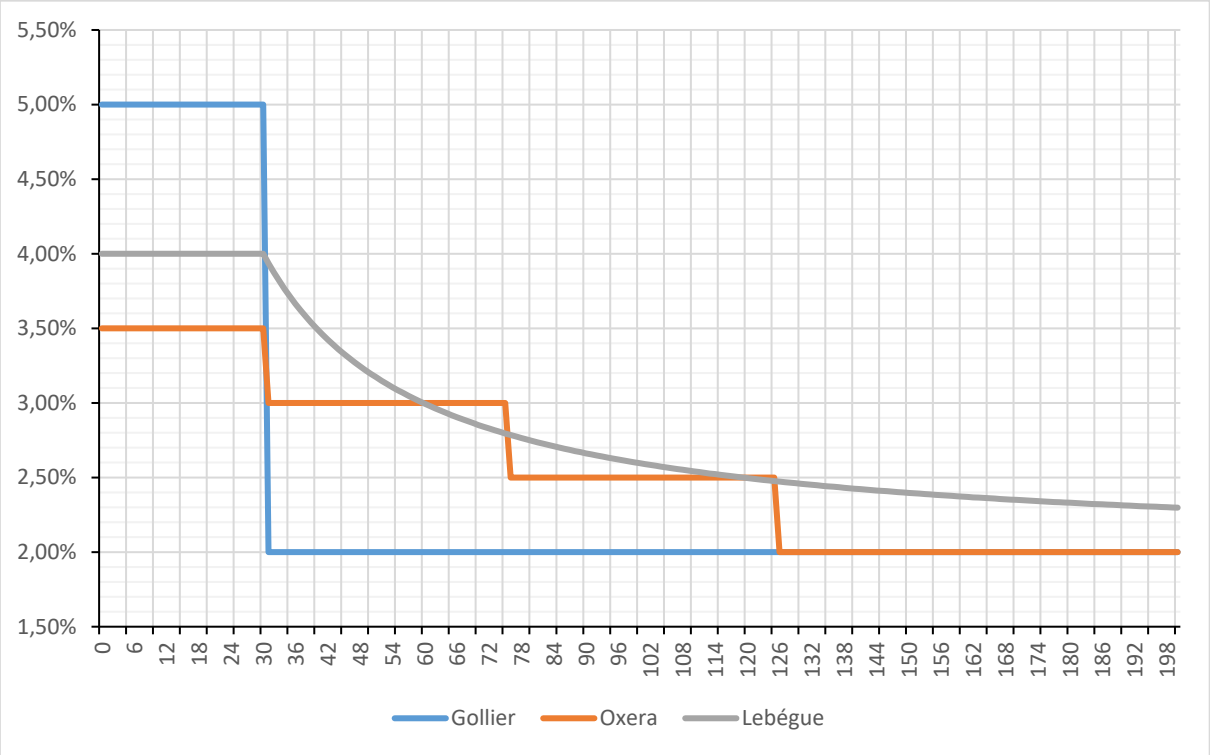

4.3 – RESULTS AND DISCUSSION

4.3.1 – Total costs

The results of the calculation, with a 0% discount rate, are represented in a boxplot in Figure 51 and Figure 52. The total back-end fuel cycle costs calculated for the reference case are lower for the OFC route than that of the CFC route, as expected. The total estimated cost for the CFC is between 2.5 and 3 times greater than the costs of the OFC. The difference is primarily the result of the cost of reprocessing facilities. According to OECD/NEA (124), the costs of an integrated reprocessing plant, albeit large, are “paid back” by the savings in fresh fuel requirements. Given the history of difficulties faced by the Brazilian government to support the national nuclear projects, it would be preferable, from a purely economic point of view, the signing of international agreements for the reprocessing of the Brazilian SNF. This choice would be more advantageous for the following reasons: the Brazilian nuclear area faces historical financing difficulties, and it is not clear whether there is a political will to implement a high-cost facility to supply a small nuclear program. The life cycle costs of an integrated reprocessing plant are estimated to be between $19.2 Billion to $57.1 Billion,

depending on the scenario chosen. In comparison, the construction cost of CNAAA's plants - Angra 1, Angra 2, and Angra 3 - is estimated at $23.5 Billion[34] (135).

Figure 51 – Total back-end costs – OFC route.

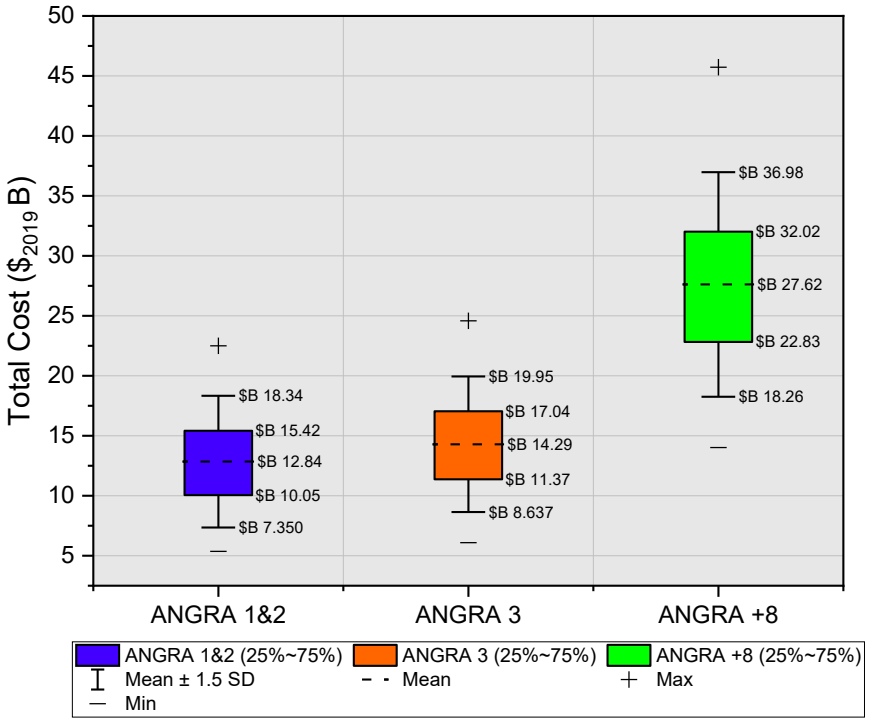

Figure 52 – Total back-end costs – CFC route.

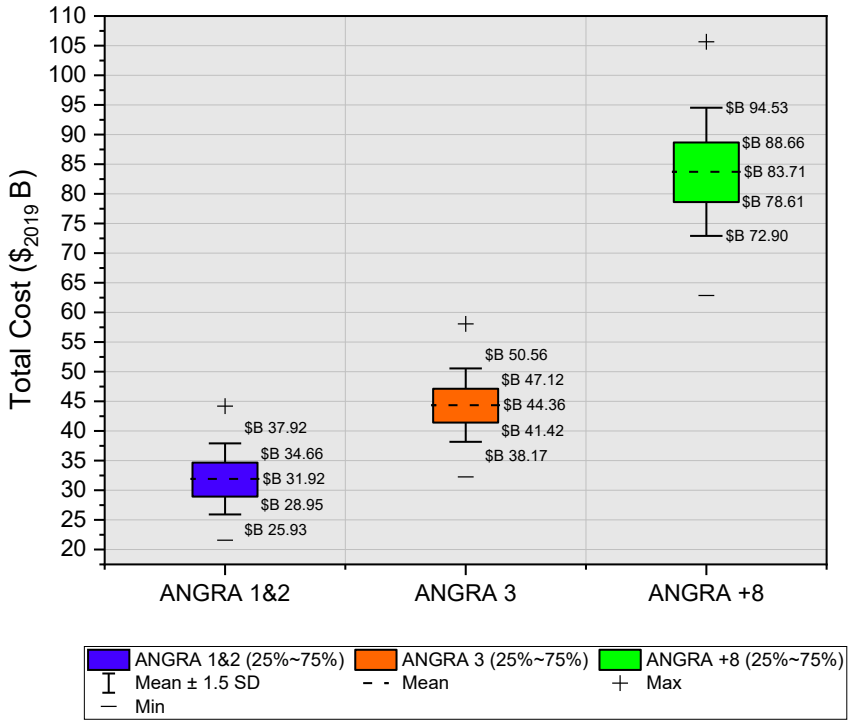

[34] The original amount is R$ 51.3 billion in 2018 and was updated by the IPCA inflation index to the value of 12/2019 at R$ 53.6 billion and converted by the 2019 power purchase parity index (PPP) of 2,281 R$/US$.

In addition to the total cost estimate, an additional amount for contingencies was estimated, as shown in Table 24. Except for the ***ANGRA+8*** scenario, this amount is between $5.32 - 5.59 billion. For the ***ANGRA+8*** scenario, the amount is between $8.90 - 9.77 billion. The histograms for the total cost estimations for each scenario are available in Appendix C.

Table 24 – The net present cost of implementation of different back-end strategies is $\$_{2019}$ Billion.

	ANGRA1&2		**ANGRA3**		**ANGRA+8**	
	OFC	**CFC**	**OFC**	**CFC**	**OFC**	**CFC**
Mean	12.84	31.92	14.29	44.36	27.62	83.71
Standard Deviation	3.66	4.00	3.77	4.13	6.24	7.21
95% CI (±)	0.10	0.11	0.10	0.11	0.17	0.20
P90	18.16	37.51	19.66	49.91	36.52	93.48
Supplementary Amount	5.32	5.59	5.37	5.55	8.90	9.77

Figure 53 shows the result of the sensitivity analysis and shows the variation in the average cost as a function of the variation in the values of the cycle components. In all cases analyzed, the installations with the greatest influence on the cost of the back-end are the geological repository and the reprocessing plant.

Figure 53 – Change in Output Mean Across Range of Input Values at a 0% discount rate. a) ***ANGRA1&2 OFC***; b) ***ANGRA1&2 CFC***; c) ***ANGRA3 OFC***; d) ***ANGRA3 CFC***; e) ***ANGRA+8 OFC***; f) ***ANGRA+8 CFC***.

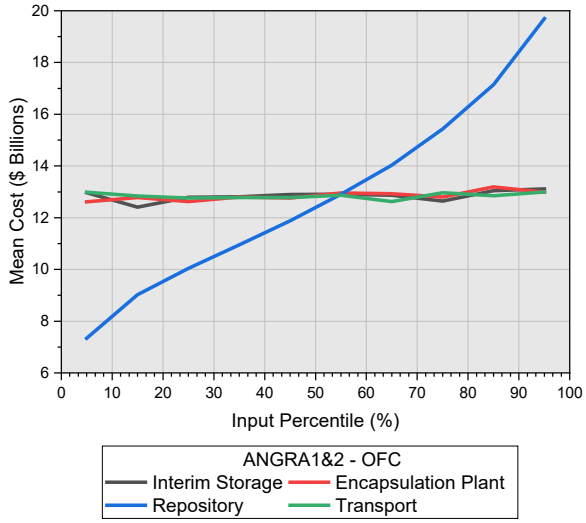

a)

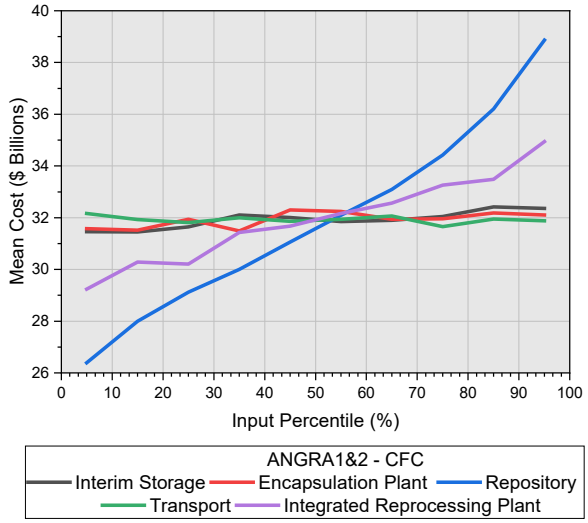

b)

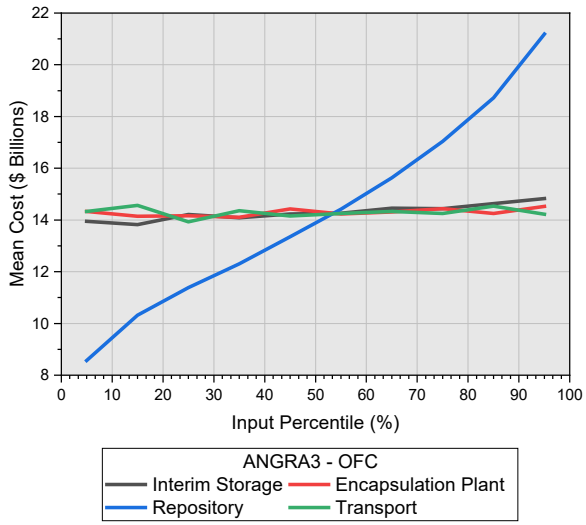

c)

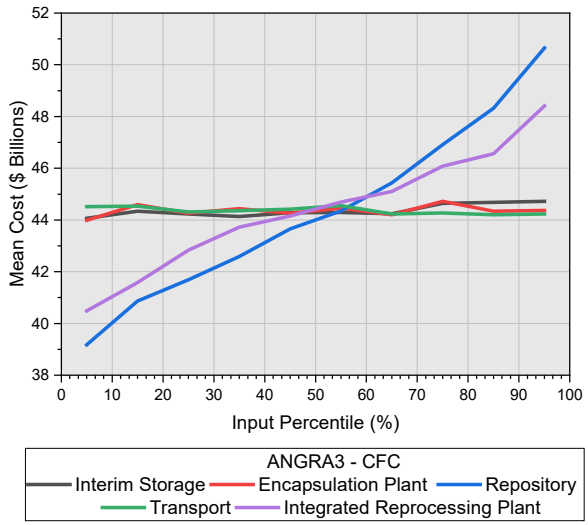

d)

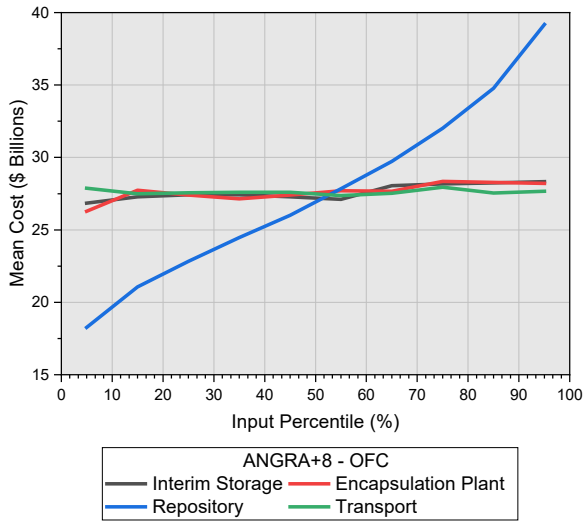

e)

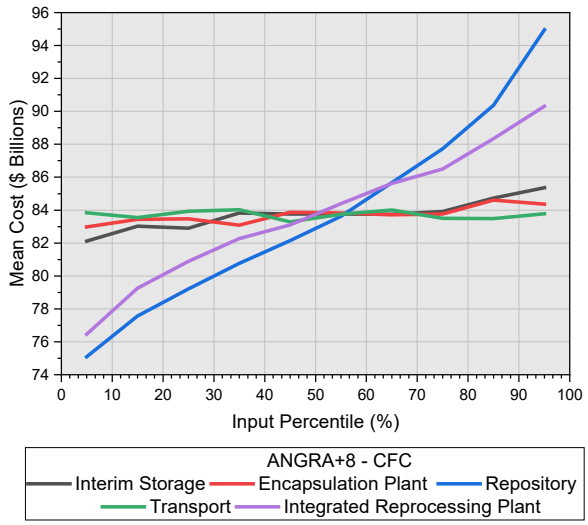

f)

4.3.2 – LCOE

In addition to the total cost, the LCOE was calculated for the scenarios, shown in Figure 54 and Figure 55. The LCOE cost is an interesting indicator because it allows estimating the full cost of nuclear energy generation in Brazil. As stated before, Brazilian law does not require the entity generating the nuclear waste to keep a dedicated fund to pay for the disposal of waste. The entity must reimburse the future expenditure of the disposal facilities, which is the responsibility of CNEN. Eletronuclear currently keeps a fund to cover the decommissioning expenses of the plants based on the amount received from the sale of electricity.

The unit variable cost[35] (Portuguese: Custo Variável Unitário – CVU) of the Angra 1 and Angra 2 NPPs is 13.90 $\$_{2019}$/MWh and 8.82 $\$_{2019}$/MWh. The average value weighted by the capacity of the plants is 10.46 $\$_{2019}$/MWh. In the OFC route, for a null discount rate, only the ***ANGRA+8*** scenario has a flat cost below the average CVU value of the current NPPs and the CVU value of the Angra 2 NPP. The ***ANGRA3*** scenario reaches this level with a discount rate higher than 1% while the ***ANGRA1&2*** scenario with a discount rate above 1.8%. The LCOEs for variable discount rates are, in all scenarios, with values between 1.6 and 3.2%.

[35] The CVU is the cost per unit of energy produced by a thermoelectric plant.

Figure 54 – Sensitivity of the LCOE to the discount rate – OFC Route.

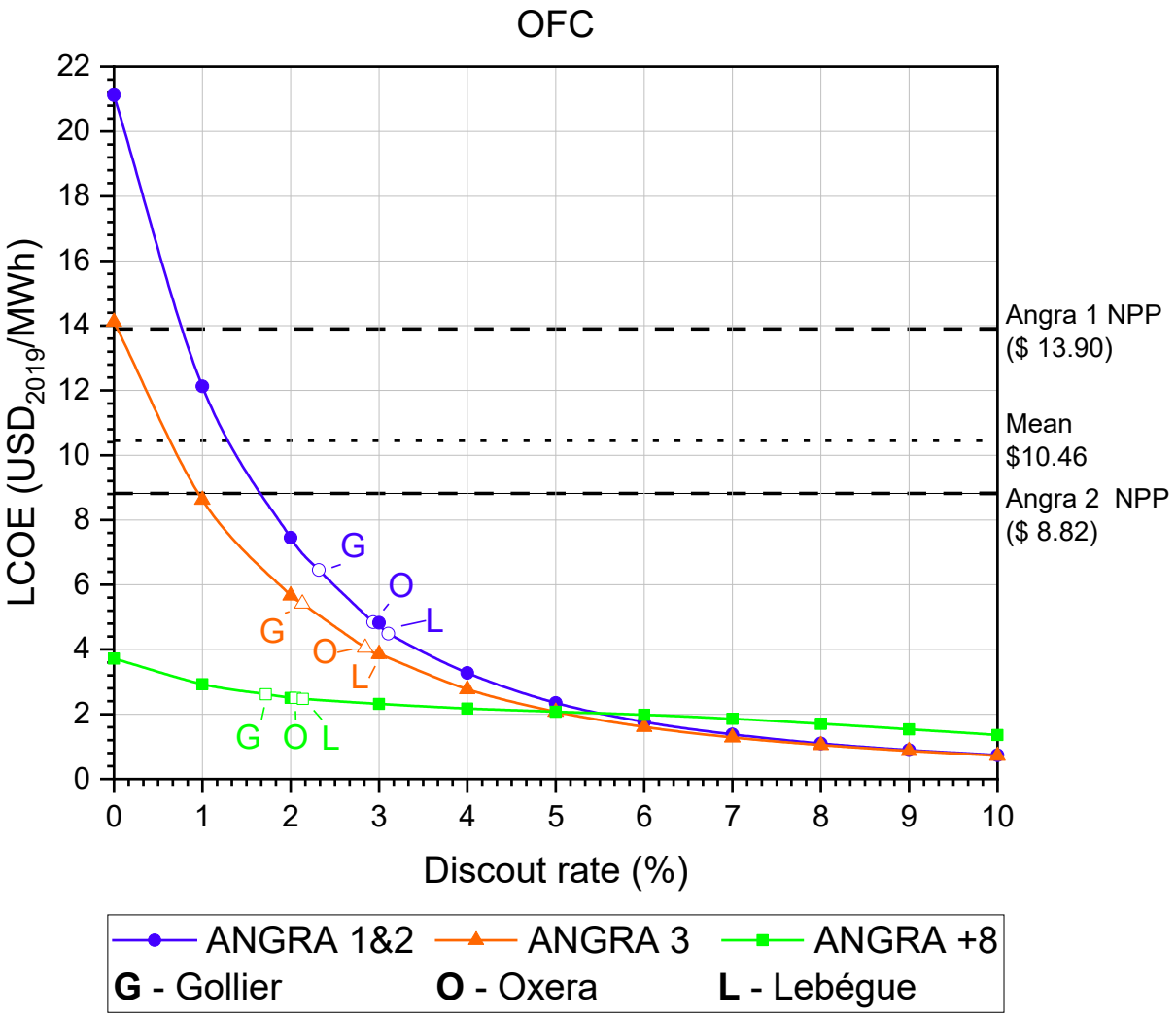

In the case of the CFC route, all scenarios present an LCOE higher than the average CVU, while the discount rate is less than 9.5%. The ***ANGRA+8*** scenario is discarded once again, as it is the only scenario with an LCOE below the CVU of Angra 1 for any discount rate used. In this case, the LCOEs for variable discount rates are, in all scenarios, with values between 3 to 4%, except for the Gollier rate for the ***ANGRA+8*** scenario, whose LCOE is close to the fixed rate of 9.4%. In the specific case of the ***ANGRA+8*** scenario, it is seen that from a discount rate of 2% to 6%, the calculated LCOE showed an increase. This occurs with the increase in the contribution of the facilities that are built at the beginning of the scenarios, such as the interim storage facilities and the reprocessing plant, as shown in Figure 55.

Figure 55 – Sensitivity of the LCOE to the discount rate – CFC Route.

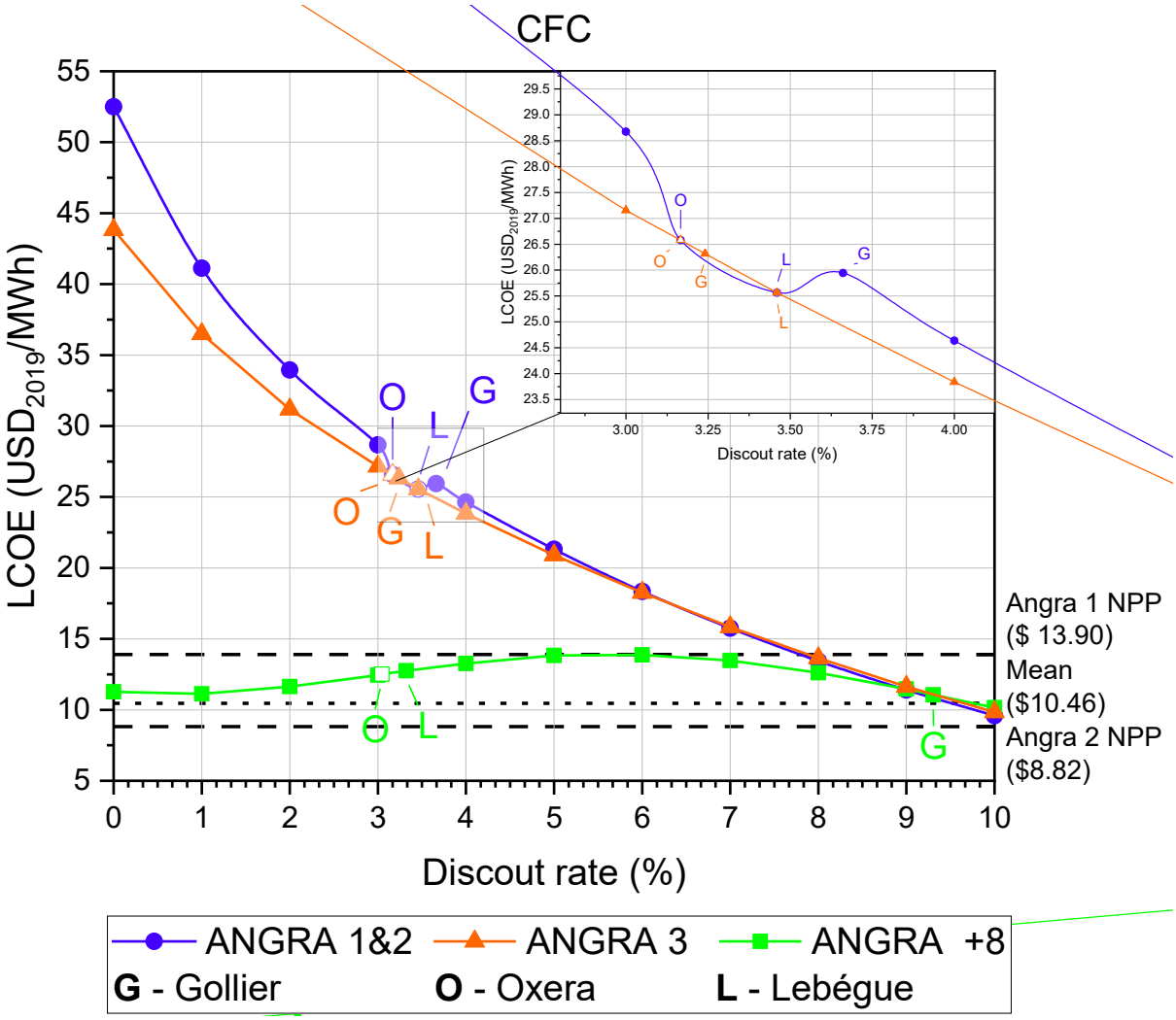

However, this analysis is weighted by the amount of energy generated since the beginning of the NPPs operation. In this way, it becomes a flawed indicator for nuclear programs such as the Brazilian one, that is, in which there is no obligation to create a fund to finance the waste disposal activities. Therefore, since there exists an idea of the amount that should be collected by Eletronuclear to cover the expenses with the back end of the nuclear cycle, a second analysis was conducted, considering the energy produced only from 2019 onwards.

As expected with a smaller denominator, generated energy, the LCOE value increases (Equation 19). With the introduction of non-zero discount rates, two distinct behaviors occur for LCOE values. The first is marked by a rapid fall in LCOE values followed by

a stabilization of values for higher discount rates, as observed by the ANGRA 1&2 OFC and ANGRA 3 OFC scenarios in Figure 56. The second behavior is similar to the first, there is LCOE values decrease with increasing discount rates, as observed by the ANGRA +8 OFC scenario (Figure 56) and by all scenarios shown in Figure 57. However, instead of stabilizing, the LCOE values grow again with the increase in the discount rate. These behaviors are linked to the decrease in energy generated in the future, associated with the increase in the discount rate, as well as the influence of the construction costs of facilities built in the initial period of the analysis, which is insensitive to the discount rate.

Figure 56 – Sensitivity of the LCOE for the electricity generation beginning in 2019 to the discount rate – OFC Route.

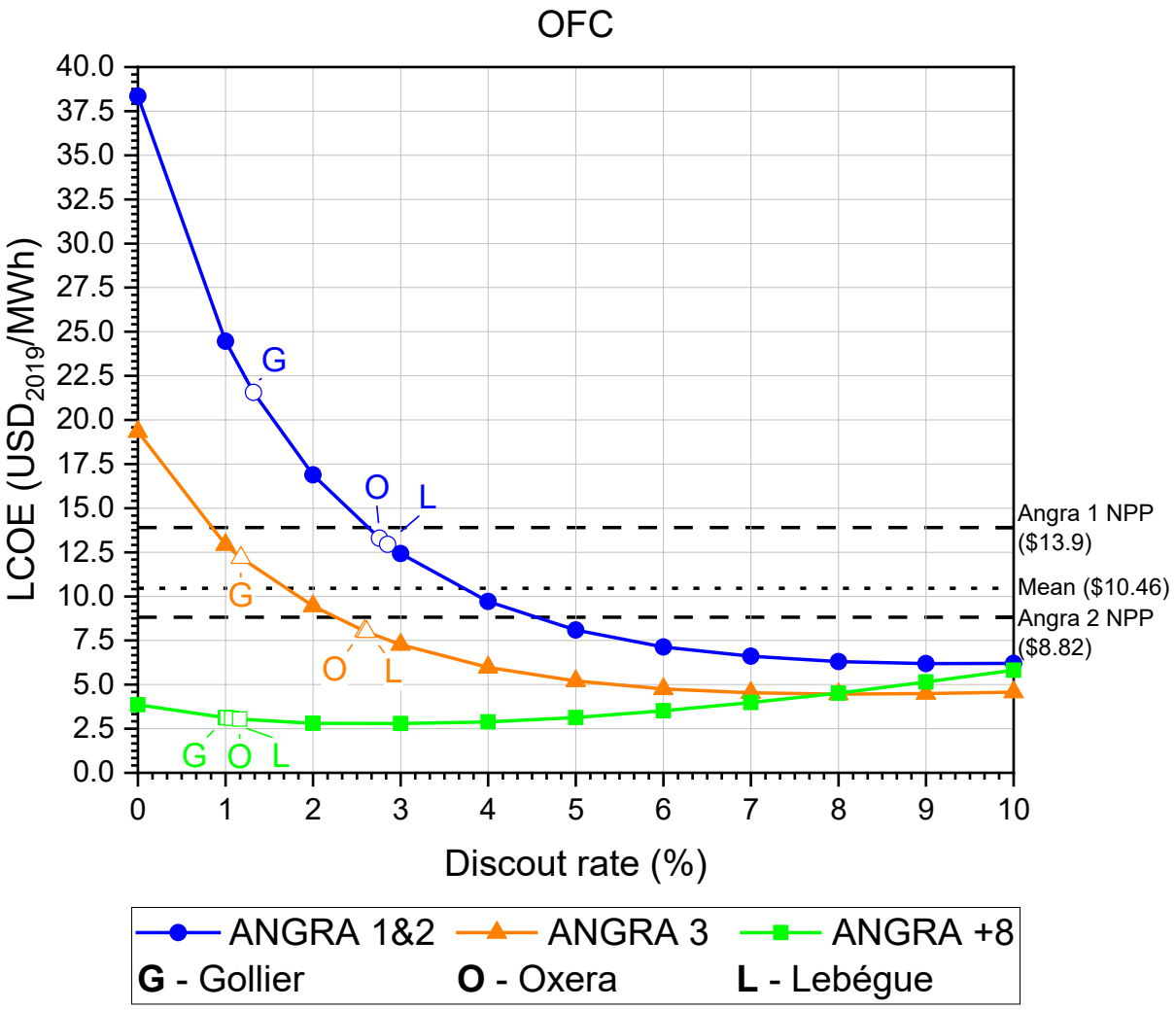

Figure 57 – Sensitivity of the LCOE for the electricity generation beginning in 2019 to the discount rate – CFC Route.

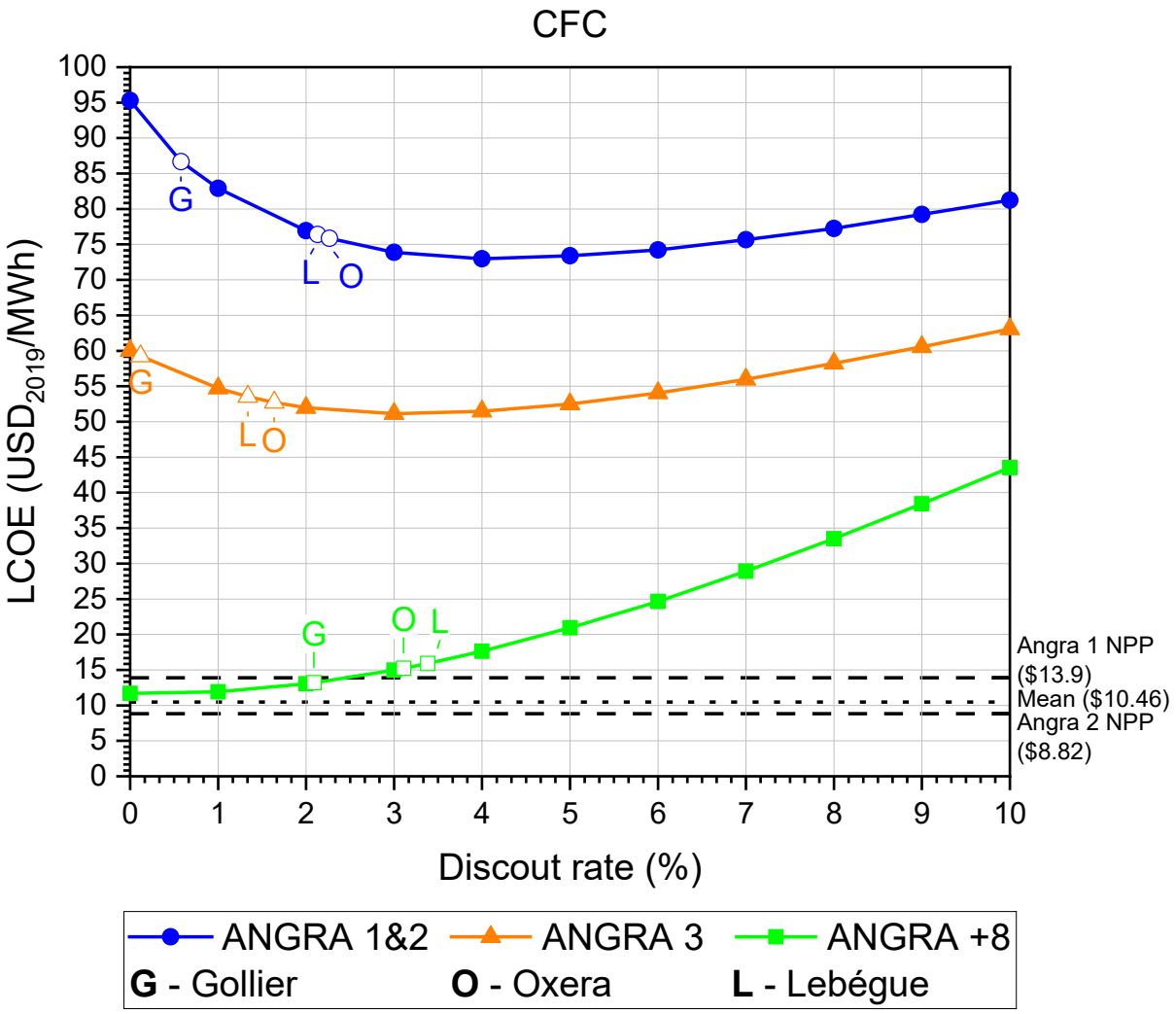

To estimate the average energy generation cost of Brazilian NPPs that includes the cost of waste disposal, only the OFC Route was considered, since the uncertainty about the implementation of reprocessing activities, even if it is conducted abroad, is exceptionally large. In addition, the energy generated from 2019 and the discount rate adopted by EPE of 8% were considered. Considering that the weighted average CVU is 10.46 $/MWh, the energy generation cost for the ***ANGRA1&2***, ***ANGRA3,*** and ***ANGRA+8*** scenarios is, respectively. 16.76 $/MWh, 14.92 $/MWh, and 14.97 $/MWh. These values correspond to an increase of 60.2%, 42.6%, and 43.2% of the current average CVU for the ***ANGRA1&2***, ***ANGRA3,*** and ***ANGRA+8*** scenarios, respectively.

4.4 – CONCLUSION

This chapter sought to estimate the costs of the nuclear fuel cycle back-end associated with the uncertainties of the Brazilian fuel cycle. To deal with the lack of concrete predictions, different options for expanding the Brazilian nuclear energy system were considered.

The net present cost of implementation increases as the size of the systems increase. However, despite the higher uncertainty ranges in the costs of small-sized systems, they have higher LCOE when compared to larger-sized systems, which become more evident as the discount rate decreases. The CFC has a higher LCOE due to reprocessing, which always presents the highest costs of the back end. For the OFC, the highest back-end costs are due to the repository or interim storage depending on the discount rate applied. Long-term facilities costs, such as the repository, decrease with the increase in the discount rate since they are implemented later.

The Monte Carlo analysis and the sensitivity analysis resulted in a ROM estimate of the implementation costs and specific costs to deal with the uncertainties of the scenarios. A well-planned nuclear policy considering the results presented could reduce the costs of the fuel cycle back-end. Also, such results can be useful for strategies and planning of the nuclear sector in the country.

5 – CONCLUSION

This thesis aimed to analyze holistically the disposal of Brazilian SNF. For that, studies were carried out related to the thermal design of a Brazilian DGR, selection of an adequate area for further studies for the installation of a DGR, and, finally, the estimation of the related costs.

Regarding the simulations of heat transfer processes, this thesis contributed to the determination of the minimum spacing between each SMOX canister for a range of temperature values for the Brazilian subsoil. Even in the case of simplified simulations, these results are important for the area selection processes. With the advance of research in the area and with the choice of a site for the construction of the Brazilian DGR, more complex simulations can then be carried out.

The investigation of a suitable location for a DGR in Brazil used a method proposed for Brazil, due to the lack of criteria for the selection of a repository for HLW and SNF. An area of interest for future studies was identified in the municipality of Ponto Belo, Espirito Santo, with an area of 99 km². However, the method was designed exclusively for DGR in hard rocks. It is understood that for other types of rocks, a new expert consultation must be carried out to determine new weights. In addition, popular opinion must be considered, since, as described, state legislation can prevent the construction of a DGR and there are social movements that actively work against the implementation of NPPs in Brazil. It should be kept in mind that more criteria may be considered by ANSN in the future, and this would alter the suitability values found in this work.

A crucial part of this work was the estimation of back-end costs in Brazil. Currently, Eletronuclear, despite having the responsibility to indemnify CNEN for the final disposal of the tailings, does not maintain a specific fund for the final disposal. There are two reasons: The first is that SNF is not considered nuclear waste. The second is that CNEN still does not have a plan for the construction of a Brazilian DGR. Funds accumulated for decommissioning will be insufficient for SNF or HLW disposal

activities as they were not created for this purpose. In the power generation and fuel cycle scenarios considered, it was estimated that the total cost of the back end in Brazil will cost between $\$_{2019}$ 12.84 billion to $\$_{2019}$ 83.71 billion, with the cost of the OFC being between $\$_{2019}$ 12.84 billion to $\$_{2019}$ 27.62 billion, while the CFC will cost between $\$_{2019}$ 31.92 billion to $\$_{2019}$ 83.71 billion. Given the significantly higher costs of the CFC and the historical difficulties in financing nuclear activities in Brazil, it is expected that, at least, the reprocessing of the fuel to be carried out entirely in Brazil may be abandoned. Considering that the OFC is officially adopted in Brazil, it is estimated that the energy generation cost of present and future NPPs, which are sufficient to cover the disposal costs, is 40% to 60% higher than the average costs of the current generation.

Despite being considered a strategic area, the Brazilian nuclear sector suffers from a lack of definition concerning its future, as in many countries around the world. The costs associated with the construction of NPPs, changes in the way of planning the electrical system, and the fear associated with nuclear accidents are obstacles for the sector. Although the Brazilian government is still planning and considering the use of nuclear energy, the sector faces financing data, making it impossible to predict the number of NPPs to be built by the end of the century. In addition, there are gaps in Brazilian legislation related to the backend of the nuclear fuel cycle caused by political inaction, such as the formal and legal definition of the fuel cycle to be adopted, since so far there are only indications about the adoption of SNF reprocessing. It was, therefore, necessary to adopt a series of assumptions, such as the type of rock to be adopted by the nuclear waste disposal program or the type of SNF to be disposed of, so that this work could be carried out. Consequently, the conclusions of this study must be carefully analyzed given the various assumptions made and the uncertainties related to the Brazilian civil nuclear program.

6 – REFERENCES

1. TSOULFANIDIS, Nicholas. *The Nuclear Fuel Cycle*. La Grange Park, Illinois, USA : American Nuclear Society, 2013. ISBN 978-0-89448-460-5. TK9360 .C53 2013

2. BONIN, Bernard. The Scientific Basis of Nuclear Waste Management. In : CACUCI, Dan Gabriel (ed.), *Handbook of Nuclear Engineering* [online]. Boston, MA : Springer US, 2010. p. 3253–3419. [Accessed 13 October 2018]. ISBN 978-0-387-98130-7. Available from: http://link.springer.com/10.1007/978-0-387-98149-9_28

3. COMISSÃO NACIONAL DE ENERGIA NUCLEAR. *NE 6.06 Seleção e escolha de locais para depósitos de rejeitos radioativos* [online]. 1989. NORMA CNEN NE 6.06. Available from: http://appasp.cnen.gov.br/seguranca/normas/pdf/Nrm801.pdf

4. BRASIL. *Decreto nº9.600, de 5 de dezembro de 2018. "Consolida as diretrizes sobre a Política Nuclear Brasileira".* [online]. 2018. [Accessed 3 October 2019]. Available from: http://www.planalto.gov.br/ccivil_03/_ato2015-2018/2018/decreto/D9600.htmConsolida as diretrizes sobre a Política Nuclear Brasileira.

5. *Spent Fuel Reprocessing Options* [online]. Vienna : INTERNATIONAL ATOMIC ENERGY AGENCY, 2009. TECDOC Series (CD-ROM), 1587. ISBN 978-92-0-150309-1. Available from: https://www.iaea.org/publications/8143/spent-fuel-reprocessing-options

6. ARGONNE NATIONAL LABORATORY. *History of Argonne Reactor Operations* [online]. 1970. [Accessed 13 September 2019]. Available from: https://www.ne.anl.gov/About/reactors/History-of-Argonne-Reactor-Operations.pdf

7. COMMITTEE ON WASTE DISPOSAL OF THE DIVISION OF EARTH SCIENCES. *Disposal of Radioactive Waste on Land; Report* [online]. Washington, D.C. : National Academies Press, 1957. [Accessed 13 October 2018]. ISBN 978-0-309-29378-5. Available from: http://www.nap.edu/catalog/18527

8. INTERNATIONAL ATOMIC ENERGY AGENCY, Vienna (Austria). *Disposal of Radioactive Wastes Vol I Proceedings of the Scientific Conference on the Disposal of Radioactive Wastes* [online]. International Atomic Energy Agency (IAEA) : IAEA, 1960. ISBN 0074-1884. Available from: http://inis.iaea.org/search/search.aspx?orig_q=RN:45016844

9. KUBO, A. S. and ROSE, D. J. Disposal of Nuclear Wastes: At an increased but still modest cost, more options can be explored, and the outlook can be improved. *Science*. 21 December 1973. Vol. 182, no. 4118, p. 1205–1211. DOI 10.1126/science.182.4118.1205.

10. MITCHELL, NT, GRAY, DA, HOOKWAY, BR, LAUGHTON, AS, STOTT, G and WEBB, G. Options for the disposal of high-level radioactive waste. Radioactivity Management. In : *Proc. Intern. Conf., Salzbourg, Autriche*. 1977. p. 2–13.

11. PARKER, Frank L, BROSHEARS, Robert E and PASZTOR, Janos. *The Disposal of High-level Radioactive Waste 1984: A Comparative Analysis of the State-of-the Art in Selected Countries*. Beijer Institute, the International Institute for Energy and Human Ecology …, 1984.

12. INTERNATIONAL ATOMIC ENERGY AGENCY. *Status and trends in spent fuel and radioactive waste management*. Vienna, 2018. IAEA nuclear energy series, no. NW-T-1.14. ISBN 978-92-0-108417-0.

13. WALKE, Russell and KWONG, Gloria. *International Conference on Geological Repositories 2016. Conference Synthesis, 7-9 December 2016, Paris, France*. Organisation for Economic Co-Operation and Development, 2017.

14. POSIVA OY. General Time Schedule for Final Disposal. *Posiva* [online]. 2019. [Accessed 3 October 2019]. Available from: http://www.posiva.fi/en/final_disposal/general_time_schedule_for_final_disposal

15. U.S. DEPARTMENT OF ENERGY. DOE/EIS-0046F: *Management of Commercially Generated Radioactive Waste* [online]. Environmental Impact Statement. Washington, D.C. : U.S. Department of Energy, 1980. Available from: https://www.energy.gov/sites/default/files/EIS-0046-FEIS-1980.pdf

16. IKONEN, Kari and RAIKO, Heikki. *Thermal dimensioning of Olkiluoto repository for spent fuel*. Posiva Oy, 2012.

17. POSIVA OY. Posiva - Excavation of joint functional test final disposal tunnel started at Posiva's ONKALO. [online]. 2021. [Accessed 23 April 2021]. Available from: https://www.posiva.fi/en/index/news/pressreleasesstockexchangereleases/2021/excavationofjointfunctionaltestfinaldisposaltunnelstartedatposiva8217sonkalo.html

18. ANDRA INTERNATIONAL. Key figures. [online]. 2021. [Accessed 23 April 2021]. Available from: https://international.andra.fr/projects/cigeo/cigeos-facilities-and-operation/key-figures

19. Long process nearing completion. [online]. September 2020. [Accessed 23 April 2021]. Available from: http://www.skb.com/news/long-process-nearing-completion/

20. NUCLEAR ENERGY AGENCY. No. 7532: *Management and Disposal of High-Level Radioactive Waste: Global Progress and Solutions* [online]. Paris : Organisation for Economic Co-Operation and Development, 2020. Radioactive Waste Management. Available from: https://www.oecd-nea.org/jcms/pl_32567/management-and-disposal-of-high-level-radioactive-waste-global-progress-and-solutions

21. COURANT, Richard. *Variational methods for the solution of problems of equilibrium and vibrations*. Verlag nicht ermittelbar, 1943.

22. CHEN, Xiaolin and LIU, Yijun. *Finite element modeling and simulation with ANSYS Workbench*. 2015. ISBN 978-1-4398-7385-4.

23. MADENCI, Erdogan and GUVEN, Ibrahim. Introduction. In : MADENCI, Erdogan and GUVEN, Ibrahim, *The Finite Element Method and Applications in Engineering Using ANSYS®* [online]. Boston, MA : Springer US, 2015. p. 1–13. [Accessed 6 November 2019]. ISBN 978-1-4899-7549-2. Available from: http://link.springer.com/10.1007/978-1-4899-7550-8_1

24. NUCLEAR ENERGY AGENCY. NEA/RWM/R(2013)2: *Underground Research Laboratories (URL)* [online]. Paris : Organisation for Economic Co-Operation and Development, 2013. Radioactive Waste Management. Available from: https://www.oecd-nea.org/rwm/reports/2013/78122-rwm-url-brochure.pdf

25. INTERNATIONAL ATOMIC ENERGY AGENCY. *Use of numerical models in support of site characterization and performance assessment studies of geological repositories.* [online]. 2013. [Accessed 1 November 2019]. Available from: http://www-pub.iaea.org/MTCD/Publications/PDF/TE-1717_web.pdf

26. CHOI, Heui-Joo, and CHOI, Jongwon. Double-layered buffer to enhance the thermal performance in a high-level radioactive waste disposal system. *Nuclear Engineering and Design*. October 2008. Vol. 238, no. 10, p. 2815–2820. DOI 10.1016/j.nucengdes.2008.04.017.

27. LEE, S. Y., HENSEL, S. J. and DE BOCK, C. Thermal Analysis of Geologic High-Level Radioactive Waste Packages. In : *ASME 2010 Pressure Vessels and Piping Conference: Volume 7* [online]. Bellevue, Washington, USA : ASME, 2010. p. 421–432. [Accessed 6 November 2019]. ISBN 978-0-7918-4926-2. Available from: http://proceedings.asmedigitalcollection.asme.org/proceeding.aspx?articleid=1619084

28. BULUT ACAR, Banu and ZABUNOĞLU, H. Okan. Comparison of the once-through and closed nuclear fuel cycles with regard to waste disposal area required in a geological repository. *Annals of Nuclear Energy*. October 2013. Vol. 60, p. 172–180. DOI 10.1016/j.anucene.2013.04.039.

29. BULUT ACAR, Banu and ZABUNOĞLU, Okan H. Impact assessment of alternative back-end fuel cycles on geological disposal of resultant spent fuels and high-level wastes. *Annals of Nuclear Energy*. August 2019. Vol. 130, p. 452–472. DOI 10.1016/j.anucene.2019.03.014.

30. HÖKMARK, Harald. *Strategy for thermal dimensioning of the final repository for spent nuclear fuel*. Svensk kärnbränslehantering AB (SKB), 2010.

31. CHOI, Heui Joo, LEE, Jong Youl and KIM, SS. *Korean reference HLW disposal system*. Korea Atomic Energy Research Institute, 2008.

32. INTERNATIONAL ATOMIC ENERGY AGENCY. *Geological disposal facilitie for radioactivity waste: specific safety guide*. Vienna : International Atomic Energy Agency, 2011. Safety Standards Series, SSG-14. ISBN 978-92-0-111510-2.

33. BRASIL. *National Report of Brazil for the 6th Review Meetingof the Joint Convention on the Safety of Spent Fuel Management and on the Safety of Radioactive Waste Management* [online]. 2018. Available from:

https://www.iaea.org/sites/default/files/national_report_of_brazil_for_the_6th_review_meeting_-_english.pdf

34. ELETRONUCLEAR. BP-U-0061.2-0085-200010 (Rev.0): *Unidade de Armazenamento Complementar a Seco de Combustível Irradiado – UAS-Situação Atual UAS – Abril/2020*. 2020.

35. ELETRONUCLEAR. BP-U-UAS-170007: *Solução de Armazenamento Complementar para Elementos Combustíveis Irradiados de Angra 1 e Angra 2* [online]. Relatório Técnico. 2017. Available from: https://www.eletronuclear.gov.br/Documents/politicas-empresariais/POL%C3%8DTICA%20PARA%20O%20GEERENCIAMENTO%20SEGURO%20DE%20RES%C3%8DDUOS%20RADIOATIVOS%20E%20COMBUST%C3%8DVEL%20CENTRAL%20NUCLEAR.pdf

36. BRASIL. *MEDIDA PROVISÓRIA Nº 1.049, DE 14 DE MAIO DE 2021. "Cria a Autoridade Nacional de Segurança Nuclear e altera a Lei nº 4.118, de 27 de agosto de 1962, a Lei nº 6.189, de 16 de dezembro de 1974, a Lei nº 8.691, de 28 de julho de 1993, a Lei nº 9.765, de 17 de dezembro de 1998, a Lei nº 6.453, de 17 de outubro de 1977, e a Lei nº 10.308, de 20 de novembro de 2001"* [online]. 14 May 2021. [Accessed 4 October 2019]. Available from: https://www.in.gov.br/en/web/dou/-/medida-provisoria-n-1.049-de-14-de-maio-de-2021-320065436

37. COMISSÃO NACIONAL DE ENERGIA NUCLEAR. *NN 9.02 Gestão dos Recursos Financeiros Destinados ao Descomissionamento de Usinas Nucleoelétricas* [online]. October 2016. NORMA CNEN NN 9.02. Available from: https://www.gov.br/cnen/pt-br/acesso-rapido/normas/grupo-9/grupo9-nrm902.pdf

38. COMISSÃO NACIONAL DE ENERGIA NUCLEAR. *NN 9.01 Descomissionamento de Usinas Nucleoelétricas* [online]. November 2012. NORMA CNEN NN 9.01. Available from: http://appasp.cnen.gov.br/seguranca/normas/pdf/Nrm901.pdf

39. COMISSÃO NACIONAL DE ENERGIA NUCLEAR. *Posição Regulatória 1.26 / 001 Gerenciamento de Rejeitos Radioativos em Usinas Nucleoelétricas* [online]. 2008. Posição Regulatória 1.26 / 001. Available from: http://appasp.cnen.gov.br/seguranca/normas/pdf/pr126_01.pdf

40. BRASIL. *DECRETO Nº 5.935, DE 19 DE OUTUBRO DE 2006."Promulga a Convenção Conjunta para o Gerenciamento Seguro de Combustível Nuclear Usado e dos Rejeitos Radioativos.".* [online]. 2006. [Accessed 3 October 2019]. Available from: http://www.planalto.gov.br/ccivil_03/_ato2004-2006/2006/decreto/d5935.htm

41. COMISSÃO NACIONAL DE ENERGIA NUCLEAR. *NE 5.02 Transporte, Recebimento, Armazenagem e Manuseio de Elementos Combustíveis de Usinas Nucleoelétricas* [online]. 2003. NORMA CNEN NE 5.02. Available from: http://appasp.cnen.gov.br/seguranca/normas/pdf/Nrm502.pdf

42. BRASIL. *Lei nº 10.308, de 20 de novembro de 2001. "Dispõe sobre a seleção de locais, a construção, o licenciamento, a operação, a fiscalização, os custos, a indenização, a responsabilidade civil e as garantias referentes aos depósitos de*

rejeitos radioativos, e dá outras providências" [online]. 2001. [Accessed 4 October 2019]. Available from: http://www.planalto.gov.br/ccivil_03/leis/LEIS_2001/L10308.htm

43. BRASIL. *LEI Nº 9.765, DE 17 DE DEZEMBRO DE 1998. "Institui taxa de licenciamento, controle e fiscalização de materiais nucleares e radioativos e suas instalações."* [online]. 17 December 1998. [Accessed 4 October 2019]. Available from: http://www.planalto.gov.br/ccivil_03/leis/l9765.htm

44. COMISSÃO NACIONAL DE ENERGIA NUCLEAR. *NE 1.26 Segurança na Operação de Usinas Nucleoelétricas* [online]. 1997. NORMA CNEN NE 1.26. Available from: http://appasp.cnen.gov.br/seguranca/normas/pdf/Nrm126.pdf

45. BRASIL. *CONSTITUIÇÃO DA REPÚBLICA FEDERATIVA DO BRASIL DE 1988* [online]. 1988. [Accessed 4 October 2019]. Available from: http://www.planalto.gov.br/ccivil_03/constituicao/constituicao.htmCONSTITUIÇÃO DA REPÚBLICA FEDERATIVA DO BRASIL DE 1988

46. BRASIL. *LEI Nº 6.453, DE 17 DE OUTUBRO DE 1977. "Dispõe sobre a responsabilidade civil por danos nucleares e a responsabilidade criminal por atos relacionados com atividades nucleares e dá outras providências."* [online]. 1977. [Accessed 4 October 2019]. Available from: http://www.planalto.gov.br/ccivil_03/LEIS/L6453.htm

47. INSTITUTO BRASILERIO DO MEIO AMBIENTE E DOS RESCURSOS NATURAIS RENOVÁVEIS - IBAMA. *Licença Prévia nº 279/2008* [online]. 23 July 2008. Available from: https://servicos.ibama.gov.br/licenciamento/consulta_empreendimentos.php

48. INSTITUTO BRASILERIO DO MEIO AMBIENTE E DOS RESCURSOS NATURAIS RENOVÁVEIS - IBAMA. *Licença de Instalação nº591/2009* [online]. 5 March 2009. Available from: https://servicos.ibama.gov.br/licenciamento/consulta_empreendimentos.php

49. INSTITUTO BRASILERIO DO MEIO AMBIENTE E DOS RESCURSOS NATURAIS RENOVÁVEIS - IBAMA. *PARECER nº 022 /2011/COEND/CGENE/DILIC/Ibama - Análise parcial de atendimento das Condicionantes de Angra 3.* [online]. 13 May 2011. Available from: https://servicos.ibama.gov.br/licenciamento/consulta_empreendimentos.php

50. TRIBUNAL DE CONTAS DA UNIÃO. *ACÓRDÃO 1108/2014 - PLENÁRIO* [online]. 30 April 2014. Available from: https://pesquisa.apps.tcu.gov.br/#/documento/acordao-completo/AC-1108-14%252F14-P/%2520/DTRELEVANCIA%2520desc%252C%2520NUMACORDAOINT%2520desc/0/%2520

51. MARTINS, Vívian Borges. Metodologia Baseada em Sistemas de Informação Geográfica e Análise Multicritério para a Seleção de Áreas para a Construção de um Repositório para o Combustível Nuclear Usado. . 2009.

52. AGESKOG, Lars and JANSSON, Patrik. *Heat propagation in and around the deep repository. Thermal calculations applied to three hypothetical sites: Aberg, Beberg and Ceberg*. Swedish Nuclear Fuel and Waste Management Co., 1999.

53. IKONEN, K., KUUTTI, J. and RAIKO, H. Thermal Dimensioning for the Olkiluoto Repository—2018 Update. *Posiva Oy, Working-report*. 2018. Vol. 26.

54. SVENSK KARNBRANSLEHANTERING AB. *RD&D-Programme 98* [online]. 1998. Available from: https://www.osti.gov/etdeweb/servlets/purl/337240

55. UNITED KINGDOM NIREX LIMITED. 502644: *Technical Note: Outline Design for a Reference Repository Concept for UK High-Level Waste/Spent Fuel* [online]. 2005. Available from: https://rwm.nda.gov.uk/publication/technical-note-outline-design-for-a-reference-repository-concept-for-uk-high-level-waste-spent-fuel-2005/?download

56. PEREIRA, Claubia, ACHILLES, Jéssica P., CARDOSO, Fabiano, CASTRO, Victor F. and VELOSO, Maria Auxiliadora F. Criticality safety analysis of spent fuel pool for a PWR using UO2, MOX,(Th-U) O2 and (TRU-Th) O2 fuels. *Brazilian Journal of Radiation Sciences*. 2019. Vol. 7, no. 3A.
DOI https://doi.org/10.15392/bjrs.v7i3A.833.

57. ANSYS. ANSYS Modeling and Meshing Guide. . 2005.

58. JASAK, Hrvoje, JEMCOV, Aleksandar and TUKOVIC, Zeljko. OpenFOAM: A C++ library for complex physics simulations. In : *International workshop on coupled methods in numerical dynamics*. IUC Dubrovnik Croatia, 2007. p. 1–20.

59. ROACHE, P. J. Perspective: A Method for Uniform Reporting of Grid Refinement Studies. *Journal of Fluids Engineering*. 1 September 1994. Vol. 116, no. 3, p. 405–413. DOI 10.1115/1.2910291.

60. ROACHE, Patrick J. *Fundamentals of verification and validation*. Socorro, New Mexico : hermosa publ, 2009. ISBN 978-0-913478-12-7.

61. PUT, M. and HENRION, P. Modelling of radionuclide migration and heat transport from an HLW-repository in Boom Clay. *EUR(Luxembourg)*. 1992.

62. ANSYS, INC. *Ansys® Workbench, 2019 R3, Help System, Mechanical APDL 2019 R3 - CHAPTER 3:TRANSIENT THERMAL ANALYSIS*. ANSYS, Inc., 2019.

63. COLEMAN, Hugh W., STERN, Fred, DI MASCIO AND, Andrea and CAMPANA, Emilio. The Problem With Oscillatory Behavior in Grid Convergence Studies. *Journal of Fluids Engineering*. 1 June 2001. Vol. 123, no. 2, p. 438–439. DOI 10.1115/1.1362672.

64. HAMZA, Valiya, VIEIRA, Fabio, GOMES, Jorge Luiz dos Santos, GUIMARAES, Suze, ALEXANDRINO, Carlos and GOMES, Antônio. Update of Brazilian Heat Flow Data, within the framework of a multiprong referencing system. *International Journal of Terrestrial Heat Flow and Applications*. 10 March 2020. Vol. 3, no. 1, p. 45–72. DOI 10.31214/ijthfa.v3i1.42.

65. INSTITUTO NACIONAL DE METEOROLOGIA - INMET. BDMEP - Dados Históricos. *Instituto Nacional de Meteorologia* [online]. Available from: https://portal.inmet.gov.br/servicos/bdmep-dados-hist%C3%B3ricos

66. ANSYS, INC. *Ansys® Workbench, 2019 R3, Help System, Mechanical APDL 2019 R3 - 15.2. Transient Analysis*. ANSYS, Inc., 2019.

67. VIII. The deferred approach to the limit. *Philosophical Transactions of the Royal Society of London. Series A, Containing Papers of a Mathematical or Physical Character*. January 1927. Vol. 226, no. 636–646, p. 299–361. DOI 10.1098/rsta.1927.0008.

68. CHO, Won-Jin and KIM, Geon Young. Reconsideration of thermal criteria for Korean spent fuel repository. *Annals of Nuclear Energy*. February 2016. Vol. 88, p. 73–82. DOI 10.1016/j.anucene.2015.09.012.

69. INTERNATIONAL ATOMIC ENERGY AGENCY. *Planning and design considerations for geological repository programmes of radioactive waste.* [online]. 2014. [Accessed 11 May 2020]. Available from: http://www-pub.iaea.org/MTCD/Publications/PDF/TE-1755_web.pdf

70. EMPRESA DE PESQUISA ENERGÉTICA. Plano nacional de energia 2030. *Ministério de Minas e Energia: Brasília, Brazil*. 2007.

71. ELETRONUCLEAR. Novos Empreendimentos. *Novos Empreendimentos* [online]. [Accessed 12 November 2020]. Available from: https://www.eletronuclear.gov.br/Canais-de-Negocios/Paginas/Novos-Empreendimentos.aspx

72. MARTA SALOMON. Acidente no Japão atrasa usinas do nordeste - Sustentabilidade. *O Estado de São Paulo* [online]. São Paulo, 9 November 2011. [Accessed 22 October 2020]. Available from: https://sustentabilidade.estadao.com.br/noticias/geral,acidente-no-japao-atrasa-usinas-do-nordeste,716834

73. LUÍS ANTONIO TERRIBILE DE MATTOS. *ANÁLISE PRELIMINAR SOBRE A DISPOSIÇÃO DE REJEITOS RADIOATIVOS DE ALTA ATIVIDADE EM FORMAÇÕES GEOLÓGICAS DO ESTADO DE SAO PAULO* [online]. Dissertação. São Paulo : Instituto de Pesquisas Energéticas e Nucleares, 1981. Available from: http://pelicano.ipen.br/PosG30/TextoCompleto/Luis%20Antonio%20Terribile%20de%20Mattos_M.pdf

74. CYRO T. ENOKIHARA. *O armazenamento de rejeitos radioativos no Brasil com enfase especial em rochas* [online]. Dissertação. São Paulo : Instituto de Pesquisas Energeticas e Nucleares - IPEN-CNEN/SP, 1983. Available from: http://repositorio.ipen.br/bitstream/handle/123456789/9836/11272.pdf?sequence=1&isAllowed=y

75. SILVA, Corbiniano, HEILBRON, Monica Da Costa Pereira Lavalle and FILHO, Paulo Fernando Lavalle Heilbron. SITE SELECTION OF A GEOLOGICAL REPOSITORY FOR THE SAFE DISPOSAL OF HIGH-LEVEL WASTE IN THE

STATE OF RIO DE JANEIRO. *Revista Internacional de Ciências*. 7 July 2015. Vol. 5, no. 1, p. 83–105. DOI 10.12957/ric.2015.16615.

76. PEREIRA, Claubia, JONUSAN, Raoni A. S., SILVA, Raphael H. M. and SILVA, Clarysson Alberto M. Seleção de áreas para a construção de um repositório geológico em Minas Gerais. *Brazilian Journal of Radiation Sciences* [online]. 4 July 2019. Vol. 7, no. 3. [Accessed 27 January 2021]. DOI 10.15392/bjrs.v7i3.831. Available from: https://www.bjrs.org.br/revista/index.php/REVISTA/article/view/831

77. MACHADO, Marcely Ferreira and SILVA, Sandra Fernandes da. *Geodiversidade do estado de Minas Gerais*. CPRM, 2010. ISBN 85-7499-091-4.

78. SILVA, Sandra Fernandes da and MACHADO, Marcely Ferreira (eds.). *Geodiversidade do estado do Espiríto Santo*. Belo Horizonte : CPRM, Serviço Geológico do Brasil, 2014. Programa Geologia do Brasil. Levantamento da Geodiversidade. ISBN 978-85-7499-139-9. QE38 .G33 2010

79. *Brasil em Relevo* [online]. [map]. Campinas : Embrapa Monitoramento por Satélite, 2005. [Accessed 25 June 2021]. Available from: http://www.relevobr.cnpm.embrapa.br/

80. DNIT - DEPARTAMENTO NACIONAL DE INFRAESTRUTURA DE TRANSPORTES. *Mapa Rodoviário Brasileiro* [online]. [map]. 2021. Available from: https://servicos.dnit.gov.br/dnitcloud/index.php/s/oTpPRmYs5AAdiNr/download?path=%2FSNV%20Bases%20Geom%C3%A9tricas%20(2013-Atual)%20(SHP)&files=202104A.zip

81. IBGE - FUNDAÇÃO INSTITUTO BRASILEIRO DE GEOGRAFIA E ESTATÍSTICA. *Base Cartográfica Contínua do Brasil* [online]. [map]. IBGE, 2019. Available from: https://geoftp.ibge.gov.br/cartas_e_mapas/bases_cartograficas_continuas/bc250/versao2019/shapefile/bc250_shapefile_06_11_2019.zip

82. FERNANDO F. ALKMIM. História Geológica de Minas Gerais. In : *Recursos Minerais de Minas Gerais On Line: síntese do conhecimento sobre as riquezas minerais, história geológica, e meio ambiente e mineração de Minas Gerais* [online]. Belo Horizonte : Companhia de Desenvolvimento de Minas Gerais (CODEMGE), 2018. Available from: http://recursomineralmg.codemge.com.br

83. WALLENIUS, Jyrki, DYER, James S., FISHBURN, Peter C., STEUER, Ralph E., ZIONTS, Stanley and DEB, Kalyanmoy. Multiple Criteria Decision Making, Multiattribute Utility Theory: Recent Accomplishments and What Lies Ahead. *Management Science*. July 2008. Vol. 54, no. 7, p. 1336–1349. DOI 10.1287/mnsc.1070.0838.

84. BHUSHAN, Navneet and RAI, Kanwal. *Strategic decision making: applying the analytic hierarchy process*. London ; New York : Springer, 2004. Decision engineering. ISBN 978-1-85233-756-8. HD30.23 .B5 2004

85. SAATY, Thomas L. How to make a decision: the analytic hierarchy process. *European journal of operational research*. 1990. Vol. 48, no. 1, p. 9–26.

86. IBGE - FUNDAÇÃO INSTITUTO BRASILEIRO DE GEOGRAFIA E ESTATÍSTICA. *Mapa de Cobertura e Uso da Terra do Brasil* [online]. [map]. Brasil : IBGE, 2018. Available from: https://geoftp.ibge.gov.br/informacoes_ambientais/cobertura_e_uso_da_terra/monitoramento/grade_estatistica/Brasil/vetores/Cobertura_uso_da_terra_Brasil.zip

87. CPRM - SERVIÇO GEOLÓGICO DO BRASIL. *Mapa Geológico do Estado da Minas Gerais* [online]. [map]. CPRM, 2021. Available from: https://rigeo.cprm.gov.br/jspui/bitstream/doc/21828/4/sig_minas_gerais.zip

88. MINISTÉRIO DOS TRANSPORTES. *Mapa Ferroviário Brasileiro* [online]. [map]. 2019. Available from: https://www.gov.br/infraestrutura/pt-br/centrais-de-conteudo/ferrovias-zip

89. ANDRÉ RODRIGO FARIAS, RAFAEL MINGOTI, LAURA BUTTI DO VALLE, CLÁUDIO A. SPADOTTO, and ELIO LOVISI FILHO. *Identificação, mapeamento e quantificação das áreas urbanas do Brasil* [online]. [map]. EMBRAPA, 2017. Available from: http://geoinfo.cnpm.embrapa.br/geoserver/wfs?format_options=charset%3AUTF-8&typename=geonode%3Aareas_urbanas_br_15&outputFormat=SHAPE-ZIP&version=1.0.0&service=WFS&request=GetFeature

90. NUCLEAR ENERGY AGENCY. NEA No. 7331: *Japan's Siting Process for the Geological Disposal of High-level Radioactive Waste: An International Peer Review*. 2016.

91. NUCLEAR WASTE MANAGEMENT ORGANIZATION OF JAPAN. NUMO-TR-13-05? *Safety of the Geological Disposal Project 2010 - Safe Geological Disposal Based on Reliable Technologies (English Summary)*. 2013.

92. KÄRN BRÄNSLE SÄKERHET. *Handling of spent nuclear fuel and final storage of vitrified high-level reprocessing waste*. Sweden : Safety analysis Stockholm, 1977.

93. JAPAN, Nuclear Waste Management Organization of. *Evaluating site suitability for a HLW repository, scientific background, and practical application of NUMO's siting factors*. NUMO Tokyo, 2004.

94. SFOE (SWISS FEDERAL OFFICE OF ENERGY). *Sectoral Plan for Deep Geological Repositories: Conceptual Part*. Department of the Environment, Transport, Energy and Communications (DETEC) Bern, 2008.

95. AGENCY, OECD Nuclear Energy and SITES, NEA Working Group on Assessment of Future Human Actions at Radioactive Waste Disposal. *Future Human Actions at Disposal Sites: A Report of the NEA Working Group on Assessment of Future Human Actions at Radioactive Waste Disposal Sites*. OECD, 1995. ISBN 92-64-14372-6.

96. HEINECK, Carlos Alberto, LEITE, Carlos Augusto da Silva, SILVA, M. A. and VIEIRA, Valter Salino. Mapa geológico do Estado de Minas Gerais, Escala 1: 1.000. 000. *Belo Horizonte: Convênio COMIG/CPRM*. 2003. Vol. 1.

97. MATOS, Gerson Manoel Muniz de, MELLO, Ivan Sergio de Cavalcanti and GONÇALVES, João Henrique. Áreas de relevante interesse mineral no Brasil-ARIM. . 2009.

98. LADEIRA NETO, José Francisco. *Mapa de declividade em percentual do relevo brasileiro* [online]. [map]. Brasil : CPRM, 2013. Available from: http://www.cprm.gov.br/publique/Gestao-Territorial/Gestao-Territorial/Mapa-de-Declividade-em-Percentual-do-Relevo-Brasileiro-3497.html

99. DNIT - DEPARTAMENTO NACIONAL DE INFRAESTRUTURA DE TRANSPORTES. *Sistema Nacional de Viação* [online]. [map]. DNIT, 2016. Available from: http://servicos.dnit.gov.br/vgeo/

100. *Encyclopedia of GIS* [online]. 2008. [Accessed 14 September 2020]. ISBN 978-0-387-35973-1. Available from: https://doi.org/10.1007/978-0-387-35973-1

101. INSTITUTO BRASILEIRO DE GEOGRAFIA E ESTATÍSTICA. *Divisão Regional do Brasil em Regiões Geográficas Imediatas e Regiões Geográficas Intermediárias*. Instituto Brasileiro de Geografia e Estatística Rio de Janeiro, 2017.

102. NILO HENRIQUE BALZANI LOPES, PEDRO HENRIQUE SILVA BARBOSA, ALANNA LEITE DOS SANTOS, LUCAS EUSTÁQUIO DIAS AMORIM, MÔNICA ELIZETTI DE FREITAS, and FRANCISCO JAVIER RIOS. A migração de fluidos como ferramenta de avaliação da viabilidade da implantação de repositórios de rejeitos radioativos geológicos (RARN) em rochas granitoides: testes em granitos submetidos a deformação natural vs. não deformados. In : *2017 International Nuclear Atlantic Conference - INAC 2017 Belo Horizonte,*. Belo Horizonte, October 2017. ISBN 978-85-99141-07-6.

103. VALTER SALINO VIEIRA and RICARDO GALLART DE MENEZES (eds.). *Geologia e Recursos Minerais do Estado do Espírito Santo: texto explicativo do mapa geológico e de recursos minerais*. Belo Horizonte : CPRM, Serviço Geológico do Brasil, 2015. ISBN 978-85-7499-252-5. QE38 .G33 2010

104. MINAS GERAIS. *LEI nº 9,547, DE 30/12/1987."Proíbe a instalação de lixo atômico ou de rejeitos radioativos no Estado de Minas Gerais e dá outras providências."* [online]. 30 December 1987. Available from: https://www.almg.gov.br/consulte/legislacao/completa/completa.html?tipo=LEI&num=9547&comp=&ano=1987&aba=js_textoOriginalProíbe a instalação de lixo atômico ou de rejeitos radioativos no Estado de Minas Gerais e dá outras providências.

105. MINAS GERAIS. *DECRETO nº 40,969, DE 23/03/2000. “Proíbe o ingresso, no Estado, de rejeito radioativo.”* [online]. 23 March 2000. Available from: https://www.almg.gov.br/consulte/legislacao/completa/completa.html?tipo=DEC&num=40969&comp=&ano=2000Proíbe o ingresso, no Estado, de rejeito radioativo.

106. ESPÍRITO SANTO. *LEI Nº 4,033, DE 23 DE DEZEMBRO DE 1987* [online]. 23 December 1987. Available from: http://www3.al.es.gov.br/Arquivo/Documents/legislacao/html/LEI40331987.html

107. SUPREMO TRIBUNAL FEDERAL. PGR contesta normas estaduais que proíbem ou restringem a construção de usinas e depósitos nucleares. *Supremo*

Tribunal Federal [online]. 30 June 2021. [Accessed 30 June 2021]. Available from: http://portal.stf.jus.br/noticias/verNoticiaDetalhe.asp?idConteudo=467798&ori=1

108. IAEA. *Costing Methods and Funding Schemes for Radioactive Waste Disposal Programmes* [online]. Vienna : IAEA, 2020. [Accessed 5 July 2021]. ISBN 978-92-0-111720-5. Available from: http://public.eblib.com/choice/PublicFullRecord.aspx?p=6416360

109. KING, David. A low carbon nuclear future: Economic assessment of nuclear materials and spent nuclear fuel management in the UK. *Smith School of Enterprise and the Environment, University of Oxford*. 2011.

110. BOSTON CONSULTING GROUP. *Economic Assessment of Used Fuel Management in the United States* [online]. 2006. Available from: http://image-src.bcg.com/Images/BCG_Economic_Assessment_of_Used_Nuclear_Fuel_Management_in_the_US_Jul_06_tcm9-132990.pdf

111. MATTHEW BUNN, STEVE FETTER, JOHN P. HOLDREN, and BOB VAN DER ZWAAN. DE-FG26-99FT4028: *The Economics of Reprocessing vs. Direct Disposal of Spent Nuclear Fuel* [online]. Cambridge, MA, United States. : Belfer Center for Science and International Affairs, John F. Kennedy School of Government, Harvard University, 2003. Available from: https://www.belfercenter.org/sites/default/files/files/publication/repro-report.pdf

112. ROTHWELL, GS and WOOD, T. *The Value of Spent Nuclear Fuel Retrievability*. a working paper for the International Atomic Energy Agency, Pacific …, 2011.

113. OECD. PUBLISHING. *Advanced Nuclear Fuel Cycles and Radioactive Waste Management*. Organisation for Economic Co-operation and Development, 2006. ISBN 92-64-02486-7.

114. MASSACHUSETTS INSTITUTE OF TECHNOLOGY. *The future of nuclear fuel cycle: an interdisciplinary MIT study.* [online]. Cambridge, Mass. : Massachusetts Institute of Technology, 2011. [Accessed 2 July 2021]. ISBN 978-0-9828008-4-3. Available from: http://web.mit.edu/ceepr/www/publications/MIT%20Future_of_Nuclear_Fuel_Cycle.pdf

115. DIXON, B. W., GANDA, F., WILLIAMS, K. A., HOFFMAN, E. and HANSON, J. K. INL/EXT--17-43826, 1423891: *Advanced Fuel Cycle Cost Basis – 2017 Edition* [online]. 2017. [Accessed 2 July 2021]. Available from: http://www.osti.gov/servlets/purl/1423891/

116. HOLT, Derek. *Financing the nuclear option: modelling the cost of new build* [online]. Oxford : OXERA, 2005. Available from: https://www.oxera.com/wp-content/uploads/2018/03/Financing-the-nuclear-option-3.pdfpublisher: Oxera, Oxford, available from: http://www. oxera. com/cmsDocuments/Agenda_June

117. PB POWER (FIRM) and ROYAL ACADEMY OF ENGINEERING (GREAT BRITAIN). *The cost of generating electricity* [online]. London : Royal Academy of Engineering, 2004. ISBN 978-1-903496-11-4. Available from:

https://www.eusustel.be/public/documents_publ/links_to_docs/cost/cost_generation_report.pdf

118. TOLLEY, George, JONES, Donald, CASTELLANO, M, CLUNE, W, DAVIDSON, P, DESAI, K, FOO, A, KATS, A, LIAO, M and IANTCHEV, E. The economic future of nuclear power. *University of Chicago* [online]. 2004. Available from: https://www.eusustel.be/public/documents_publ/links_to_docs/cost/uoc-study.pdf

119. YANGBO DU and JOHN E. PARSONS. Update on the Cost of Nuclear Power. *SSRN Electronic Journal* [online]. 2009. [Accessed 2 July 2021]. DOI 10.2139/ssrn.1470903. Available from: http://www.ssrn.com/abstract=1470903

120. DE ROO, Guillaume and PARSONS, John E. A methodology for calculating the levelized cost of electricity in nuclear power systems with fuel recycling. *Energy Economics*. September 2011. Vol. 33, no. 5, p. 826–839. DOI 10.1016/j.eneco.2011.01.008.

121. MORATILLA SORIA, B. Yolanda, URIS MAS, Maria, ESTADIEU, Mathilde, VILLAR LEJARRETA, Ainhoa and ECHEVARRIA-LÓPEZ, David. Recycling versus Long-Term Storage of Nuclear Fuel: Economic Factors. *Science and Technology of Nuclear Installations*. 2013. Vol. 2013, p. 1–7. DOI 10.1155/2013/417048.

122. HAMEL, J. An Economic Analysis of Select Fuel Cycles Using the Steady-State Analysis Model for Advanced Fuel Cycles Schemes (SMAFS). *Energy Resources International, Inc.: Washington, DC, USA*. 2007.

123. RECKTENWALD, GD and DEINERT, MR. Cost probability analysis of reprocessing spent nuclear fuel in the US. *Energy Economics*. 2012. Vol. 34, no. 6, p. 1873–1881.

124. LOKHOV, Alexey, URSO, Maria Elena and CAMERON, Ron. OECD/NEA study on economics of the Back-end of the Nuclear Fuel Cycle. . 2013.

125. INTERNATIONAL ASSOCIATION FOR ENVIRONMENTALLY SAFE DISPOSAL OF RADIOACTIVE MATERIALS – EDRAM. *Guidelines for comparing cost assessments for geological repository projects* [online]. EDRAM, 2012. Available from: http://www.edram.info/fileadmin/user_upload/_imported/guidelines_comparative_analysis_cost_assessments.pdf

126. IAEA. *Management of Spent Fuel from Nuclear Power Reactors Learning from the Past, Enabling the Future.* [online]. Vienna : IAEA, 2020. [Accessed 17 November 2020]. ISBN 978-92-0-108720-1. Available from: http://public.eblib.com/choice/PublicFullRecord.aspx?p=6244680

127. SPEKTOR, Matias. Without Reversal: Brazil as a Latent Nuclear State. *Nuclear Latency and Hedging*. 2019. P. 175.

128. INTERNATIONAL ATOMIC ENERGY AGENCY. Power Reactor Information System (PRIS). [online]. 10 June 2020. [Accessed 19 June 2020]. Available from: https://pris.iaea.org/pris/CountryStatistics/CountryDetails.aspx?current=BR

129. MINISTÉRIO DE MINAS E ENERGIA. EMPRESA DE PESQUISA ENERGÉTICA. *Plano Decenal de Expansão de Energia 2029* [online]. Brasília, 2020. Available from: http://www.epe.gov.br/sites-pt/publicacoes-dados-abertos/publicacoes/Documents/PDE%202029.pdf

130. Governo prevê construção de seis novas usinas nucleares até 2050. *Valor Econômico* [online]. [Accessed 16 April 2020]. Available from: https://valor.globo.com/brasil/noticia/2019/09/26/governo-preve-a-construcao-de-seis-novas-centrais-nucleares-ate-2050.ghtmlEmpreendimentos devem somar 6,6 mil megawatts e demandarão US$ 30 bilhões em investimentos

131. TOGZHAN KASSENOVA, LUCAS PEREZ FLORENTINO, and MATIAS SPEKTOR. *Prospects for Nuclear Governance in Brazil* [online]. São Paulo : FGV RI, 2020. [Accessed 10 March 2020]. Available from: https://ri.fgv.br/en/news/2020-03-10/prospects-nuclear-governance-brazil

132. LEONARD, Barry. *GAO Cost estimating and assessment guide: Best practices for developing and managing capital program costs*. Diane Publishing, 2009. ISBN 1-4379-1702-X.

133. ANGELIS, Diana I., FRANCK, Raymond, MELESE, Francois and DILLARD, John. *Applying insights from Transaction Cost Economics (TCE) to improve DoD cost estimation* [online]. 2007. Available from: http://hdl.handle.net/10945/601Calhoun

134. MELESE, F., RICHTER, A. and SOLOMON, B. (eds.). *Military Cost-benefit Analysis: Theory and Practice*. London : Routledge/Taylor & Francis Group, 2015. Routledge studies in defence and peace economics, Volume 14. ISBN 978-1-138-85042-2. UA25.5 .M55 2015

135. TRIBUNAL DE CONTAS DA UNIÃO. *036.751/2018-9 - Relatório de Auditoria* [online]. 5 February 2020. 3/2020-Plenário. [Accessed 10 June 2020]. Available from: https://pesquisa.apps.tcu.gov.br/#/documento/acordao-completo/%2522angra%25203%2522%2520conclus%25C3%25A3o/%2520/DTRELEVANCIA%2520desc%252C%2520NUMACORDAOINT%2520desc/1/%2520

136. LARISSA FAFÁ. Pernambucana Itacuruba é o local “preferencial” para instalação de nova usina nuclear. *Agência EPBR* [online]. 29 August 2020. Available from: https://epbr.com.br/pernambucana-itacuruba-e-o-local-preferencial-para-instalacao-de-nova-usina-nuclear/

137. GIOVANNA CARNEIRO. Instalação de usina nuclear no Sertão de Pernambuco é debatida na Alepe. *Folha de Pernambuco* [online]. 7 October 2019. Available from: https://www.folhape.com.br/noticias/instalacao-de-usina-nuclear-no-sertao-de-pernambuco-e-debatida-na-alep/118237/

138. PERNAMBUCO. *LEI Nº 10.088, DE 21 DE DEZEMBRO DE 1987. “Proíbe a instalação de usina nuclear, derivadas e similares; a guarda de lixo atômico, e de química letal, assim consideradas; e a celebração de convênios ou concessões de licenças pertinentes, e disciplina o transporte desses produtos no Estado de Pernambuco.”* [online]. 21 December 1987. Available from: https://legis.alepe.pe.gov.br/texto.aspx?id=9351&tipo=

139. IMPRENSA CNBB. IGREJA RECEBE APOIO CONTRA PROJETO DE CONSTRUÇÃO DE USINA NUCLEAR. *Conferência Nacional dos Bispos do Brasil* [online]. 29 November 2019. Available from: https://cnbbne2.org.br/cnbb-ne-2-tem-apoio-do-governo-e-da-oab-contra-usina-nuclear-em-pe/

140. IMPRENSA ALEPE. Usina nuclear: João Paulo aponta riscos para população de Itacuruba. *Assembleia Legislativa do Estado de Pernambuco* [online]. 1 March 2021. Available from: https://www.alepe.pe.gov.br/2021/03/18/usina-nuclear-joao-paulo-aponta-riscos-para-populacao-de-itacuruba/

141. OPERADOR NACIONAL DO SISTEMA ELÉTRICO - ONS. ONS NT-0020/2017: *IMPORTÂNCIA DA UTN ANGRA 3 PARA O ATENDIMENTO DO SIN* [online]. Rio de Janeiro : ONS, 2017. Available from: https://www.eletronuclear.gov.br/Sociedade-e-Meio-Ambiente/Documents/NT_0020_2017_Importancia_Angra_3_.pdf

142. EMPRESA DE PESQUISA ENERGÉTICA. *Plano Nacional de Energia 2050 - Energia Nuclear*. 2020.

143. *Modelling Nuclear Energy Systems with MESSAGE: A User's Guide* [online]. Vienna : INTERNATIONAL ATOMIC ENERGY AGENCY, 2016. Nuclear Energy Series, NG-T-5.2. ISBN 978-92-0-109715-6. Available from: https://www.iaea.org/publications/10861/modelling-nuclear-energy-systems-with-message-a-users-guide

144. RAMONA ORDOÑEZ. Eletronuclear e Westinghouse assinam acordo para extensão da vida útil de Angra 1. *O Globo* [online]. 30 January 2020. [Accessed 19 June 2020]. Available from: https://oglobo.globo.com/economia/eletronuclear-westinghouse-assinam-acordo-para-extensao-da-vida-util-de-angra-1-24220916

145. ELETRONUCLEAR. Informações de Angra 1. [online]. [Accessed 3 June 2020]. Available from: http://www.eletronuclear.gov.br/Nossas-Atividades/Paginas/Informacoes-de-Angra-1.aspx

146. ELETRONUCLEAR. Informações de Angra 2. [online]. [Accessed 3 June 2020]. Available from: http://www.eletronuclear.gov.br/Nossas-Atividades/Paginas/Informacoes-de-Angra-2.aspx

147. AREVA. Status Report 78: *The Evolutionary Power Reactor (EPR)* [online]. 2011. [Accessed 30 April 2020]. Available from: https://aris.iaea.org/PDF/EPR.pdf

148. DANIEL W. MULLIGAN. *IMPROVED MODELING OF THREE-POINT ESTIMATES FOR DECISION MAKING: GOING BEYOND THE TRIANGLE* [online]. Master's thesis. MONTEREY, CALIFORNIA : NAVAL POSTGRADUATE SCHOOL, 2016. Available from: https://apps.dtic.mil/sti/pdfs/AD1027514.pdf

149. TOLMASQUIM, Mauricio Tiomno. Energia termelétrica: gás natural, biomassa, carvão, nuclear. *Rio de Janeiro: EPE*. 2016. P. 25.

150. EMPRESA DE PESQUISA ENERGÉTICA – EPE. *Premissas e Custos da Oferta de Energia Elétrica no horizonte 2050*. 2018. ESTUDOS DE LONGO PRAZO.

151. GOLLIER, Christian. Discounting an uncertain future. *Journal of public economics*. 2002. Vol. 85, no. 2, p. 149–166.

152. OXERA, A. Social Time Preference Rate for Use in Long-term Discounting. *The office of the Deputy Prime Minister, Department for transport and Department for the Environment, food and rural affairs, London*. 2002.

153. GÉNÉRAL DU PLAN, Commissariat. Révision du taux d'actualisation des investissements publics. *Présidé par D. Lebegue, La Documentation Française*. 2005.

154. ESRI. What is Empirical Bayesian kriging? *Kriging in Geostatistical Analyst* [online]. Available from: https://desktop.arcgis.com/en/arcmap/10.6/extensions/geostatistical-analyst/what-is-empirical-bayesian-kriging-.htm

155. CARLOS HENRIQUE ALEXANDRINO, SANIELY EDUARDA MAGALHÃES COUY, and FLAVIANY LOPES RODRIGUES. AVALIAÇÃO DOS RECURSOS GEOTÉRMICOS DE MINAS GERAIS. *Revista Vozes dos Vales: Publicações Acadêmicas* [online]. May 2012. No. 01. Available from: http://site.ufvjm.edu.br/revistamultidisciplinar/files/2011/09/Avalia%C3%A7%C3%A3o-dos-recursos-geot%C3%A9rmicos-de-Minas-Gerais.pdf

156. NUCLEAR WASTE MANAGEMENT ORGANIZATION - NWMO. *Programs around the world for managing used nuclear fuel* [online]. NWMO, 2020. Available from: https://www.nwmo.ca/~/media/Site/Files/PDFs/2020/08/05/14/52/IntPrograms_2020-Web.ashx?la=en

APPENDIX A – CALCULATION OF THE SUBSURFACE TEMPERATURE

An important part of the SNF heat transfer simulation is the determination of the thermal and temperature properties of the host rock. As shown in Figure 21, for a given geometric configuration of the SNF disposal panel, at each every 1ºC of enhancement in host rock temperature, is observed an increase of 1ºC maximum temperature at the surface of the canister. In this way, locations with a lower geothermal gradient and, consequently, lower rock temperatures in the depth of the repository are preferable.

Therefore, the temperature of the Brazilian subsoil rocks at the depth, 500m, of the repository was calculated. The calculation was made with the help of the work by Hamza et al, who compiled data on the thermal properties of the Brazilian subsoil. This work has the temperature gradients, thermal conductivity, heat flux, and radiogenic heat production of 406 sites in Brazil. Figure 58 shows the location of the measurement points. In addition, data on the average surface temperature observed in 2020 were used, from a total of 700 meteorological collection stations throughout Brazil, as shown in Figure 59

Figure 58 – Location of the heat data source. Adapted from (64).

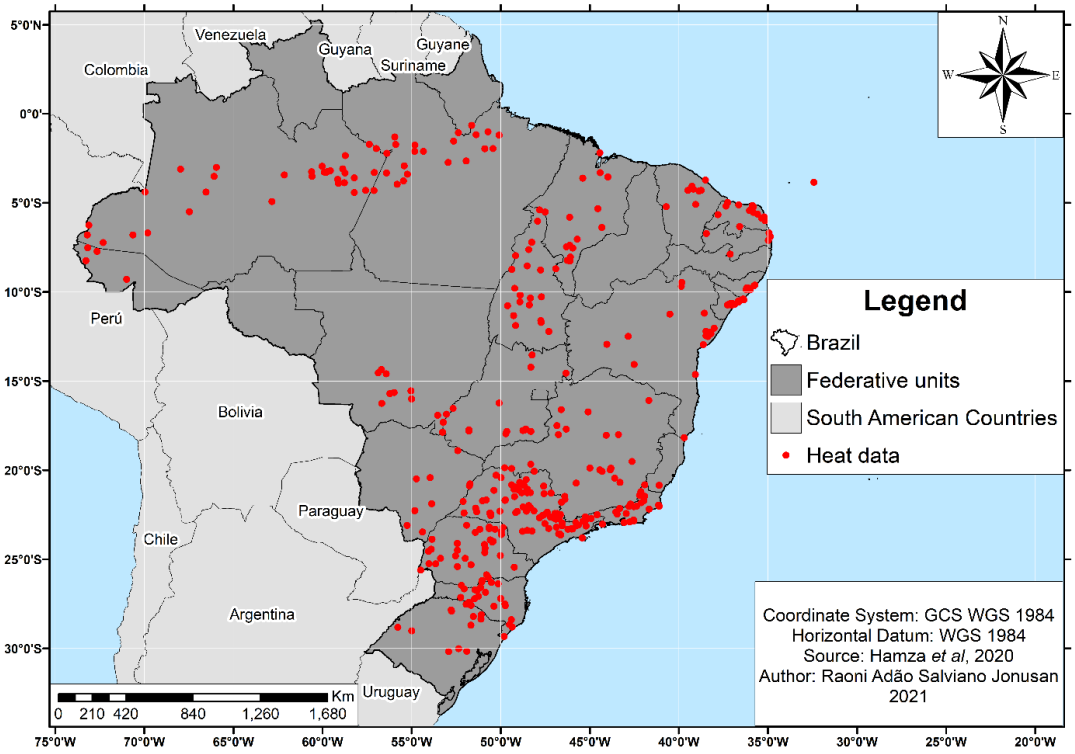

Figure 59 – Location of the surface temperature data source. Adapted from (65).

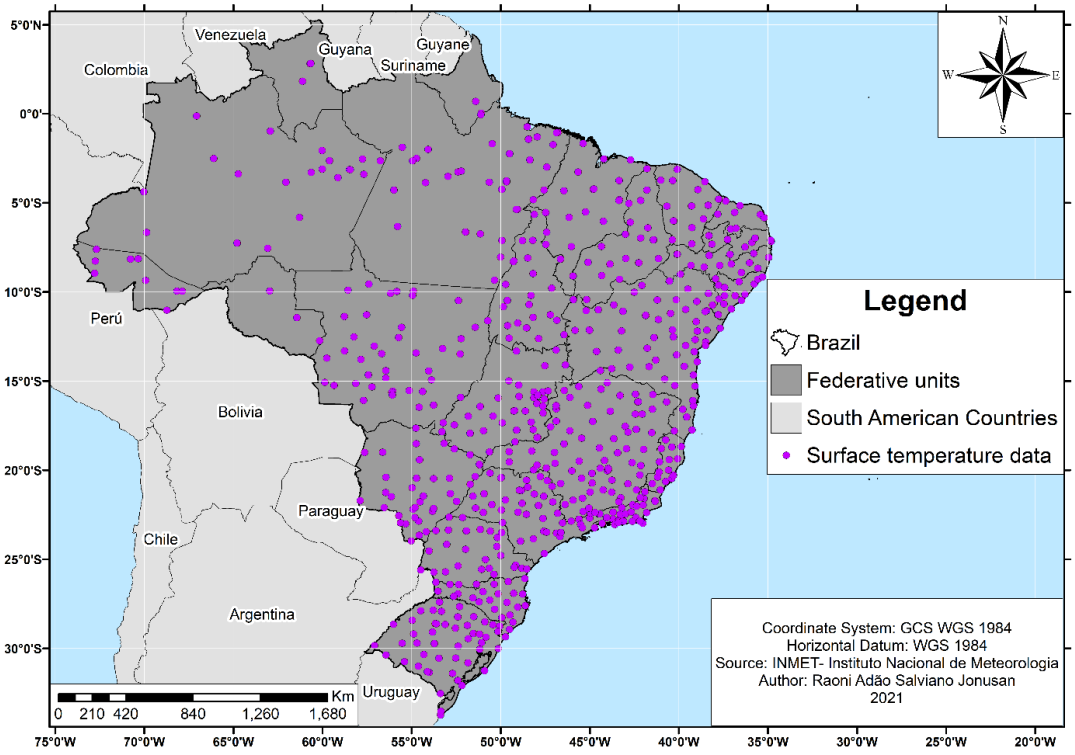

With the raw data, interpolations were performed to estimate the distribution of thermal properties in Brazil. It should be noted that especially for the Midwest and North, there are large regions without direct measurement of properties, which affects the quality of the interpolation. The interpolation was performed with the help of ArcMap 10.60.1 and geostatistical analyst tools. The Empirical Bayesian Kriging tool was used for all cases. We chose to use this tool for the following reasons (154):

- Requires minimal interactive modeling.
- Standard errors of prediction are more accurate than other kriging methods.
- Allows accurate predictions of moderately nonstationary data.
- More accurate than other kriging methods for small datasets.

During the interpolation process, the properties shown in Table 25 were used for the geostatistical interpolation of the data.

Table 25 – Properties for the Empirical Bayesian Kriging tool.

Properties	**Conductivity**	**Heat Flow**	**Mean Surface Temperature**	**Geothermal Gradient**	**Radiogenic Heat Production**
Subset Size	500				
Overlap Factor	5				
Nº of Simulation	1000				
Transformation	Empirical				
Semivariogram Type	K-Bessel Detrended			K-Bessel	Whittle Detrended

It is important to emphasize that geostatistical interpolation techniques, such as kriging, depend on the notion of autocorrelation. Autocorrelation is assumed to be a function of distance, taking as a true one of the basic principles of geography: things close together are more similar than things that are far apart. Geostatistical techniques, therefore, use information from the spatial location of the parameters to calculate the distances between observations and model the autocorrelation as a function of distance. Even with a considerable number of observations used, the values estimated in this work should be used with care, given the large distance between each observation and the different lithologies existing between then in the Brazilian territory.

The Brazilian thermal conductivity has values between 1.88 W/mK and 3.16 W/mK. The lowest values found are in two anomalies in the North region. The highest values are found in the states of Minas Gerais and the interior of Bahia. Figure 60 shows the thermal conductivity map of Brazil.

Figure 60 – Thermal conductivity map of Brazil.

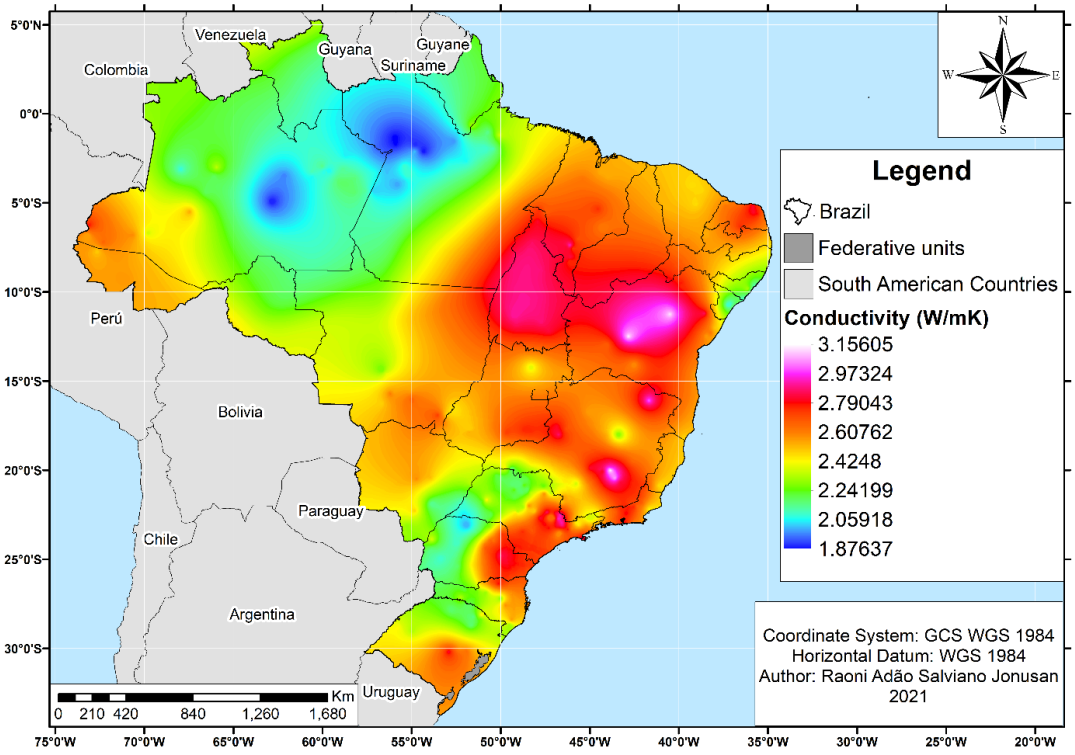

The variation of heat flux in Brazil is exceptionally large. Values range between 36.06 W/m² and 105.62 W/m². The state of Rio de Janeiro is marked by low heat fluxes, while the state of Ceará is marked by high thermal conductivity values. Figure 61 shows the thermal heat flux map of Brazil.

Figure 61 – Heat flow map of Brazil.

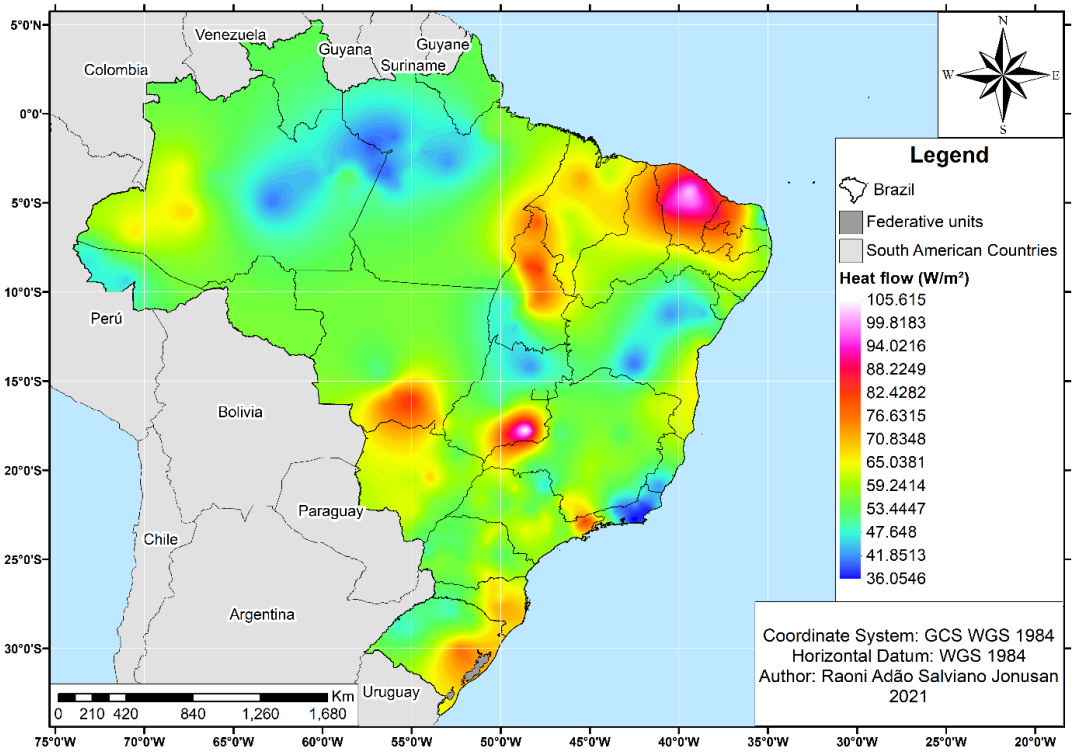

The highest values of radiogenic heat production area in the interior of the Bahia, in Goiás, and the eastern portion of Rio Grande do Sul. The Bahian anomaly is located near the uranium deposit of Caetité. Figure 62 shows the map of radiogenic heat production in Brazil.

Figure 62 – Radiogenic heat production map of Brazil.

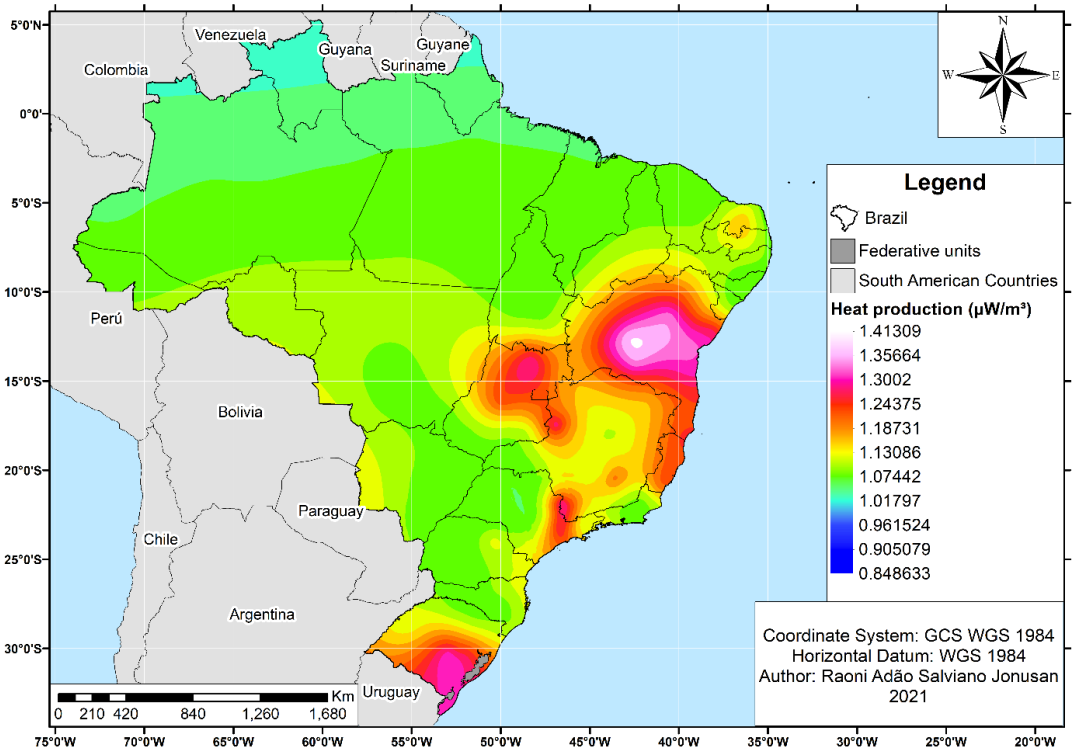

Brazil is marked by low values of the geothermal gradient. Most of the country has values around 25ºC/km. Rio de Janeiro has the lowest values of the geothermal gradient, close to 16ºC/km. Three places are marked by large grids, the state of Ceará, the border region between Minas Gerais and Goiás, and the border region between São Paulo and Rio de Janeiro. Figure 63 shows the map of the Brazilian geothermal gradient.

Figure 63 – Geothermal gradient map of Brazil.

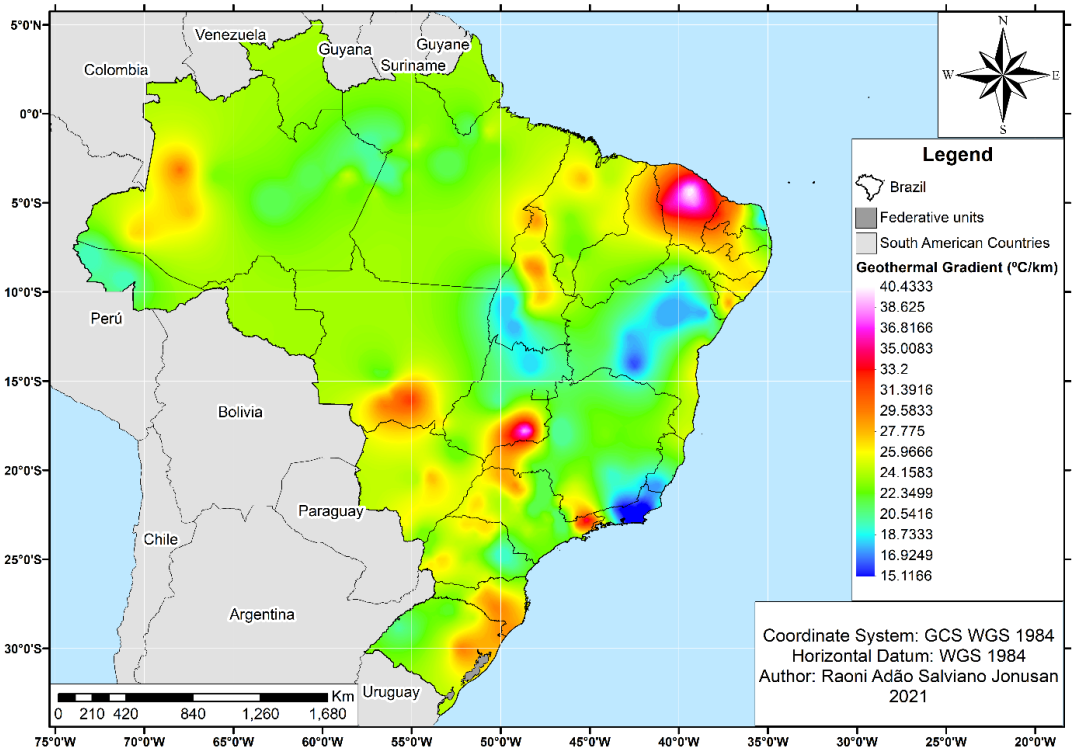

Another essential piece of information is the average surface temperature in Brazil. Brazil can be divided into three regions. The first, concentrated in the north and northeast region, has the highest average annual temperatures, with temperatures above 26ºC. The second, with intermediate average temperatures, is in the Southeast and Midwest regions. The latter in the southern region has the lowest average annual temperatures, below 20ºC. Figure 64 shows the map of the 2020 average annual temperature of Brazil.

Figure 64 – Mean surface temperature of 2020 map of Brazil.

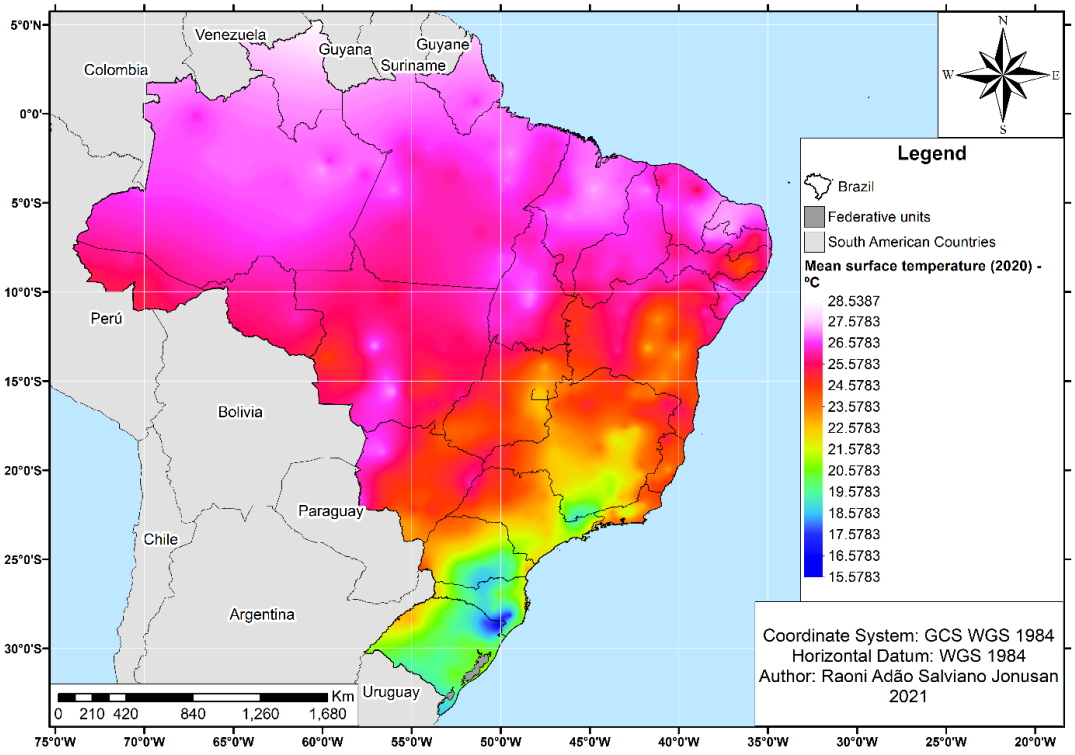

Based on these data, it is possible to calculate the temperature of the Brazilian subsoil at different depths. Temperatures were calculated for the upper limit of the model in chapter 01, 475 m; for the repository tunnel depth, 500m; and for the lower limit of the model, 532.5m. The temperature is calculated using the formula (155):

$$T_z = \frac{q_0 * z}{\lambda} - \frac{A_0 * z^2}{2\lambda} + T_0 \qquad (20)$$

Where T_z is the crust temperature in ºC, q_0 is the heat flux in W/m², z is the depth in m, λ is the thermal conductivity in W/mK, A_0 is the radiogenic heat production mW/m³, and T_0 is the mean surface temperature in ºC. The results are shown in Figure 65, Figure 66, and Figure 67.

Figure 65 – Rock temperature at 475 m depth map of Brazil.

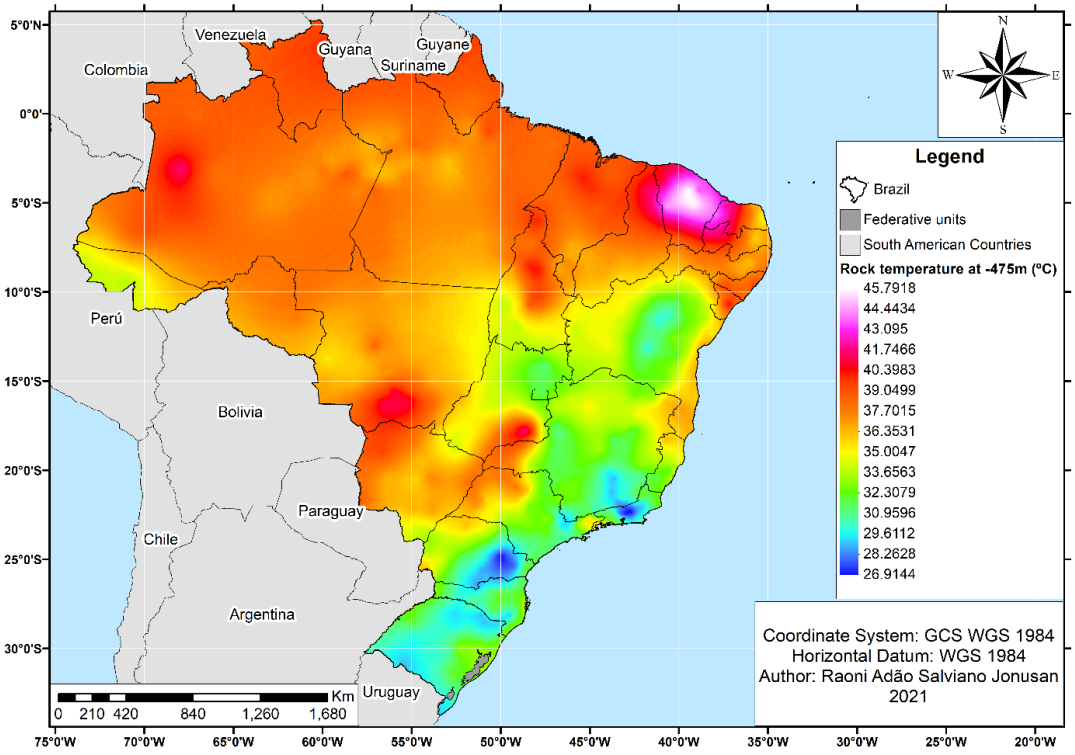

Figure 66 – Rock temperature at 500 m depth map of Brazil.

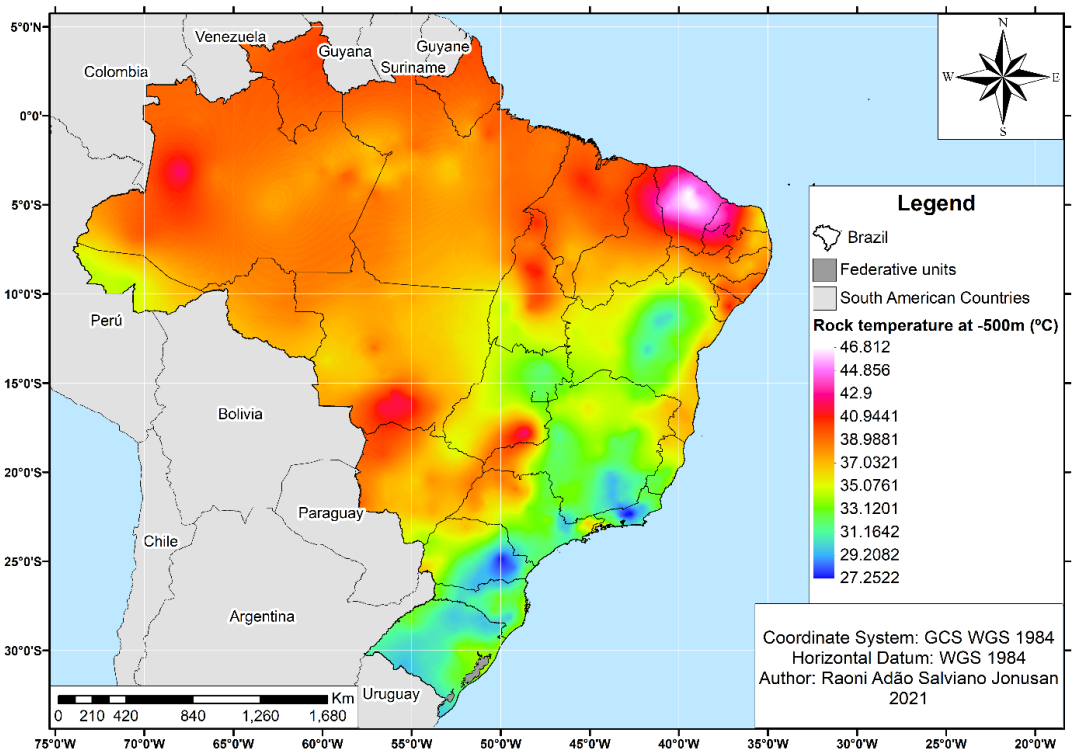

Figure 67 – Rock temperature at 532.5 m depth map of Brazil.

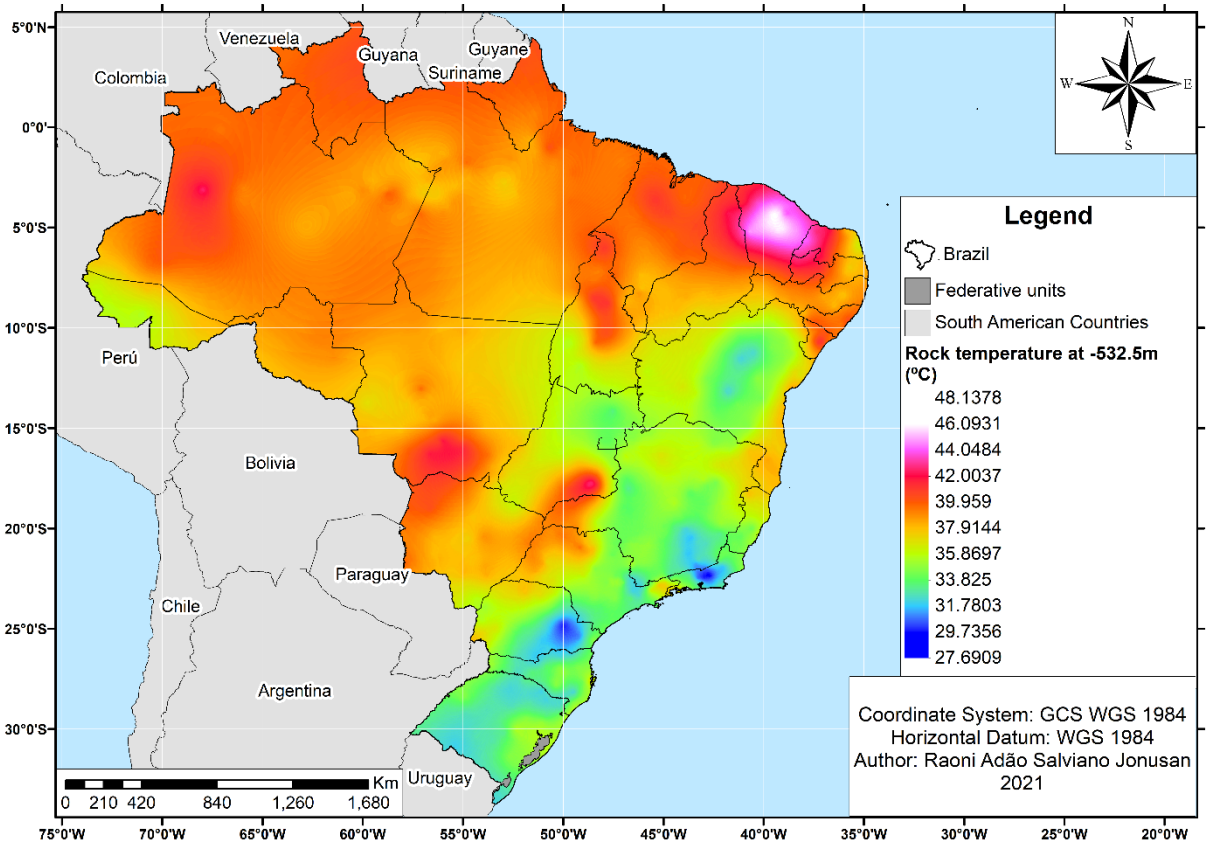

APPENDIX B – DISTRIBUTION CURVES FOR THE INPUT DATA

Figure 68 – Interim storage ***ANGRA1&2 OFC.***

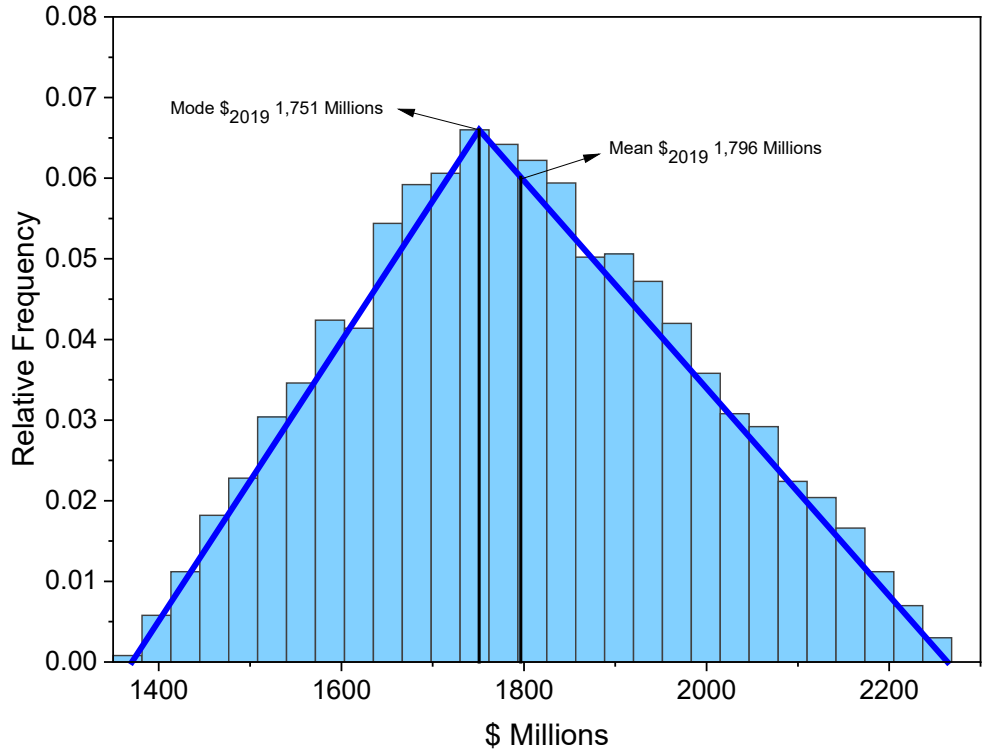

Figure 69 – Encapsulation plant ***ANGRA1&2 OFC.***

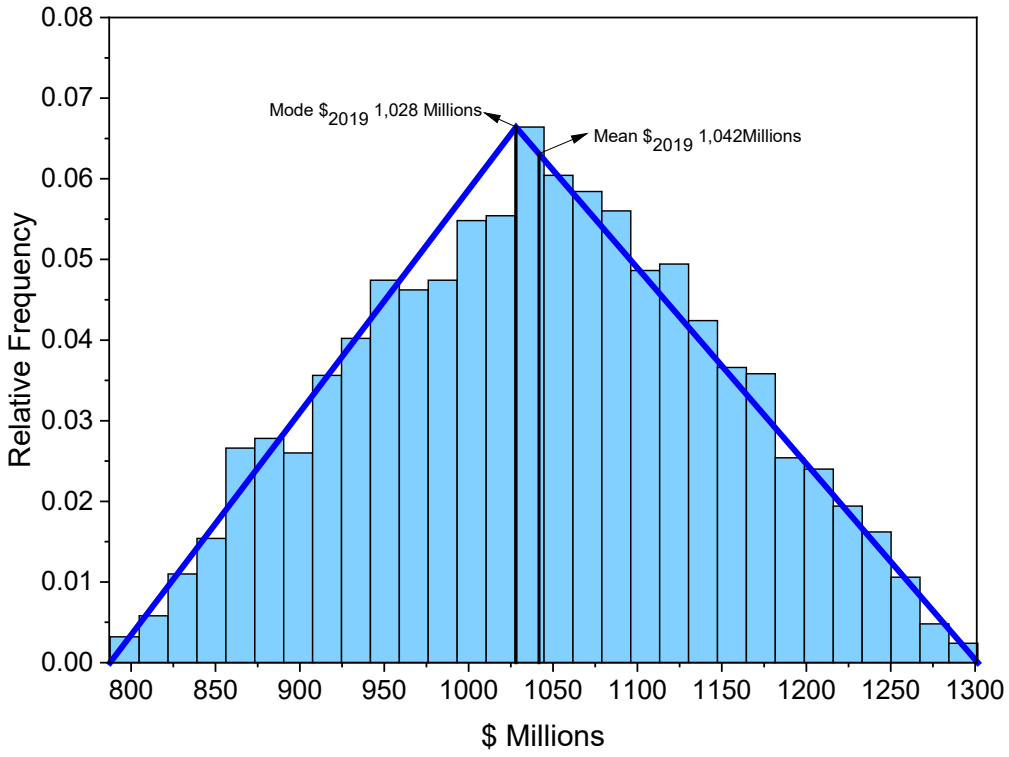

Figure 70 – Repository ***ANGRA1&2 OFC.***

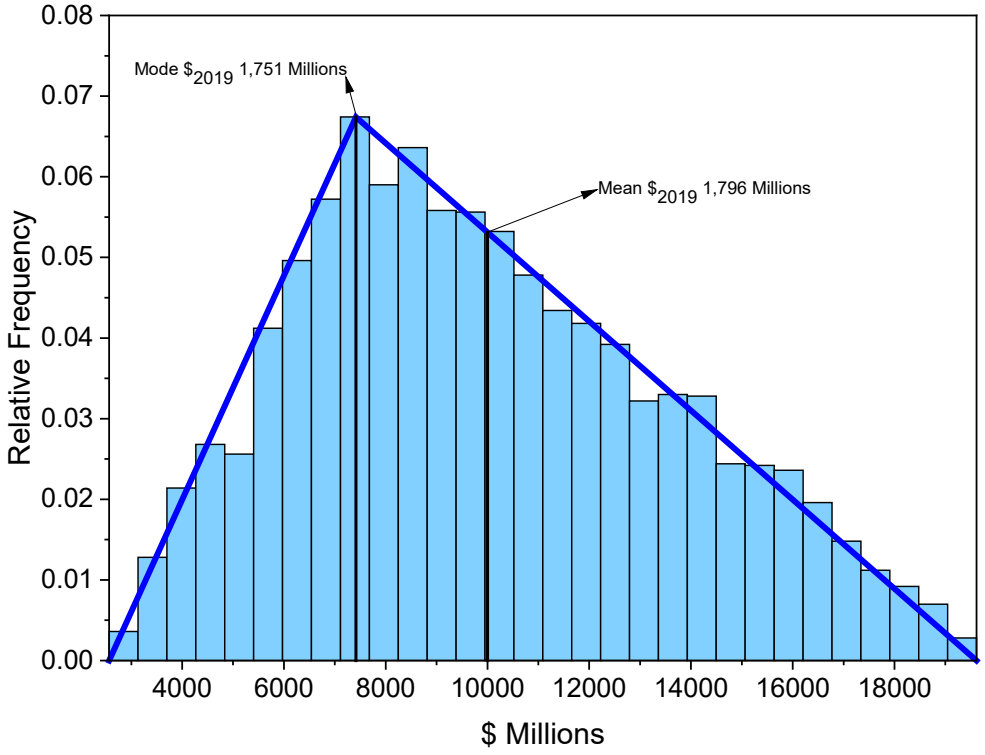

Figure 71 – Transport ***ANGRA1&2 OFC.***

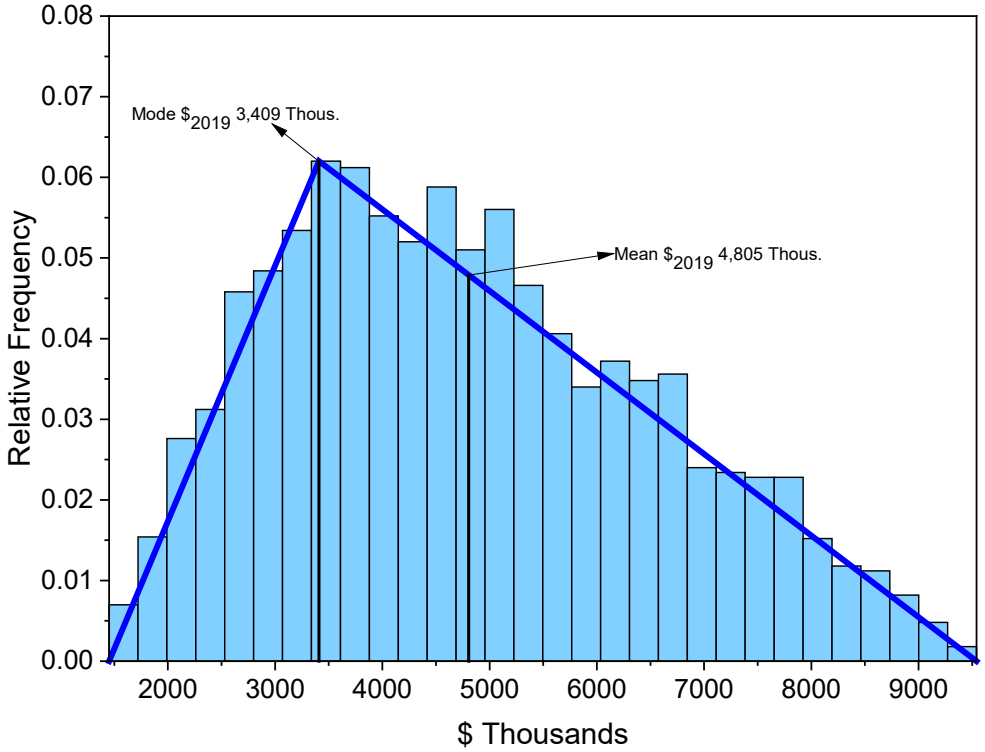

Figure 72 – Interim storage ***ANGRA3 OFC.***

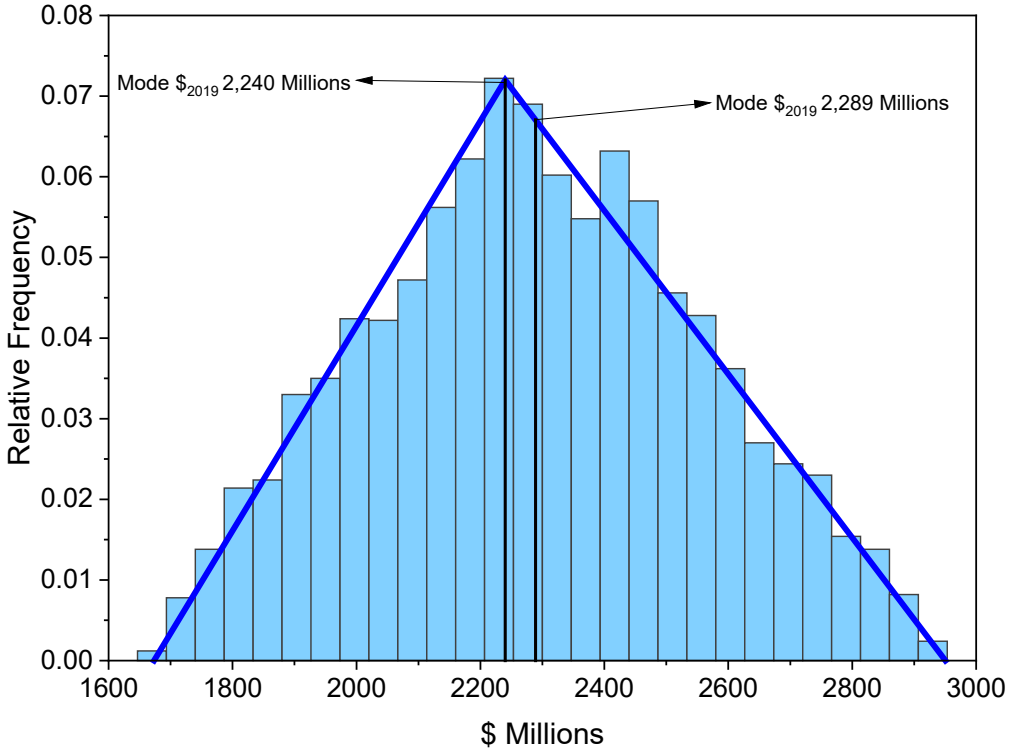

Figure 73 – Encapsulation plant ***ANGRA3 OFC.***

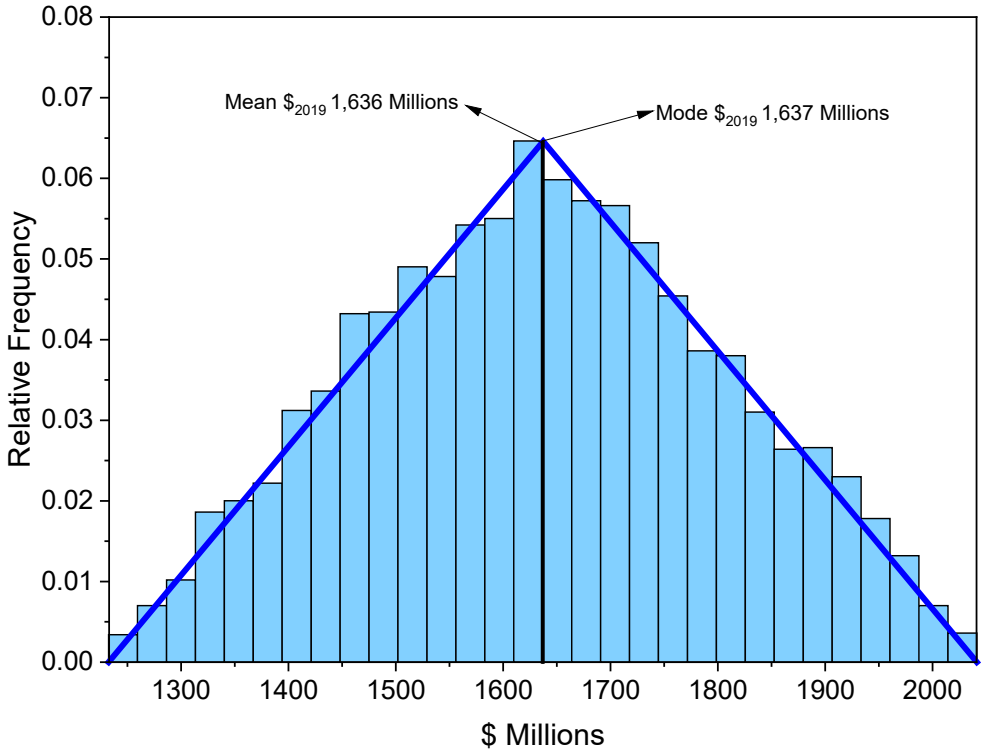

Figure 74 – Repository ***ANGRA3 OFC.***

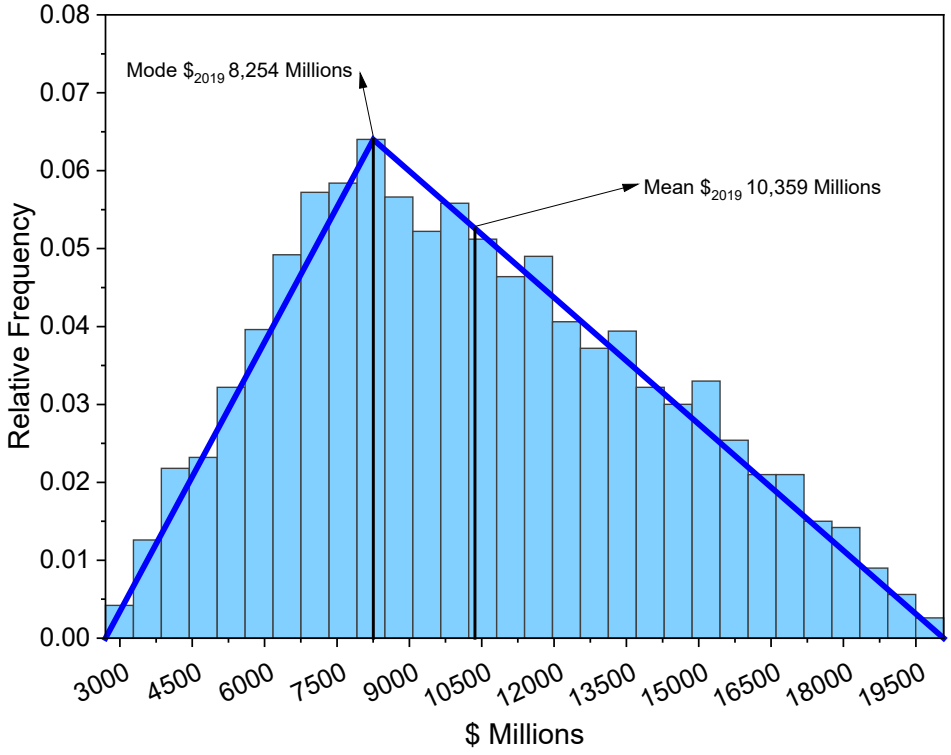

Figure 75 – Transport ***ANGRA3 OFC.***

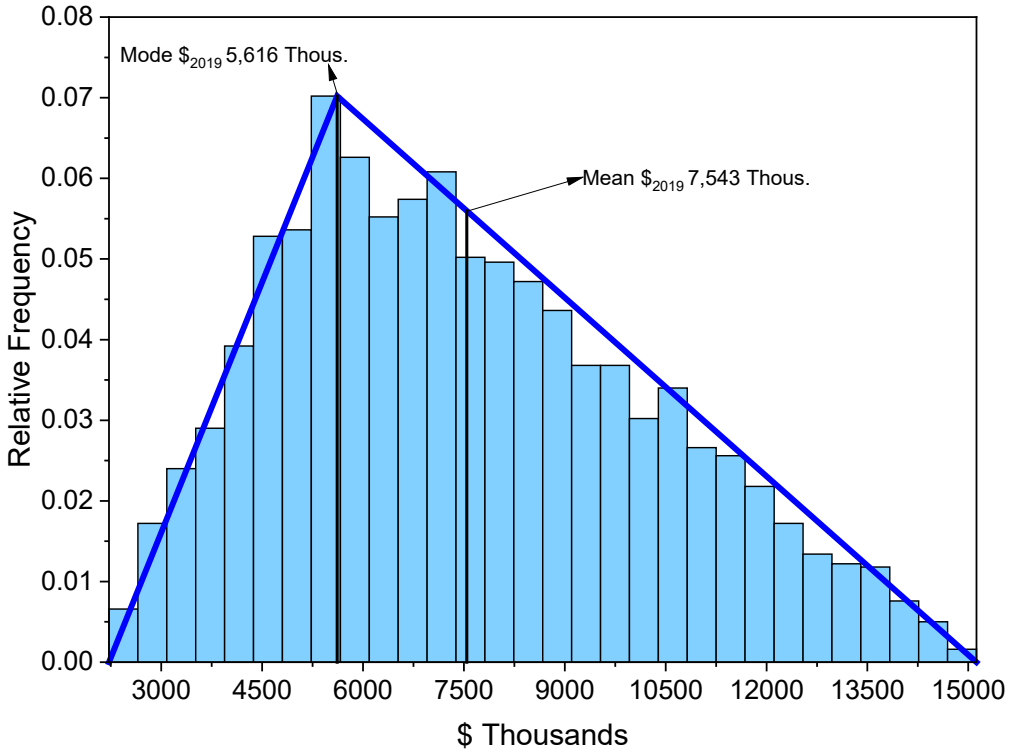

Figure 76 – Interim storage ***ANGRA+8 OFC.***

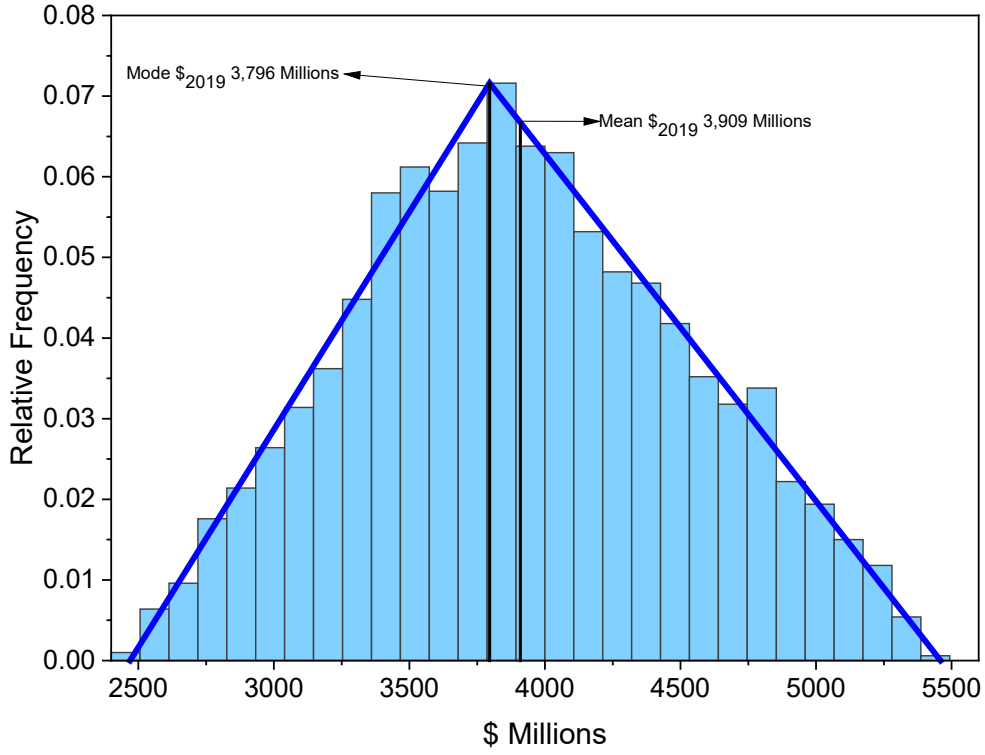

Figure 77 – Encapsulation plant ***ANGRA+8 OFC.***

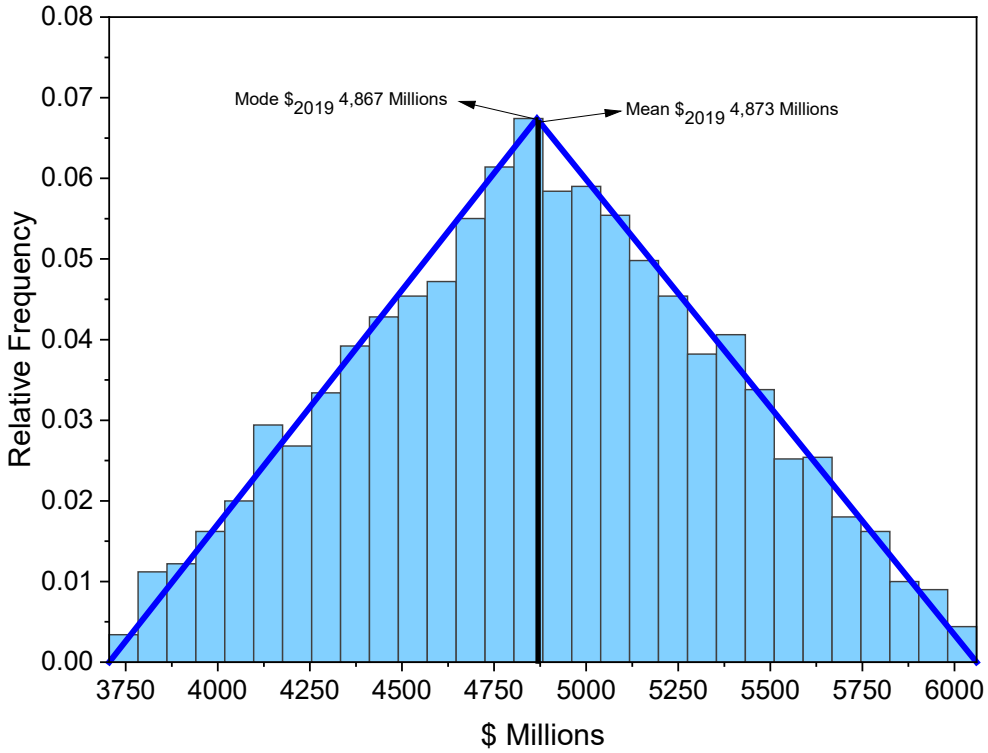

Figure 78 – Repository ***ANGRA+8 OFC.***

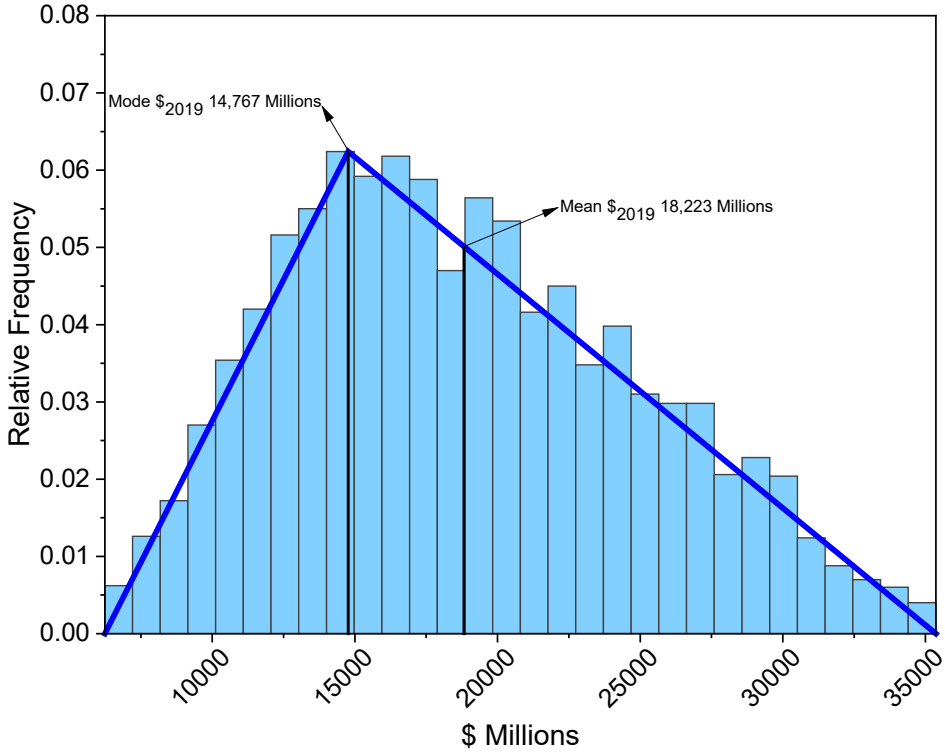

Figure 79 – Transport ***ANGRA+8 OFC.***

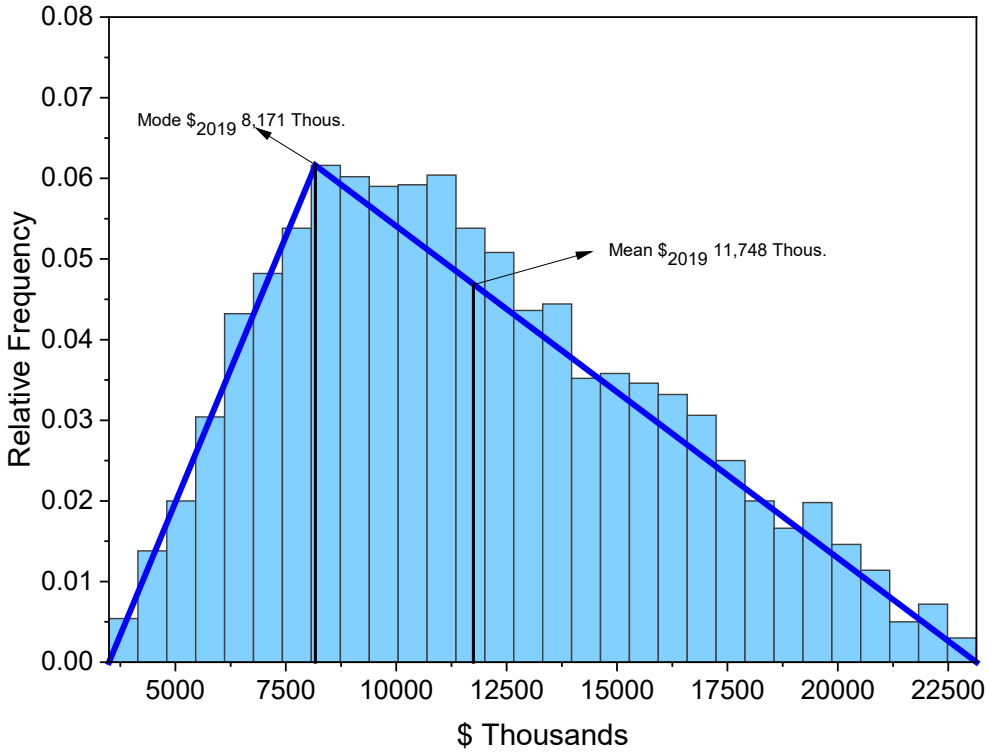

Figure 80 – Interim storage ***ANGRA1&2 CFC.***

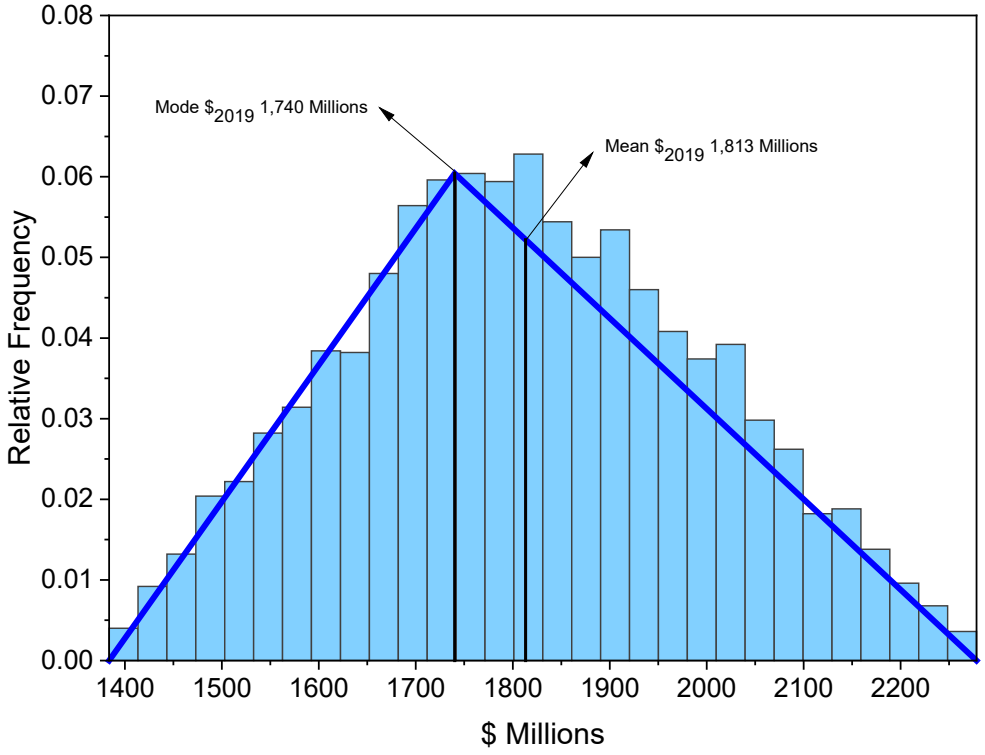

Figure 81 – Reprocessing plant ***ANGRA1&2 CFC.***

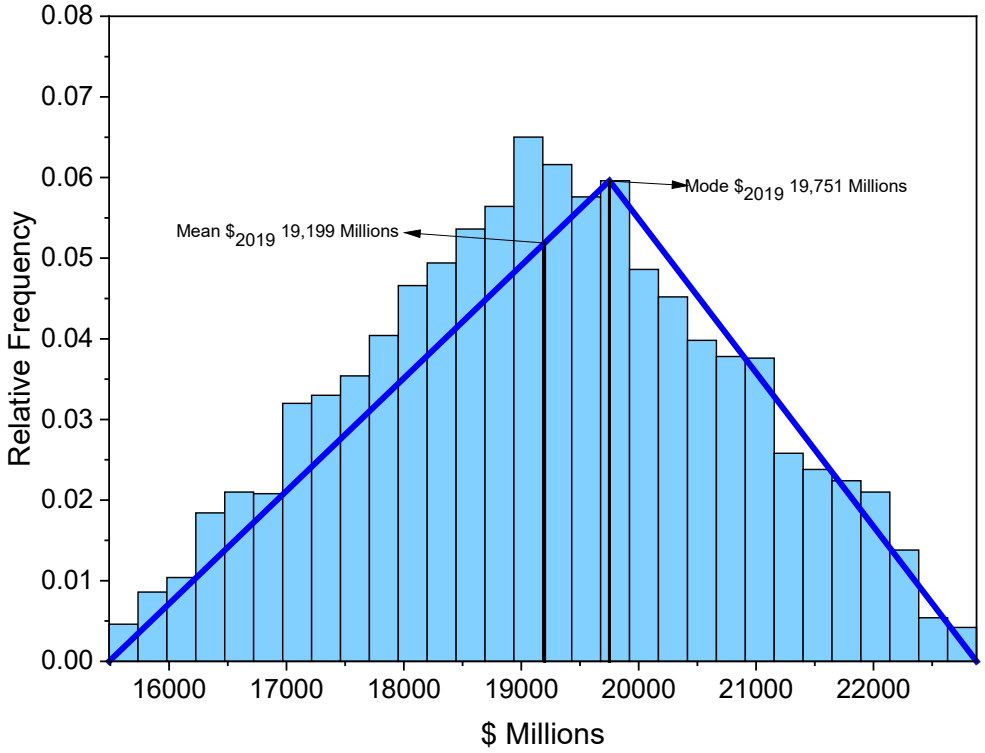

Figure 82 – Encapsulation plant ***ANGRA1&2 CFC.***

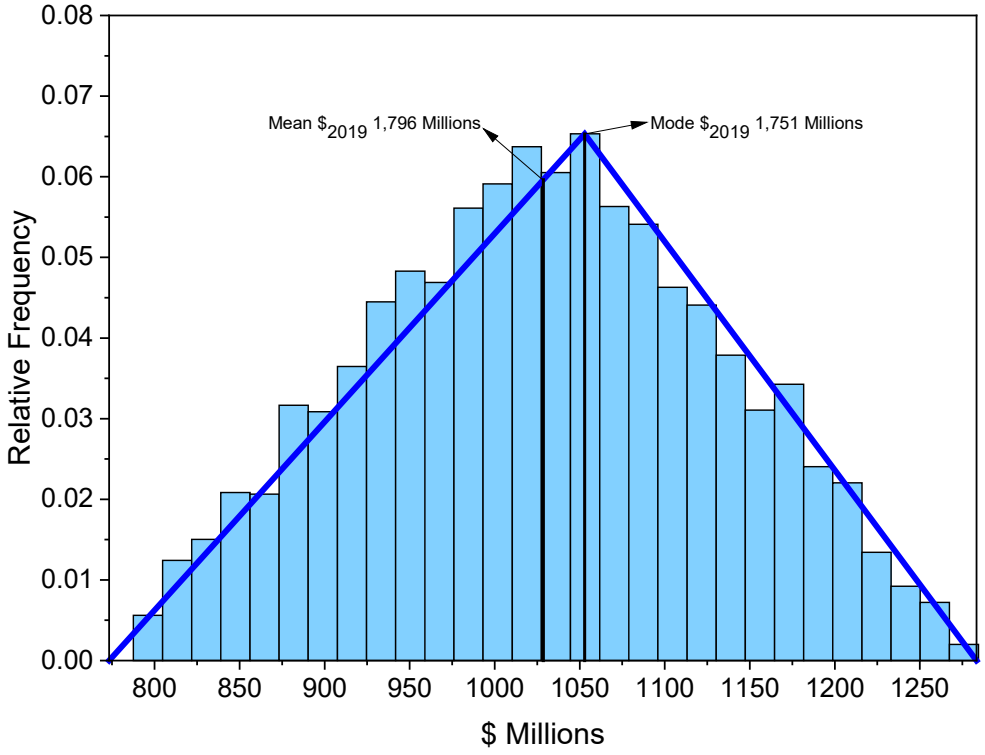

Figure 83 – Repository ***ANGRA1&2 CFC.***

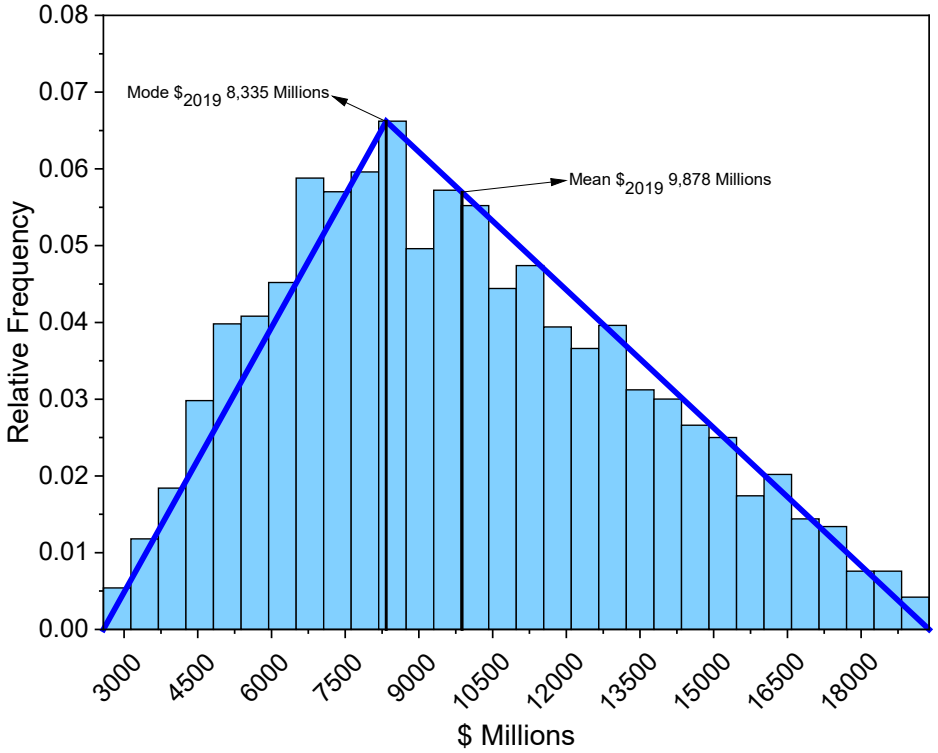

Figure 84 – Transport ***ANGRA1&2 CFC.***

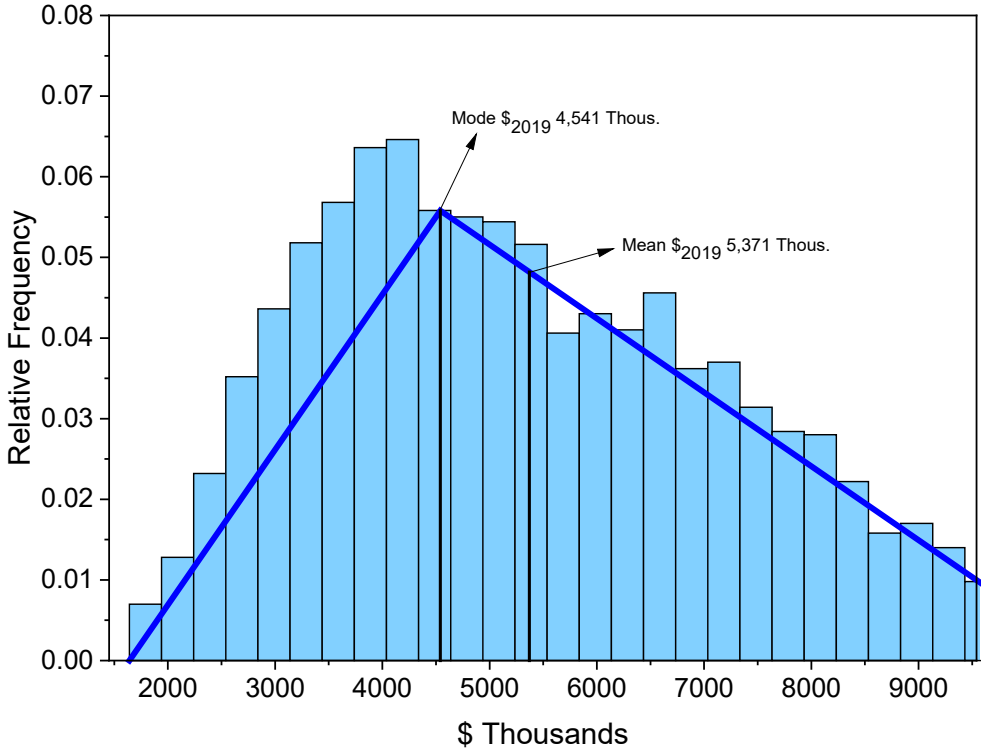

Figure 85 – Interim storage ***ANGRA3 CFC.***

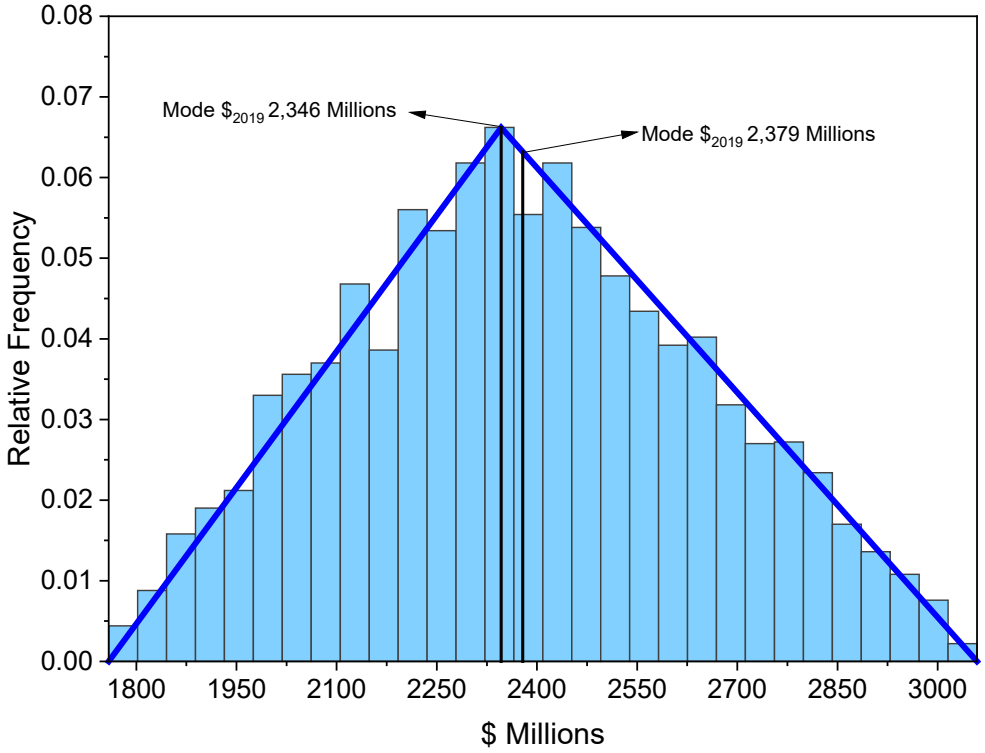

Figure 86 – Reprocessing plant ***ANGRA3 CFC.***

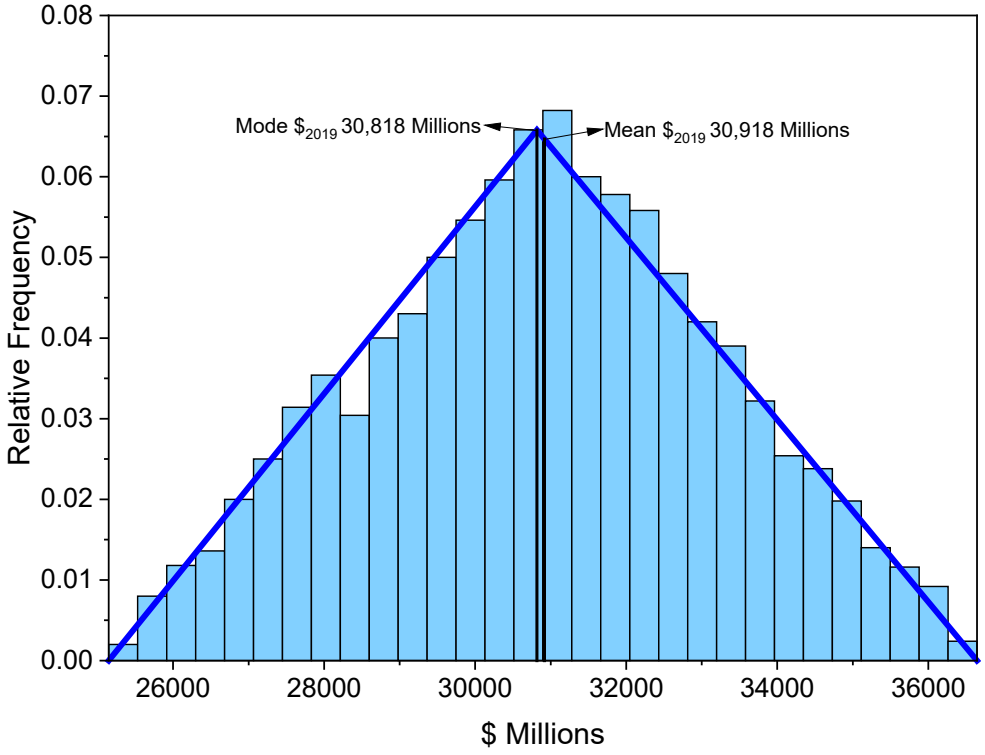

Figure 87 – Encapsulation plant ***ANGRA3 CFC.***

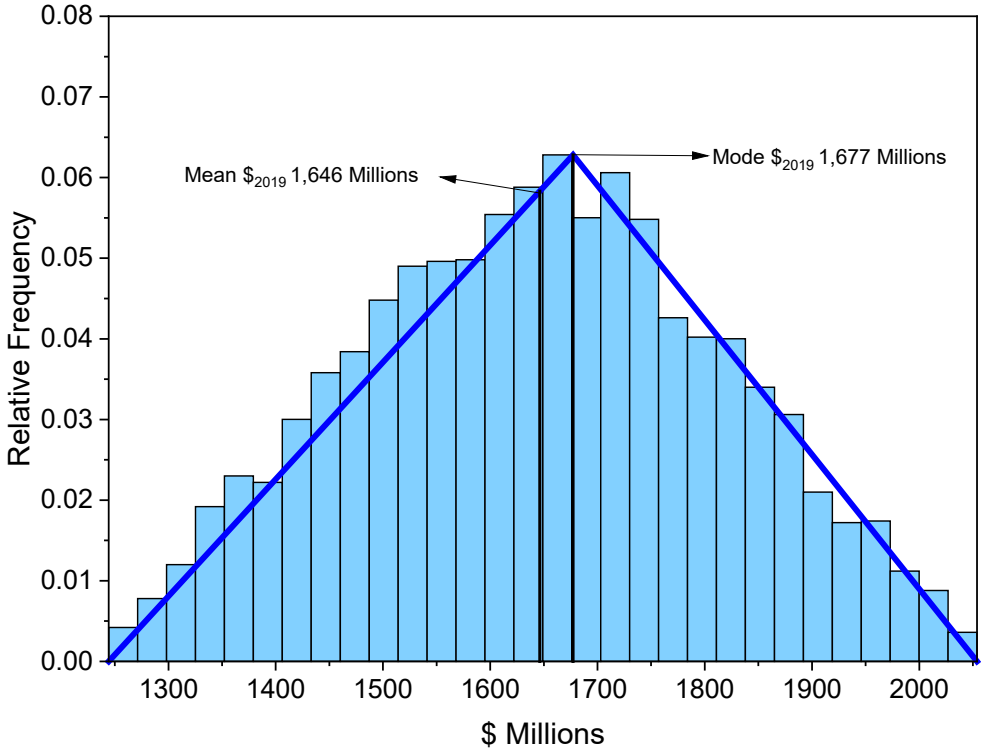

Figure 88 – Repository ***ANGRA3 CFC.***

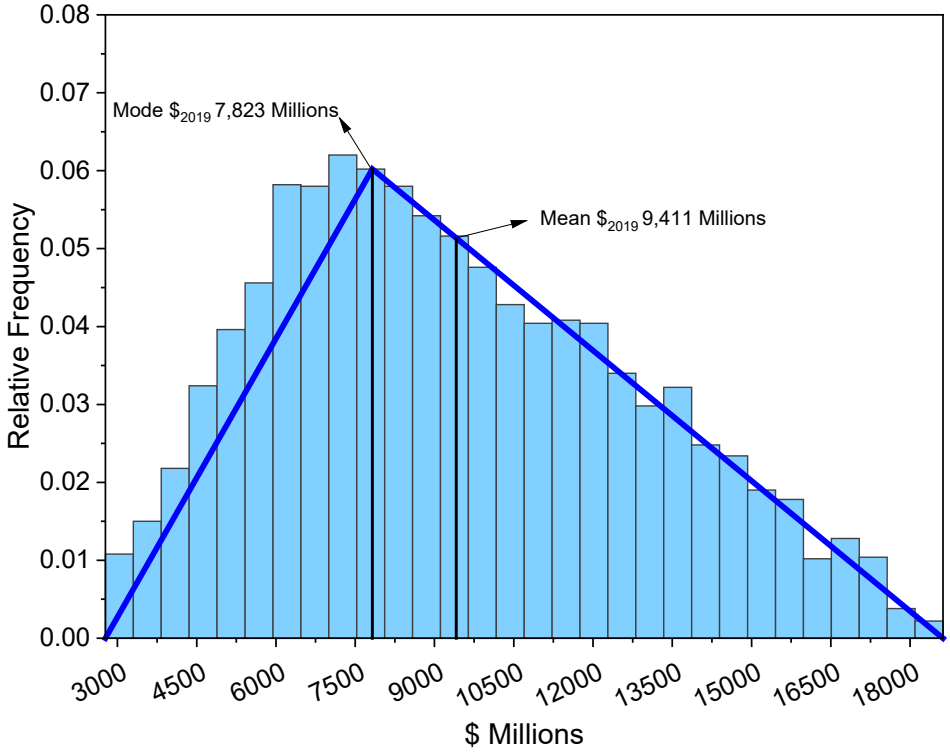

Figure 89 – Transport ***ANGRA3 CFC.***

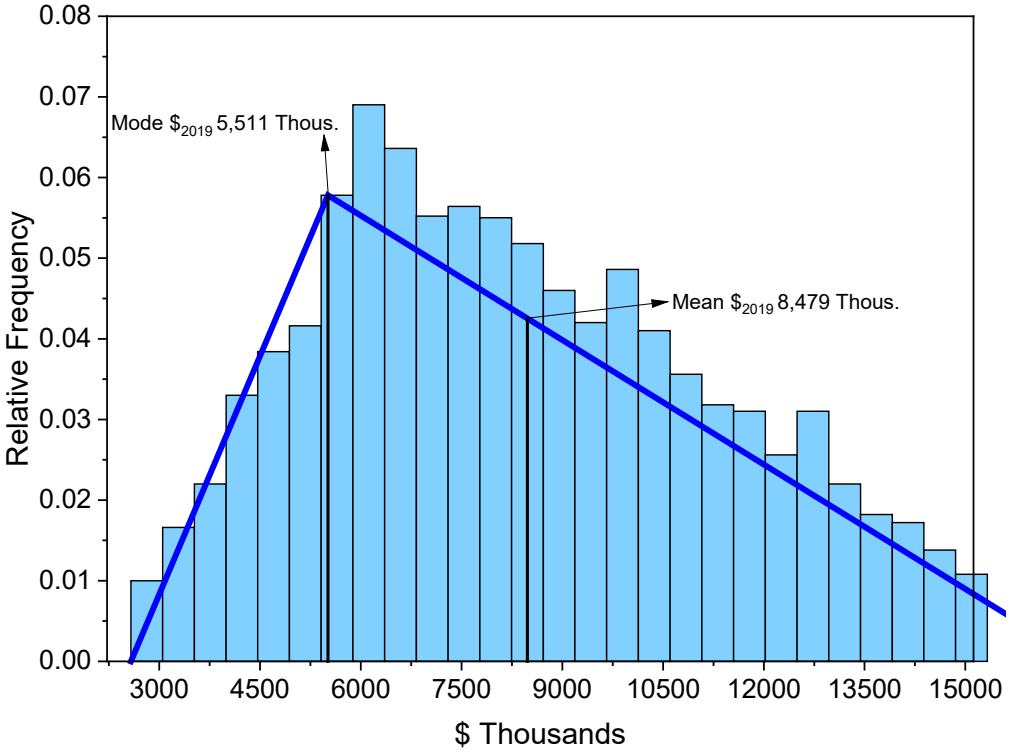

Figure 90 – Interim storage ***ANGRA+8 CFC.***

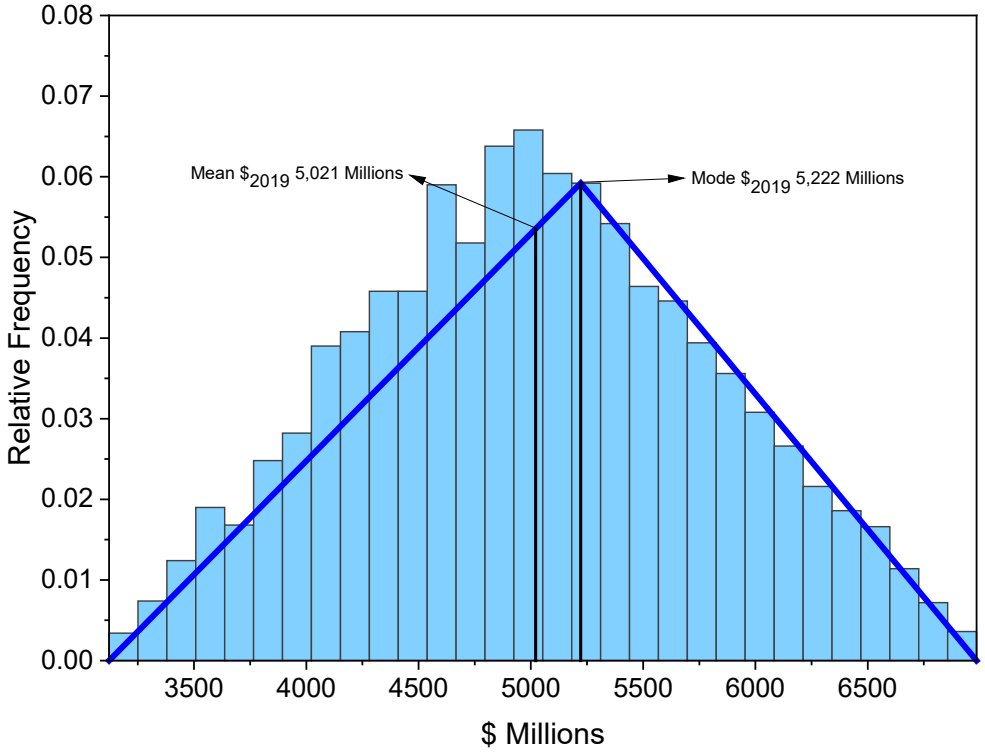

Figure 91 – Reprocessing plant ***ANGRA+8 CFC.***

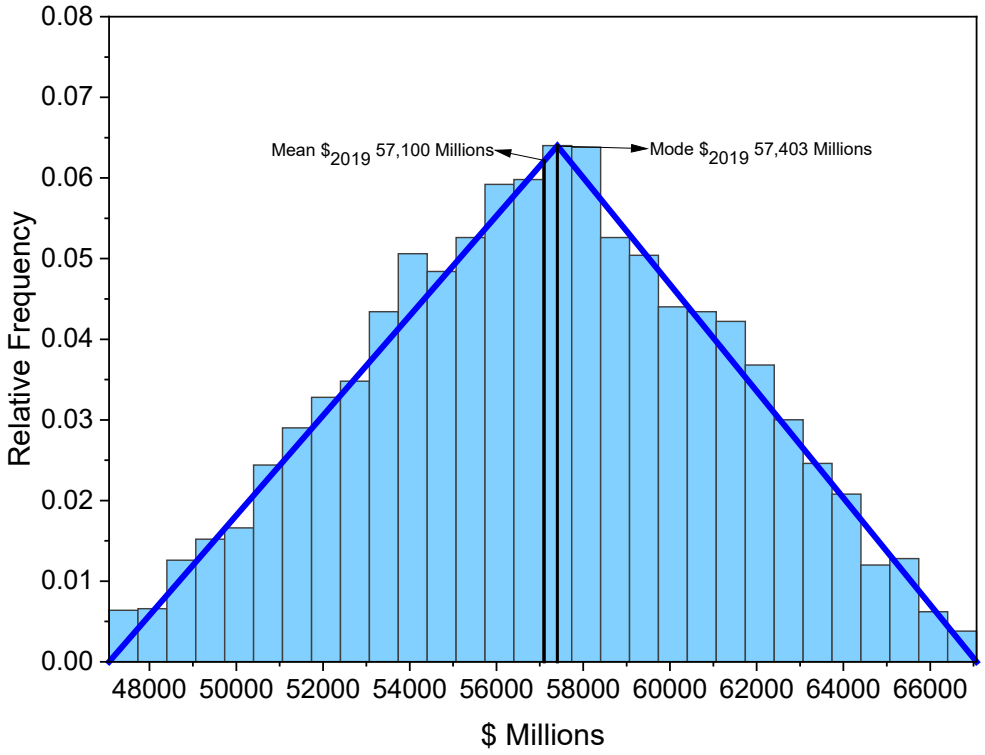

Figure 92 – Encapsulation plant ***ANGRA+8 CFC.***

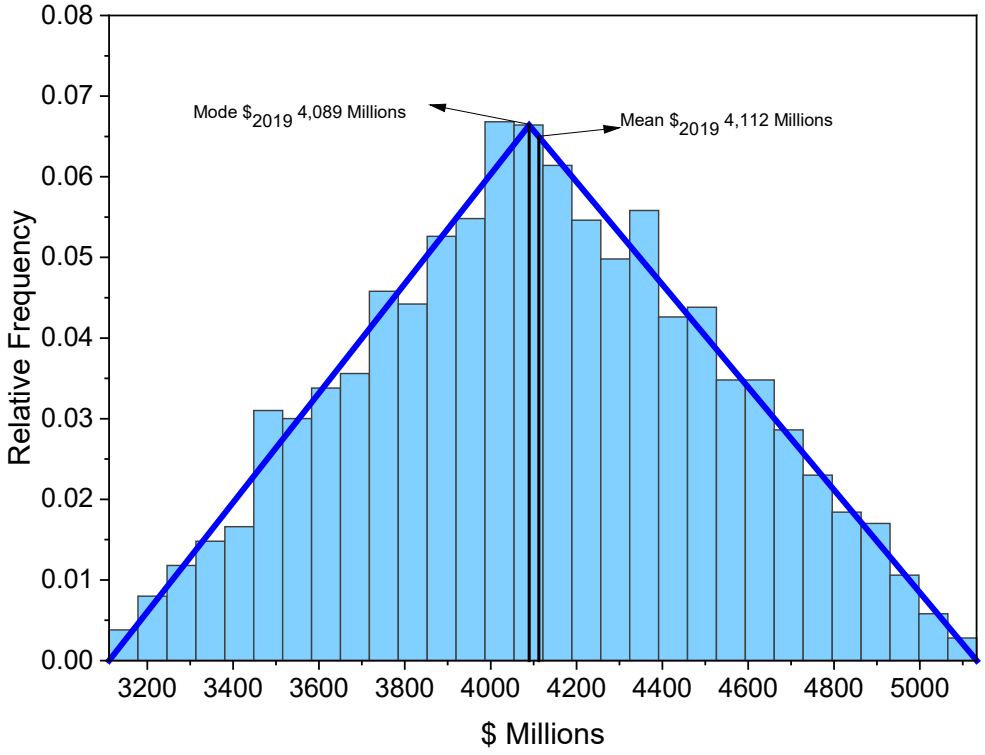

Figure 93 – Repository ***ANGRA+8 CFC.***

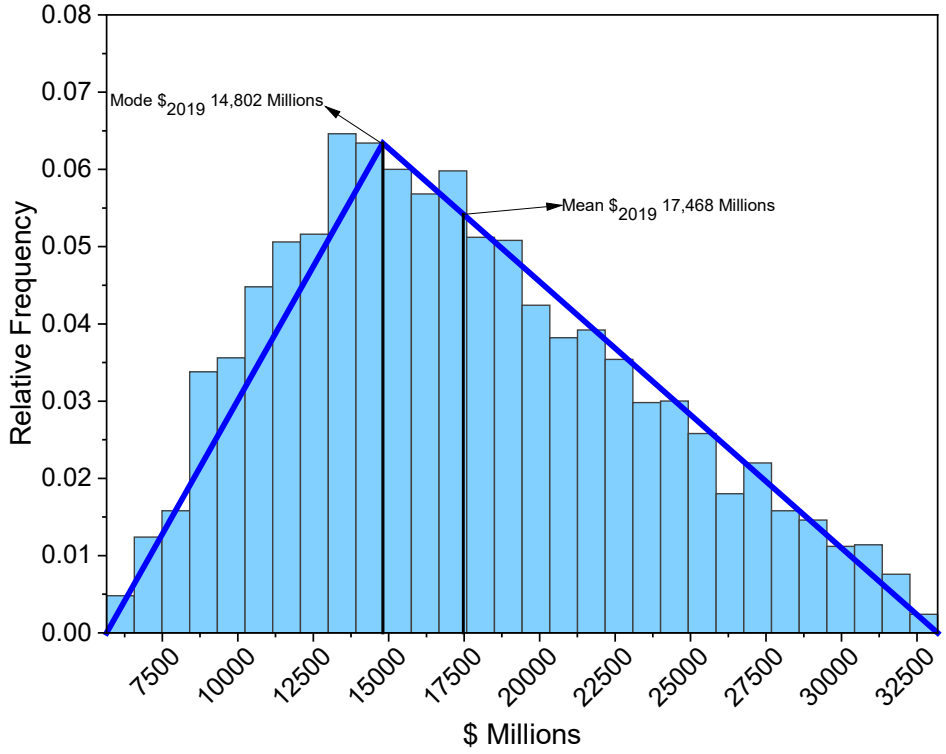

Figure 94 – Transport ***ANGRA+8 CFC.***

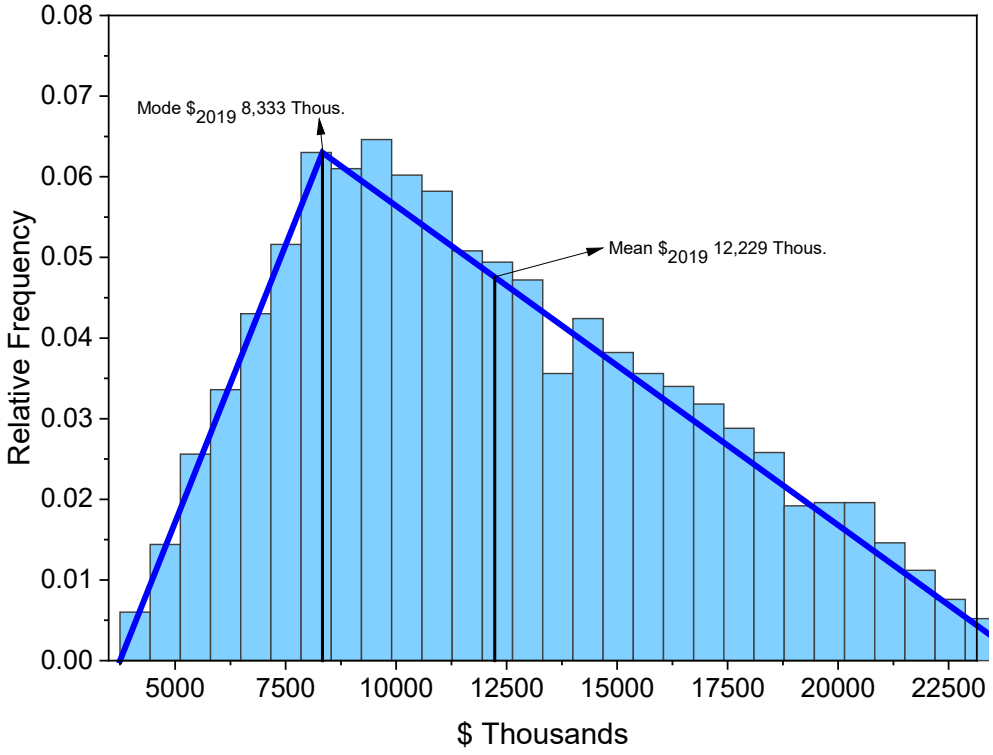

APPENDIX C - DISTRIBUTION CURVES FOR THE OUTPUT DATA

Figure 95 – Total cost histogram – ***ANGRA1&2 OFC***.

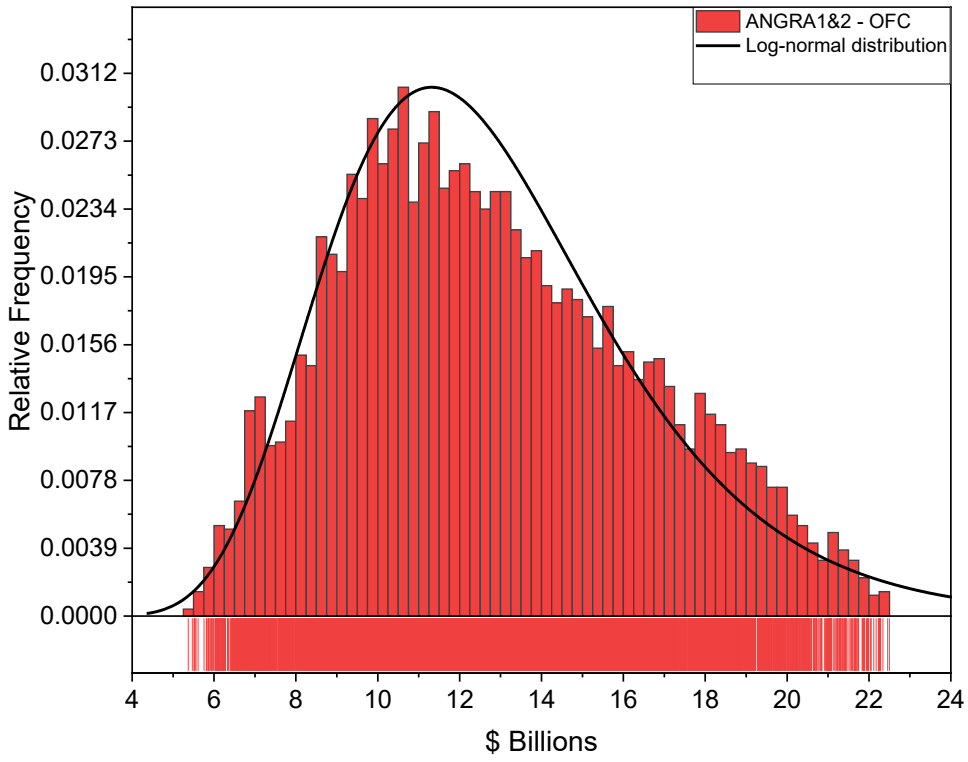

Figure 96 – Total cost histogram – ***ANGRA3 OFC***.

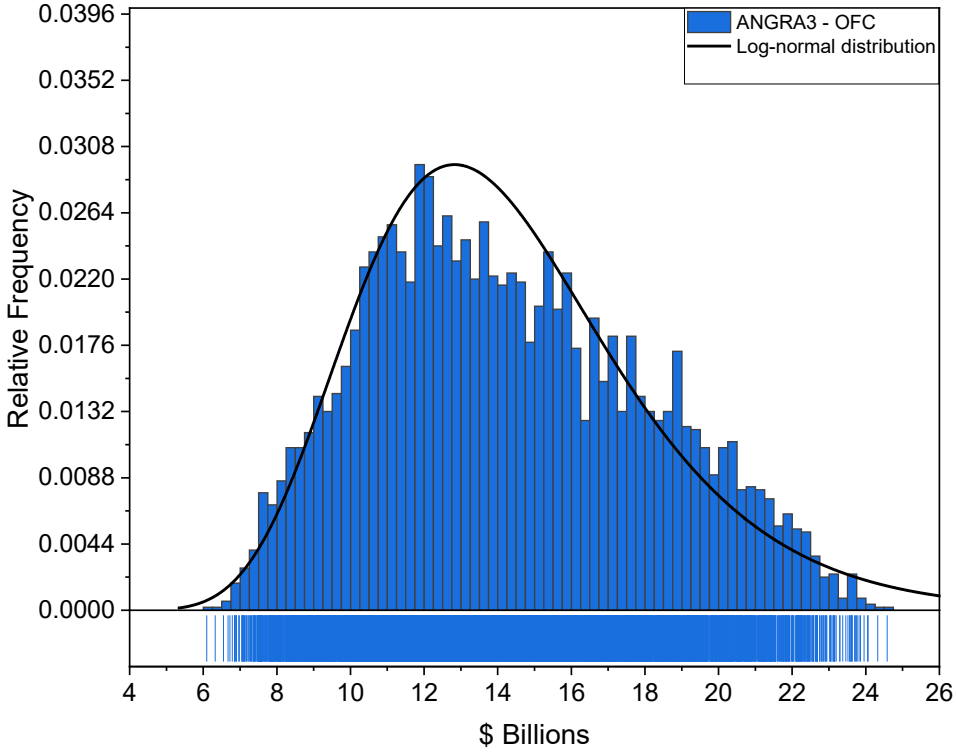

Figure 97 – Total cost histogram – ***ANGRA+8 OFC***.

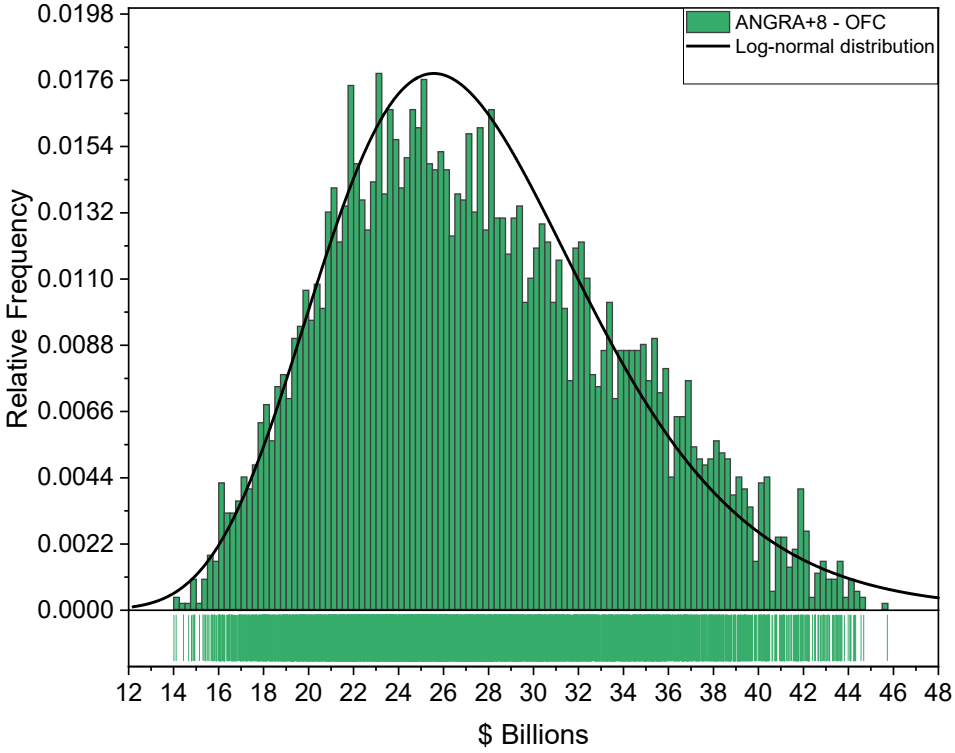

Figure 98 – Total cost histogram – ***ANGRA1&2 CFC***.

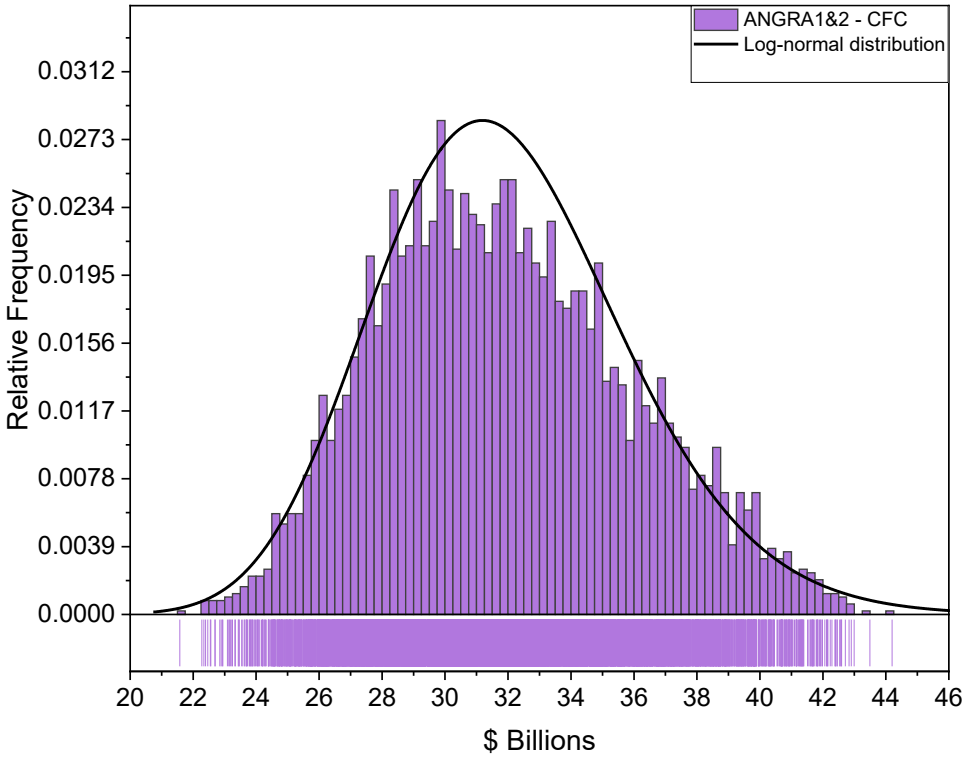

Figure 99 – Total cost histogram – ***ANGRA3 CFC***.

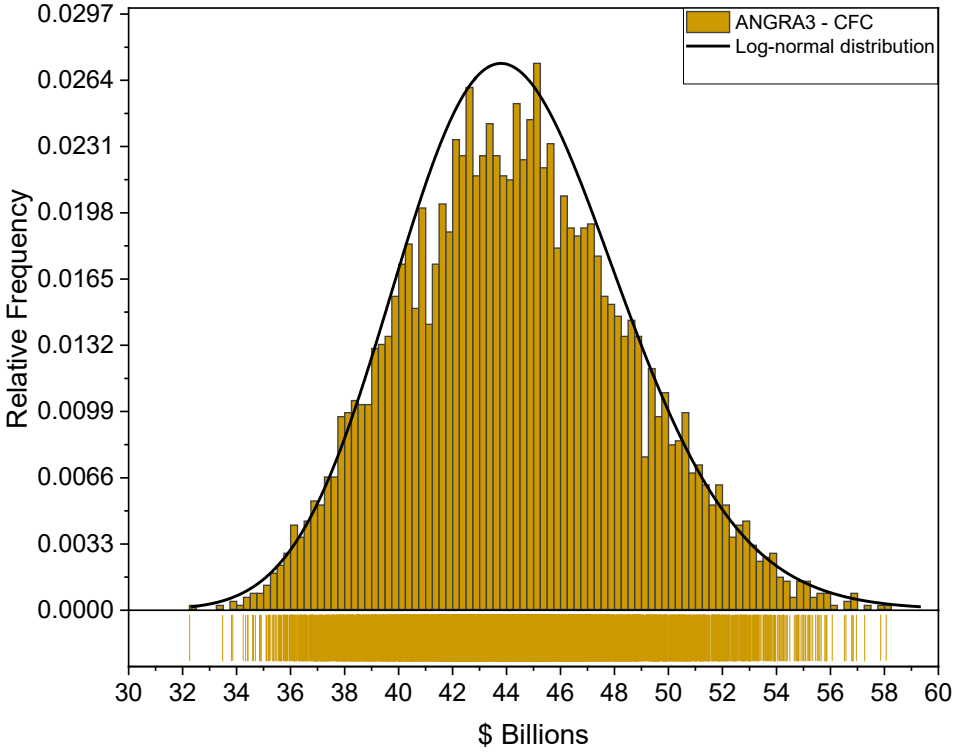

Figure 100 – Total cost histogram – ***ANGRA+8 CFC***.

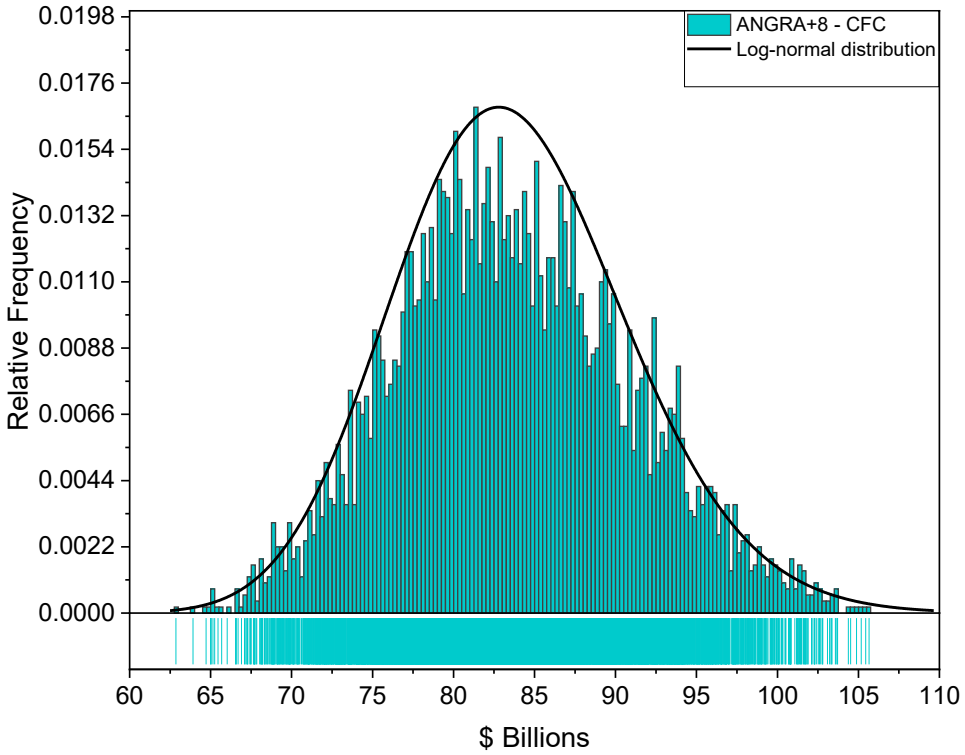

APPENDIX D - BACK-END COST BREAKDOWN FOR ALL SCENARIOS

Figure 101 – Back-end cost breakdown for ***ANGRA1&2*** OFC scenario.

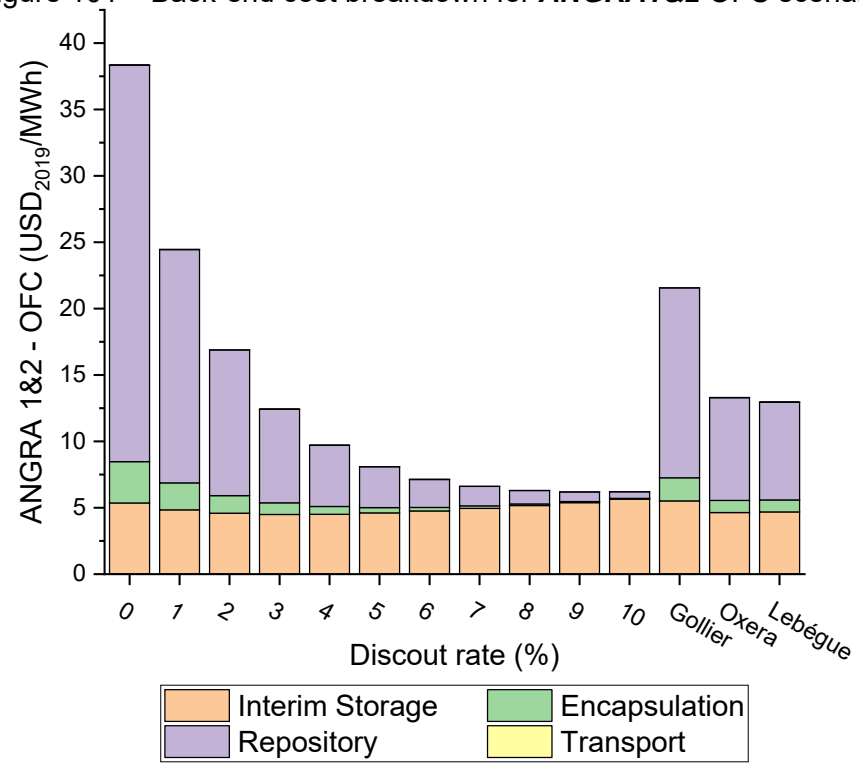

Figure 102 – Back-end cost breakdown for ***ANGRA1&2*** CFC scenario.

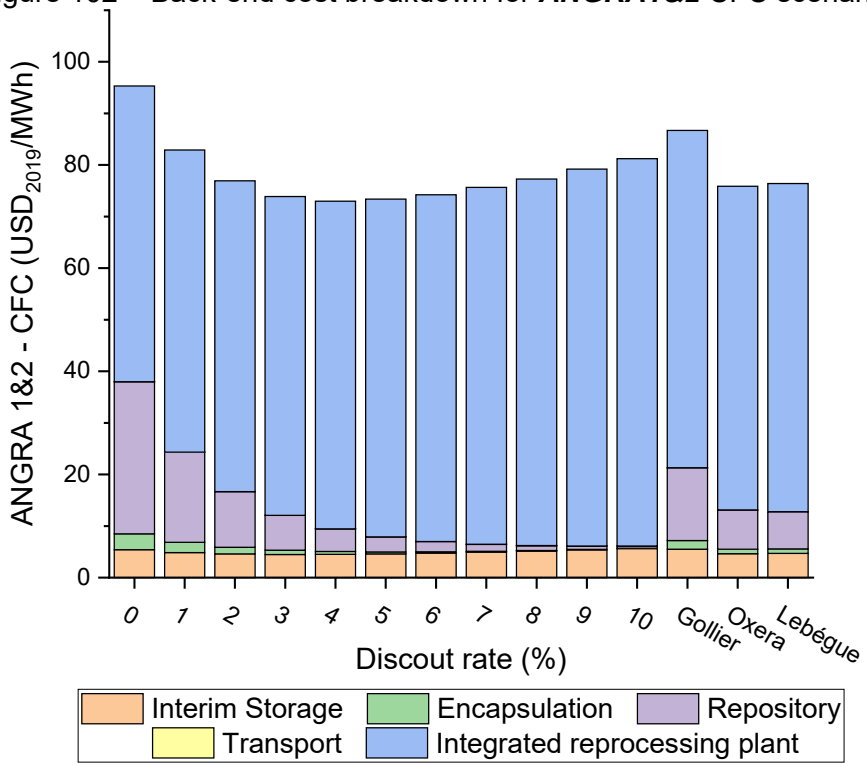

Figure 103 – Back-end cost breakdown for ***ANGRA3*** OFC scenario.

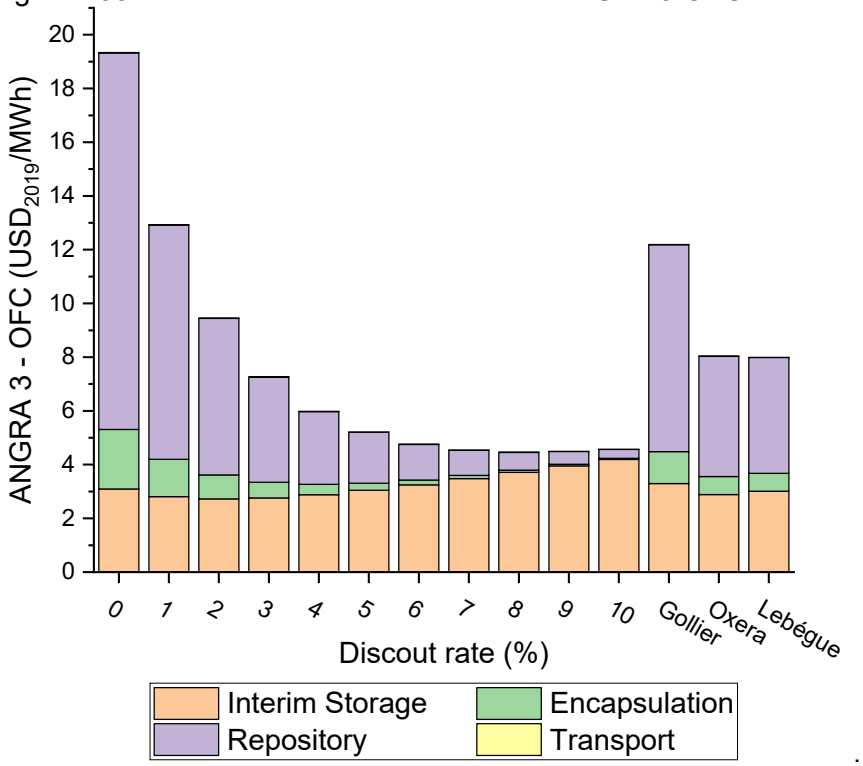

Figure 104 – Back-end cost breakdown for ***ANGRA3*** CFC scenario.

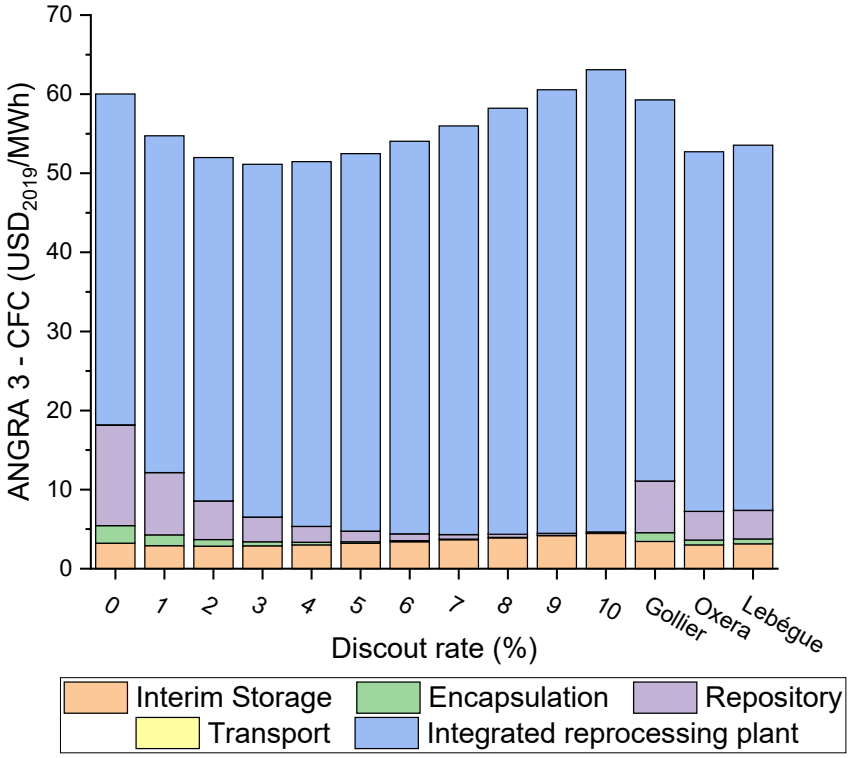

Figure 105 – Back-end cost breakdown for ***ANGRA+8*** OFC scenario.

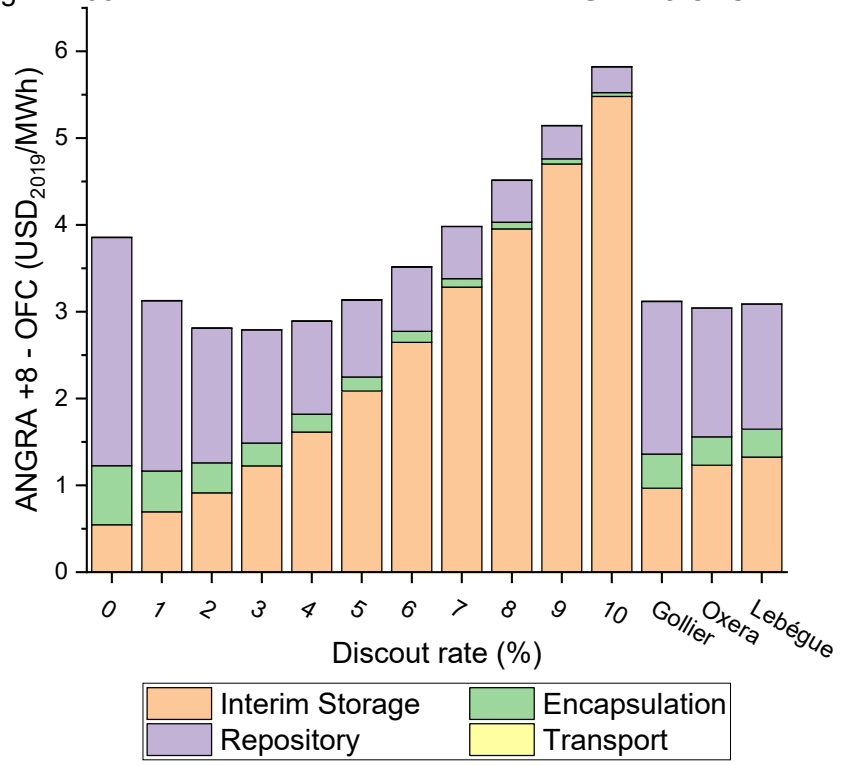

Figure 106 – Back-end cost breakdown for ***ANGRA+8*** CFC scenario.

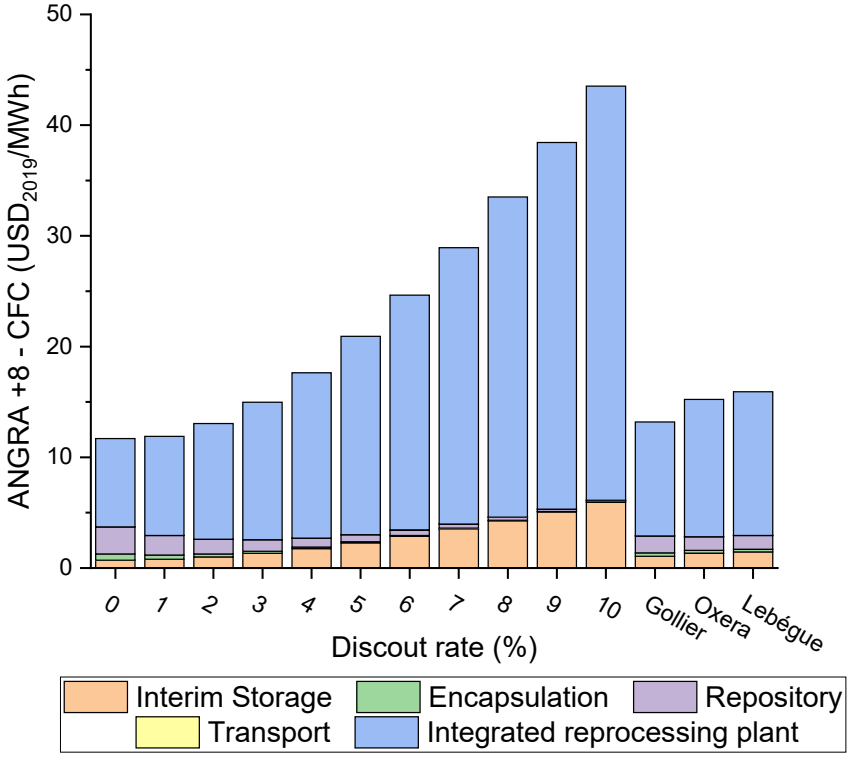

ANNEX A - STATUS OF NATIONAL WASTE DISPOSAL PROGRAMMES

Table 26 – Status of national waste disposal programs. Adapted from(156).

(continues)

Country	Name of organization	Long-term management strategy	Status	Type of geology
Argentina	N/A	No decision	N/A	N/A
Armenia	N/A	No decision	N/A	N/A
Belgium	National Agency for Radioactive Waste and Enriched Fissile Materials (ONDRAF/ NIRAS)	No decision	Decided to build a deep geological repository	N/A
Brazil	Comissão Nacional de Energia Nuclear (CNEN)	No decision	N/A	N/A
Bulgaria	N/A	No decision	N/A	N/A
Canada	Nuclear Waste Management Organization (NWMO)	Deep geological repository for used nuclear fuel	Active site selection process	Crystalline and sedimentary
China	China National Nuclear Corporation (CNNC)	Deep geological repository for used nuclear fuel and high-level waste	Active site selection process	Crystalline
Croatia		No decision		
Czech Republic	Radioactive Waste Repository Authority (SÚRAO)	Deep geological repository for used nuclear fuel and high-level waste	Early site selection process	Crystalline
Finland	Posiva	Deep geological repository for used nuclear fuel	Construction underway	Crystalline
France	French National Agency for Radioactive Waste Management (ANDRA)	Deep geological repository for used nuclear fuel and high-level waste	Site selected	Sedimentary
Germany	Bundesgesellschaft für Endlagerung (BGE)	Deep geological repository for used nuclear fuel and high-level waste	Active site selection process	Crystalline, sedimentary, and salt
Hungary	Public Limited Company for Radioactive Waste Management (PURAM)	Deep geological repository for used nuclear fuel and high-level waste	Active site selection process	Clay

(continues)

Country	Name of organization	Long-term management strategy	Status	Type of geology
India	India Atomic Energy Commission (AEC)	Deep geological repository for high-level waste	Active site selection process	Crystalline, sedimentary, and basalt
Iran	N/A	No decision	N/A	N/A
Italy		No decision		
Japan	Nuclear Waste Management Organization of Japan (NUMO)	Deep geological repository for high-level waste	Active site selection process	Crystalline and sedimentary
Mexico		No decision		
Netherlands	Central Organization for Radioactive Waste (COVRA)	Deep geological repository for used nuclear fuel and high-level waste	Decided to build a deep geological repository	Salt and clay
Pakistan		No decision		
Romania	Nuclear and Radioactive Waste Agency (ANDR)	Deep geological repository for used nuclear fuel and high-level waste	Early site selection process	Salt, clay, crystalline, and green schists
Russia	National Operator for Radioactive Waste Management (NO RAO)	Deep geological repository for high-level waste	Site Selected	Crystalline
Slovakia	Nuclear Regulatory Authority of the Slovak Republic (UJD SR)	Deep geological repository for used nuclear fuel and high-level waste	Active site selection process	Crystalline and sedimentary

(conclusion)

Country	Name of organization	Long-term management strategy	Status	Type of geology
Slovenia	Agency for Radwaste Management (ARAO)	Deep geological repository for used nuclear fuel and high-level waste	Decided to build a deep geological repository	N/A
South Africa	National Radioactive Waste Disposal Institute (NRWDI)	Deep geological repository for used nuclear fuel and high-level waste	Decided to build a deep geological repository	N/A
South Korea	Korea Radioactive Waste Agency (KORAD)	Deep geological repository for used nuclear fuel and high-level waste	Decided to build a deep geological repository	N/A
Spain	National Company of Radioactive Waste (ENRESA)	Deep geological repository for used nuclear fuel and high-level waste	Decided to build a deep geological repository	Crystalline, clay and salt
Sweden	Swedish Nuclear Fuel and Waste Management Company (SKB)	Deep geological repository for used nuclear fuel	Submitted a licensing application to build a repository	Crystalline
Switzerland	National Cooperative for the Disposal of Radioactive Waste (NAGRA)	Deep geological repository for used nuclear fuel and high-level waste	Active site selection process	Clay
Taiwan	Institute of Nuclear Energy Research (INER)	Deep geological repository for used nuclear fuel	Early site selection process	Crystalline
Ukraine	State Agency of Ukraine on Exclusion Zone Management (SAUEZM)	Deep geological repository for high and intermediate level waste	Decided to build a deep geological repository	Crystalline, Clay and Salt
United Kingdom	Radioactive Waste Management Limited (RWM)	Deep geological repository for used nuclear fuel and high-level waste	Active site selection process	Crystalline, sedimentary, and salt
United States	Department of Energy (DOE)	Deep geological repository for used nuclear fuel and high-level waste	Decided to build a deep geological repository	N/A

ANNEX B - OVERNIGHT AND O&M COSTS OF BACK-END FACILITIES

Figure 107 – Interim storage facility: Overnight investment costs (124).

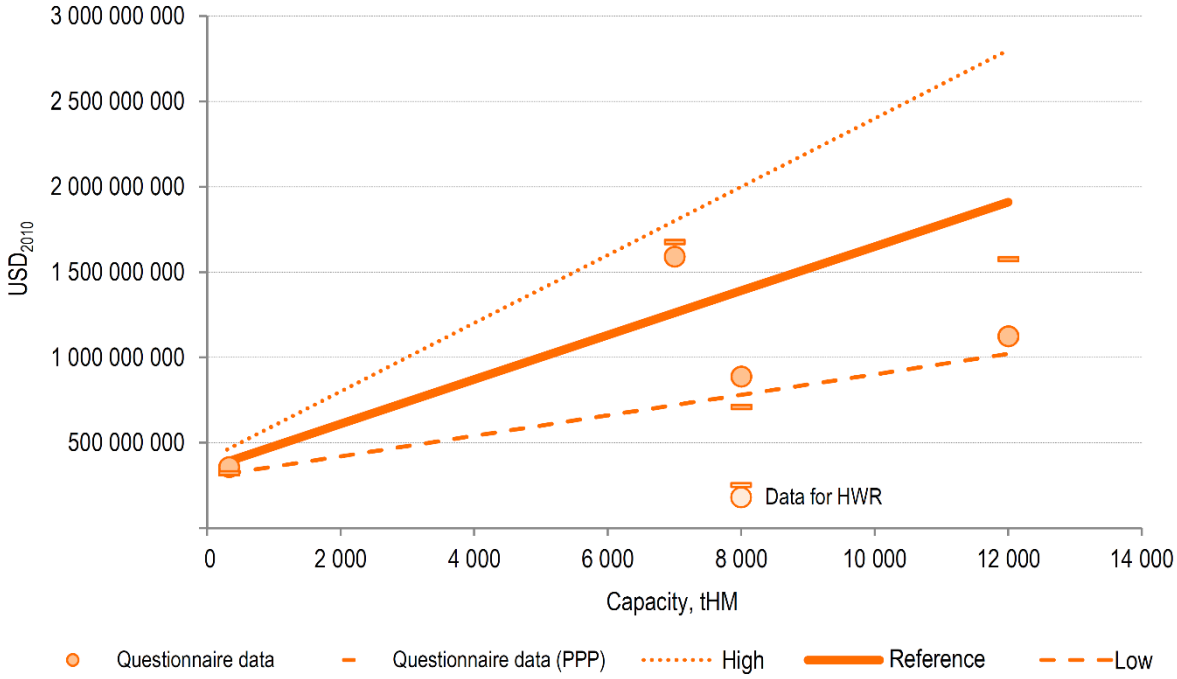

Figure 108 – Interim storage facility: O&M costs (124).

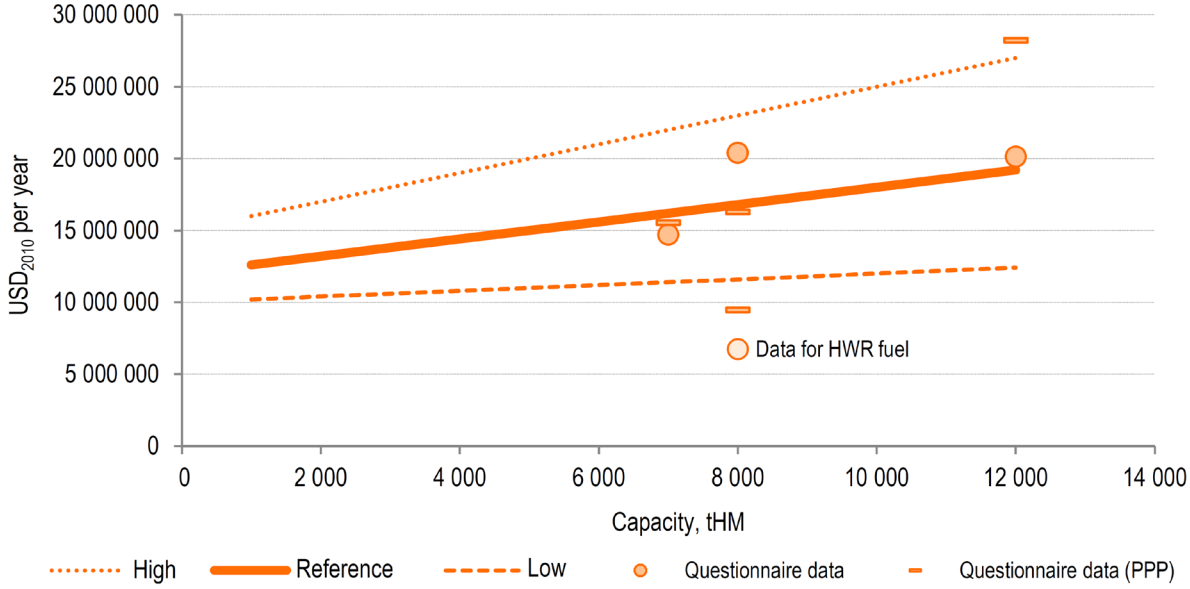

Figure 109 – Integrated reprocessing plant: Overnight investment costs (124).

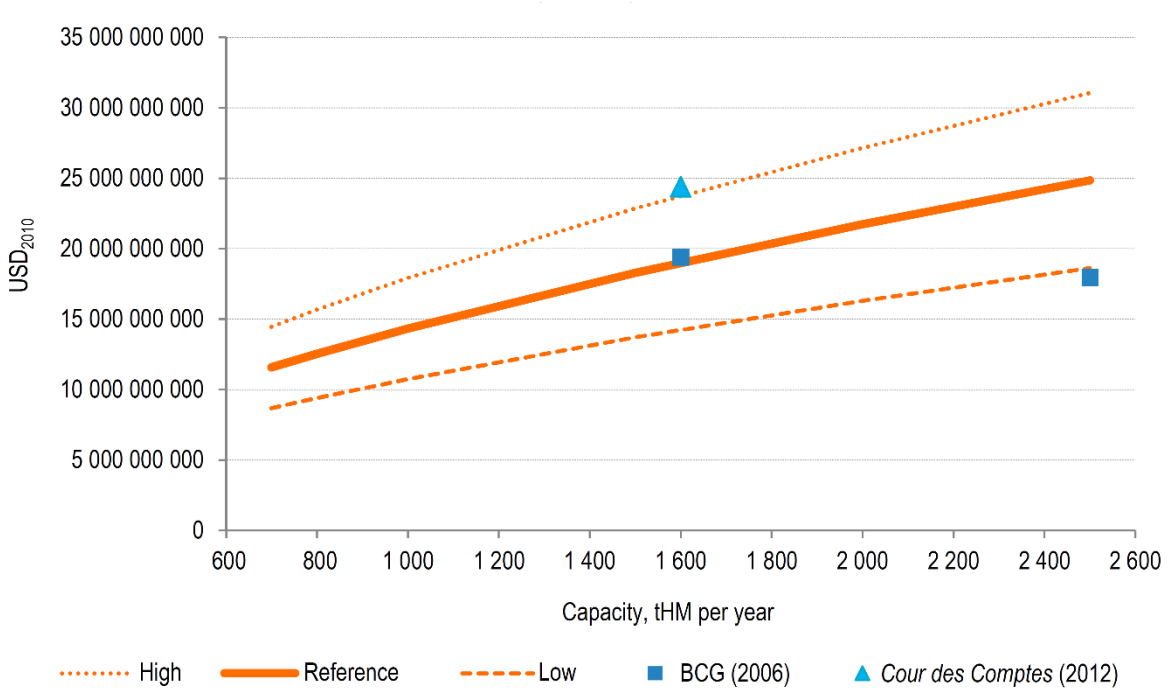

Figure 110 – Integrated reprocessing plant: O&M costs (124).

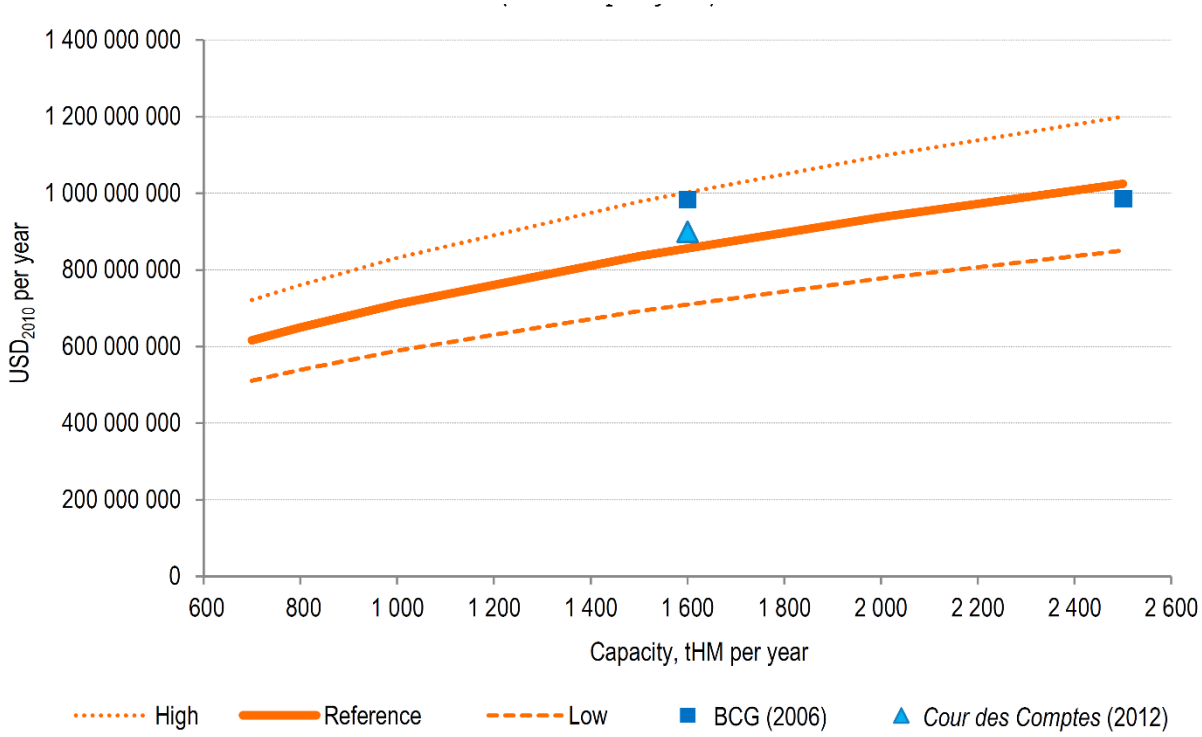

Figure 111 – SNF encapsulation plant: Overnight investment costs (124).

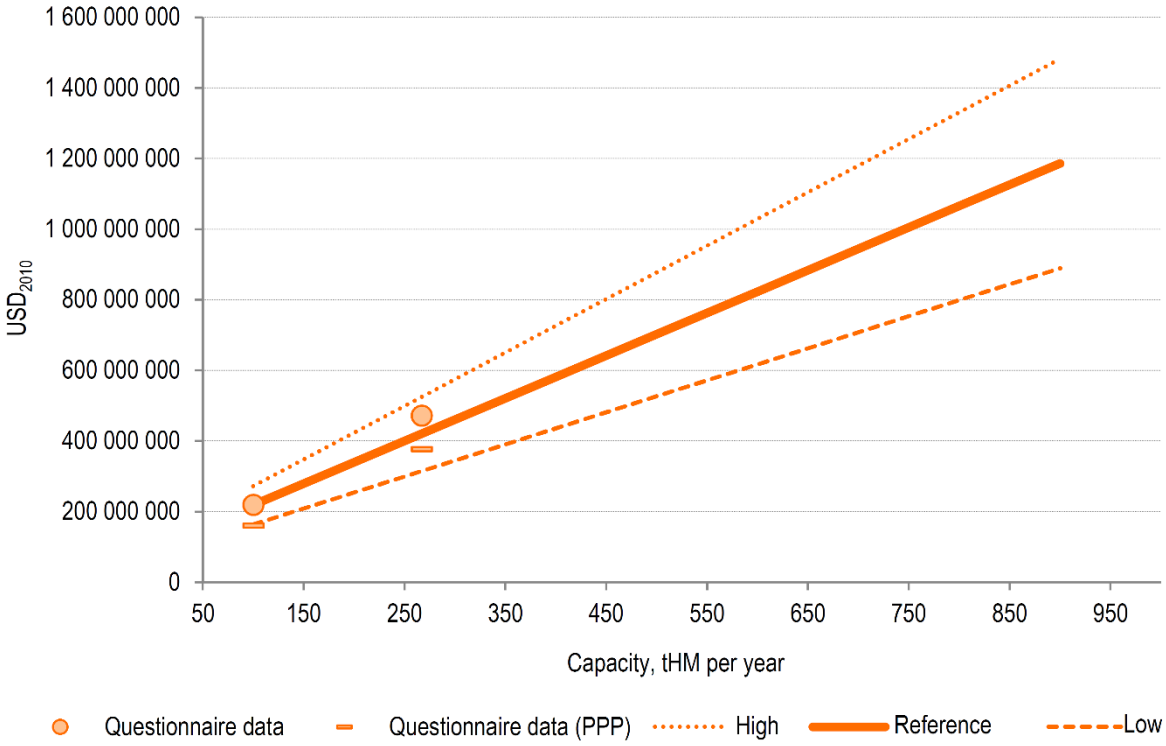

Figure 112 – SNF encapsulation plant: O&M costs (124).

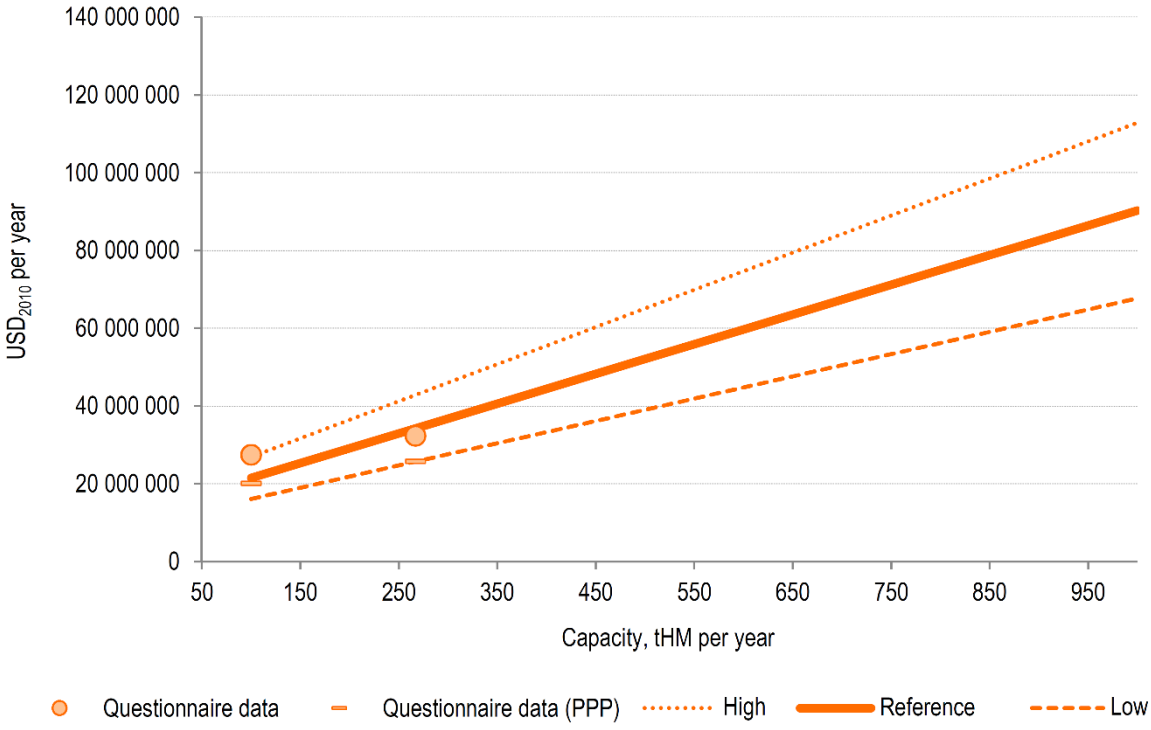

Figure 113 – Geological repository: Overnight investment cost (124).

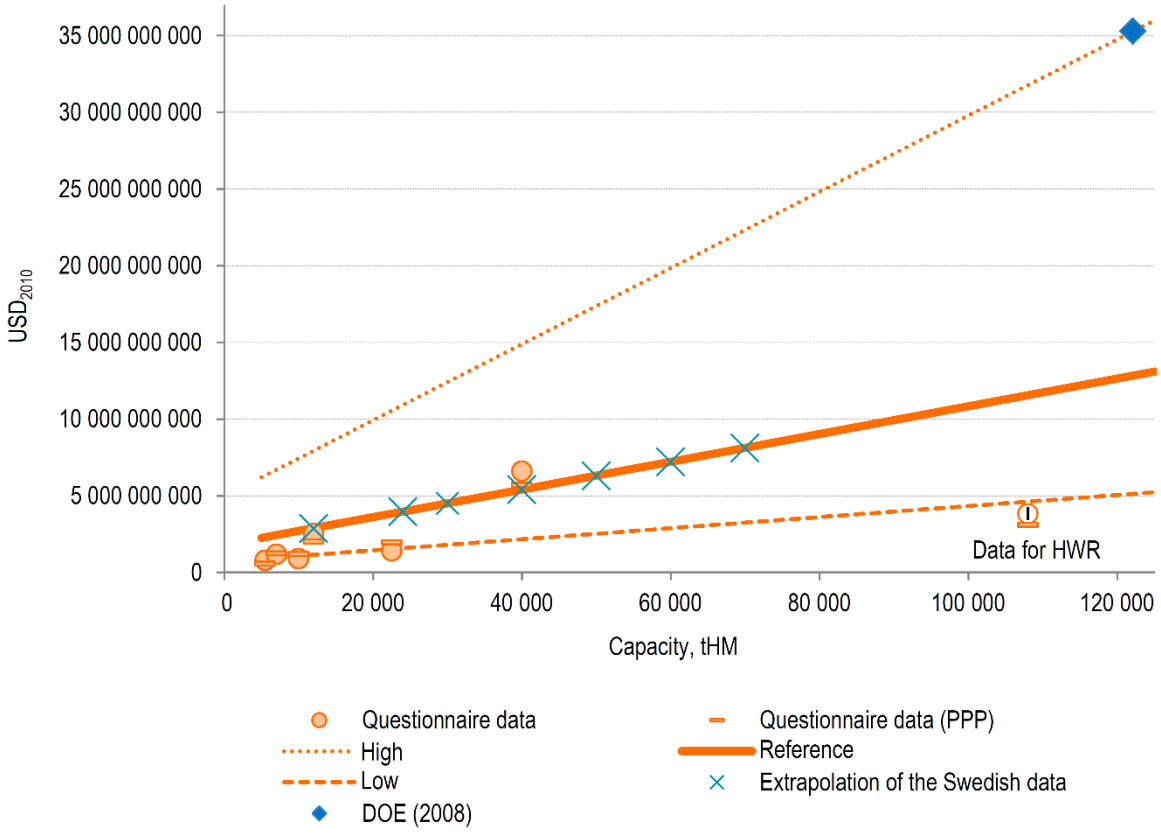

Figure 114 – Geological repository: Annual O&M costs (normalized for 60 years of operation) (124).

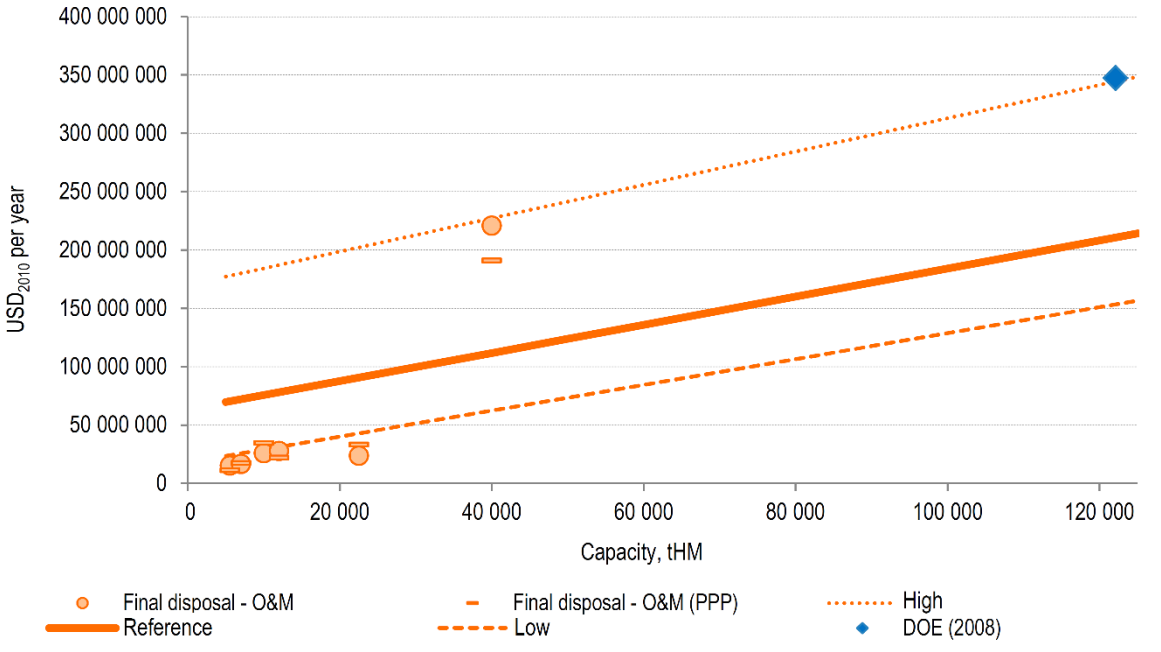

Figure 115 – Geological repository: Closure costs (124).

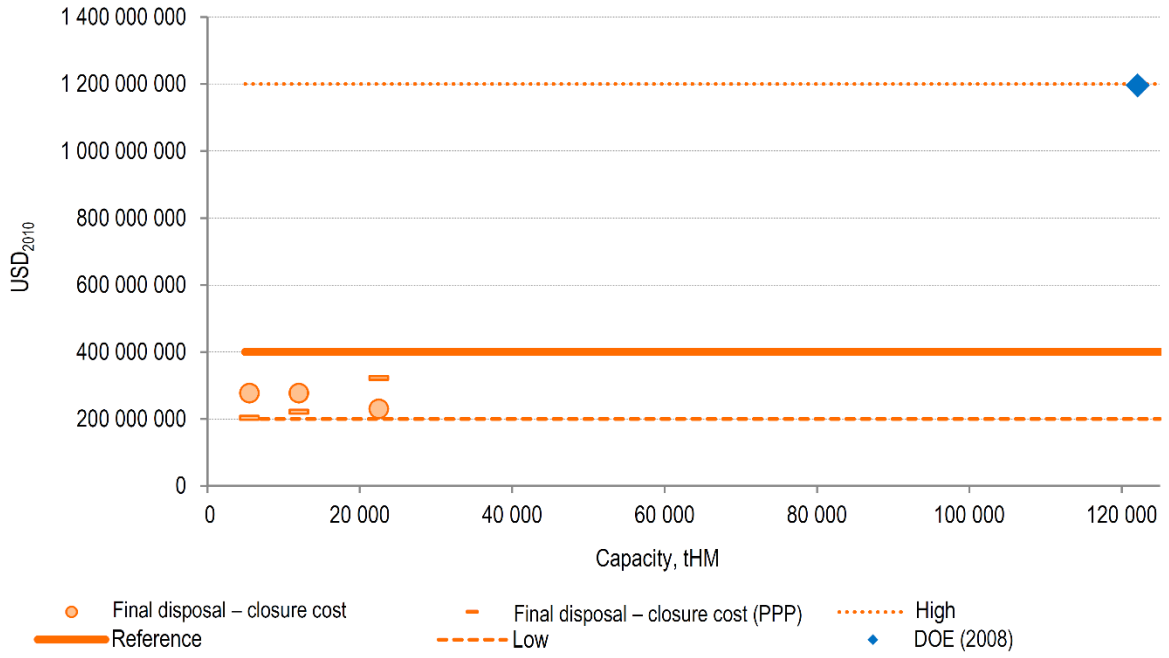

Figure 116 – Specific transport costs (124).